Till Vännen Henrik
från Texas

ARKIV FÖR FYSIK

UTGIVET AV

KUNGL. SVENSKA VETENSKAPSAKADEMIEN

Band 12 nr 1

E. RUNE LINDGREN

The transition process and other phenomena in viscous flow

ALMQVIST & WIKSELL/STOCKHOLM

1957

THE TRANSITION PROCESS AND OTHER PHENOMENA IN VISCOUS FLOW

By

E. RUNE LINDGREN

AVHANDLING

som med tillstånd av Kungl. Tekn. Högskolan
för teknisk doktorsgrads vinnande
framlägges till offentlig granskning
å hörsal 187, Teknologgården 22, Kungl. Tekn. Högskolan,
onsdagen den 29 maj 1957 kl. 10

UPPSALA 1957
ALMQVIST & WIKSELLS BOKTRYCKERI AB

ARKIV FÖR FYSIK Band 12 nr 1

Communicated 23 January 1957 by Hilding Faxén and Hannes Alfvén

The transition process and other phenomena in viscous flow

By E. Rune Lindgren

With 65 figures in the text

Preface

The present study contains an account of some experiments on the transition process and other phenomena of liquid flow, mainly in cylindrical tubes. The experimental indications in many respects do not agree with current ideas regarding basic flow characteristics. However, in several cases these indications appear to remove apparent discrepancies between various determinations of flow phenomena as reported in the literature of Hydrodynamics, indications which might justify the publication of the paper in its present form, even though several misinterpretations may possibly have to be corrected in the light of future research.

The investigation could scarcely have been carried out if it had not been for the helpful interest and co-operation of numerous persons at various institutions, particularly because the work has been performed in the realm of a purely theoretical institution, without any experimental facilities. It would therefore appear appropriate to present my acknowledgements and the background of the investigation in this preface.

In the spring of 1951 Professor Bo Hellström at the Hydraulics Laboratory of the Royal Institute of Technology (KTH) employed me to develop a Demonstration Fluid Polariscope applying the stream birefringence technique about which he had received information during a visit to the United States. This project was discontinued fairly soon. In my spare time, however (after receiving a sample of White Hector bentonite as a gift from the *Baroid Sales Division, National Lead Company,* California), I worked out some preliminary tests which demonstrated the great possibilities of this technique for studying flow phenomena.

The idea of making flow experiments using the bentonite technique materialized when a series of seminars, arranged at the Institute by Professors H. Alfvén and O. H. Faxén, suggested that even the macroscopic course of the transition process, and of the mechanism of turbulence, did not appear fully clarified in many respects. This state of affairs induced me to arrange some primitive demonstration experiments on the transition process in flow of a bentonite sol through a glass tube, which attracted the interest of Professor Faxén. He promised to support an investigation as far as means allowed and also gave his permission to let graduation students volunteer as assistants.

A first series of experiments was completed at the end of 1952 and resulted in a paper, *Some aspects of the change between laminar and turbulent flow of liquids in cylindrical tubes* (Lindgren 1954*a*). The first part of the experiments was carried out in the Photographic Laboratory, by permission of Professor H. Bäckström, while the subsequent parts were performed in a laboratory of my own, thanks to the Rector of the Institute, Professor Ragnar Woxén.

As a consequence of the above paper the *State Council of Technical Research* granted economic support so that an improved flow apparatus could be built and I could devote more than my spare time to carrying on further experiments.

During the period of erection of the new apparatus the experiments in the old flow apparatus were continued and extended. These experiments, together with those reported in the paper mentioned above, form Part 2 of the present study. Other experiments, which were carried on now and then with the old apparatus during the years 1952–1955, are reported in Part 3. Some of these were reported preliminarily in *Note on the flow of liquids in tubes* (Lindgren 1954*b*). The illustrations in that paper, however, are of little value because of poor print.

The new flow apparatus, located in the Laboratory of Chemical Engineering Equipment by kind permission of Professor Otto Stelling on the recommendation of Professor Lage Malm and Professor Anders Rasmusson, was completed in the late spring of 1954. In this connection I am specially indebted to Professor Rasmusson who, without restrictions, placed all the laboratory facilities of the Division of Chemical Engineering Equipment at my disposal.

The experiments carried out with the new apparatus and reported in Part 4 of this study consist of visual observations of the transition process simultaneously recorded at various locations in pairs along long cylindrical tubes. After finishing these experiments at the end of 1954, extended measurements were made by inclusion of automatically recorded simultaneous measurements of the pressure drop over various measuring distances along the tubes. These experiments, completed early in 1955, are reported in Part 5.

In the course of some complementary viscosity measurements I found it necessary to make a rather extensive study of the viscosity of bentonite sols and, further, that it was necessary to collect detailed information regarding the viscous properties of liquids in general and of water in particular. This time-consuming work was done during the second half of 1955 and the results are reported in Part 1 of the paper. Here, I have to express my gratitude to Docent E. Forslind who devoted much time to numerous discussions on rheologic problems during the various phases of the work.

The 6th and last part of the paper, which contains a summary of the most important experimental indications and a discussion of their coordination with theories and other experiments reported in the literature, has been made possible through a generous initiative taken by Professor Sten Luthander, head of the Division of Aeronautics KTH and through the support and sponsorship of the *Air Research and Development Command, United States Air Force*, through its European Office under Contract No. AF 61(514)-1202.

The names of those who in one way or another participated directly in the preparations or the experimental work will be found in pertinent passages of the text. I wish to express my gratitude to them all for their valuable help. It should also be mentioned that most of the measuring equipment used in the experiments reported in Parts 4 and 5, except for some specially designed units, was placed at my disposal by courtesy of Mr. D. Östensson, Hydraulics Laboratory; Mr. Paul Mitlid. Electro-

nics Laboratory; Mr. Helge von Koch, Physics Laboratory; Mr. N. Åhrberg, Laboratory of Electrical Measurements, Mr. T. Koch, Photographic Laboratory; Mr. Anders Norén, Hydraulic Eng. Laboratory; all of KTH and Mr. Sven Hellman, Research Institute of National Defense. The majority of the instrumental equipment, however, was obligingly placed at my disposal by Mr. A. Söderholm, head of the Measuring Section of the Aeronautics Laboratory. In fact, it would not have been possible to carry out the experiments to their present extent had it not been for the co-operation of Mr. Söderholm and his staff.

I am also indebted to Dr. Tore Lundin at the Division of Applied Inorganic Chemistry for help and advice in various respects, as well as to Professor E. Ingelstam who kindly allowed me to micrograph the tube surfaces with his metallographic microscope in the Physics Laboratory, and to Mr. L. Johansson for his helpful instructions regarding the use of the microscope.

I also have great pleasure of expressing my gratitude towards my friend and supervisor Professor O. H. Faxén, head of the Division of Mechanics I, KTH, who has devoted much time and work in securing the necessary grants from the various sponsors among which, besides those named previously, mention should also be made of the KTH through Professor Faxén's institution. My thanks to him include my heart-felt gratitude for the many hours he has devoted to discussion of the various aspects of the problems attacked. It is my belief that if I have managed to express myself adequately in the paper presented here, this is not least a result of Professor Faxén's work as a teacher of "logics and facts".

Mr. Alan McLean as also Docent Forslind and my wife have revised my English, Mrs. Ulla McLean did the beautiful drawings, and most valuable help was given by Miss Dagmar Odqvist and her staff at the Institute Library. The manuscript has been typed by Miss Märta Lundquist, Mrs. Rut Kumlin, Miss Sonja Persson, Mrs. Ingegerd Westerlund, Miss Greta Mobach, and Mrs. Alice Sylwén. My sincere thanks are due to them all.

There are still numerous persons at many institutions to whom I should like to express my gratitude for help in many ways, but it is impossible to mention them all by name.

Stockholm, January 1957

Rune Lindgren

Introduction

Some primary definitions

In real fluid motion—flow of liquids and gases—a distinction is made between the two fundamental conceptions: laminar and turbulent flow. Although these two terms are commonly used, their meaning is vague and a closer examination makes it evident that it is quite difficult to give exact definitions of these two manifestations of fluid flow.

Osborne Reynolds in his fundamental investigations 1874–1883 distinguished between *steady* and *sinuous* fluid motion, which, however, is no proper definition of the two states of fluid flow. First it can be questioned whether the words steady and sinuous refer to variations of the flow characteristics in space or in time. Secondly the term sinuous usually has the meaning of regular variations, quite different from the highly irregular turbulent fluctuations which actually were in Professor Reynolds' mind.

Horace Lamb in his *Hydrodynamics* (1953 pp. 663–4) describes the turbulent flow as a wildly irregular motion appearing to consist of interlacing and constantly varying streams crossing and recrossing the main flow. C. W. Oseen at the *3rd International Congress for Applied Mechanics in Stockholm,* 1930, tried to define the turbulent flow by the words: "Turbulent ist eine Flüssigkeitsbewegung wenn sie so kompliziert ist, dass man von einer genauen Kenntnis derselben absieht und sich mit der Kenntnis einer mittleren Bewegung begnügt."

According to Professor Lamb it was Lord Kelvin who introduced the very descriptive term "*turbulence*" (Lamb: *Hydrodynamics* 1953, p. 664) which is not quite satisfactorily defined by the descriptions made by Lamb and Oseen above.

In the following, *laminar* flow will be understood as steady flow showing a stationary regular flow pattern, in which the macroscopic velocity of the fluid elements in every point is tangential to continuous and smooth streamlines which, at least in the immediate neighbourhood of the walls bounding the space of flow, proceed parallel to these boundaries.

The descriptions above imply the existence of an indefinite number of different types of turbulent flow as well as the existence of other types of flow which are neither of the turbulent nor of the laminar type and which have to be described as they occur. In this paper, however, a distinction will be made between (generally) "*disturbed flow*", and flow with "*selfmaintaining turbulence*" which concepts both would be covered by the word "turbulence" according to classical ideas.

The onset of turbulence

The German engineer G. Hagen in 1839 made experiments on flow of water through cylindrical glass tubes and actually deduced the Poiseuille formula for laminar flow almost two years before the French physician J. L. M. Poiseuille published his famous paper 1840–41. At the same time Hagen reported observations of transition between steady and irregular flow. The statements differ, but this seems to be the first time the transition phenomenon and the existence of turbulence have been expressly reported in the literature.

It has been commonly assumed that laminar flow of real liquids and gases spontaneously changes to the turbulent state when certain "critical" velocities are exceeded and vice versa. Until recently the onset of turbulence was supposed always to take place after a certain distance of accumulation of laminar flow, so that continuous turbulent flow would establish itself downstream of the distance of accumulation provided the velocity was higher than its "critical" value. Apart from Reynolds' original work as reported in 1883, the first experimental evidences expressively indicating quite another course of the transition process were published by A. M. Binnie 1945. His experiments showed for certain that transition of flow in tubes took place by an increasing (decreasing) number of turbulent "flashes" when the velocity was increased (decreased) around the appropriate "critical" velocity. (Reynolds introduced the term "flash" for short regions of disturbed flow which he observed to appear in otherwise laminar tube flow.) Binnie's later experiments together with J. S. Fowler in 1947 also show that the mechanism of transition is a random phenomenon.

The observations of the transition process as consisting of random bursts of turbulence have later been noted by H. W. Emmons in 1951 when studying flow of water layers over a slightly inclined "smooth" glass plate. Recently, in 1955, these observations were confirmed by G. B. Schubauer and P. S. Klebanoff who reported this transition process to be valid also for flow of air over plane surfaces.

The efforts of many of the most prominent theoretical physicists and mathematicians since the middle of the last century, have as yet failed to give a theoretical explanation of the initiation of turbulence consistent with the experimental experiences. This conclusion appears to be true in spite of a statement by Herman Schlichting in his *Grenzschicht-Theorie* (1951 pp. 300–1):

> "Im ganzen ergibt sich aus diesen sehr sorgfältigen Messungen [Professor Schlichting here refers to experiments reported by G. B. Schubauer and H. K. Skramstad 1943] eine so vollständige Bestätigung der Theorie der kleinen Schwingungen, dass nunmehr an der Gültigkeit dieser Theorie nicht mehr gezweifelt werden kann. Die Reynoldsche Vermutung, dass der Umschlag laminar-turbulent auf eine Instabilität der Laminarströmung zurückzuführen ist, ist damit endgültig bestätigt."

In the light of the experimental experiences of random bursts of turbulence according to Reynolds, Binnie, Emmons and Schubauer & Klebanoff as well as to my own observations, Schlichting's statement seems to be questionable. Of course the instability theory of small oscillations cannot be objected to in itself, but in most cases it does not at all give results consistent with experimental facts, neither qualitatively nor quantitatively, with respect to the transition process. It also is desirable to point out that Reynolds seems not to have expressed any definite hypothesis regarding the transition process, though this is implied in the Schlichting statement above.

The transition process

The current conceptions associated with the transition mechanism of the flow of liquids and gases mainly derive from the Prandtl school in Göttingen 1920–40 and particularly from the works by Ludwig Schiller 1920, 1921, 1924, 1925, 1930, 1934; W. Tollmien 1929, 1953, and Schlichting 1934, 1951, while at the same time Reynolds' original statements seem to have been rather neglected.

1 Reynolds introduced the only possible dimensionless quantity characterizing homogeneous incompressible viscous flow

$$R = \frac{U d}{\nu} \quad \text{(the Reynolds number)}, \tag{0.1}$$

where U = mean flow velocity,
d = a length characterizing the flow space which in the case of flow in cylindrical tubes is specified as the tube diameter (or the radius),
ν = kinematic viscosity of the fluid.

The Reynolds number is usually interpreted as a measure of the quotient of the inertia forces divided by the viscous forces but can also be given other meanings. The concept of the Reynolds number is used in characterizing different states of any type of flow and is analysed by Th. v. Kármán 1923.

The idea is that, if transition occurs at a certain R in one case of a certain type of flow, this transition value of R ought to be valid under arbitrary conditions of the same type of flow notwithstanding variations in U, d and ν.

From experiments on tube flow Schiller 1921 concluded that if the flow is highly agitated at the tube entrance and provided the entrance length is long enough there occurs an instantaneous increase of the flow resistance when a critical Reynolds number $R = R_k$ is exceeded. This discontinuity of the flow resistance was currently interpreted as an instantaneous onset of turbulence.

Schiller performed his experiments by measuring the pressure drop of flow of water through "smooth" cylindrical brass tubes of about 8 and 16 mm diameter. He showed that the least necessary entry length (distance of accumulation) in order to create an abrupt breakdown of the laminar flow must be not less than 100–130 tube diameters. The necessary disturbance level was secured by a circular disc of larger diameter than the tube diameter and placed a short distance in front of the tube inlet. When the disc was moved closer to the tube opening, transition occurred at decreasing Reynolds numbers. However, the transition value of R did not decrease under a certain value $R = R_k = 2320$ when the disc was moved nearer than 1.2 mm to the tube inlet. Schiller concluded that this specified condition corresponds to the least necessary disturbance level essential to cause instantaneous onset of turbulence by the shortest possible distance of accumulation.

Reynolds 1883 made much the same experimental observations by pressure measurements as did Schiller 1921. He, however, specially pointed out that the disturbances exhibited a very intermittent character, before a permanent rise in the flow resistance was brought about by further increasing the velocity.

In a later paper Schiller 1924 concluded that even at very small levels of entrance disturbance, transition should occur spontaneously at Reynolds numbers which, at least asymptotically, tend to the value $R_k = 2320$, provided only that a long enough distance of accumulation is allowed for.

Schiller's experimental observations of the spontaneous onset of turbulence in tube flow are currently explained in terms of the theory of instability of small oscillations as developed by Tollmien 1929 and the problem is often supposed to have been principally solved by T. Tatsumi 1952 who, using the Tollmien method, obtained a lowest possible critical Reynolds number of $R_k \approx 9700$.

The course of the breakdown of laminar flow due to the Tollmien theory as solved by Tatsumi can be roughly described in the following manner; Laminar flow entering the tube inlet possesses a more or less plane velocity profile. During the passage through the tube the velocity distribution gradually changes to the parabolic profile. (This development was calculated by J. Boussinesq in a series of papers 1890–91 and later by Schiller 1922.) It is assumed that the entrance flow must be highly disturbed by oscillations of a wide spectrum of frequencies. At lower Reynolds numbers the velocity profiles as developed along the tube are stable to most of the disturbances. Those disturbances fade away sooner or later depending on their original intensity. However, certain velocity profiles as developed along the entrance length might be unstable to oscillations of one or another frequency. These disturbances increase their amplitude as they proceed along the tube and finally, after a least necessary distance of accumulation, they cause breakdown of the predominantly steady flow. The smallest R at which the flow might possibly become unstable owing to the presence of disturbances of some frequency, is considered to correspond to the critical Reynolds number $R = R_k$. The necessary distance of accumulation is dependent on the original amplitude of the disturbances (Germ. Anfachungsgrösse) which induce the transition to turbulence.

It is interesting to note the difference between the above explanation of the transition process and Reynolds' ideas about the same matter. He writes (Reynolds 1883, p. 78):

"..., it became clear to me that, if in a tube of sufficient length the water were at first admitted in a high state of disturbance, then as the water proceeded along the tube, the disturbance would settle down into a steady condition, which condition would be one of eddies or steady motion, according to whether the velocity was above or below what may be called the real critical value."

On p. 64 in the same paper Reynolds concludes that his experiments have confirmed the assumption quoted above.

Reynolds also worked with low levels of entrance disturbance and reached quite high Reynolds numbers without transition to turbulence. He studied the onset of turbulence in 1.5 m long cylindrical glass tubes of diameters 3.68, 1.53 and 0.79 cm fitted with smooth trumpet mouthpieces. Those experiments were performed by the colour-band method which was introduced by Reynolds. (Coloured liquid is injected a short distance in front of the tube entrance through a thin tubular probe placed parallel to the test tube along its axis of symmetry. A colour filament is thus formed and extends down the tube in a straight line as long as the flow is laminar.)

Valfrid W. Ekman in 1911 repeated Reynolds' experiments with low entrance disturbances, using Reynolds' original apparatus and reached $R \approx 54000$ without transition to turbulence.

So far Reynolds' observations as well as those of Ekman do not exclude a possible course of the transition process as associated with the Tollmien instability theory. However, in the colour-band experiments Reynolds observed the peculiar phenomenon of transition which he described as turbulent flashes and which is not consistent with previously accepted ideas of the transition mechanism. Consequently these observations have been quite neglected until recently. In S. Goldstein, *Modern Developments in Fluid Dynamics* (1938 Vol. I pp. 324–5) all that appears is the statement:

"In the neighbourhood of the critical Reynolds number, Schiller and Naumann observed (as did Reynolds) that the laminar flow was occasionally interrupted for a short distance by a vigorous eddying motion. Reynolds called such regions of turbulence 'flashes', but no explanation of them has yet been given."

We quote Reynolds' own words also in this matter (Reynolds 1883, pp. 76–7):

"Another phenomenon very marked in the smaller tubes, was the intermittent character of the disturbance. The disturbance would suddenly come on through a certain length of the tube and pass away and then come again, giving the appearance of flashes, and these flashes would often commence successively at one point in the pipe. The appearance when the flashes succeeded each other rapidly was as shown in Fig. 16.

"This condition of flashing was quite as marked when the water in the tank was very steady, as when somewhat disturbed."

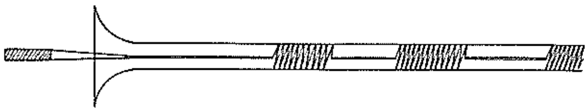

Fig. 0.1. The appearance of turbulent flashes in flow of water through a cylindrical glass tube according to Osborne Reynolds (1883 Fig. 16) as visualized by means of the colour band method.

Further on he writes:

"As the velocity was further increased these flashes became more frequent until the disturbance became general.

"I did not see a way to any very crucial test as to whether the steady motion became unstable for a large disturbance before it did so for a small one; but the general impression left on my mind was that it did in some way—as though disturbances in the tank, or arising from irregularities in the tube, were necessary to the existence of a state of instability."

It is interesting to note how careful and accurate is Reynolds' experimental work in spite of the rather primitive instrumental technique of the time. Having the opportunity to work with an extensive and quite refined experimental equipment I have been able to confirm Reynolds' observations in almost every respect as did Binnie 1945, 1947, though the latter worked only with high levels of entrance disturbance.

1. Properties of certain liquid systems

In the course of numerous flow experiments it was found necessary to undertake a rather detailed investigation concerning the properties of bentonite sols used in the experiments. This was also desirable in view of several advances in Rheology which seem to be of importance in the field of pure Hydrodynamics.

The concept of viscosity

Taking account of some recent rheological developments, which in the main seem to have passed unnoticed by authors concerned with pure Hydrodynamics, it appears desirable to call attention to some aspects of the concept of viscosity.

In classical Rheology (e.g. as presented by W. Philippoff, *Viskosität der Kolloide* 1942 or J. J. Hermanns, *Flow properties of disperse systems* 1953) the liquids are commonly divided into two classes, Newtonian and non-Newtonian, the Newtonian liquids being assumed to behave in accordance with the well-known hypothesis of Isaac Newton in *Principia Mathematica* 1687 (Part II, Sect. IX)

$$\tau = \mu \frac{\mathrm{d}U}{\mathrm{d}n}, \tag{1.1}$$

where τ = shear stress per unit area in a plane containing the velocity vector $\boldsymbol{U}$, perpendicular to the flow space vector $\boldsymbol{n}$,
$\mathrm{d}U/\mathrm{d}n$ = the rate of shear,
μ = the coefficient of viscosity, considered to be a physical constant, characterizing the fluid in question independent of external influences.

Single-phase "pure" liquids such as water, mercury and alcohol have been considered Newtonian while, in general, poly-phase liquids such as gel-forming colloids have been classified as non-Newtonian, possessing structural viscosity.

In the classical meaning "structural viscosity" implies a variation of viscosity with the rate of shear (or with the strength of the shear forces) as illustrated by Fig. 1.1 (see also Philippoff 1942 p. 113). According to this representation the liquid possesses a high viscosity value μ_0 when its molecular structure is undisturbed by external forces, while the viscosity value decreases to a lower limit μ_∞ when the structure is completely broken down by external forces exceeding certain yield values. Both the μ_0 and the μ_∞ values are considered physical constants of the liquid in question. However, the classical conception of viscosity and structural viscosity presented above has proven to imply over-simplifications of the complicated processes of deformation in liquid systems. R. Metrot 1946 stated:

"La viscosité, quand on parle d'un système plastique comme une boue de forage, est une grandeur complexe et mal définie. On est obligé pour traiter scientifiquement le problème de définir d'autres grandeurs qui sont de véritables constantes physiques...."

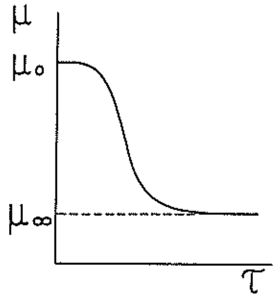

Fig. 1.1. Diagram illustrating the classical concept of structural viscosity. (μ = dynamic viscosity, τ = shear stress.)

E. R. Ballantyne 1949 in an unpublished paper has shown experimentally that the viscosity of bentonite sols depends not only on the dynamic treatment but also on the external boundary conditions of the liquid, thus confirming the Metrot statement above that neither μ_0 nor μ_∞ are physical constants.

W. J. Morris and R. Schnurmann 1951 concluded from experiments on liquid flow in tubes that increasing rates of shear would probably cause a decrease of the viscosity of any liquid.

Dealing with internal boundary conditions of clay-water systems, E. Forslind, in a series of papers 1948, 1952*a* and 1953, has advanced similar ideas concerning the concept of viscosity from the theoretic point of view. Further, Forslind and co-workers have confirmed Ballantyne's observations in extended measurements on low-concentration clay sols (unpublished work).

From the present point of view, the classical conception of viscosity as a physical constant, at its best, implies quite an approximation. The viscosity has rather to be considered a compound function of several variables which depend on the molecular properties, the dynamic conditions and on the external and internal boundary conditions as well as on the geometric dimensions of the liquid system. This state of matters seems to provide the answer to many peculiarities observed in experimental Hydrodynamics. The determination of the viscosity of water is one typical case.

The standard calibration values of the viscosity of water hitherto presented in the *Handbook of Chemistry and Physics*, are those given by Eugene C. Bingham and Richard F. Jackson 1918, obtained by means of the capillary method. These authors determined the dynamic viscosity of water at 20°C to be $1.005 \cdot 10^{-3}$ kg/ms while the new recommended calibration value given by J. F. Swindells, J. R. Coe and T. B. Godfrey 1952 is $(1.0019 \pm 0.0003)\ 10^{-3}$ kg/ms, though in the same year F. Höppler 1952 determined the value $(1.008 \pm 0.001)\ 10^{-3}$ kg/ms. Evidently the discrepancies between these viscosity values considerably exceed the formal measuring errors.

A survey of determinations of the viscosity of water at different temperatures published by Wolf Weber 1955, undesignedly gives a clear view of the discrepancies between the viscosity values due to various authors, Here, mention should also be made of the surprisingly low flow resistance values obtained by Schiller 1924 for flow of water through 60 and 120 mm cylindrical tubes, corresponding to very low apparent viscosity values.

Perhaps the discrepancies between various determinations of the viscosity of water receive a natural explanation in terms of structural viscosity. In this connection it is of interest to note that theoretical investigations by Forslind 1952*b* indicate water to be an anomalous liquid possessing pronounced structural viscosity properties.

The use of the Reynolds number in Hydrodynamics

For the present no definite limits can be given between which the viscosity of various liquid systems might vary depending on the flow conditions.

In viscous flow the rate of shear varies from zero at the point of maximum velocity, to certain maximal values close to the bounding walls, their absolute magnitude depending on the rate of flow and the geometric shape of the flow space. Thus, considering the structural properties of liquids reported in the previous section, it is in general impossible to assign a distinct viscosity value to liquid flow in bulk, which also means that the classical definition of the Reynolds number is only a rough approach to a model law for viscous flow.

However, close to the walls there seems to exist an intermediate layer in which the molecular structure of the phase-boundary is quite stable although direct wall co-ordination effects are considerably reduced. The specific structural properties of this surface zone differ from those within the bulk liquid, where, moreover, the properties vary. According to J. C. Henniker 1949 the molecular orientation of the surface zone might be observable at considerable depths. *The viscosity of the surface zone at rates of shear exceeding certain yield limits probably is independent of the geometric shape of the flow space and might provide an acceptable substitute for true relationships of viscous flow when used in defining the Reynolds number.* This the more as the rate of shear in viscous flow in practice always has its maximum value at the bounding walls, and flow experiments indicate that the transition phenomenon is intimately connected with the surface zone of the flow medium.

By using the above viscosity value of the surface zone a distinct Reynolds number might be assigned to any particular viscous flow.

It seems quite conceivable that the results of the experiments, described in the following, might be interpreted along the lines indicated in the above discussion. The validity, however, of the present definition of the Reynolds number for general comparisons of the transition processes under various flow conditions, cannot be stated *a priori* but has to be learned from experiments.

The standard calibration values of the viscosity of water due to Bingham and Jackson 1918 are obtained by the use of thin glass capillaries implying measurements of the viscosity of thin water films at high rates of shear, which at least means an approach to the desired viscosity values. Consequently the viscosity values given by Bingham and Jackson will be used throughout the present paper. Though the absolute errors cannot be estimated, it is to be noted that viscosity values obtained on thin water films under high rates of shear, by various experimenters, seem not to differ by more than 1 % relative to each other.

Characteristics of bentonite sols used in the present flow experiments

The use of bentonite sols in flow experiments is based on their "stream-double-refraction" properties which allow direct visual flow observations to be made.

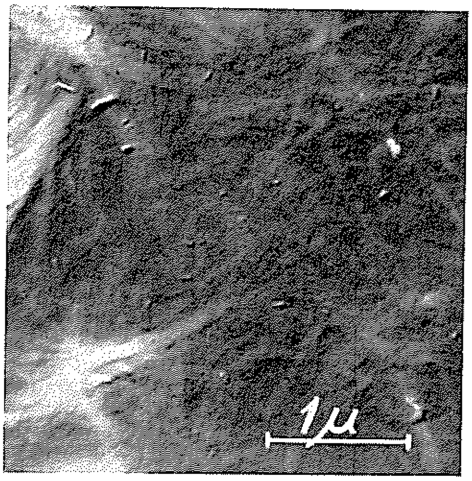

Fig. 1.2. Electron micrograph of a sample of White Hector bentonite sol, obtained by Tore Lundin, *Div. of Appl. Inorg. Chem., KTH*. The sample has been Pd-shadowed prior to the exposure. 19000 diameters magnification.

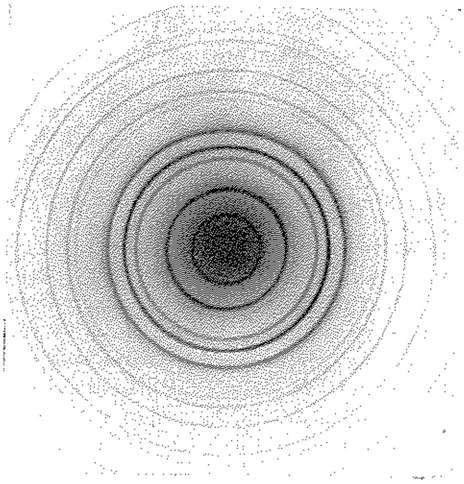

Fig. 1.3. Electron diffraction diagram of White Hector bentonite obtained by Å. Grudemo at the *Swed. Cem. and Concr. Res. Inst.*

G. Gran at the *Swedish Forest Products Research Laboratory* and R. Eklund at the *Div. of Appl. Inorg. Chem. KTH* prepared a 5 % storage suspension in aqua distillata from parts of a mineral sample of *White Hector bentonite* in accordance with recommendations given by M. B. McPherson and R. E. Nece 1950.

According to McPherson and Nece the maximum apparent particle size must not exceed 0.5 μ in order to secure satisfactory optical activity of the sols. Consequently the bentonite lump was passed several times through a colloidal mill prior to the preparation of the standard sol.

The clean opaline bentonite suspensions were very stable when stored in pyrex bottles. After use in the experimental apparatus (where the circulation pumps were made of stainless steel) for periods of about two months, the sols turned a dirty greenish colour and showed tendencies to flocculate when left undisturbed for some time. After stirring or agitating by circulation through the apparatus the flocculated material rapidly redispersed and no influence on the experimental results has been traced to these ionic effects. Allowing a three months storage time after preparation, the high optical activity of the Hectorite suspensions has shown no change due to ageing effects even after a considerable change in colour.

The presence of bentonite cannot be traced by the unaided eye when suspensions of less than 2‰ (per mille) bentonite concentration are viewed in an ordinary 15 mm test tube. On the other hand the suspensions exhibit pronounced thixotropic properties at concentrations exceeding about 15 ‰. (For a definition of thixotropy see e.g. Philippoff 1942, pp. 317, 416 or Hermanns 1953, pp. 12–38.) Above this concentration the sols of the type used exhibit a permanent double refraction which gradually develops with progressing gelation. This double refraction seems to be less distinct than the stream double refraction but is nevertheless clearly visible.

The photograph of Fig. 1.2 of 19000 diameters magnification shows that the

Table1.1. Density values of bentonite sols used for computing kinematic viscosity values.

t °C	14	16	18	20	22	24
γ ‰	ϱ kg/m³					
0	999	999	999	998	998	997
0.8	999	999	999	998	998	997
1.0	1000	1000	999	999	998	998
1.3	1001	1000	1000	999	999	998
1.7	1001	1001	1000	1000	999	999
2.0	1002	1001	1001	1000	1000	999
2.5	1003	1002	1001	1001	1000	1000
5.0	1004	1003	1003	1002	1001	1000
10.0	1006	1005	1005	1004	1003	1002
20	1008	1007	1007	1006	1005	1004

sols must be polydisperse, the maximum particle size being about $2 \cdot 10^{-3} \times 10^{-4}$ mm² with an estimated thickness of about 10^{-5} mm (personal communication by Docent Forslind, *Div. of Phys. Chem. KTH*). The electron diffraction diagram of Fig. 1.3 is shown for purposes of identification and check on the purity of the bentonite used.

The density of the bentonite suspensions

Density values ϱ of the bentonite sols of various concentration γ have been determined at different temperatures t by means of a "precision" areometer designed for the measuring range 950–1015 kg/m³ at 15°C with a reading accuracy of ± 1 kg/m³. A simple calculation shows that the thermal volume expansion of the glass areometer should not cause any observable measuring error within the temperature interval involved and accordingly does not need to be corrected for.

The areometer was calibrated by repeated measurements of the density of distilled water at various temperatures within the interval 15–25°C, prior to the measurements of the density of the various bentonite sols.

Table 1.1 contains the density values obtained for the various suspensions as well as the calibration values of pure water. The formal accuracy of the measured values certainly is kept within ± 3 kg/m³ which means an error of about 0.3 %.

Primary viscosity measurements

Viscosity measurements of various bentonite sols have been performed on several occasions by means of an ordinary Höppler precision viscometer, the first reproducible measurements being accomplished at the *Centr. Res. Lab. of the Swedish Paint and Varnish Ind., KTH*, by courtesy of Börje Andersson, though in too short a series of measurements. Almost a year later A. Ramgard, who assisted in flow experiments for a long period, obtained several series of reproducible measurements which have been reproduced and completed by myself after a further period of almost one year.

The thermostat used in connection with the viscometer kept temperatures above room temperature (about 18°C) constant within ± 0.01–0.02°C, and around the temperature 17°C (cooling with ice) the variations were about ± 0.02–0.03°C which increased in some cases to a maximum of about ± 0.06°C when the temperature was as low as 15°C.

The experiences with the Höppler viscometer showed the necessity of closely following the instructions given by the instrument manufacturer. The test tube as well as the measuring glass ball were thoroughly cleaned with a brush and a mixture of ethyl-acetate and ether plus 5 % ammonia, and afterwards rinsed in distilled water. Neither air nor the hands of the operator were allowed to touch any wetted surface of the apparatus. Also following given instructions, every liquid sample to be measured was heated to a temperature of 35–40°C before it was carefully introduced into the test tube. This procedure prevented any formation of air bubbles during the measurements.

Mr. Ramgard introduced an extra arrangement by which troublesome irregularities of the measurements were suppressed to some extent. Besides the measuring glass ball, two extra balls (one small glass ball and one big steel ball belonging to the viscometer set and intended as measuring balls for other ranges of viscosity) were introduced into the test tube in such succession that, when the apparatus was put in measuring position, the small glass ball was forced by the steel ball to move downwards quite fast, developing strong oscillations, causing intensive turbulent motion of the fluid along the walls as it passed by. The measuring ball followed at much slower speed behind the two "stirring balls", which were chosen so that they came to rest on the bottom of the test tube well before the measuring ball entered the measuring distance.

The dynamic viscosity μ measured by means of the Höppler viscometer is evaluated according to the formula

$$\mu = C(\varrho_b - \varrho)\,T, \tag{1.2}$$

where C is a calibration constant, ϱ_b is the density of the measuring ball and ϱ is the density of the test liquid. T is the measured time for the ball to pass the measuring length.

In the temperature interval $15 \leq t \leq 25$°C, ϱ_b is determined to be constant at 2461 kg/m^3 correct to the fourth digit and the calibration constant C is to be determined.

In Table 1.2 are given the mean values T of 6–10 measurements at each temperature value t. Also is given the maximal observed deviation $\pm \Delta T/T = (T_{\max} - T_{\min})/2\,T$ in each sequence of measurements. The calibration values of the dynamic viscosity μ are those according to Bingham and Jackson 1918 and the density values ϱ are taken from Table 1.1.

From Table 1.2 is obtained the mean value of the calibration constant $C = 8.087 \cdot 10^{-9}$ m^2/s^2 with a mean square error of $\pm 0.009 \cdot 10^{-9}$ m^2/s^2.

The scale of the thermometer belonging to the viscometer is divided in 1/10°C and the temperature can be estimated with an accuracy of ± 0.01°C. Comparison with a standard thermometer calibrated at *Deutsche Reichsanstalt* (the accuracy given to be ± 0.01°C) has shown that the instrument thermometer indicated 0.03°C too low values at 15°C, the error increasing monotonically to 0.07°C too low values at 25°C. The t values given in Table 1.2 are corrected with respect to this error. The maximum systematic error in C due to the inaccuracy of the temperature readings can be estimated not to exceed 0.5 % which error should be added to the formal statistical error of C given above.

Table 1.2. Determination of the calibration constant C of an ordinary Höppler precision viscometer.

The C values determined from Mr. Ramgard's measurements are slightly lower than those obtained by the author. This might be due to the fact that Ramgard did not use the special cleaning liquid mentioned on p. 14 but merely rinsed the test tube with aqua distillata.

t °C	T s	$\pm \Delta T/T$ %	ϱ kg/m³	$\mu \cdot 10^3$ kg/ms	$C \cdot 10^9$ m²/s²	Evaluated from measurements performed by
17.44	90.40	0.2	999	1.071	8.105	Ramgard
21.17	82.59	0.2	998	0.978	8.093	
25.07	75.94	0.3	997	0.893	8.033	
17.36	90.57	0.3	999	1.073	8.105	
19.45	86.33	0.1	998	1.019	8.066	
21.33	82.52	0.2	998	0.973	8.059	
16.35	93.00	0.2	999	1.101	8.098	Lindgren
20.45	83.74	0.3	998	0.994	8.113	
24.95	75.55	0.3	997	0.895	8.094	

The chronometer (stop watch) is read with an accuracy of ± 0.05 s and has been controlled by a series of comparisons with the official standard time. In each case, without exception, the chronometer indicated constant reading very close to 0.1 % too short time, even over extended periods of time. This systematic error, as well as a possible error in the standard time, does not need to be corrected for, since the same chronometer is used, also in the viscosity measurements of the bentonite sols.

The value obtained for the calibration constant, $C = (8.09 \pm 0.02)\ 10^{-9}$ m²/s², differs from the value given by the manufacturer $C = (8.03 \pm 0.04)\ 10^{-9}$ m²/s², the difference being traced to the presence of the two extra "strirring balls" in the viscometer during the present calibration measurements. It was shown that the fall time of the measuring ball as well as the random irregularities of the measurements increased when the "stirring balls" were removed from the test tube.

Using the same instrument components, the measuring process of the calibration measurements has been applied also in determining the viscosity values of the bentonite sols at various temperatures.

Table 1.3 contains the results, evaluated by means of formula (1.2) in which the calibration constant C has the value $(8.09 \pm 0.02)\ 10^{-9}$ m²/s². The time values T are in each case the mean value of 6–12 observations. In order to give an idea of the statistical variations within each sequence of measurements the maximum deviations observed, $\pm \Delta T/T$, are also given as defined in connection with Table 1.2. The mean square error of T in any sequence of measurements does not exceed 0.1 %. The kinematic viscosity values ν in the last column of the table are calculated according to the definition

$$\nu = \frac{\mu}{\varrho}. \tag{1.3}$$

Formally, the maximum probable error of any of the ν values given in Table 1.3 is found to be about 0.8 % or say less than 1 % by logarithmic differentiation of the combined equations (1.2) and (1.3) and consideration of the estimated errors of C, T, ϱ and $\varrho_b - \varrho$.

Table 1.3. Viscosity values of White Hector bentonite sols determined by means of an ordinary Höppler precision viscometer.

Diameter of the test tube, 15.88 mm.

γ ‰	t °C	T s	$\pm \Delta T/T$ %	$\mu \cdot 10^3$ kg/ms	ϱ kg/m³	$\nu \cdot 10^6$ m²/s	Calculated from measurements performed by
0.40	15.36	99.78	0.2	1.181	999	1.181	Ramgard
	17.24	95.68	0.3	1.132	999	1.132	
	19.33	90.63	0.2	1.072	998	1.074	
	21.31	85.98	0.1	1.017	998	1.019	
0.68	17.44	96.92	0.5	1.147	999	1.147	
	20.25	90.54	0.3	1.071	998	1.073	
	21.16	87.95	0.5	1.041	998	1.043	
	25.08	80.53	0.2	0.953	997	0.957	
1.02	15.59	105.60	0.2	1.249	1000	1.247	
	17.46	100.60	0.1	1.190	999	1.190	
	19.53	95.48	0.2	1.130	999	1.130	
	21.29	91.42	0.2	1.082	998	1.084	
1.33	15.24	109.20	0.2	1.292	1000	1.290	
	17.48	103.10	0.2	1.220	1000	1.218	
	19.69	97.63	0.2	1.155	999	1.155	
	21.97	92.42	0.3	1.093	999	1.093	
1.94	17.36	111.33	0.1	1.317	1001	1.313	
	19.45	105.45	0.1	1.248	1000	1.246	
	21.31	101.02	0.1	1.195	1000	1.193	
	23.49	95.50	0.2	1.130	999	1.130	
3.86	15.73	145.01	0.3	1.716	1003	1.705	Lindgren
	17.94	135.86	0.3	1.607	1002	1.600	
	20.23	128.14	0.2	1.516	1001	1.511	
	22.56	120.80	0.7	1.429	1000	1.427	
	24.94	113.80	1.2	1.346	1000	1.344	
7.72	16.53	247.62	0.1	2.930	1004	2.906	
	18.14	236.33	0.1	2.796	1004	2.774	
	20.20	224.27	0.0	2.653	1003	2.636	
	22.54	212.13	0.4	2.510	1002	2.498	
	25.10	199.70	0.2	2.363	1001	2.356	

The values of the bentonite concentration γ have been obtained by means of an ordinary analysis balance of ± 0.2 mg accuracy. The same balance has been used throughout the measurements except for some controls of the reproducibility. The Pt-container, used in the quantitative analysis of the bentonite concentration of the sols, was first thoroughly cleaned and rinsed in distilled water, dried in a heating box at 110°C and left to cool in a siccator with silica gel. It was then weighed on the balance and the sample of the bentonite sol poured into the container to be immediately weighed. Without touching the container by hand it was afterwards exposed to an infra-red radiator and a smooth current of air. The air was led through a battery of active carbon, cotton and silica gel before reaching the liquid surface.

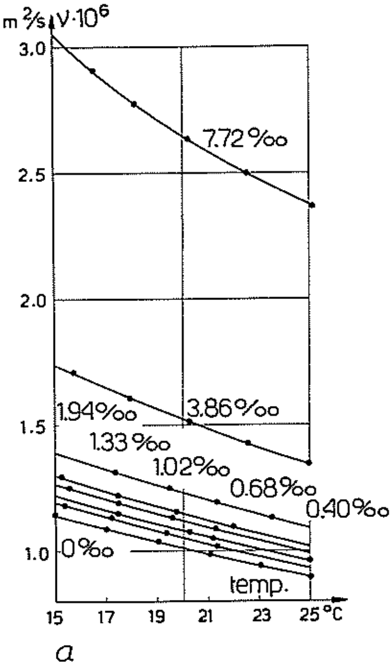

Fig. 1.4*a*. Relations between viscosity ν and temperature t of bentonite sols of various concentrations γ obtained by means of an ordinary Höppler precision viscometer.

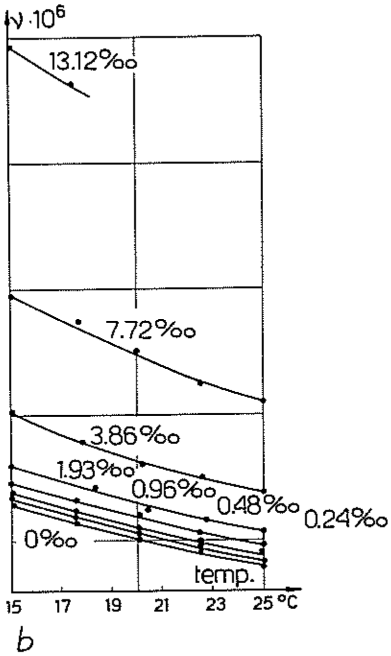

Fig. 1.4.*b*. Relations between viscosity ν and temperature t of bentonite sols of various concentrations γ obtained by means of a Höppler Rheo-Viskometer.

After completely drying the sample, the container again was put into the siccator to cool after which the final weighing was carried out.

A simple error calculation gives an accuracy of the determined concentrations of better than 1 %. Repeated measurements of some of the sols on two different balances likewise indicated a reproducibility within 1 %.

The results of the primary viscosity measurements as given in Table 1.3 are illustrated in the diagram Fig. 1.4*a* showing the relation between the kinematic viscosity ν and the temperature t for bentonite sols of various concentrations γ. This diagram has been transformed in Fig. 1.6*a* to show the relationship between $\log \nu$ and γ at three selected temperatures. Below 3 ‰ concentration, rectilinear relations seem to exist between $\log \nu$ and γ but at higher γ the $\log \nu$ values deviate from the straight lines towards higher viscosity values.

The present viscosity measurements by means of the Höppler viscometer are performed on quite thin liquid layers as the measuring glass ball fits very closely in the test tube, the diameter difference being less than 0.01 mm (tube diameter $\approx$ 15.88 mm). However, the light glass ball cannot be expected to cause high enough shear rates so as to obtain the desired yield viscosity values. Even when rather diluted, the bentonite sols possess a rigid structure, the "rigidity" increasing progressively with increasing concentration which might explain the shape of the curves in Fig. 1.6*a*.

The assumptions above are supported also when considering the ν values obtained at 18°C by the *Paint and Varnish Lab.* (marked with open circles in Fig. 1.6*a*). At lower concentrations there is an acceptable agreement between the different viscosity determinations but at 5 ‰ concentration the *Paint and Varnish Lab.* has obtained a value situated considerably below the straight line in question. This deviation is explained by the replacement of the measuring glass ball by a steel ball of smaller diameter (15.50 mm), which considerably increases the rate of shear as well as the thickness of the liquid layer measured.

Final viscosity measurements

In order to obtain the desired viscosity values of thin layers of bentonite sols at high enough rates of shear the viscosity measurements were further carried on by means of a *Höppler Rheo-Viskometer.*

The Rheo-Viskometer consists of a vertical test tube of about 16 mm diameter in which a ball (both made of glass) fastened to a rod, is forced to travel measuring distances of 2 to 30 mm at various speeds (also here the measuring glass ball fits very closely in the test tube). The rod is linked to one end of a balance arm by a ball bearing. This arm is to be loaded with different weights and is also equipped with a decimal unit for compensating the density of the test liquids. The balance arm is supported by a ball bearing and is balanced by a weight at its other end. The measuring distance travelled is continuously indicated by an indicator clock connected to a pin on the balance arm at a short distance from the main bearing. The test tube and a precision thermometer are inserted in a metal housing, designed for connection to a thermostat. (An older variant of the Rheo-Viskometer is described by Philippoff 1942 (pp. 91–2). See also Höppler 1952.)

It should be noted that the working principle of the measuring ball in this viscometer is not quite the same as in the ordinary Höppler viscometer where the ball *rolls* down the steeply inclined test tube. It is furthermore to be mentioned that the weak point of the Rheo-Viskometer seems to be the main ball bearing. Even with careful handling of the apparatus the friction in this bearing might cause troublesome random disturbances of the measurements.

The formula valid for this type of viscometer is given to be

$$\mu = CPT, \tag{1.4}$$

where C = calibration constant
P = load per unit area of the cross-section of the test tube
T = measured time for the glass ball to travel a certain distance.

The thermometer belonging to the instrument has shown no deviation from the standard thermometer within the temperature interval of interest as far as could be observed by the reading accuracy ± 0.01°C. The same chronometer, used before, was employed both for calibration measurements and for viscosity determinations.

The results of the calibration measurements are reported in Table 1.4.

Every T in the table represents the mean value of 10–12 observations. The weights determining the P values have been controlled with an analysis balance and found to agree within 0.05 % accuracy. The weights determining the 25 and 50 kg/m^2 loads do not belong to the original apparatus but were added after some preliminary tests. The other symbols used are defined in connection with Table 1.2.

For loadings below $P = 200$ kg/m^2 the mean values C increase with increasing P

Table 1.4. Determination of the calibration constant C of a Höppler Rheo-Viskometer.

Diameter of the test tube, about 16 mm.

P kg/m^2	t °C	T s	$\pm \Delta T/T$ %	$\mu \cdot 10^3$ kg/ms	$C \cdot 10^7$ m/s^2	$C \cdot 10^7$ m/s^2	$\Delta C \cdot 10^7$ m/s^2
	15.06	61.85	1.1	1.138	7.360		
	17.54	58.64	1.9	1.069	7.292		
	17.55	58.49	2.2	1.069	7.314		
	20.08	53.59	1.3	1.003	7.488		
	22.42	51.82	1.0	0.949	7.328		
	24.92	50.28	1.6	0.896	7.128		
25.00	19.90	57.50	3.1	1.008	7.012	7.236	+0.252 −0.224
	20.10	55.44	1.5	1.003	7.236		
	15.07	63.59	0.9	1.138	7.160		
	17.54	59.08	1.7	1.069	7.236		
	20.05	55.99	2.0	1.004	7.172		
	22.50	52.81	0.9	0.947	7.172		
	24.94	49.91	1.0	0.895	7.172		
	15.09	31.05	1.3	1.137	7.322		
	17.54	29.07	1.0	1.069	7.354		
	20.08	26.96	0.7	1.003	7.440		
	22.42	25.75	0.4	0.949	7.370		
	24.92	24.64	0.8	0.896	7.272		
	19.90	28.06	0.7	1.008	7.184		
50.00	20.10	27.41	1.1	1.003	7.318	7.296	+0.144 −0.112
	15.08	31.45	1.3	1.138	7.238		
	17.53	29.64	1.3	1.069	7.214		
	17.55	29.02	0.3	1.069	7.368		
	20.05	27.80	0.7	1.004	7.224		
	22.50	25.99	0.8	0.947	7.288		
	24.95	24.67	2.0	0.895	7.256		
	15.07	15.60	1.0	1.138	7.295		
	17.54	14.57	0.7	1.069	7.337		
	20.08	13.58	0.7	1.003	7.386		
	22.42	12.95	0.8	0.949	7.328		
	24.92	12.21	0.8	0.896	7.338		
	19.90	13.83	1.1	1.008	7.289		
100.0	20.10	13.69	0.7	1.003	7.327	7.322	+0.064 −0.037
	20.10	13.64	1.1	1.003	7.353		
	15.03	15.49	0.6	1.139	7.356		
	17.54	14.65	0.7	1.069	7.299		
	20.05	13.77	0.7	1.004	7.294		
	22.50	12.97	1.2	0.947	7.301		
	24.93	12.30	1.6	0.896	7.285		
	15.12	7.795	1.9	1.136	7.285		
	15.04	7.850	1.9	1.139	7.255		
	17.53	7.440	1.1	1.069	7.185		
	20.08	7.055	1.1	1.003	7.110		
	22.42	6.630	0.8	0.949	7.155		
	24.92	6.780	1.5	0.896	6.608		
200.0	19.90	7.010	0.7	1.008	7.190	7.128	+0.157 −0.420
	20.10	6.940	1.4	1.003	7.225		
	15.18	7.825	1.7	1.135	7.250		
	15.10	7.805	1.3	1.137	7.285		
	17.54	7.420	1.1	1.069	7.205		
	20.05	7.000	1.4	1.004	7.170		
	22.50	6.820	2.2	0.947	6.945		
	24.93	6.465	2.8	0.896	6.930		

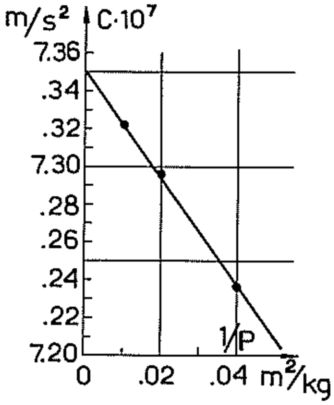

Fig. 1.5. Extrapolation of the μ_∞ value of water according to measurements with a Höppler Rheo-Viskometer.

values, simultaneous with a decrease of the observed maximum deviations ΔC from each mean value C. At $P = 200$ kg/m² there is an abrupt change to a lower value of C together with a considerable increase of the observed deviations from the mean value. This tendency is still more pronounced for $P = 300$ kg/m², which load gave $C = 5.6 \cdot 10^{-7}$ m/s².

The decrease of C obtained for the loads 200 and 300 kg/m² almost certainly is caused by the onset of turbulence. The values of C belonging to this region will not be taken account of in the following.

In Fig. 1.5 is plotted the calibration constant C versus the reciprocal of P. Extrapolation of the obtained rectilinear relationship to the ordinate axis gives $C = 7.35 \cdot 10^{-7}$ m/s² for $P \to \infty$. However, due to the uncertainty related to the alternatives of structural viscosity of the water or instrument frictions being responsible for the drift of the C values, the extrapolation process perhaps cannot be considered reliable. Instead the nearest measured value $C = 7.32 \cdot 10^{-7}$ m/s² is selected to be used as the calibration constant in the following measurements. Considering the deviations of the C values recorded in Table 1.4 as well as the extrapolation diagram Fig. 1.5, the formal error of the chosen calibration constant is estimated not to exceed $\pm 0.07 \cdot 10^{-7}$ m/s².

Knowing the calibration constant $C = (7.32 \pm 0.07)\ 10^{-7}$ m/s² the kinematic viscosity ν of the bentonite sols can be measured and evaluated by combining the formulae (1.3) and (1.4).

The viscosity measurements of the bentonite sols were performed in the same way as the calibration measurements using the same instrument components. The detailed results of the measurements are shown in the Tables 1.5*b*–*h*. Table 1.5*a* contains the viscosity values of water calculated from the calibration measurements by use of the chosen calibration constant. This is done for the purpose of comparison with the standard viscosity values of water and the viscosity values obtained for the various bentonite sols. The maximum formal error of any of the ν values given in the Tables 1.5 might be estimated not to exceed 3 %.

The test samples have all been prepared from the same parent suspension of 7.72 ‰ bentonite concentration by successive dilution to twice the volume for each subse-

Table 1.5a. Viscosity values of aqua distillata transformed from the calibration measurements of Table 1.4.

t °C	P kg/m²	T s	$\pm\Delta T/T$ %	$\mu\cdot 10^3$ kg/ms	$\mu_\infty 10^3$ kg/ms	ϱ kg/m³	$\nu\cdot 10^6$ m²/s
	300	6.42	10.1	1.410			
	200	7.82	2.6	1.145			
15.08	100	15.54	1.0	1.138	1.14	999	1.14
	50	31.25	1.8	1.144			
	25	62.72	4.8	1.148			
	300	6.28	5.6	1.379			
	200	7.43	1.3	1.088			
17.54	100	14.61	0.8	1.069	1.07	999	1.07
	50	29.24	1.9	1.070			
	25	58.74	2.3	1.075			
	300	6.13	9.8	1.346			
	200	7.00	2.4	1.025			
20.03	100	13.70	1.8	1.003	1.00	998	1.00
	50	27.56	2.5	1.009			
	25	55.63	5.2	1.018			
	300	6.11	9.2	1.342			
	200	6.75	2.2	0.988			
22.46	100	12.96	1.0	0.949	0.95	998	0.95
	50	25.87	1.4	0.947			
	25	52.31	1.8	0.957			
	300	6.18	8.4	1.357			
	200	6.47	2.7	0.947			
24.93	100	12.26	1.6	0.897	0.90	997	0.90
	50	24.66	2.0	0.903			
	25	50.09	1.4	0.917			

quent series of measurements. The sample of 13.12 ‰ (as well as a sample of 19.12 ‰) bentonite concentration has been prepared by evaporating parts of the parent suspension at 90°C. Also the 7.72 and 3.86‰ sols measured by means of the ordinary Höppler viscometer, reported in the previous section, are derived from the same parent sample.

As previously, the preparations of the test samples for the viscosity measurements in each case have included a heating of the liquid to 35–40°C, preventing the formation of air bubbles during the measurements. After cooling to room temperature the heating process to 35°C released numerous minute air bubbles in the evaporated 13.12 ‰ sample, the bubbles originating from previously microscopically dissolved (invisible)

Table 1.5b. Viscosity values of White Hector bentonite sol of concentration 0.24‰ measured by means of a Höppler Rheo-Viskometer.

t °C	P kg/m²	T s	$\pm \Delta T/T$ %	$\mu \cdot 10^3$ kg/ms	$\mu_\infty 10^3$ kg/ms	ϱ kg/m³	$\nu \cdot 10^6$ m²/s
	300	5.82	1.7	1.278			
	200	8.03	1.9	1.176			
15.08	100	16.03	1.3	1.173	1.17	999	1.17
	50	31.99	0.6	1.171			
	25	64.22	0.9	1.175			
	300	6.73	1.5	1.478			
	200	7.63	0.9	1.117			
17.55	100	15.05	1.0	1.102	1.10	999	1.10
	50	30.13	1.0	1.103			
	25	60.58	1.3	1.109			
	300	6.19	4.8	1.359			
	200	7.31	1.4	1.070			
20.04	100	14.09	0.7	1.031	1.03	998	1.03
	50	28.25	0.7	1.034			
	25	56.65	0.7	1.037			
	300	5.94	2.5	1.304			
	200	6.91	1.4	1.012			
22.47	100	13.33	0.8	0.976	0.98	998	0.98
	50	26.64	1.5	0.975			
	25	53.80	1.5	0.985			
	300	5.34	3.7	1.173			
	200	6.47	1.5	0.947			
24.99	100	12.58	0.8	0.921	0.92	997	0.92
	50	25.21	0.4	0.923			
	25	50.75	0.8	0.929			

air. The rigidity of this sol seemed to prevent the escape of the air bubbles from the liquid. The sample was therefore poured into the test tube and left over night at room temperature (≈ 18°C) in the apparatus, giving the bubbles time to disappear. The measurements the next morning were started by cooling the device to 15°C during the performance of repeated measuring cycles at very high rates of deformation (heavy loads) for the purpose of breaking the structural links of the liquid and if possible to remove any remaining air bubbles. After stationary conditions were well established, the actual measurements were performed first at 15.1°C and then at 17.5°C. However, when the temperature was raised to 20.0°C the measured T values increased noticeably together with an increasing irregularity of the values obtained.

Table 1.5c. Same as Table 1.5*b*, 0.48 ‰ bentonite sol.

t °C	P kg/m²	T s	$\pm \Delta T/T$ %	$\mu \cdot 10^3$ kg/ms	$\mu_\infty 10^3$ kg/ms	ϱ kg/m³	$\nu \cdot 10^6$ m²/s
15.07	300 200 100 50 25	5.91 8.15 16.31 32.69 65.86	1.1 1.8 0.9 0.8 2.1	1.298 1.193 1.194 1.196 1.205	1.19	999	1.19
17.53	300 200 100 50 25	5.87 7.64 15.24 30.38 62.36	8.5 1.3 1.6 0.5 1.4	1.289 1.118 1.116 1.112 1.141	1.12	999	1.12
20.04	300 200 100 50 25	6.04 7.40 14.38 29.17 60.01	3.3 1.4 1.0 1.2 2.7	1.326 1.083 1.053 1.068 1.098	1.05	998	1.05
22.43	300 200 100 50 25	5.94 6.99 13.59 27.32 55.62	5.1 1.4 2.2 0.5 0.8	1.304 1.023 0.995 1.000 1.018	1.00	998	1.00
24.90	300 200 100 50 25	5.83 6.59 13.02 26.02 52.21	6.9 1.5 1.3 0.8 0.4	1.280 0.965 0.953 0.952 0.955	0.95	997	0.95

These peculiarities I have traced to being caused by the formation of air bubbles from previously microscopically dissolved air as soon as the temperature increased over the actual equilibrium value (in this case about 18°C). Quite high T values obtained for the 13.12‰ bentonite sol at the temperatures 20.0, 22.4 and 25.0°C have been omitted from the records of Table 1.5*h* by selecting series of measurements of about 12 observations not broken by any extreme value, but even so the viscosity values obtained at these temperatures cannot be accepted.

The statements concerning the 13.12‰ sample are still more pronounced for the 19.12‰ sol, the irregularities of the measurements being judged unacceptable.

Trapped air as observed in the evaporated samples of 13.12 and 19.12 ‰ bentonite

Table 1.5d. Same as Table 1.5*b*, 0.96 ‰ bentonite sol.

t °C	P kg/m²	T s	$\pm \Delta T/T$ %	$\mu \cdot 10^3$ kg/ms	$\mu_\infty 10^3$ kg/ms	ϱ kg/m³	$\nu \cdot 10^6$ m²/s
15.00	300	6.22	3.2	1.366	1.23	1000	1.23
	200	8.45	1.8	1.237			
	100	16.80	0.6	1.230			
	50	33.84	0.6	1.238			
	25	70.20	0.8	1.285			
17.56	300	6.18	9.7	1.357	1.16	999	1.16
	200	7.94	3.2	1.162			
	100	15.88	0.8	1.162			
	50	32.19	0.6	1.178			
	25	66.20	0.8	1.211			
20.08	300	6.12	4.9	1.344	1.10	999	1.10
	200	7.69	2.6	1.126			
	100	15.05	1.0	1.102			
	50	29.97	1.0	1.097			
	25	61.65	1.3	1.128			
22.42	300	6.19	6.9	1.359	1.03	998	1.03
	200	7.22	2.8	1.057			
	100	14.11	1.2	1.033			
	50	28.17	0.4	1.031			
	25	57.48	0.9	1.052			
25.00	300	6.19	5.7	1.359	0.98	998	0.98
	200	6.95	2.2	1.017			
	100	13.39	1.1	0.980			
	50	26.78	1.1	0.980			
	25	54.56	0.7	0.998			

sols might explain observations made by E. A. Hauser and D. S. le Beau 1938. These authors observed a considerable increase of the viscosity of sols of Wyoming bentonite evaporated at 75 and 90°C when compared with the viscosity of unevaporated sols of the same quite high concentrations. The Wyoming bentonite sols used by Hauser and le Beau were polydisperse with a particle size distribution similar to that of the presently used bentonite sols.

The results of the viscosity measurements recorded in the Tables 1.5 are plotted in Fig. 1.4*b*, the diagrams obtained being transformed in Fig. 1.6*b* to show the relationship determined between $\log \nu$ and γ at three selected temperatures for comparison with the corresponding diagrams of Fig. 1.6*a*, obtained by means of the ordinary Höppler viscometer.

Table 1.5e. Same as Table 1.5*b*, 1.93 ‰ bentonite sol.

t °C	P kg/m²	T s	$\pm \Delta T/T$ %	$\mu \cdot 10^3$ kg/ms	$\mu_\infty 10^3$ kg/ms	ϱ kg/m³	$\nu \cdot 10^6$ m²/s
14.99	300 200 100 50 25	5.98 8.88 18.18 37.23 78.29	1.3 1.1 0.7 1.2 0.8	1.313 1.300 1.331 1.363 1.433	1.30	1001	1.30
18.29	300 200 100 50 25	5.70 8.29 16.75 34.46 73.33	2.6 1.2 0.6 0.7 0.8	1.252 1.214 1.226 1.261 1.342	1.21	1001	1.21
20.38	300 200 100 50 25	6.02 7.62 15.78 32.33 68.32	2.8 1.3 0.6 0.8 0.7	1.322 1.116 1.155 1.183 1.250	1.12	1000	1.12
22.67	300 200 100 50 25	5.20 7.35 14.89 30.49 63.89	4.8 0.7 1.5 1.0 0.7	1.142 1.076 1.090 1.116 1.169	1.08	1000	1.08
24.96	300 200 100 50 25	5.38 7.08 14.15 28.92 61.04	3.7 1.4 1.8 1.4 1.4	1.181 1.037 1.036 1.058 1.117	1.04	999	1.04

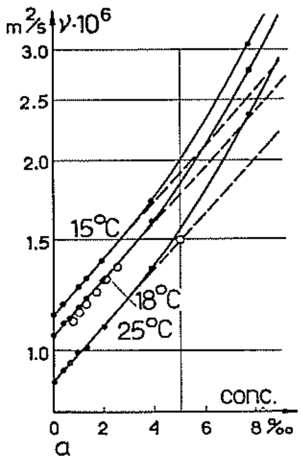

Fig. 1.6*a*. Log ν related to γ at various t as transformed from Fig. 1.4*a*.

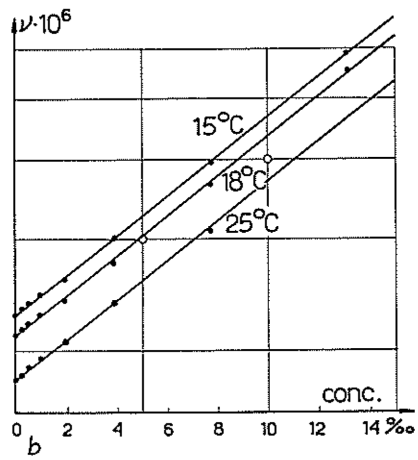

Fig. 1.6*b*. Log ν related to γ at various t as transformed from Fig. 1.4*b*.

The open circles in the diagrams indicate viscosity values at 18°C obtained with an ordinary Höppler viscometer at the *Res. Lab. of the Swed. Paint and Varnish Ind.*

Table 1.5f. Same as Table 1.5*b*, 3.86 ‰ bentonite sol.

t °C	P kg/m²	T s	$\pm\Delta T/T$ %	$\mu \cdot 10^3$ kg/ms	$\mu_\infty 10^3$ kg/ms	ϱ kg/m³	$\nu \cdot 10^6$ m²/s
15.05	300	6.94	2.5	1.524	1.52	1003	1.51
	200	10.36	1.0	1.517			
	100	21.27	0.7	1.557			
	50	44.85	1.0	1.642			
	25	92.04	1.1	1.684			
17.82	300	6.51	2.3	1.430	1.39	1002	1.39
	200	9.52	1.8	1.394			
	100	19.81	0.8	1.450			
	50	41.71	3.7	1.526			
	25	87.05	1.6	1.593			
20.20	300	6.68	3.0	1.467	1.30	1002	1.30
	200	8.89	1.1	1.301			
	100	18.16	0.8	1.329			
	50	37.86	0.5	1.386			
	25	78.93	0.7	1.444			
22.54	300	6.61	3.0	1.452	1.25	1001	1.25
	200	8.55	1.2	1.252			
	100	17.23	0.9	1.261			
	50	35.93	2.6	1.315			
	25	76.69	2.1	1.403			
25.12	300	6.48	3.9	1.423	1.18	1000	1.18
	200	8.03	1.2	1.176			
	100	16.21	0.9	1.187			
	50	33.49	0.6	1.226			
	25	70.77	1.4	1.295			

Fig. 1.6*b* exhibits rectilinear relations between $\log \nu$ and γ over all the concentration range investigated, thus differing from the relationships given by Fig. 1.6*a* in which rectilinearity is obtained only at lower concentrations, the viscosity values being higher than those of Fig. 1.6*b* even at very low concentrations γ.

The viscosity value of 5‰ bentonite sol at 18°C, obtained at the *Paint och Varnish Lab.* (marked by an open circle in the figure) by using a measuring ball of steel (diameter 15.50 mm) in the ordinary Höppler viscometer apparently seem to agree with the results obtained by using the Rheo-meter, while the viscosity value of the 10‰ sol obtained by using a still smaller steel ball (diameter 15.00 mm) deviates considerably towards lower viscosity values. These deviations indicate that the viscosity decreases

Table 1.5g. Same as Table 1.5*b*, 7.72 ‰ bentonite sol.

t °C	P kg/m²	T s	$\pm\Delta T/T$ %	$\mu\cdot 10^3$ kg/ms	$\mu_\infty 10^3$ kg/ms	ϱ kg/m³	$\nu\cdot 10^6$ m²/s
15.00	400	6.80	3.7	1.991	1.98	1004	1.97
	200	13.54	1.5	1.982			
	100	28.31	0.9	2.072			
	50	59.85	2.1	2.190			
	25	127.0	2.4	2.324			
17.67	400	6.43	1.9	1.883	1.88	1004	1.87
	200	12.90	1.7	1.889			
	100	27.25	2.0	1.995			
	50	57.56	2.1	2.107			
	25	124.3	1.6	2.275			
19.87	400	6.15	4.1	1.801	1.76	1003	1.75
	200	12.04	0.8	1.763			
	100	25.53	1.4	1.869			
	50	54.64	4.5	2.000			
	25	114.8	5.0	2.101			
22.44	400	6.71	1.9	1.965	1.62	1002	1.62
	200	11.06	1.4	1.619			
	100	23.51	1.5	1.721			
	50	45.79	0.4	1.676			
	25	110.0	3.4	2.013			
24.96	400	6.51	7.7	1.906	1.55	1001	1.55
	200	10.55	0.5	1.545			
	100	22.02	0.8	1.612			
	50	47.25	1.0	1.729			
	25	104.7	1.7	1.916			

with increasing thickness of the liquid layer which is in agreement with experiences from flow experiments.

The viscosity measurements have clearly indicated the impossiblility of assigning a distinct viscosity value to any bulk liquid. Though the formal error of the ν values given in Tables 1.5 does not exceed 3 %, nothing is known about the actual limits between which the viscosity values might vary in actual flow experiments, even when considering only the surface zone of the liquid flow. For the present, however, I can see no other possibility in evaluating the following flow experiments than by use of the relations obtained from Fig. 1.6*b*

Table 1.5h. Same as Table 1.5*b*, 13.12 ‰ bentonite sol.

t °C	P kg/m²	T s	$\pm\Delta T/T$ %	$\mu\cdot 10^3$ kg/ms	$\mu_\infty 10^3$ kg/ms	ϱ kg/m³	$\nu\cdot 10^6$ m²/s
15.08	600	6.79	4.4	2.982	2.98	1006	2.96
	400	10.85	1.6	3.177			
	200	24.16	3.0	3.537			
	100	57.55	4.9	4.213			
	50	145.3	13.2	5.318			
17.50	600	6.42	2.3	2.820	2.82	1005	2.81
	400	10.22	1.5	2.992			
	200	23.44	1.3	3.432			
	100	52.56	1.0	3.847			
	50	126.0	4.2	4.612			
20.00	600	7.19	3.5	3.158	—	1005	—
	400	10.03	1.5	2.937			
	200	22.35	0.7	3.272			
	100	50.09	1.3	3.667			
	50	120.3	5.6	4.403			
22.38	500	7.37	8.1	2.697	—	1004	—
	400	9.54	0.5	2.793			
	300	13.23	1.1	2.905			
	200	21.17	1.4	3.099			
	100	48.55	1.4	3.554			
24.97	500	7.60	22	2.782	—	1003	—
	400	8.92	1.2	2.612			
	300	12.42	0.8	2.724			
	200	19.95	1.0	2.921			
	100	46.10	7.6	3.375			

$$\log \nu(\gamma, t) = \log \nu_o(t) + k\gamma \tag{1.5}$$

or

$$\nu(\gamma, t) = \nu_o(t)\cdot 10^{k\gamma}, \tag{1.6}$$

where $\nu(\gamma, t)$ = kinematic viscosity of the bentonite sols of concentration γ at the temperature t,

$\nu_o(t)$ = kinematic viscosity of water at the same temperature t,

k = an empirical constant, its value being $k = 0.0314$ provided γ is expressed in ‰.

In the absence of a true comprehension of the variables involved in the mechanism of liquid flow the justification af the approximations and definitions presented is only to be decided from numerical evaluations of flow experiments.

SUMMARY

The conception of viscosity is discussed from the Hydrodynamic point of view taking account of recent developments in Rheology. The classical concept of viscosity of a liquid as a physical constant, is found not to be correct. Discrepancies between viscosity values of water due to various authors are reviewed and found perhaps to be explainable in terms of non-Newtonian behaviour of liquids.

Considering the transition phenomenon, a definition of the Reynolds number is proposed, consistent with the new rheological concept of viscosity.

General properties concerning certain White Hector bentonite suspensions are described and viscosity measurements have been performed by means of both an ordinary Höppler viscometer and a Höppler Rheo-Viskometer, the measurements with the Rheo-meter determining rectilinear relations between bentonite concentration and logarithmic values of the kinematic viscosity over all the concentration range investigated.

For lack of thorough knowledge of the mechanism of liquid flow, the definitions and viscosity data presented are to be adopted in evaluating the following flow experiments although it is realized that this implies an approximation of true relationships.

2. Confirmative experiments on the transition process in flow through cylindrical tubes[1]

The following experimental investigation of the change between laminar and turbulent flow of liquids in cylindrical tubes is intended as a confirmative test of observations, reported by Schiller 1921 and Binnie 1945, 1947 which do not seem to be consistent with each other. Accordingly the onset of turbulence has been studied both by measurements of the pressure drop (Schiller) and by visual observations using the stream double refraction technique (Binnie).

Experimental procedure

Bi-refringent suspensions of White Hector bentonite in distilled water have been used for the visual observations, the sols usually being of 0.8 to 10‰ concentration by weight.

The arrangement of the experimental equipment is shown in Fig. 2.1.

Three plexiglass tubes of the mean diameters 20.34 ± 0.03, 10.70 ± 0.02 and 6.55 ± 0.01 mm have been used in the experiments. The mean diameter of each tube was determined by filling the tube with known volumes of water by means of a graduated glass, alternatively with a burette. The measuring glasses were calibrated by weighing their content of various volumes of water using a chemical analysis balance. The error in the determination of the mean diameter values was found not to exceed 0.2 % corresponding to the reading accuracy of the graduated glasses which in both cases mostly appeared better than 0.1 %. However, the local diameter values along each tube were found to deviate considerably from the mean diameter value, though probably within the limits ± 4 %.

The 20 and 10 mm tubes had been processed by centrifugal casting while the 6 mm tube had been manufactured by extrusion. Fig. 2.2 exhibits the various appearances of the inner tube surfaces compared to the surface of a pyrex glass tube (of 12 mm diameter). Evidently the surface of the 6 mm tube is more rough than the surfaces of the 20 and 10 mm tubes.

The pressure drop measurements were performed only on flow in the 10 mm tube, the manometer holes situated as marked in Fig. 2.1. These holes were drilled after the completion of all other measurements. A close visual inspection along the tube, under various flow conditions, by use of the polarizing device did not give any evidence of the manometer holes disturbing the flow, provided stationary laminar flow conditions were established.

The least necessary disturbance level of the entrance flow, claimed necessary by Schiller 1921, for spontaneous onset of turbulence at the "critical" Reynolds number R_k was secured by means of a disturbance plate situated a distance of 0.5 mm from the tube mouth.

[1] Some parts preliminarily reported in: *Some aspects on the change between laminar and turbulent flow of liquids in tubes*, 1954.

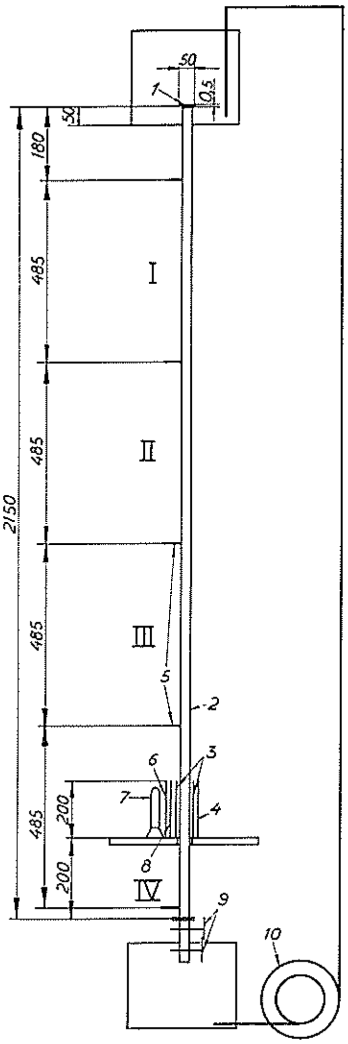

Fig. 2.1. Experimental equipment. 1 Disturbance plate; 2 Experiment tube; 3 $\frac{1}{4}$-wavelength plates; 4 Analyzer; 5 Manometer connections; 6 Opaloid glass plate; 7 Na-lamp; 8 Polarizer; 9 Cocks; 10 Pump.

In order to obtain homogenous flow conditions, the experiments in each case were performed after first agitating the suspensions by circulation through the apparatus for a while.

The flow motions have been pictured by means of cine-cameras according to arrangements shown in Fig. 2.3.

Much of the construction work of the experimental equipment and some of the first measurements have been performed by Y. Dagel as a graduation work.

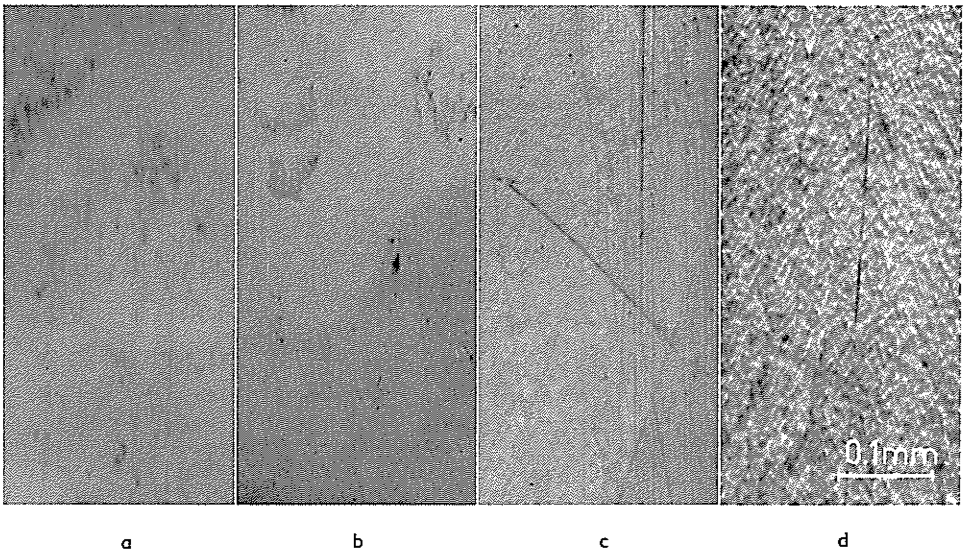

Fig. 2.2. Micrographs of the inner surfaces of the experiment tubes compared to the surface of an ordinary pyrex test tube. *a*, 12 mm pyrex test tube; *b*, 20 mm cast plexiglass tube; *c*, 10 mm cast plexiglass tube; *d*, 6 mm extruded plexiglass tube.

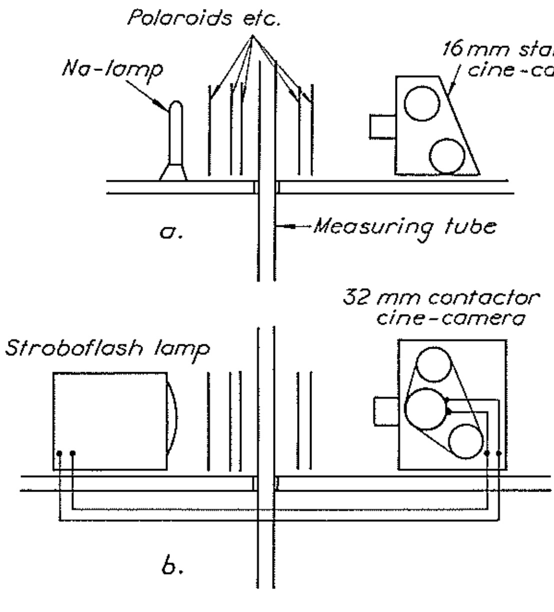

Fig. 2.3. Arrangement of the photographic equipment.

Fig. 2.4. The appearance of flow of 2.5‰ bentonite sol for various velocities in a 20.3 mm tube at about 50 diameters distance from the tube inlet. Increasing velocity from left to right. The arrow indicates the flow direction. High disturbance level of the entrance flow is secured by a disturbance plate at 0.5 mm distance in front of the tube mouth. The photographs are obtained by means of the photographic equipment shown in Fig 2.3*a*.

Qualitative observations of flow of high entrance disturbance level

Incipient laminar tube flow is observed as an illumination of the outer parts of the viewed flow field, with continuous transition to darker parts in the flow centre where the shearing forces tend to zero. As long as the flow is purely laminar, increasing flow velocity causes a gradual contraction of the dark flow area to a thin but steady black stripe in the flow centre.

It is to be emphasized that no streamlines are visualized by means of the stream double-refraction technique. The intensity of the illumination at various locations of the flow field viewed through the analyzer (crossed 90° to the polarizer) seems to be a measure of the shear stresses present in the various locations. Places of no shearing forces appear black, while increasing rates of shear cause increase of the illumination until saturation effects appear already at quite moderate rates of shear. The stream double refaction properties of White Hector bentonite sols have been investigated by Harold J. Weyland 1955.

In spite of the disturbance plate at the tube entrance, visual inspections have shown purely laminar flow even close to the tube inlet, provided Reynolds numbers of the order $R \approx 200$ were not exceeded. Above this limit there appears a region of generally disturbed flow extending some distance from the inlet and in which, now and then, is observed the whiplike formation of turbulent flashes possessing turbulent structure, quite different from the rather "soft" fluctuations of the disturbed entrance flow. Increasing Reynolds numbers cause an increase of the flash frequency and extend the disturbed flow region further downstream which, however, is visible only within rather restricted limits (around 50–70 diameters from the tube inlet). Also the intensity of the small scale turbulent fluctuations of the flashes increases with increasing Reynolds numbers. (The Reynolds number is defined on pp. 6 and 11.)

Below certain Reynolds numbers $\underline{R}$ the turbulent flashes seem to be damped and

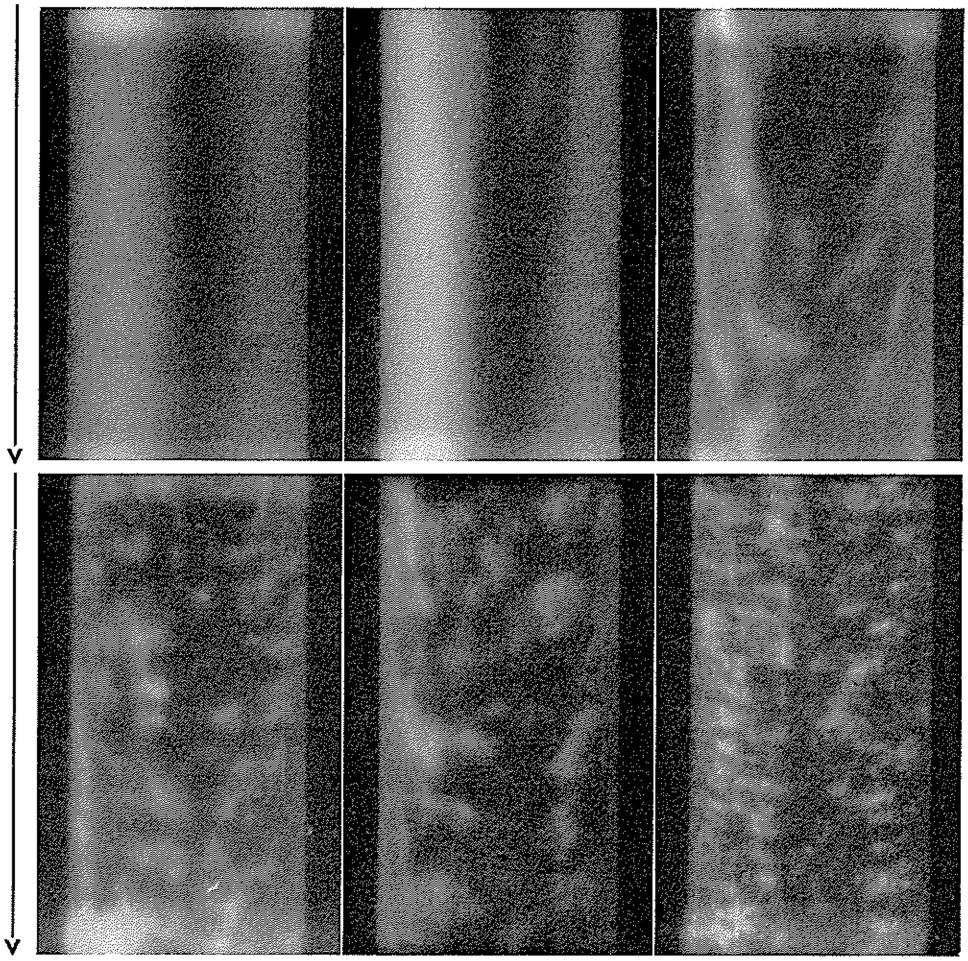

Fig. 2.5. The same flow as in Fig. 2.4 but pictured by means of the equipment shown in Fig. 2.3*b*. Increasing velocity from upper left to lower right.

disappear after travelling some distance along the tube. This lower limit $\underline{R}$ has a magnitude of the order of $\underline{R} \approx 2000$ for technically smooth tubes, below which value the flashes seem to disappear within travelling distances of about 100–130 tube diameters. Above the $\underline{R}$ value the damping effect often seems to cease and the flashes appear to become more or less self-maintaining. On further raising the Reynolds number, the flash frequency increases until the flashes overlap each other forming turbulent streaks and finally continuous turbulence (no laminar intervals) at a Reynolds number $\overline{R}$. Above this $\overline{R}$ value there appears direct transition from disturbed entry flow to continuous turbulence, the transition zone moving upstream towards the tube inlet with increasing R.

The development of the flow pattern for flow of 2.5 ‰ bentonite sol in the 20 mm

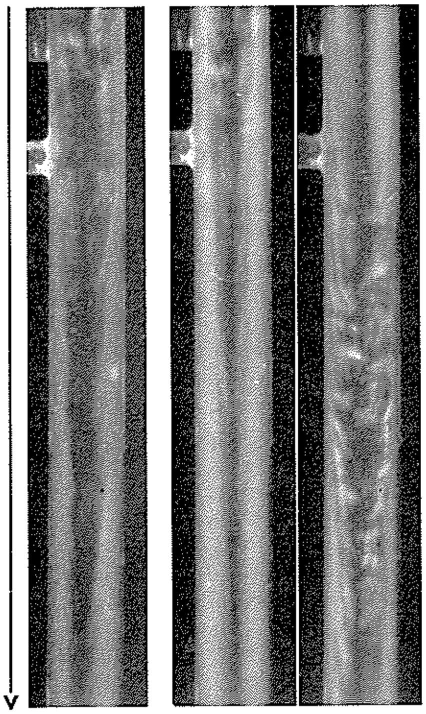

Fig. 2.6. The appearance of turbulent flashes in flow through a 10.7 mm tube at about 160 diameters distance from the tube inlet.

Picture *a* shows a rather weak turbulent flash in flow of 2.5‰ bentonite sol at a Reynolds number of $R \approx 2500$. Picture *b* shows the appearance of the fore end and the main body of two separate flashes in flow of 5.0‰ bentonite sol at about the same Reynolds number. High disturbance level of the entrance flow.

tube at about 50 diameters distance from the tube inlet is illustrated by Fig. 2.4. Disturbed entrance flow conditions have been secured by means of the disturbance plate at 0.5 mm distance in front of the tube mouth. The pictures have been obtained by using the arrangement shown in Fig. 2.3*a* while Fig. 2.5 shows corresponding pictures taken by means of a synchronized cine-camera and a strobo-flash lamp according to Fig. 2.3*b*.

Studying the flow some distance, say 150 diameters, from the tube inlet, the black line in the flow centre remains steady, giving the impression of purely laminar flow until the Reynolds number $\underline{R}$, around which value the black line is often observed to perform slow oscillatory motions, indicating a tendency to instability. Some of these oscillations can be traced as the last appearance of fading turbulent flashes, but mostly the jerky motions of the black line are due to disturbance eddies which emanate from the disturbed entry flow region, and which by themselves are almost invisible. After exceeding the $\underline{R}$ value, self-maintaining turbulent flashes appear in the otherwise laminar flow. Disturbance eddies observed at such a large distance from the tube inlet were never observed to initiate turbulent flashes but mostly, within the range of Reynolds numbers $R \approx 0$–3000, fade away completely within distances of around 200 diameters from the tube inlet.

The striking feature of the turbulent flashes is their arrow-like shape with the cusp in the flow direction as shown in Fig. 2.6. They always appeared in this shape and almost continuous turbulent flow gives an impression of being composed of discrete flashes overlapping each other.

During the performance of transition experiments with flow in the 10 mm tube (the disturbance plate still placed 0.5 mm in front of the tube mouth) an increase of the flash frequency was observed each time the circulation was started delivering test liquid into the container (through a plastic hose). Some while after turning off the pump the flash frequency retained its former lower value, indicating that the variation of flash number was due to variations of the disturbance level, set up by motions in the supply liquid.

According to Schiller 1921 there occurs a discontinuous increase of the pressure drop at a lowest possible "critical" Reynolds number, $R_k = 2320$ (the "real critical" Reynolds number), provided the disturbance plate is situated a distance not exceeding 1.2 mm from the tube inlet, which should correspond to a highest disturbance level obtainable. The qualitative observations reported here, however, show that still higher disturbance levels are possible. This means that *either there does not exist a definite R_k value or there must be a specific development of the turbulent flashes during their passage through the entry length of the tube, differing, according to whether the Reynolds number is below or above the "critical" value $R_k = 2320$.*

Also the significance of axial rotational velocities of the inlet flow with respect to the initiation of turbulence was investigated in some unpretentious tests. For this purpose cylindrical brass guide bars of 0.3 to 2.5 mm diameter were mounted between the disturbance plate and the tube mouth and directed tangential to the tube circumference so as to set the incoming fluid into rotational motion around the tube axis. In each case the bars also served to fix the distance of the disturbance plate from the tube inlet. No influence on the appearance of turbulent flashes in the flow was ever observed by fitting and removing these bars. No investigation was undertaken regarding the effect of such guide bars in the absence of the disturbance plate.

Qualitative observations of flow of low entrance disturbance level

When the disturbance level of the flow at the tube entrance was rather low (removal of the disturbance plate and smoothening of the tube mouth) the flashes appeared first at higher R values. Above certain Reynolds numbers the black line in the middle of the flow in most cases gradually moved to an unsymmetric position in the tube indicating an asymmetric velocity distribution as shown by picture *f* in Fig. 2.7. This asymmetry manifests itself at quite long distances from the tube inlet depending on the entrance conditions in combination with the rate of flow. A further increase of the velocity usually causes a vague oscillatory motion of the asymmetric but hirtherto straight line as demonstrated by Fig. 2.7*g*. Above this R value the oscillating line now and then is knotted up as by a whiplike motion some distance from the tube entrance, each time forming a turbulent flash.[1] Further increase in velocity

[1] This course of the transition process for low entrance disturbances is described similarly by Reynolds 1883 (see p. 8).

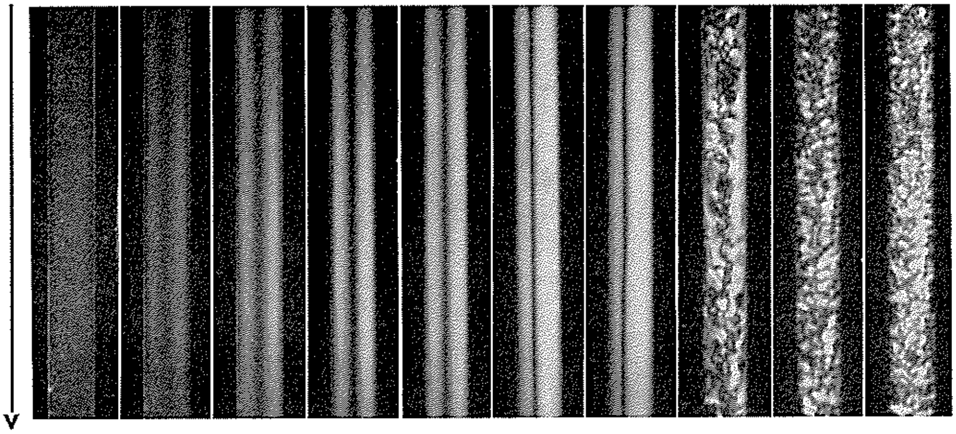

Fig. 2.7. The appearance of flow of 10‰ bentonite sol through a 10 mm glass tube at various velocities in the case of small entrance flow disturbances. The pictures are taken at a distance of about 70 diameters from the tube inlet.

causes a higher frequency of flashes until the turbulence is general. The further development of the turbulent flow with increasing velocity is illustrated by the pictures *h*, *i* and *k* in Fig. 2.7.

If we assume that the Navier-Stokes equations (See Lamb 1953 p. 577) imply proper macroscopic approximations of viscous flow, it is easy to prove that there cannot exist a stationary laminar flow of asymmetric velocity distribution as apparently exhibited by Fig. 2.7*f*.

In this connection one has to bear in mind the generalized Navier-Stokes equations as for instance defined by O. H. Faxén 1927 using tensor expressions, thus avoiding any hypothesis regarding the deformation processes. Starting from such ideas Bengt Andersson 1952 has shown formally that even though the Navier-Stokes equations are satisfied by, for instance, the experimentally confirmed parabolic velocity profile of the Poiseuille flow, this is no proof of the correctness of these equations as was pointed out already by Faxén (1927 p. 816).

However, even when considering structural properties of the flowing media, we have some reason to trust the Navier-Stokes equations provided only that the elastic effects are small compared to the viscous effects. This, of course, cannot be proved, but there exist quite a few elegant experimental verifications of theoretical predictions concerning more delicate flow problems. Among these is to be recalled the investigation of the Couette flow by G. I. Taylor 1922/23 and the experimental verification by Schubauer and Skramstad 1943 of the instability theory of the Blasius flow due to Tollmien 1929.

In 1914 Fritz Kohlrausch reported asymmetric velocity distributions for flow of air through a tube of 29.8 mm diameter as shown in Fig. 2.8, taken from Kohlrausch's paper. The length of the tube was 2.4 m and the velocity distribution is measured at a distance of 0.3 m before the outlet end. The inlet flow seems to have been moderately disturbed. The figure shows how the velocity profile gradually develops to become more and more asymmetric with increasing velocity. I take this state of

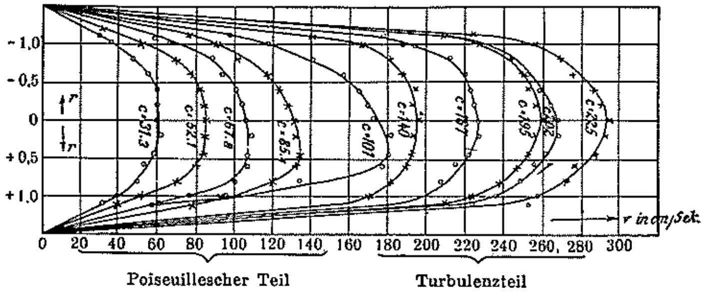

Fig. 2.8. Development of the velocity profile of flow of air through a 2.4 m long cylindrical tube of 29.8 mm diameter at a distance of 70 diameters from the inlet end according to Fritz Kohlrausch as shown in *Ann. d. Ph.* (4) 44, p. 316 (1914).

matters as a confirmation of the assumption above that the asymmetric position of the black line in Fig. 2.7*f* really implies an asymmetric velocity distribution. Presently, I cannot explain this peculiarity otherwise than as caused by the presence of vorticity, superposed on the basic laminar flow, but invisible depending on the high rates of shear by which the saturation value of the stream double refraction is exceeded. This interpretation is in agreement with experimental observations reported by Schiller 1930, 1934, A. Nauman 1931 and Hermann Kurzweg 1933, which indicate that flow contraction (laminar separation) at the tube inlet causes a successive regular formation of closed, mainly asymmetric, toroidal vortices which roll along the tube walls following the mean flow. Kurzweg (1933 pp. 198–199) even stated that: "Hinter dem Rohranlauf ist also eine Wirbelstrasse vorhanden, die sich bis zu einer gewissen Länge ins Rohr erstreckt, aber bald wieder abklingt, und mit turbulenter Rohrströmung nichts zu tun hat." It was further observed by Kurzweg that the onset of turbulence was connected with beginning irregularity of the generation of the primary vortices. In these experiments, however, the onset of turbulence was studied only within a distance of less than some few tube diameters from the tube inlet. Experimental observations reported by A. H. Gibson 1933 are also noteworthy in this connection.

Professor Gibson used the colour band method and studied the breakdown of "laminar" flow in "smooth" cylindrical glass pipes of diameters 12.7–38.1 mm. He found that the colour band indicated breakdown of the steady flow for least velocity values at certain "critical" radial positions of 0.66–0.60 r from the tube centre (r = tube radius), while higher velocities were necessary to destroy the colour band when situated on either side of the "critical" r value. This is illustrated in Fig. 2.9, taken from Gibson's article. The figure shows that the difference between the "critical" velocities at various radial positions of the colour band, diminishes with increasing distance from the tube inlet. Also was observed a general decrease of the absolute values of the "critical" velocities with increasing entry lengths until certain limits were reached. Furthermore, Gibson noted a decrease of the asymmetric position of the "critical" radial distance from the tube centre when the entry length was increased from 16 to 120 diameters, whereafter it seemed to be constant. The observations reported were valid when the entrance flow was rather undisturbed as when it was somewhat disturbed, the critical velocities being considerably lower in the latter case.

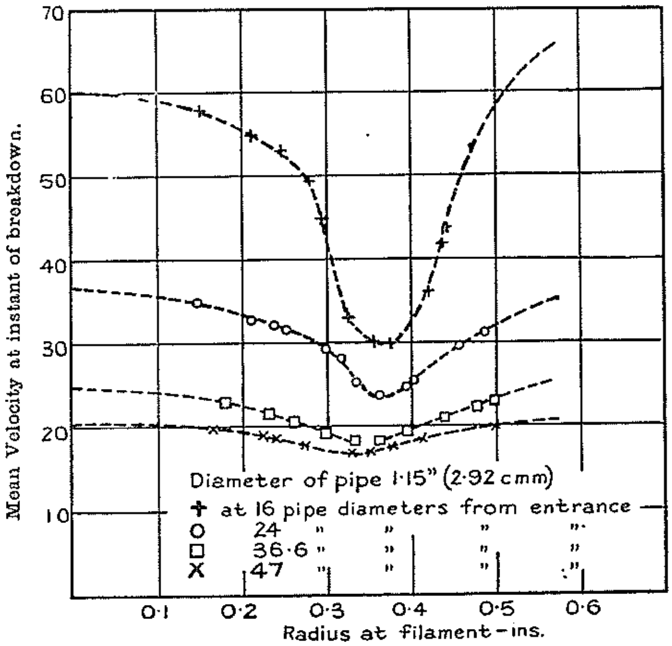

Fig. 2.9. The onset of turbulence in flow of water through a cylindrical glass pipe at various distances from the tube inlet and related to radial distances from the tube centres as observed by A. H. Gibson by means of the colour band method. The diagram is taken from the *Phil. Mag.* (7) 15:1, p. 643 (1933).

No disturbance plate was used in any of the experiments reported above nor in the following investigation carried out by means of the same apparatus used previously (shown in Fig. 2.1) equipped with the 6 mm tube; its rounded inlet end concentrically connected to a 0.1 m long piece of the 20 mm tube which formed the flow outlet of the liquid container. In these experiments, the liquid level in the supply container was allowed to drop slowly from a height of 20 cm above the bottom of the container (0.3 m above the inlet end of the 6 mm tube), filling the basin below while the circulation pump was turned off. Accordingly there was a decrease of the flow velocity during the emptying process owing to the decrease of the static pressure head. When the liquid level reached a lowest height of 4 cm above the bottom the pump was started and the surface was again raised to its 20 cm height without changing the settings of the apparatus.

During the pumping period of each flow cycle there appeared turbulence in the flow while a short time after filling the container and turning off the pump, the turbulent disturbances disappeared and undisturbed flow conditions were established. However, in spite of the decreasing flow velocity, there again appeared turbulent flashes in the flow after the liquid surface dropped to a certain level. The flashes were replaced by turbulent streaks and even continuous turbulence appeared as the liquid level dropped further. I cannot see any other explanation of this effect than that it was caused by flow contraction (laminar separation) at the tube inlet, the contraction being suppressed when the liquid level was high enough but being released when the static pressure head fell below a certain value.

Discussion of the qualitative observations

Per unit tube length, each half of the symmetric flow field (parallel to the tube axis), of undisturbed laminar flow in tubes, possesses flow circulation of the same magnitude but of opposite signs, so that the resulting flow circulation of the whole flow field becomes zero. By the action of viscosity the flow circulation develops along the entry length of the tube from certain entry values, depending on the inflow conditions, until stationary flow conditions are established. The amount of circulation is determined by the maximum value of the symmetric velocity profile. In reality, unavoidable unsymmetry of the entrance flow, random disturbances in the supply fluid and flow contraction at the tube inlet will induce extra circulation of one or both of the previously assumed symmetric parts of the flow field. According to Lord Kelvin's circulation theorem, this extra circulation can disappear only gradually by the action of viscosity. Thus, the present observations, together with those of Reynolds 1883; Ekman 1911, Kohlrausch 1914; Schiller 1921, 1930, 1934; Naumann 1931; Kurzweg 1933; Gibson 1933 and other authors indicate that the temporary preservation of the extra entry flow circulation is secured by the initiation of more or less asymmetric toroidal vortices moving with the flow by rolling along the tube walls, and extending their transverse dimensions as they pass by. This state of matters gives a natural explanation of observed unsymmetric velocity distributions and the flickering of the black line observed in the present experiments, as well as the same behaviour of colour bands observed by most of the authors cited above. Why, however, in some cases low energetic entry vortices, as it seems, spontaneously might turn into turbulent flashes of quite high order of energy transposition, is not explained by any of the experiments reported.

It is significant that the presented course of the transition process is valid for any disturbance level of the entrance flow as due to the presence of primary disturbance vortices, which in themselves are damped but which might transform into more or less self-maintaining turbulent flashes before they fade out. *Neither the present experiments nor experiments reported in the literature support some current ideas that, at least for flow of low entrance disturbance level, the transition process should imply breakdown of laminar flow, unstable to infinitesimal disturbances.*

There is a noteworthy similarity between the present observations of the transition process in tube flow and those for flow over plane surfaces reported by Emmons 1951, Schubauer and Klebanoff 1955 and others.

Quantitative observations on flow of high entrance disturbance level

In the first series of quantitative observations was determined the rate of flow $Q=\bar{Q}$ (volume V of liquid passing a cross-section of the tube during the time T) at which the laminar intervals disappeared and continuous turbulence established itself. The experiments were carried out in the apparatus of Fig. 2.1, the disturbance plate situated 0.5 mm in front of the tube mouths.

The results obtained are recorded in Table 2.1 in which are given the $\bar{Q}$ values for flow of bentonite suspensions of various concentrations γ through the three plexi-

Table 2.1. Determination of the Reynolds number $\bar{R}$ at which no laminar intervals could be observed in flow of bentonite sols of various concentrations through cylindrical plexiglass tubes of 20.3, 10.7 and 6.55 mm diameter. High disturbance level of the entrance flow.

$d\cdot 10^3$ m	γ ‰	temp °C	$\bar{Q}\cdot 10^6$ m³/s	$\nu\cdot 10^6$ m²/s	$\bar{R}$	$\pm\Delta\bar{R}/\bar{R}$ %	Calculated from observations performed by
20.34 ± 0.02	20	15.3	284	4.86	3660	2.3	Dagel
	10	14.8	116.4	2.36	3090	2.1	
	5.0	15.8	74.6	1.60	2920	1.6	
	3.3	16.5	64.5	1.39	2900	1.6	
	2.5	15.3	52.0	1.35	2410	2.6	
	2.0	15.8	55.9	1.29	2710	1.8	
	1.7	16.8	49.8	1.23	2540	1.0	
	1.3	15.3	52.4	1.24	2650	2.4	
10.70 ± 0.01	10	17.6	55.1	2.20	2980	3.9	Dagel and Lindgren
	5.0	17.9	36.1	1.52	2830	2.9	
	3.3	17.7	33.7	1.35	2970	5.3	
	2.5	18.0	30.2	1.27	2830	4.1	
	1.7	17.9	27.7	1.20	2750	2.3	
	1.3	18.0	26.1	1.16	2680	2.7	
	1.0	18.0	26.1	1.14	2720	3.6	
	0.8	17.9	26.7	1.12	2840	5.4	
6.55 ± 0.01	10	17.8	32.9	2.19	2920	3.6	Lindgren
	5.8	17.8	25.7	1.61	3100	4.5	
	4.4	17.5	23.0	1.47	3040	7.6	
	2.6	17.7	20.3	1.28	3080	1.0	
	2.1	18.0	18.9	1.23	2990	3.4	
	1.1	18.0	17.5	1.14	2980	5.1	

glass tubes and also the temperature t, and the ν values, calculated by means of the formula

$$\nu(\gamma, t) = \nu_0(t)\, e^{0.0314\,\gamma}$$

(where $\nu_0(t)$ = the viscosity of water at the temperature t according to Bingham and Jackson 1918) derived from measurements reported previously. The $\bar{R}$ values are calculated by use of the mean diameter values of the tubes. Each quantity given in the table represents the mean value of 4–10 observations, the $\Delta\bar{R}/\bar{R}$ quantities showing the maximum deviation observed ($\Delta\bar{R}/\bar{R} = \pm(\bar{R}_{\max} - \bar{R}_{\min})/2\bar{R}$).

The thermometer used in the experiments was read with an accuracy of ±0.1°C and comparison with a standard thermometer showed that it indicated 0.2°C too high values over all the temperature interval made use of. The V values were measured by means of a graduated glass (volume 1000 cm³) which could be read within ±5 cm³. Control weighings showed that this glass actually gave 0.5 % too high volume values.

The quantities given in Table 2.1 are corrected with respect to the systematic errors mentioned above.

Although the results reported in Table 2.1 should not be considered too significant, some interesting points can be noted.

The $\bar{R}$ values for flow through the widest tube decrease when the bentonite concentration γ decreases from high values, tending to a constant value at lower γ. On the other hand, the $\bar{R}$ values for flow through the narrowest tube seem not to depend systematically on γ. Further is to be noted a tendency to increasing $\bar{R}$ for decreasing tube diameter. Within the concentration range $1.3 - \gamma - 2.6$ ‰, where no systematic relations between γ and $\bar{R}$ can be traced, the mean values of $\bar{R}$ are 2600 (2580), 2800 (2760) and 3000 (3010) for flow through the 20, 10 and 6 mm tubes respectively. The independence of the $\bar{R}$ values with respect to γ within this concentration interval, indicates that probably the same $\bar{R}$ values should be valid for flow of pure water.

The observed tendency of decreasing $\bar{R}$ with increasing diameter d is in full agreement with experimental results reported already by Hagen 1854, as evaluated in L. Prandtl and O. Tietjens; *Hydro- und Aeromechanik* (1931 Vol. II, p. 33).

The decrease of $\bar{R}$ with increasing tube diameter might be interpreted as due to a relative increase of the disturbance level of the entrance flow. If the disturbance plate is situated at the same distance in front of the mouth of tubes of different diameters, as in the present experiments, the absolute inlet flow velocity is independent of the tube diameter for the same Reynolds number (constant temperature is presumed), while the mean flow velocity is lower in a wider tube as compared to flow through a narrower tube. This means that the entry flow velocity, relative to the tube mean flow velocity, is higher in the wider tube than in the thinner one, which also must imply a higher disturbance level for the flow in the wider tube. Alternatively, but less probably, the variation in $\bar{R}$ might be connected with the various entry lengths of the tubes, which are $90d$ for the 20 mm tube, $180d$ for the 10 mm tube and $280d$ for the 6 mm tube.

The relative constancy of the $\bar{R}$ values with respect to variations in γ might be considered an indication that the chosen method of viscosity determination reported previously allows a proper approximative estimation of the Reynolds number when studying the transition phenomenon.

Here it is desirable to correct misstatements made in a previous paper, Lindgren 1954*a*, p. 296, in which is stated: "The viscosities were measured, after vigorous shaking of the samples, both by means of an Ostwald capillary viscometer and a Hoeppler viscometer and were finally checked by the free fall of a glass ball in larger samples of the suspensions. No systematic difference between the results from the three methods of measuring the viscosities has been observed." This information, which does not cover real conditions, is due to poor control of the performance of the viscosity measurement at the time and should be left out of consideration.

Binnie 1945 observed the appearance of turbulent flashes at a Reynolds number $\underline{R} = 1970$ in flow of 0.25 ‰ benzopurpurin sol through a glass tube of 25 mm diameter after 95 diameters entry length, under highly disturbed entrance flow conditions, while continuous turbulence was established at $\bar{R} = 2900$. For flow of a suspension of 0.05 ‰ benzopurpurin through a 6 mm glass tube Binnie and Fowler 1947 observed the first flashes at $\underline{R} = 1900$ after 130 diameters entry length and continuous turbulence at $\bar{R} = 3000$.

Binnie's observations are in full agreement with the present experiments which also indicate some other deviations from generally accepted ideas due to Schiller. In order to co-ordinate Schiller's observations with those of the present experiments, simultaneous visual and pressure drop observations were performed on flow in the 10 mm tube. Distilled water and bentonite suspensions of 1.1 and 5.8 ‰ concentration

Table 2.2. Measurements of the pressure drop Δp along 0.485 m long test sections and determination of values of the apparent dynamic viscosity μ of water, transposed to the mean temperature 16.8°C, flowing through a plexiglass tube of mean diameter 10.70 mm.

The mean diameter d and the entry length l_0 of each test section are: I. d = 10.98 mm, $l_0 = 17d$; II. d = 10.83 mm, $l_0 = 52d$; III. d = 10.48 mm, $l_0 = 107d$; IV. d = 10.53 mm, $l_0 = 153d$. High disturbance level of the entrance flow is secured by means of a disturbance plate 0.5 mm in front of the tube mouth.

Temp	$V \cdot 10^6$	T	$Q \cdot 10^6$	$\nu \cdot 10^6$	R	Pressure drop Δp along the measuring sections N/m²				Apparent values of dynamic viscosity $\mu \cdot 10^3$ at 16.8 °C kg/ms			
°C	m³	s	m³/s	m²/s		I	II	III	IV	I	II	III	IV
16.3	860	50.0	17.2	1.104	1840	50	34	34	29	2.1	1.39	1.19	1.04
16.5	810	36.9	22.0	1.098	2370	80	50	60	39	2.7	1.6	1.6	1.1
16.8	870	33.7	25.8	1.090	2800	100	70	90	80	2.8	2.0	2.1	1.9
16.8	840	24.9	33.7	1.090	3660	140	140	140	130	3.1	2.9	2.5	2.4
	850	21.7	39.2		4250	190	160	190	170	3.6	2.9	3.0	2.7
	870	73.3	11.9		1290	20	15	24	20	1.23	0.90	1.3	1.04
	890	58.6	15.2		1650	30	23	29	22	1.45	1.08	1.17	0.90
	830	40.5	20.5		2220	44	37	36	29	1.58	1.28	1.07	0.88
	820	34.4	23.9		2590	60	65	80	55	1.8	1.9	2.0	1.4
	860	28.2	30.5		3310	95	100	120	100	2.3	2.3	2.4	2.0
	910	26.7	34.1		3700	130	120	160	120	2.8	2.5	2.9	2.2
	860	37.3	23.0		2500	60	60	60	40	1.9	1.9	1.6	1.1
	840	39.4	21.3		2310	50	44	44	50	1.7	1.5	1.3	1.5
	850	54.3	15.7		1700	30	24	29	24	1.40	1.09	1.13	0.95
	860	79.4	10.8		1170	16	17	20	17	1.09	1.12	1.13	0.98
	850	61.9	13.7		1490	24	20	24	20	1.29	1.04	1.07	0.91
	840	42.0	20.0		2170	44	34	44	30	1.6	1.2	1.3	0.93
	840	36.9	22.8		2470	55	60	60	44	1.8	1.9	1.6	1.2
	840	30.1	27.9		3030	80	90	100	85	2.1	2.3	2.2	1.9
	840	23.5	35.7		3880	12	—	—	—	2.5	—	—	—
	850	38.7	22.0		2390	50	51	52	44	1.7	1.7	1.4	1.2
	850	48.4	17.6		1910	31	31	35	34	1.3	1.2	1.2	1.2
16.8	850	41.2	20.6	1.090	2230	44	40	40	34	1.6	1.2	1.2	1.03

were used in the experiments. The results obtained are reported in the Tables 2.2, 2.3 and 2.4.

The measurements of the pressure drop Δp along the four test sections were performed by direct reading of open manometer tubes made of 4 mm plexiglass tubes. The diameter of the manometer borings in the test tube was 2 mm. The readings were made with the aid of a millimetre scale placed behind the manometer tubes. Preliminary tests showed that the capillary forces caused a very irregular behaviour of the manometer liquid levels. By inserting a droplet of photographic wetting agent in each of the manometer tubes this irregularity, as far as could be observed with the unaided eye, was completely eliminated. The pressure drop values could be read only by two digits depending on the small pressure differences at low velocities, and fluctuations caused by turbulence disturbances in the flow at higher velocities. The pressure differences read in mm liquid gauge have been transformed to N/m² in the tables by multiplying with the local gravitational constant $g = 9.82$ (9.818) m/s².

Table 2.3. Measurements of the pressure drop and determination of values of the apparent dynamic viscosity μ of 1.1‰ bentonite suspension, transposed to the mean temperature 17.5°C.

Experimental data are reported in connection with Table 2.2.

Temp	$V \cdot 10^6$	T	$Q \cdot 10^6$	$\nu \cdot 10^6$	R	Pressure drop Δp along the measuring sections N/m²				Apparent values of dynamic viscosity $\mu \cdot 10^3$ at 17.5 °C kg/ms			
°C	m³	s	m³/s	m²/s		I	II	III	IV	I	II	III	IV
17.3	170	90.1	1.9	1.16	190	4	4	4	4	1.5	1.5	1.3	1.3
	540	60.1	9.0		920	14	16	17	15	1.15	1.31	1.15	1.04
	495	47.5	10.4		1060	16	18	20	20	1.13	1.27	1.35	1.38
	605	35.6	17.0		1730	45	31	36	29	1.95	1.30	1.29	1.06
	715	29.2	24.5		2500	70	60	60	60	2.1	1.7	1.5	1.5
	780	29.0	26.9		2740	80	90	80	80	2.2	2.3	1.8	1.9
	745	22.7	32.8		3350	120	120	140	120	2.7	2.6	2.6	2.3
	680	17.8	38.2		3900	150	160	180	160	2.9	3.0	2.9	2.6
	820	26.5	30.9		3150	110	110	120	110	2.6	2.6	2.4	2.2
	720	25.8	27.9		2850	80	90	100	90	2.1	2.3	2.2	2.0
	680	26.6	25.6		2610	70	60	80	70	2.0	1.6	1.8	1.7
	770	31.9	24.1		2460	60	60	60	50	1.8	1.8	1.5	1.3
	755	34.7	21.8		2220	54	51	45	37	1.8	1.67	1.20	1.11
	755	36.2	20.9		2130	45	45	45	34	1.58	1.53	1.32	1.01
	750	41.3	18.2		1860	41	36	39	30	1.65	1.41	1.31	1.03
	605	58.8	10.3		1050	18	18	20	18	1.29	1.25	1.18	1.08
	505	72.1	7.0		710	11	11	14	12	1.15	1.12	1.22	1.06
	475	91.0	5.2		530	7	8	10	10	0.96	1.1	1.17	1.19
	620	66.6	9.3		950	16	15	18	16	1.26	1.14	1.19	1.07
	680	57.6	11.8		1200	21	21	22	22	1.31	1.27	1.13	1.16
	665	41.6	16.0		1630	34	29	31	29	1.57	1.29	1.18	1.13
	645	34.1	18.9		1930	41	37	38	32	1.59	1.39	1.22	1.06
	690	34.2	20.2		2060	49	39	44	34	1.79	1.37	1.33	1.05
	745	33.3	22.4		2280	50	60	50	40	1.6	1.9	1.3	1.1
	810	34.7	23.3		2380	60	60	60	50	1.9	1.9	1.6	1.3
	660	25.7	25.7		2620	90	70	90	70	2.6	1.9	2.1	1.7
	620	23.6	26.3		2680	80	80	90	80	2.2	2.4	1.8	1.9
	655	21.9	29.9		3050	90	110	110	110	2.2	2.6	2.3	2.3
	640	22.8	28.1		2870	90	100	100	90	2.4	2.6	2.2	2.0
	640	20.0	32.0		3260	100	130	130	120	2.3	2.9	2.5	2.4
	490	12.7	38.6		3940	150	170	170	160	2.9	3.1	2.9	2.6
17.3	520	14.2	36.6	1.16	3730	150	140	160	150	3.0	2.7	2.9	2.6

The values of the apparent dynamic viscosity μ given in the tables have been calculated by means of the formula

$$\mu = \frac{\pi}{128} \frac{\Delta p}{l} \frac{d^4}{Q} \tag{2.1}$$

valid for fully developed Poiseuille flow, provided μ is a constant.

Here Δp = pressure drop along the test section
l = length of the test section
d = mean tube diameter of the test section
Q = volume V flowing through a cross-section of the tube during a time interval T.

Table 2.4. Measurements of the pressure drop and determination of values of the apparent dynamic viscosity μ of 5.8 ‰ bentonite sol, transposed to the mean temperature 16.0°C.

Experimental data are given in the text to Table 2.2.

Temp	$V \cdot 10^6$	T	$Q \cdot 10^6$	$\nu \cdot 10^6$	R	Pressure drop Δp along the measuring sections N/m²				Apparent values of dynamic viscosity $\mu \cdot 10^3$ at 16.0 °C kg/ms			
°C	m³	s	m³/s	m²/s		I	II	III	IV	I	II	III	IV
15.8	445	59.2	7.5	1.70	520	15	20	23	22	1.46	1.89	1.86	1.81
	505	42.4	11.9		830	29	27	38	32	1.78	1.61	1.93	1.66
	440	59.2	7.4		520	17	18	24	21	1.68	1.72	1.96	1.76
	520	49.9	10.4		720	26	26	32	28	1.83	1.77	1.87	1.66
	425	36.7	11.6		810	28	28	37	32	1.76	1.71	1.93	1.71
	500	31.0	16.1		1120	39	45	49	41	1.77	1.98	1.84	1.58
	550	26.0	21.2		1480	60	62	64	57	2.07	2.07	1.83	1.66
	615	20.5	30.0		2090	98	88	99	77	2.39	2.07	2.00	1.59
	525	15.9	33.0		2300	103	113	101	85	2.28	2.42	1.85	1.59
	640	17.6	36.4		2530	120	130	120	100	2.4	2.5	2.0	1.7
	565	14.8	38.2		2660	130	160	140	120	2.5	3.0	2.2	2.3
15.8	630	15.8	39.9	1.70	2780	140	150	190	140	2.6	2.7	2.9	2.2
15.9	630	15.0	42.0	1.69	2940	170	190	200	190	3.0	3.2	2.9	2.8
15.9	580	14.5	40.0		2800	150	160	180	160	2.8	2.8	2.7	2.5
16.0	650	17.5	37.1		2600	140	140	140	110	2.8	2.7	2.3	1.8
16.0	640	18.1	35.4		2480	130	120	130	100	2.7	2.4	2.2	1.8
16.1	607	17.9	33.9		2370	120	110	110	90	2.6	2.3	2.0	1.6
	647	20.4	31.7		2220	100	100	104	80	2.3	2.2	2.0	1.6
	650	22.2	29.3		2050	93	93	90	76	2.33	2.26	1.87	1.61
16.1	590	24.3	24.3	1.69	1700	69	72	73	66	2.09	2.11	1.83	1.69
16.2	570	31.1	18.3	1.68	1290	48	47	56	49	1.94	1.84	1.88	1.68
	555	36.7	15.1		1060	39	38	43	41	1.91	1.80	1.75	1.74
	590	55.4	10.6		750	26	26	32	30	1.81	1.75	1.85	1.77
	560	71.0	7.9		560	18	19	24	24	1.68	1.73	1.87	1.90
16.2	600	42.7	14.1		990	35	36	40	39	1.83	1.83	1.74	1.73
16.3	550	30.4	18.1		1270	48	49	54	49	1.96	1.94	1.83	1.70
	630	30.1	20.9		1470	60	57	65	55	2.12	1.95	1.91	1.65
	675	25.6	26.4		1860	78	83	81	71	2.18	2.25	1.88	1.68
	650	21.5	30.2		2130	103	93	98	78	2.52	2.21	2.00	1.62
	640	19.1	33.5		2360	113	113	103	83	2.49	2.41	1.88	1.55
16.3	660	18.9	34.9	1.68	2460	130	120	113	93	2.7	2.5	1.99	1.67
16.4	620	16.5	37.6	1.67	2660	140	120	140	110	2.8	2.3	2.3	1.8
	660	17.2	38.4		2720	120	150	150	130	2.3	2.8	2.4	2.1
	680	17.5	38.9		2750	130	170	170	150	2.5	3.1	2.7	2.4
	600	14.7	40.8		2890	130	180	190	170	2.4	3.2	2.9	2.6
	615	14.7	41.8		2960	150	180	200	180	2.7	3.1	2.9	2.7
16.4	665	15.9	41.2	1.67	2960	170	180	210	190	3.0	3.1	3.1	2.9

The mean diameter d of each test section of the tube was determined in the same way as described previously in connection with the determination of the total mean diameter values of various tubes. The diameter values obtained are:

Test section	I	II	III	IV
Mean diameter d	10.98	10.83	10.48	10.53 ± 0.01 mm

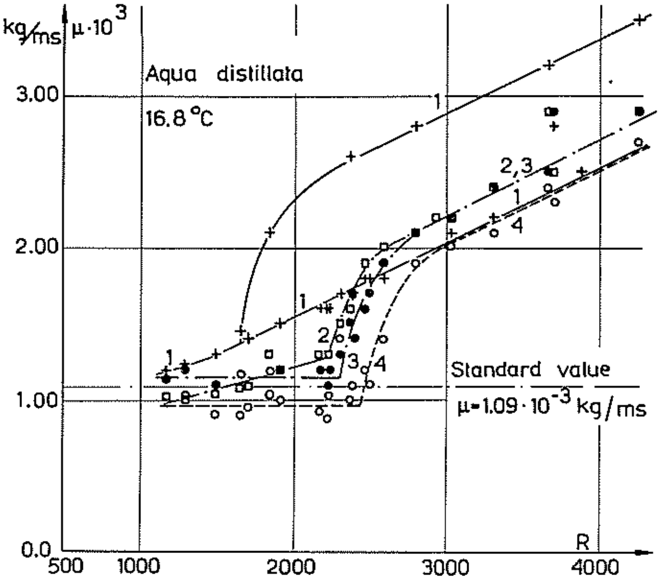

Fig. 2.10. The apparent dynamic viscosity μ of water and the onset of turbulence for flow of water in a 10.7 mm plexiglass tube obtained by means of pressure drop measurements along four test sections of 0.485 m length. Diagram 1 is determined by measurements over test section I which is preceded by an entry length of $l_0 = 17$ tube diameters d. For diagram 2, $l_0 = 52d$; for 3, $l_0 = 107d$; and for 4, $l_0 = 153d$. High disturbance level is secured for the entrance flow (see text to Fig. 2.4).

The calculated values of μ given in the Tables 2.2, 2.3 and 2.4 are quite uncertain within $\pm$ 5–10% accuracy, even relative to each other, which allows for adjustments of the obtained values within at least half the given limits of accuracy. This fact has been made use of to some extent for increasing the legibility of the diagrams Fig. 2.10; 2.11 and 2.12, illustrating the tables. Also the results of the visual observations carried on simultaneously with the pressure measurements are reported in the Figs. 2.11 and 2.12 although for practical reasons they are not given in the tables.

According to current ideas the approximately horizontal parts of the diagrams in Figs. 2.10; 2.11 and 2.12 represent laminar flow and the steep parts of the curves represent turbulent flow, while the point of "discontinuity" between the two branches of each diagram is thought to represent the "critical" Reynolds number R_k above which laminar flow spontaneously changes to turbulence, provided the disturbance level is high enough.

On comparison of the visual observations and the pressure drop measurements on test section IV for flow of the 1.1 and 5.8‰ bentonite sols as illustrated by Figs. 2.11 and 2.12 it is immediately realized that the apparent discontinuities in the pressure drop diagrams (μ diagrams) at the "critical" Reynolds number R_k, by no means imply instantaneous onset of turbulence which has been the general opinion for a long time. On the contrary, these apparent discontinuities appear somewhere in the middle of transition regions limited below by Reynolds numbers $R = \underline{R}$ at which the first turbulent flashes appear, and limited upwards by $R = \overline{R}$ where continuous turbulence establishes itself, such that $\underline{R} < R_k < \overline{R}$. The observations made, indicate

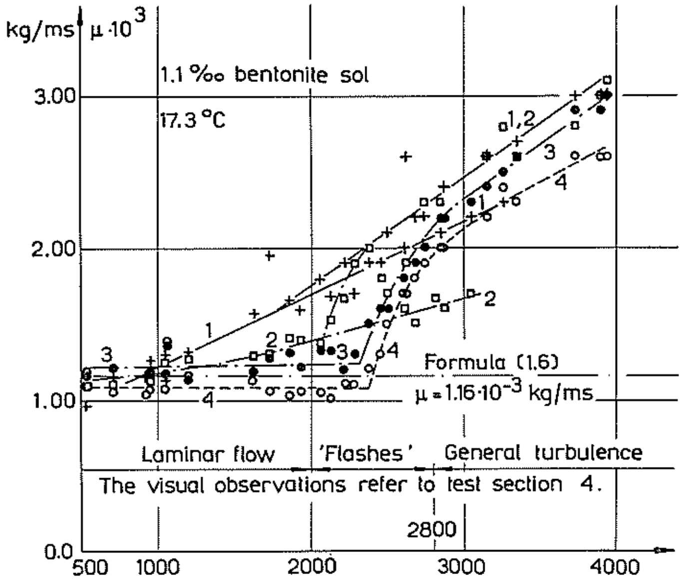

Fig. 2.11. Determination of the apparent dynamic viscosity μ and the onset of turbulence for flow of 1.1‰ bentonite sol parallel to visual observations of the transition process. (Test data given in connection with Fig. 2.10.)

that this state of matters is true also for flow of pure water and in fact for any viscous flow.

The points of discontinuity in the diagrams are not so well defined. However, it seems that they are situated at approximately the same "critical" Reynolds number R_k for flow both of pure water and of the two bentonite suspensions at test section IV with an entry length $l_o = 143d$, $R_k \approx 2400$; section III $l_o = 107d$, $R_k \approx 2300$; and section II $l_o = 52d$, $R_k \approx 2200$, while special features are attached to the curves for test section I.

There is evidently a tendency to obtain lower R_k values with decreasing entry length, provided high disturbance level of the entrance flow is secured. This tendency was also observed by Schiller (1921 pp. 440–41) but he explained it as being caused by incidental measuring errors and did not pay any attention to this peculiarity. The value $R_k \approx 2300$, obtained for test section III, is in agreement with the Schiller value $R_k = 2320$, which was obtained for flow of water through a brass tube of 8 mm diameter, its entry length being $130d$ and the measuring length about 1 m.

Depending on the development of the velocity profile in the entry length of the tube, even approximately constant μ values cannot be expected to be obtained on measurements of the laminar flow through the test sections I and II (specially section I) which also means a less abrupt change between the two curve branches. Examining the μ diagram for flow of pure water obtained for test section I (Fig. 2.10) there is to be observed not only the expected continuous transition between the disturbed inlet flow and ordinary turbulence but also an extra branch, representing some kind of high energetic flow, existing only in the entry length of the tube. Only two measuring points indicating the possible existence of such an extra branch are obtained for

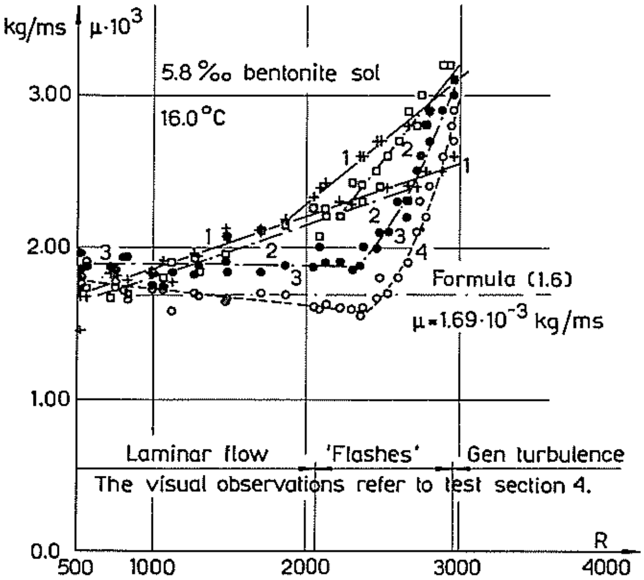

Fig. 2.12. Determination of the apparent dynamic viscosity μ and the onset of turbulence for flow of 5.8 ‰ bentonite sol parallel to visual observations of the transition process. (Test data are given in connection with Fig. 2.10.)

flow of the 1.1 ‰ bentonite suspension (Fig. 2.11) and none at all for the 5.8 ‰ sol (Fig. 2.12).

Although no definite explanation can as yet be given about the nature of the flow represented by the extra flow branch, it seems to be connected with highly disturbed entrance flow conditions. W. Sorkau 1911–15 reported observations of extra "turbulent" branches, of the above type, for flow of liquids of high fluidity such as water, alcohol, ether etc. He worked with two capillary glass tubes, 5 and 6 cm long and of about 0.4 mm diameter. The extra turbulent branches were obtained only for flow through the first capillary, which provided quite disturbed entrance flow conditions, but never in the second capillary which was carefully designed so as to avoid entrance disturbances.

The diagrams for the test sections I and II in Figs. 2.11 and 2.12 exhibit another type of extra branches for flow of the 1.1 ‰ and 5.8 ‰ bentonite sols in the turbulent region. These extra branches, situated below the branches of "normal" turbulent flow, seem to represent some kind of general disturbed flow which has not yet turned into "real" turbulence but does so before it reaches test section III. (For a further explanation of the 'extra' branches see, however, Part 6 p. 149.)

The viscosity of water as obtained for test section IV in Fig. 2.10 is about $0.96 \cdot 10^{-3}$ kg/ms which is considerably lower than the standard value $1.09 \cdot 10^{-3}$ kg/ms at 16.8°C according to Bingham and Jackson 1918. On the other hand the μ values obtained for test section III are slightly higher than the standard values. Similar statements hold also for flow of the bentonite sols with respect to μ values determined by means of the formula on p. 41. The μ values obtained from test section IV show a tendency to decrease with increasing R for flow of the 5.8 ‰ sol.

I can give no explanation of the deviations observed, even when considering structural properties of the liquids, nor do systematic measuring errors seem to be responsible for these peculiarities.

A final visual examination of the flow of 5.8 ‰ bentonite sol along the whole length of the 10 mm tube showed that the turbulent fluctuations decreased with the distance travelled. This was the case at all velocities where any change of the turbulence could possibly be observed as being limited by the relatively short length of the tube. In one typical case, fully disturbed flow entered into section I, and frequent flashes were observed in section II. Only a few flashes appeared in section III while none of the flashes was observed to reach section IV. These observations are in contradiction to those of Binnie and Fowler 1947 who did not observe damping effects of turbulent disturbances as soon as $R > \underline{R} \approx 1900$. There then remains the possibility that the quite high bentonite concentration might be the cause of the damping effect observed in the present experiments, though this is contradicted, to some extent, by the diagrams shown in Figs. 2.10, 2.11 and 2.12, which in the main indicate that the flow characteristics are rather independent of the bentonite concentration.

With the purpose of clarifying this point of discrepancy I thought it necessary to study the development of individual flashes during the tube passage by visual observations at two stations along the tube simultaneously. By this arrangement the irregularity of the appearance of the turbulent flashes was eliminated as a source of error when observing the damping effect of the fluctuations.

The experiments were performed on flow through the 6 mm tube with helpful assistance from H. Nysäter. The observing stations were situated 0.78 m (120 diameters) and 1.86 m ($282d$) downstream of the tube inlet (Stn. I and Stn. II). The counting of flashes was started simultaneously at the two stations immediately a certain well defined flash was observed at Stn. I. At not too high a flash frequency the individual flashes observed at Stn. I could easily be identified at Stn. II. In order to avoid systematic subjective errors, we now and then changed places at the observation stations. The number of turbulent flashes N_1 at Stn. I and N_2 at Stn. II were counted during time intervals τ several times under apparently unaltered flow conditions. The Reynolds number was determined in the same manner as described previously (see pp. 40–41) by use of the same instrument components.

Table 2.5 contains the results of the first series of measurements, which was performed on flow of 2.5 ‰ bentonite sol. The drift of the height of the liquid level in the supply container during the test runs caused variations of the flow velocity and is the main cause of the spreading of the R values. The observed maximum deviation of $Q = V/T$, which is about 2 %, has been adopted as the standard error in R when illustrating Table 2.5 by means of Fig. 2.13. The absolute errors of ν are unknown and have not been considered here.

The figure shows the pronounced irregularity connected with the appearance of flashes, the irregularity decreasing with increasing distance from the tube inlet. There is further to be observed a damping effect on the turbulent fluctuations, though less distinct than for flow of the 5.8 ‰ bentonite sol through the 10 mm tube. At 120 diameters distance from the tube inlet the first flashes appeared at a Reynolds number $R \approx 1850 \pm 40$ according to Fig. 2.13, while after $284d$ entry length they appeared first at $R \approx 2150 \pm 50$. At $R \approx 2460 \pm 50$ is further to be observed the damping of turbulent streaks at Stn. I to a discrete number of flashes at Stn. II.

The beginning of a series of corresponding observations on flow of 1.6 ‰ sol is

Table 2.5. Simultaneous observations of the flash frequency n at two stations along a 6.55 mm tube for flow of 2.5 ‰ bentonite sol at various Reynolds numbers R.

Stn. I (n_1) is situated at a distance of 120 tube diameters and Stn. II (n_2) at 284 diameters from the tube entrance. High disturbance level is secured by means of a disturbance plate at the tube mouth. The values $\pm\Delta n/n$ and $\pm\Delta R/R$ are calculated according to the expression $\Delta f/f = (f_{max} - f_{min})/2f_{mean}$.

N_1	N_2	τ s	$n_1 = N_1/\tau$ 1/s	$n_2 = N_2/\tau$ 1/s	$\pm\Delta n_1/n_1$ %	$\pm\Delta n_2/n_2$ %	Temp °C	$V \cdot 10^6$ m^3	T s	$Q \cdot 10^6$ m^3/s	$\nu \cdot 10^6$ m^2/s	R	$\pm\Delta R/R$ %
10	0	173	0.06	0			20.8	640	49.3	13.0			
12		169	07										
20		174	12										
9		217	04					840	64.0	13.1			
13		184	07										
16		166	10		100	—					1.18	2170	0.4
10		540	02					780	60.0	13.0			
5		158	03										
0		141	00										
16	0	173	0.09	0			20.8						
38	28	109	0.35	0.26			20.4	890	60.6	14.7			
56	27	82	0.68	0.33				720	50.8	14.2			
60	19	55	1.09	0.35									
60	33	41	1.46	0.80									
64	29	42	1.52	0.69									
62	21	32	1.94	0.66									
61	36	42	1.45	0.86	82	68					1.19	2340	1.7
52	27	75	0.69	0.36									
40	22	106	0.38	0.21									
51	35	80	0.64	0.44									
50	26	71	0.70	0.37									
50	24	67	0.75	0.36			20.4	710	49.8	14.3			
20	6	148	0.14	0.04			20.1	680	50.0	13.6			
16	3	130	12	02									
4	1	142	03	01				660	49.1	13.4			
16	2	113	14	02									
20	2	160	13	01									
7	2	199	04	01	93	75					1.20	2170	0.7
16	2	133	12	02									
18	7	179	10	04									
6	2	178	03	01									
30	2	129	0.23	0.02			20.1	680	50.2	13.6			
Almost	41	31		1.32			19.7	770	50.1	15.4			
continu-	40	27		1.48									
ous	40	30		1.33									
turbu-	40	25	—	1.60	—	10					1.21	2460	0.1
lent	31	23		1.35									
flow	27	20		1.35									
	40	28		1.43			19.8	770	50.2	15.3			
Continu-	High						19.8	810	49.8	16.3			
ous	fre-												
turbu-	quency	—	—	—	—	—					1.21	2610	0.0
lent	of turb.												
flow	flashes						19.8	810	49.8	16.3			

Table 2.5 (*continued*)

N_1	N_2	τ s	$n_1 = N_1/\tau$ 1/s	$n_2 = N_2/\tau$ 1/s	$\pm \Delta n_1/n_1$ %	$\pm \Delta n_2/n_2$ %	Temp °C	$V \cdot 10^6$ m³	T s	$Q \cdot 10^6$ m³/s	$\nu \cdot 10^6$ m²/s	R	$\pm \Delta R/R$ %
Continuous turbulent flow	Almost continuous turb. flow	—	—	—	—	—	19.8	910	50.1	18.2	1.21	2910	—
4	0	420	0.01	0				600	50.0	12.0			
14	0	362	0.04	0	65	—	19.8	590	50.1	11.8	1.21	1910	0.8
5	0	270	0.02	0				595	49.9	11.9			
60	8	54	1.11	0.15			19.8	690	49.9	13.8			
60	5	75	0.80	07									
35	2	29	1.21	07				680	50.0	13.6			
50	8	42	1.19	19	27	48					1.21	2200	0.7
50	5	35	1.43	14									
50	5	34	1.47	15									
50	4	35	1.43	0.11			19.8	685	50.0	13.7			
50	0	53	0.94	0			20.4	372	30.2	12.3			
50		49	1.02					371	30.1	12.3			
50		59	0.85					378	29.9	12.6			
50		79	0.63										
50		67	0.74		31	—		372	30.1	12.4	1.19	2020	1.2
50		67	0.74										
50		91	0.55										
50	0	77	0.65	0			20.4						
50	0	103	0.49	0			20.4	392	30.0	13.1			
40		241	17					399	31.2	12.8			
50		119	42										
50		150	33					381	30.1	12.7			
100		56	1.79					392	30.2	13.0			
100		56	1.79		100	—					1.19	2080	2.0
100		62	1.61										
100		72	1.39										
100		129	0.77					379	30.0	12.6			
50		85	0.59					388	30.0	12.9			
50		68	0.74										
10	0	115	0.09	0			20.4	382	30.2	12.7			
6	0	198	0.03	0			20.3	350	30.1	11.6			
10		50	20					357	30.1	11.9			
20		101	20										
10		65	15		78	—					1.20	1900	1.4
10		100	10										
10		107	09										
5		103	05										
10	0	206	0.05	0			20.3	348	30.1	11.6			

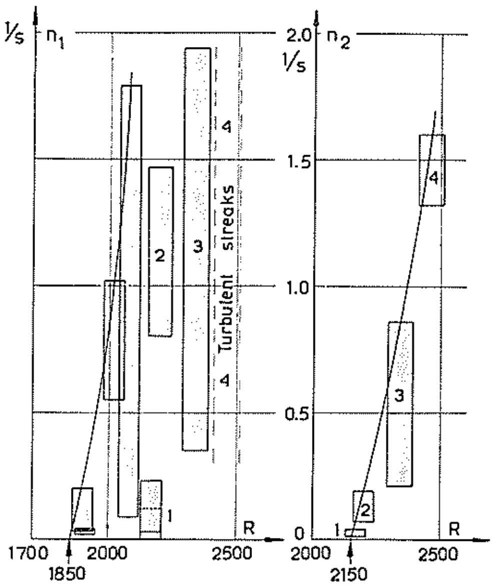

Fig. 2.13. Flash frequency n related to the Reynolds number R for highly disturbed flow of 2.5‰ bentonite suspension through a 6.55 mm plexiglass tube observed simultaneously at 120 diameters (n_1) and 284 diameters (n_2) distance from the tube inlet.

Each bar represents the region within which n was observed to vary for each corresponding R value, its accuracy given by the width of the bar. The figure clearly exhibits the very irregular nature of the mechanism that initiates the formation of flashes but also a distinct damping effect on the turbulent fluctuations.

General turbulence appears first at $R \approx 2900$ but discrete flash numbers cannot be given for Reynolds number $R > 2400$, above which value the individual flashes mostly overlapped each other, forming turbulent streaks.

reported in Table 2.6. These measurements were broken off because, above $R \approx 2180$, the damping effect ceased. In one case at $R \approx 2180$, as shown in the table, 25 flashes were observed at Stn. I while their number increased the 40 at Stn. II. This tendency became still more pronounced at higher Reynolds numbers. However, the increase of the number of flashes during the tube passage seemed to imply not creation of flashes in the flow but merely a spreading out and decomposition of longer flashes or turbulent streaks into smaller flash units. These observations, however, show that the damping effect on turbulent fluctuations observed in flow of 5.8‰ bentonite sol through the 10 mm tube might be interpreted as being due to the relative high bentonite concentration. The experiments on the flow of 1.6‰ bentonite sol not only confirm the observations of Binnie and Fowler 1947 but even lead a bit further as these authors seem not to have observed the dividing of longer turbulent flashes into several short flash units.

The present experimental investigation of the transition phenomenon, evidently, removes apparent discrepancies between observations reported by Schiller 1921 and Binnie and Fowler 1947 and indicates a course of the transition process, consistent with experimental evidences reported in the literature.

Table 2.6. The same observations for flow of 1.6‰ bentonite sol as reported for flow of 2.5‰ sol in Table 2.5.

N_1	N_2	τ s	$n_1 = N_1/\tau$ 1/s	$n_2 = N_2/\tau$ 1/s	$\pm \Delta n_1/n_1$ %	$\pm \Delta n_2/n_2$ %	Temp °C	$V \cdot 10^6$ m³	T s	$Q \cdot 10^6$ m³/s	$\nu \cdot 10^6$ m²/s	R	$\pm \Delta R/R$ %
10	10	180	0.06	0.06			19.8	355	30.1	11.8	1.14		
10	6	263	04	02									
31	20	116	27	02			19.9	360	30.0	12.0	1.13		
25	19	94	27	02	45	63						2050	2.0
33	24	147	22	02			20.1	363	30.1	12.1	1.13		
10	9	130	08	07									
16	14	198	0.08	0.07			20.2	359	30.1	11.9	1.12		
7	5	104	0.07	0.05			20.3	347	30.1	11.5			
2	2	235	01	01				350	30.2	11.6			
4	2	160	02	01	94	83					1.12	2020	3.0
7	5	156	04	03				343	28.2	12.1			
4	4	174	0.02	0.02			20.3	344	30.1	11.4			
25	40	75	0.33	0.53			20.4						
25	25	95	0.26	0.26	12	38		382	30.2	12.6	1.12	2180	—
25	26	96	0.26	0.27			20.4						

SUMMARY

The interpretation of present flow experiments and observations reported in the literature suggests that the transition phenomenon in viscous flow does not imply a change from laminar to turbulent flow. It rather means transition of some kind of low energy disturbance vortices into high energy turbulent flashes possessing intensive small scale velocity fluctuations. It is shown that this explanantion of the transition process is valid for both low and high disturbance levels of the entrance flow, in contradistinction to current ideas, according to which, at least for low levels of entrance disturbance, transition is thought to imply breakdown of laminar flow due to the presence of small disturbance oscillations as analysed theoretically by T. Tatsumi 1952.

The primary disturbance vortices, responsible for the breakdown of the "steady" flow, originate from asymmetric inflow conditions, random disturbances in the supply liquid and laminar separation at the tube inlet as a result of the principle of conservation of flow circulation according to Lord Kelvin.

Transition takes place by the appearance of an increasing number of turbulent flashes for increasing Reynolds numbers R, in full agreement with statements by Osborne Reynolds 1883 (low disturbance level of the entry flow) and A. M. Binnie and J. S. Fowler 1947 (high disturbance level). The experiments, however, do not explain why primary disturbance vortices, which by themselves seem to be damped, might in some cases turn into turbulent flashes and in other cases not.

The apparent discontinuous increase of the flow resistance when certain "critical" Reynolds numbers R_k are exceeded, as observed by Reynolds 1883, L. Schiller 1921 and other authors, does not mean instantaneous onset of turbulence. The "discontinuity" rather appears somewhere in the middle of transition regions which extend from $R = \underline{R}$ where turbulent flashes first appear until $R = \bar{R}$ where continuous turbulence is established, so that $\underline{R} < R_k < \bar{R}$. These specific R

values might vary considerably even under apparently identical flow conditions. Schiller's determination of the "real critical" Reynolds number (R_k for "fully" disturbed entrance flow conditions) as having a definite value $R_k = 2320$ is consistent neither with the present measurements nor with experiments reported by other authors. The value of the "real" R_k might vary within wide limits, although commonly $2100 > R_k > 2400$, indicating that it depends on several as yet unknown flow quantities.

Double pressure drop branches, representing different states of flow have been obtained for flow of water through the 10 mm tube measured over test-sections nearest to the tube entrance but not for test sections further downstream, These observations confirm measurements due to W. Sorkau 1911–15 who reported the existence of two types of "turbulence" for disturbed entrance flow conditions in flow through glass capillaries.

3. Visual studies of some effects of various protuberances in tube flow[1]

Primarily, the present part of the paper is intended to serve as an illustration of the practical use of the stream double refraction technique in studying flow phenomena visually, and also of the complications that might arise in the interpretations of such visual observations. Secondly, the observations give some additional knowledge about certain doubtful premises of viscous flow reported in the literature.

Experimental procedure

The experiments reported in the following have been performed by direct visual observations and by photographing the flow of bentonite sols as exhibited by their stream double refraction properties.

The previously described apparatus outlined in Fig. 2.1, was used also in carrying out the present experiments. The 2.2 m long cylindrical plexiglass tubes of 20.3 and 10.7 mm diameter, used in the earlier experiments, and a rectangular tube of inner cross-section 10×30 mm^2 and of the same length, were used for studying the effect of single protuberances inserted into the flow. By mounting a 7 mm thick plexiglass panel along one of the narrower sides inside the rectangular tube, its cross-section was changed to 10×23 mm^2. From the middle of the tube, all along the second half of the tube, the panel, which was made by Mr. Ramgard, carried regularly arranged roughness elements consisting of 0.35 mm thick rectangular brass plates spanning over the 10 mm side of the tube at right angles to the flow direction. The plates were situated at 2.0 mm intervals from each other and protruded 1.8 mm into the flow. This arrangement allowed visual studies of some flow effects caused by regularly roughened tube surfaces.

The Reynolds numbers R of the various flow experiments are calculated according to the extended definition

$$R = \frac{U\,d}{\nu}, \tag{3.1}$$

where U = mean flow velocity
ν = kinematic viscosity of the surface layer of the flow (see p. 11).
and d = hydraulic diameter which is defined by the formula

$$d = 4\,\frac{S}{P}, \tag{3.2}$$

where S = area of the flow cross-section
P = wetted perimeter of S.

This definition permits calculation of the Reynolds number also for flow through the rectangular tubes and the definition is chosen so that the hydraulic diameter

[1] Some parts preliminarily reported in *Note on flow of liquids in tubes*, 1954.

for full flow through cylindrical tubes is identical with the geometric diameter. (See Goldstein, *Modern Developments in Fluid Dynamics* 1938, p. 297.)

Transition experiments reported in the literature indicate that, under ordinary flow conditions, transition to turbulence occurs at about the same Reynolds number for flow through "smooth" channels of any cross-section, even when the flow possesses a free surface, provided calculation of the Reynolds number is based on the hydraulic diameter as defined in formula (3.2).

The Reynolds number for flow in bulk through cylindrical tubes, according to the classical definition, where d has the meaning of the geometric diameter and the kinematic viscosity ν is considered a physical constant, is derived strictly in accordance with the theory of similitude. However, the introduction of the hydraulic diameter in the Reynolds number of this meaning is not consistent with the principles of similitude.

Though devoid of an explanation, this state of matters induced Schiller 1925 to suspect a hidden crucial meaning in the notion of the hydraulic diameter.

In fact, wall effects seem to be responsible for the maintainance of turbulent disturbances, making the Schiller assumption probable and also justifying the introduction of the hydraulic diameter as being in agreement with the principles of similitude, provided the viscosity ν is defined as the viscosity of the surface layers of the flow as proposed previously (Part 1, p. 11).

The numerical values of the Reynolds numbers for the flow experiments are determined in the same manner as described in Part 2 (pp. 40–41). Each value obtained is rounded off to the nearest 50 decade (viz. $R = 2170 \to 2150$; $2180 \to 2200$) and the formal error of the Reynolds numbers thus given is estimated not to exceed $\pm 4\,\%$.

The observations are reported in connection with accompanying photographs which have been obtained by means of a 35 mm standard camera synchronized with an ordinary electronic flash. Also were obtained some motion pictures which could not be used in illustrating the present report because of their poor quality. This aim has been dropped temporarily as it was impossible to obtain the desirable cinematographic equipment without a considerable time delay and additional economic support, hard of access at the time.

Flow in cylindrical tubes and the effect of single obstacles under various circumstances

In Fig. 3.1 the flow of 1.9 ‰ bentonite sol through the 20 mm cylindrical tube is shown with the effect of a cylindrical probe of 1.0 mm diameter stretching over the whole cross-section along a tube diameter. The probe is situated about 93 diameters (1.90 m) from the tube inlet which is sharp edged but which in this case is not furnished with a disturbance plate (see p. 6). Pictures *c* and *f* are photographed from a direction at right angles to the plane containing the tube axis and the probe axis. In photographing pictures *a*, *b*, *d*, *e* and *g* the camera axis has been directed parallel to the probe axis.

The Reynolds number $R \approx 700$ and the basic flow is purely laminar in Fig. 3.1 *a*. Visually, the pin causes a symmetric disturbance in the main flow, though it disappears within a short distance downstream. It cannot be decided from the picture whether this disturbance is laminar or composed of vorticity. In picture *b* the basic flow is still purely laminar at $R \approx 900$. Here the disturbance has the character of

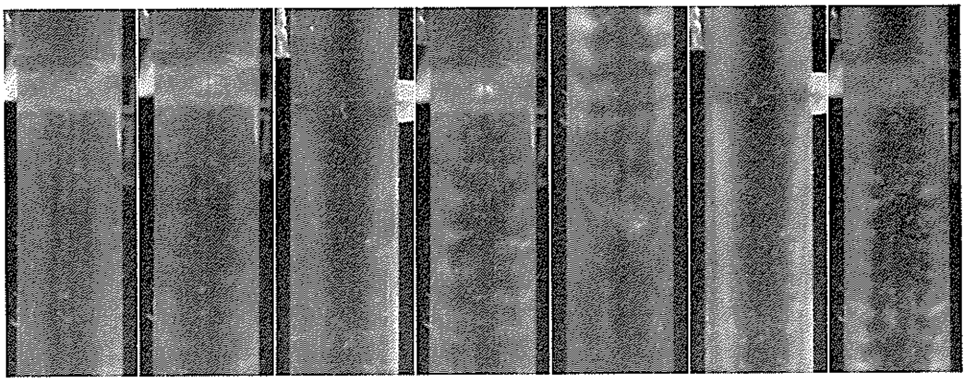

a b c d e f g

Fig. 3.1. Flow disturbances agitated by a cylindrical 1.0 mm probe in flow of 1.9‰ bentonite sol at various Reynolds numbers. The inner diameter of the polished plexiglass tube is 20.3 mm. The probe is inserted into the flow through a 2.3 mm hole in the tube wall and stretches over all the cross-section along a diameter of the tube. The tube entrance is sharp edged but no disturbance plate is adapted. The distance from the tube entrance to the probe is about 93 diameters (1.90 m).

The pictures *a*, *b*, *d*, *e* and *g* are taken from a direction at right angles to the view direction of the pictures *c* and *f*. The basic flow is purely laminar in all pictures except in the last two, where turbulent flashes frequently were observed passing by.

The temperature of the liquid in these experiments was about 19.0°C and the Reynolds number of the flow in the pictures is *a*, $R \approx 700$; *b*, $R \approx 900$; *c*, *d* and *e*, $R \approx 1300$ (picture *e* is taken 6 cm downstream of picture *d*); and *f* and *g*, $R \approx 4150$ (see note, below).

Comments to the pictures are given in the text.

Note.—The Reynolds numbers given for flow shown in the pictures of the present paper differ considerably from those given for the same pictures in the superseded paper, *Note on the flow of liquids in tubes* 1954. This is due to the correction of the viscosity values performed in accordance with results reported in Part 1.

a vorticity wake spreading out to the tube walls from its origin at the probe. Pictures *c* and *d* show that the vorticity wake caused by the probe, macroscopically seems to be composed of cylindrical vortices, their axis being parallel to the probe axis. Picture *e* is taken about 6 cm downstream of picture *d* and shows that these cylindrical whirls degenerate into a general diffuse disturbance after distending into contact with the tube walls. The Reynolds number $R \approx 1300$ for the flow shown in the pictures *c*, *d* and *e* and, as could be expected, the disturbance also here gradually vanishes and pure laminar flow re-establishes itself further downstream. Pictures *f* and *g* exhibit a similar flow pattern at $R \approx 4150$ though the wake vorticity apparently is more intensive here. Some distance downstream this flow exhibits a flow pattern similar to that of picture *e* but owing to the limited length of the tube, the further development of the disturbances could not be observed. The pictures *f* and *g* are taken during laminar intervals of the basic flow in which frequent flashes occurred.

Other series of similar experiments were performed on flow through the same tube, using cylindrical probes of 0.4; 1.0 and 2.0 mm diameter at a Reynolds number of $R \approx 2600$. In these experiments each probe first was situated 93 diameters (1.90 m)

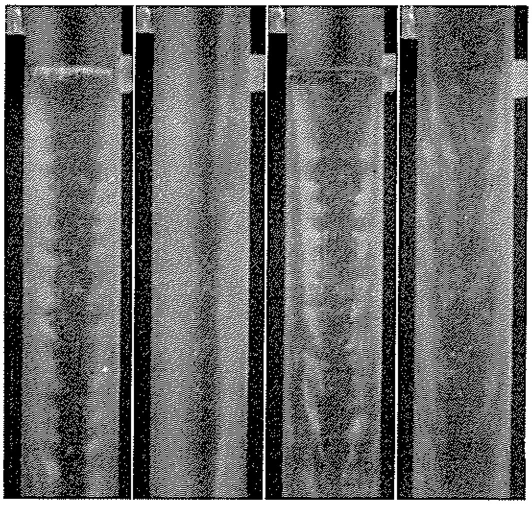

Fig. 3.2. Disturbances agitated by 0.4 and 2.0 mm cylindrical probes in flow of 1.9 ‰ bentonite sol through the 20.3 mm cylindrical plexiglass tube. The probes are inserted into the flow in the same manner as described in Fig. 3.1. The Reynolds number is $R \approx 2600$ at a flow temperature of 18.5°C. A disturbance plate was adapted at the sharp edged tube inlet so that turbulent flashes frequently appeared in the basic flow.

a Flow disturbances caused by the 0.4 mm rod covered with dust particles collected from the liquid.

b The same flow as in *a*, but pictured about 0.50 m downstream of the probe. The flow is here generally disturbed. 1.00 m further downstream, the probe disturbances remain only as weak turbulent flashes which vanish after an additional distance. The disturbances caused by the probe and those emanating from the tube inlet are easily distinguished from each other.

c In this picture the 0.4 mm probe has been exchanged for the 2.0 mm probe.

d The same flow as in *c* but 0.30 m downstream of the probe, where the flow is generally disturbed. 1.00 m further downstream there occur only turbulent flashes and it is not possible to distinguish between flashes caused by the rod and those emanating from the tube inlet.

from the tube inlet which was furnished with a disturbance plate placed 0.5 mm in front of the tube mouth as indicated in Fig. 2.1. Frequent turbulent flashes appeared in the basic flow. In Fig. 3.2*a* and *c* are shown the disturbances caused by the 0.4 and 2.0 mm probes. As judged from these pictures the thicker rod causes a higher grade of disturbance than the thinner one, which is shown covered by dust particles collected from the liquid. (A filter was later introduced into the circulation system and the dust particles were removed from the liquid. They did not however, influence the flow characteristics as observed by visual inspection.)

This series of experiments was succeeded by another during which each probe was situated 15 diameters (0.30 m) upstream of the previous position, while the flow was observed at the same position as before. Under these circumstances the flow never became laminar but was generally disturbed. The disturbed flow caused by the 0.4 mm rod is shown in picture *b* while picture *d* shows the corresponding more intensively disturbed flow caused by the 2.0 mm rod. The same type of disturbed flow is observed near the tube entrance to be agitated by the disturbance plate (see some of the pictures in Figs. 2.4 and 2.5 which are taken at a distance of about 50 diameters from the tube entrance).

Finally each probe was placed at a position 21 diameters (0.42 m) from the tube inlet. At 39 diameters (0.80 m) distance downstream of the probe, the disturbance from the 0.4 mm rod appeared as weak turbulent flashes in the laminar intervals of the basic flow. These flashes easily could be distinguished from the more energetic flashes emanating from the disturbance plate and they seemed to disappear completely within a distance of 64 diameters (1.30 m) from the probe. The disturbance agitated by the 2.0 mm rod was observed at the same distance (64 diameters) from the probe as strong turbulent flashes which individually could not be distinguished from those emanating from the tube inlet.

The observations reported here imply a confirmation of Reynolds' impression, that breakdown of steady flow occurs more readily for stronger disturbances than for weak ones and that the necessary disturbance level for breakdown decreases with increasing Reynolds numbers (see quotation of Reynolds on p. 8).

Besides the experiments presented here, numerous other observations have shown that the originally initiated disturbances must distend into contact with the tube walls—and that furthermore the "disturbed" flow thus formed has to travel an additional distance of at least several tube diameters before breakdown to turbulent flashes or to "real" turbulent flow as distinct from merely disturbed flow. This distance of accumulation seems to decrease with increasing disturbance level, though only within certain limits. The transition phenomenon actually seems to be closely connected with the flow conditions in the immediate vicinity of the bounding walls.

The conclusions made above are further supported by the appearance and behaviour of the turbulent flashes as observed by the present visual method. The characteristic features of the turbulent flashes are their arrow-like shape shown in Fig. 2.6 and their constant travelling speed, around the mean velocity of the flow, without noticeable change of their dimensions as they proceed along the tube. (At lower levels of disturbance, transition occurs at higher Reynolds numbers and the above description has to be modified in several respects.) The presented characteristics indicate that a single turbulent flash principally consists of a torus whirl (composed of smaller vortex units covering a wide spectrum of sizes and energy) continuously "rolling up" the surface layer of the liquid in contact with the tube surfaces. Since the flow velocity in the middle of the tube is higher than the mean flow velocity the flash disturbances situated there are brought forward relative to the main body of the torus. These disturbances (in the centre of the flow) do not come into contact with the tube walls and vanish after travelling a certain distance ahead of the main body depending on their radial positions and on the mean flow velocity. They of course reach farthest ahead of the flash body in the very flow centre, where the velocity is highest. Those parts of the flash, however, which are situated near the tube walls are "swallowed" by the main torus and some of these disturbances are brought into contact with the tube walls, being caught in the maintaining process of the turbulent cross-currents.

The given description explains the arrow-like form of the flashes and appears the simplest and most straightforward interpretation of the observed macroscopic behaviour of turbulent flashes. It actually implies that *selfmaintaining turbulence should originate from wall effects acting on disturbed flow in the immediate vicinity of—or in contact with—the bounding walls.*

It should be noted that the turbulent fluctuations according to the photographs seem to exist in immediate contact with the outer boundaries of the tube walls. This is due to a lens effect of the liquid-filled tubes and is of no significance as regards the flow characteristics. When the quotient between the wall thickness and the tube radius is large enough, the flow field will be visible with boundaries inside the outer boundaries of the tube. On the contrary, when this quotient is small enough, flow parts, situated considerable distances inside of the inner tube surfaces will be visible as if in contact with the outer boundaries of the tube.

The sketched maintaining process of the turbulent fluctuations as taking place at the surface of contact between the flow medium and the rigid boundaries appears to be in direct agreement with observations reported by A. Fage and H. C. H. Townend 1932. Those authors studied the flow of water through tubes, particularly the turbulent fluctuations very close to the tube surfaces, by means of an ultra-microscope. They performed their observations by studying the behaviour of sub-microscopic particles present in the water. In a passage of their paper, Fage and Townend stated (1932 p. 670): "Sometimes two or more slowly moving particles, often widely separated, were observed to shift in step, and the whole appearance suggested that the violent motion in the faster moving fluid dragged the whole surface layer bodily sideways."

Here it should be mentioned that Fage and Townend made their observations on flow through a "smooth" square tube of 22.6 mm side at a distance of 54 hydraulic diameters (1.22 m) from the tube entrance, which was equipped with a mouth trumpet so as to avoid disturbances. (The observations were reported to be valid also for flow through a cylindrical tube under similar conditions.) The weak entrance disturbances (the critical Reynolds number was visually determined to be about 3600) and the short distance of accumulation together with some other observational features of these experiments makes it doubtful that the observations of Fage and Townend in the main were carried out on selfmaintaining general, turbulent flow. It might be expected that the phenomenon quoted above would be more pronounced in experiments in which the crucial conditions according to Schiller 1921 (see p. 6) have been secured.

Here, I want to draw attention to a passage in William H. McAdams, *Heat Transmission* (1954 p. 152) referring to an unpublished experimental investigation by William H. Couch and Charles E. Herrstrom 1924. The passage runs:

"Couch and Herrstrom introduced a color band at the axis of a glass pipe through which water was flowing in turbulent motion and found that the color was quickly dissipated by the turbulence, as was the case in the classical color-band experiments of Reynolds. A second color band, laid down simultaneously near the wall, was not disturbed, thus indicating either that near the wall the flow was streamline in character or that if eddies existed, they were too feeble to dissipate the color band. This experiment showed substantial turbulence at the axis and no noticeable turbulence near the wall."

This seems to imply a definite contradiction to the present conclusions. However, after studying the report by Couch and Herrstrom[1] one quickly realizes that these authors have observed nothing but the character of high level entrance disturbances and disturbances caused by the coloured liquid injector. I do not have to explain this in detail but merely quote a passage in Couch and Herrstrom's report (1924 p. 5):

---

[1] A photostatic copy of this report was put at my disposal by courtesy of the *MIT Library* through the helpful agency of Mrs. K. Hellström at the *Royal Swedish Academy of Engineering Sciences*, Stockholm.

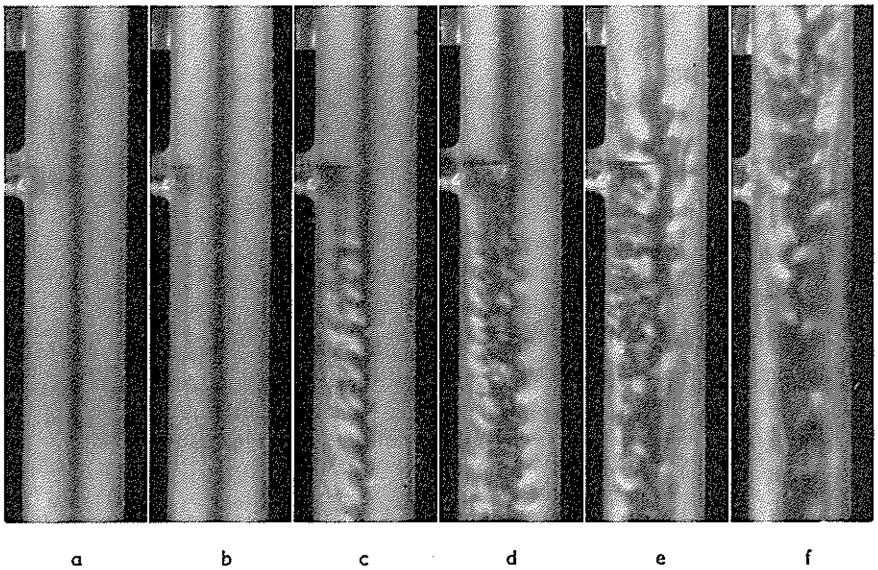

Fig. 3.3. Flow of 5 ‰ bentonite sol through the 10.7 mm cylindrical plexiglass tube at a Reynolds number of 2400 and a flow temperature of 18.4°C. A moderate frequency of turbulent flashes appeared in the basic flow. A conical shaped probe is inserted to various depths into the flow at a distance of 1.60 m from the tube inlet. (The probe is a 3 mm cylindrical brass rod formed conical along 2 cm of the end to a needle tip.)

a The probe tip is inserted about 0.5 mm into the flow. No effect of the probe on the flow pattern can be traced in this picture.
b Insertion about 2 mm. The first traces of agitated screw flow motion are visible.
c Insertion about 4.5 mm. The probe tip induces a discrete spiral or screw flow motion.
d and *e*. Insertion to the centre of the flow. The probe causes irregular disturbances in the flow. These disturbances seem to be more intensive in picture *e*, in which a turbulent flash of the basic flow just passes by, than in picture *d*, where the flow appears laminar. It is to be noted that the black line, visible upstream of the probe in picture *d*, is situated asymmetrically with respect to the tube axis, which at the instant probably indicates the presence of vorticity in the apparently laminar basic flow.
f No probe is present here. An undisturbed turbulent flash is shown in this picture, for the purpose of comparison with the turbulent flash in picture *e* disturbed by the probe.

"In order to get data on straight line flow, critical velocity, and turbulent flow, we made use of a glass condenser tube, 24″ long and 12 mm in diameter. The enlarged mouth of the tube made it possible to insert a twoholed stopper. Through one hole the water was admitted to the tube, and a capillary tube was pushed through the other hole. The colored liquid was fed into the condenser tube by means of this capillary. It was possible to fix the capillary either at the centre of the stream or at the walls, so that conditions of flow could be studied at all points. The capillary also extended far enough into the tube, so that the color band was not affected by any entrance disturbances."

Considering observations reported in the present paper the last statement in the quotation above cannot be correct specially as even the total length of the tube (51 diameters) is too short to admit observations on anything but disturbed entrance flow.

Fig. 3.3 illustrates some experiments showing the effect of a conical brass probe inserted to different depths into a flow of 5‰ bentonite sol through the 10.7 mm tube (its outer diameter being 15 mm) at a Reynolds number of about 2400. The disturbance plate was adapted at the tube entrance and turbulent flashes appeared with a moderate frequency at the position of the probe, 150 diameters (1.60 m) distance from the tube inlet.

Pictures *a* and *b* show that the probe might protrude considerably into the flow without causing any noticeable disturbance of the laminar flow. In picture *c* where the probe is inserted still more it initiates some kind of spiral or screw motion which, however, seems to be disturbed nearer the tube wall by the action of the thicker parts of the rod. The first traces of the spiral motion in the flow might be distinguished already in picture *b*. In pictures *d* and *e* the probe is inserted to the middle of the tube and causes an irregular disturbance of the main flow. This disturbance seems to be more intensive in picture *e*, which shows the conditions during the passage of a turbulent flash, than in picture *d*, obtained during a non-turbulent interval of the basic flow. This is a characteristic feature confirmed by other similar observations and is also in agreement with the long established practice in specifying the turbulence level in windtunnels. (The "critical" Reynolds number of a sphere placed in the airstream is the higher, the lower the turbulence grade is in the stream.)

The experiments above have been extended in order to investigate whether the same flow characteristics are valid for flow of different concentrations of bentonite sols and with other probes. One series of such extended measurements is illustrated by Fig. 3.4, which shows the flow of 2.5 ‰ bentonite sol through the same 10.7 mm tube at about the same Reynolds number as before, $R \approx 2500$. Also here the inlet flow was agitated by the disturbance plate, and turbulent flashes occurred with a moderate frequency in the basic flow. The 0.4 mm probe used before was placed at the same position where the conical rod previously was situated.

The effects produced by the conical rod in the flow of the 5‰ bentonite sol appeared also in these experiments. However, the constant diameter of the 0.4 mm rod prevented observable disturbances from being initiated close to the tube walls in contradistinction to the effect of the conical rod. This seems to be the reason why the spiral-like motion pointed out in Fig. 3.3*c* is shown more distinctly in Fig. 3.4*b*, *c* and *d*. The screw-motion seems to be approximatively symmetric with respect to the tube axis in picture *d*, where the pin is inserted to the middle of the flow initiating a couple of antisymmetric (?) spirals.

R. R. Rothfus and R. S. Prengle 1952 observed the same type of spiral motion in flow of water through tubes of 50.8 and 25.4 diameter. These authors performed their experiments by injecting coloured liquid through thin tubular probes inserted into the flow at considerable distances from the tube inlet. Rothfus and Prengle, however, did not realize that the probe was the origin to the "screw-motion". Consequently they made some misleading interpretations in assuming the existence of a "laminar sub-layer" not compatible with the common laminar film hypothesis, It is noteworthy that also Couch and Herrstrom 1924 did observe such spiral-like motions, though only at very low velocities of the flow, which is natural if we consider the high disturbance level of the entrance flow in their experiments.

The initiation of the "screw-motion" might be explained in terms of the principle of conservation of circulation according to Lord Kelvin's theorem, which implicates the impossibility of a momentary change of stationary flow-circulation of viscous flow. Provided the tip of the probe continuously is "rolling up" a single primary

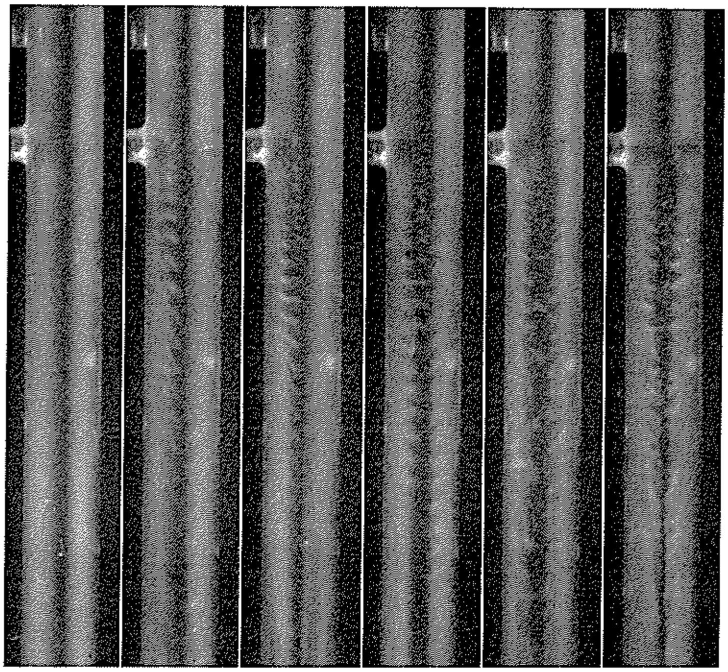

a b c d e f

Fig. 3.4. Studies on 2.5 ‰ bentonite sol flowing through the 10.7 mm cylindrical plexiglass tube at a Reynolds number of 2500 when the flow temperature was 18.3°C. High disturbance level is secured by adaption of the disturbance plate at the sharp edged tube entrance. Turbulent flashes appeared now and then in the basic flow at the place of observation. The 0.4 mm cylindrical brass rod inserted into the flow is situated 1.60 m from the tube inlet. The inserting depth of the probe varies from about 0.7 mm in picture *a* to the whole tube diameter in picture *f*. Some of the pictures (*b*, *c* and *d*) distinctly show spiral-like flow motions initiated by the probe.

whirl this would imply a prohibited instantaneous change of the rate of circulation per unit length of the tube unless the axis of such an initiated vortex follows a screw path during the next part of its tube passage. In such a case, however, the circulation of the vortex would be contradirected to its previous value, cancelling itself each full turn made by the vortex axis. After some time dissipating effects must be expected to distort the screw vortex pattern as is also shown by the pictures presented.

Flow in rectangular tubes and the effect of single obstacles under various circumstances

The following experiments have been carried out on flow through the rectangular plexiglass tube with "smooth" walls and of 10×30 mm^2 cross-section corresponding to a hydraulic diameter of $d = 15$ mm. No disturbance plate was adapted at the sharp-edged tube entrance and the probes were situated at 110 diameters (1.60 m)

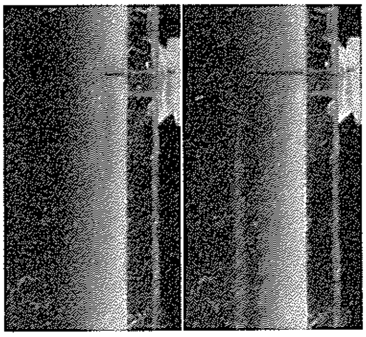

a b

Fig. 3.5. Flow of 2.5‰ bentonite sol through the "smooth" rectangular tube of 10×30 mm² cross-section (hydraulic diameter $d = 15$ mm) viewed broadside on (seen through the 30 mm side). The Reynolds number is 2600 at a flow temperature of 18.3°C. No disturbance plate was adapted at the sharp edged tube entrance and a moderate frequency of turbulent flashes appeared in the basic flow. The probe is inserted 2 mm into the flow in picture *a* and 7 mm in picture *b*, at a distance of 1.60 m from the tube entrance.

Similarly to the probe action on laminar flow in cylindrical tubes (Figs. 3.3 and 3.4) the probe induced a screw-like flow motion also in the flow through the rectangular tube as shown in picture *b*.

distance from the tube inlet and were inserted into the flow along the symmetry planes of the tube.

Fig. 3.5 shows the effect of the 0.4 mm cylindrical probe protruding into the flow of 2.5‰ bentonite suspension at a Reynolds number of $R \approx 2600$. Some turbulent flashes appeared in this flow. The probe is inserted 2 mm into the flow in picture *a* and 7 mm in picture *b*. No influence of the probe can be traced in picture *a* while picture *b* exhibits the same type of spiral motion initiated by the probe as earlier observed in the cylindrical tubes. Many tests showed that the screw-like motions reported here are initiated only at the tip of quite thin probes but never for instance by the 2 mm probe used in the experiments.

In Fig. 3.6 is shown the effect of the 2 mm probe inserted to the centre of the tube in flow of the same 2.5‰ bentonite sol used before. In pictures *a* and *b* the basic flow is purely laminar at Reynolds numbers of $R \approx 1100$ and 1600, while turbulent flashes appear now and then in the flow shown in pictures *c* and *d* at $R \approx 2700$. Picture *d* shows the development of the disturbance 7 cm downstream of the place of initiation shown in picture *c*. The first visual signs of the probe disturbances exhibit themselves first some distance downstream of the probe and a comparison of the pictures *a*, *b* and *c* indicates that this distance decreases with increasing Reynolds numbers. Probably, these disturbances are of the same two-dimensional vorticity type as exhibited in the pictures of Fig. 3.1 for flow in the 20.3 mm cylindrical tube.

Even though turbulent flashes appear in the basic flow in pictures *c* and *d* the probe disturbance seems to vanish completely farther downstream. This implies a further confirmation of earlier statements that certain levels of disturbance are necessary to cause breakdown of a predominant "steady" flow.

With respect to the undisturbed flow the pictures of Fig. 3.6 seem to indicate constant, almost zero rate of shear over the whole width of the flow field in the view

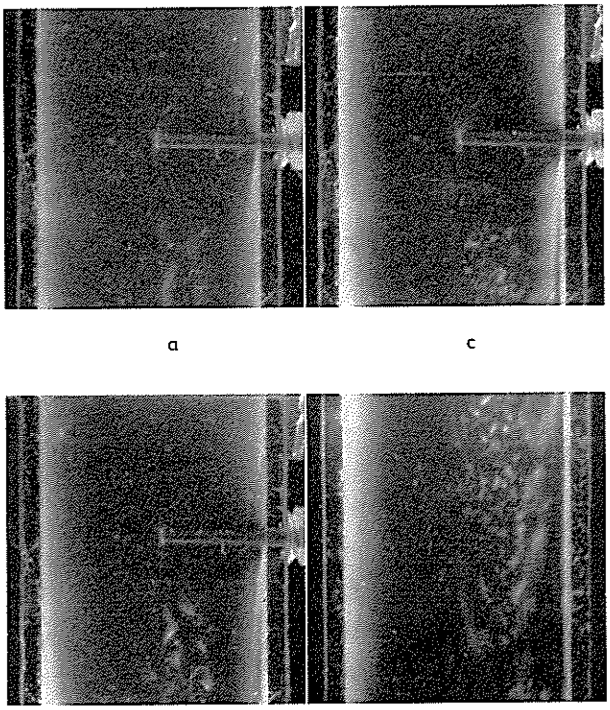

a c

b d

Fig. 3.6. Flow of 2.5‰ bentonite sol through the "smooth" rectangular tube of 10×30 mm² cross-section disturbed by the 2.0 mm cylindrical brass rod inserted to the flow centre at various Reynolds numbers, the flow temperature being 18.7°C. The probe is situated 1.60 m from the tube inlet. No disturbance plate is mounted at the sharp egded tube entrance. The flow is viewed through the 30 mm wide tube side.

a, $R \approx 1100$; the basic flow is purely laminar. *b*, $R \approx 1600$; same. *c* and *d*, $R \approx 2700$; picture *d* is taken about 7 cm downstream of picture *c*; turbulent flashes appeared with a moderate frequency in the basic flow.

plane except in the neighbourhood of the bounding walls, where luminosity indicates the presence of shear stresses. In pictures *a*, *b* and *c* the dark flow region (region of low rates of shear) extends almost symmetrically upstream and downstream of the rod approaching the bounding wall where the probe is located. The flow velocity certainly increases to a maximum in the tube cross-section containing the probe and there is no reason to believe that the mean shear rate in the view plane of the flow should decrease at this section as indicated by the pictures. On the other hand, it is evident that the probe must cause an increase of the rate of shear in planes at right angle to the probe axis (perpendicular to the viewed flow field). Further, picture *d* seems to indicate that the probe disturbance has considerably lowered the rate of shear of the flow close to the right tube wall as compared to the undisturbed flow at the left wall. Also this interpretation seems highly improbable.

Weyland 1955, and experiments reported in Part 2 have shown that saturation of the optical activity of bentonite sols occurs already at quite moderate rates of shear, though varying with the bentonite concentration. When the rate of shear exceeds the saturation value, perhaps each bentonite particle is in average "fully orientated" contributing to the total bi-refringence effect. Accordingly, a change of the rate of shear above the saturation value should not be observable visually. In the most extreme case the flow of bi-refringent sols might possess so high rates of shear in flow-planes parallel to the narrower side of the tube that saturation occurs in these planes and no optical activity is left in the planes parallel to the wider tube wall. Also intermediate stages to these extreme conditions might cause erroneous interpretations of visual observations if possible complications are not considered.

Returning to the interpretations of the photographs of Fig. 3.6, the rate of shear in the flow planes perpendicular to the view plane is considerably higher than the rate of shear in planes parallel to the view plane and probably even the saturation values are exceeded in some regions. Since the specific number of optically active particles in the flow is constant, the high rate of shear in the perpendicular planes "steal" optical activity from the view planes in which the shear stresses are comparatively low, except in the neighbourhood of the narrow tube sides where the shear rates in the two perpendicular planes are comparable to each other. This state of matters might explain the visual appearance of the undisturbed part of the flow shown in the pictures of Fig. 3.6. The increasing rate of shear around the probe section in planes perpendicular to the view plane affects an increasing number of the available optically active particles, decreasing the optical activity in the view plane (where the rates of shear ought to be about unaltered) thus giving a false impression of decreasing rate of shear close to the right wall around the probe position as shown in the pictures *a*, *b* and *c* of Fig. 3.6. A similar interpretation might be applied to picture *d* in the same figure, showing the development of the probe disturbances. Probably these disturbances mainly consist of two-dimensional vortices rolling broadside on along the right half of the tube, retarded at the wall and moving faster in the inner parts of the viewed flow field. The disturbances probably increase the rate of shear in the rotational plane, stealing optical activity from the view plane giving a false impression of no velocity gradient in the neighbourhood of the right wall. (The interpretation given above and in what follows is the simplest one I have come to think of. Other, more likely causes might remain.)

Numerous experiments indicate that changes between different states of flow are in general readily observed visually by use of the stream double refraction method, though the observations might be erroneously interpreted unless precautions are taken, considering the optical properties of the bi-refringent liquid, as for instance made in the preceding discussion of the pictures in Fig. 3.6. This is also illustrated by the photographs in Fig. 3.7 which show the effect of the 2.0 mm probe inserted to various depths in continuous turbulent flow of 2.5 ‰ bentonite sol at a Reynolds number of $R \approx 3200$.

In pictures *d*, *e* and *f* of Fig. 3.7 apparently different rates of shear are visualized in the neighbourhood of the wall where the flow is disturbed by the probe and at the opposite wall of undisturbed flow. This feature is perhaps due to the optical properties of the bentonite sol in the same manner as explained in the analysis of the pictures in Fig. 3.6. A further confirmation of the suggested relations between shear stress and stream double refraction is given by the flow photographed in picture 3.7 *c*. Here the probe seems to be inserted to such a small depth that the flow is sweeping over the tip of the probe with an increased velocity rather than increasing the velocity over

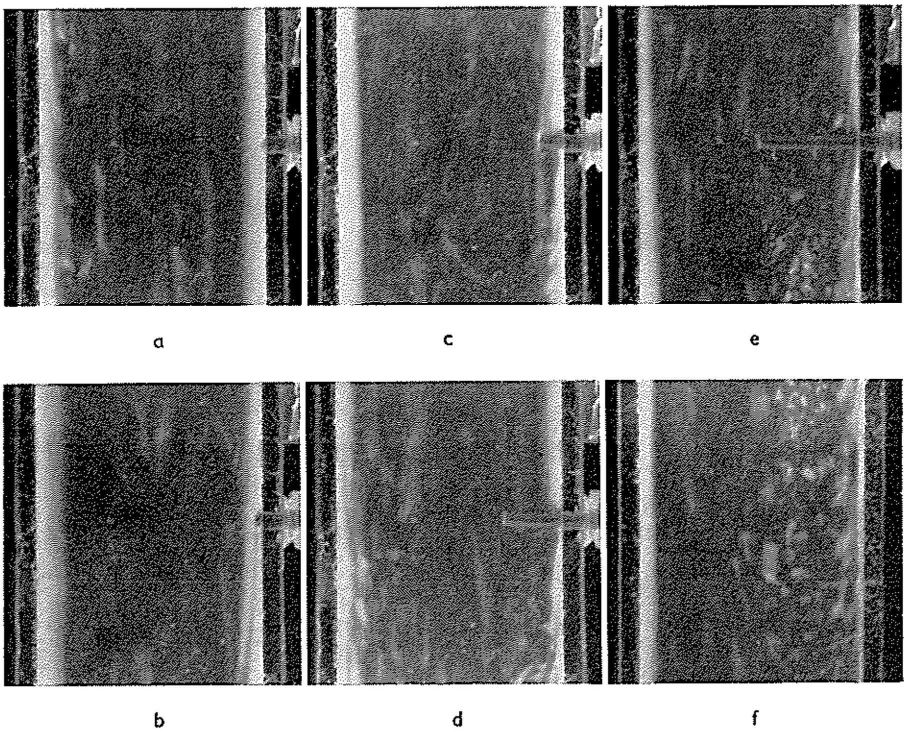

Fig. 3.7. Continuous turbulent flow of 2.5 ‰ bentonite sol through the smooth rectangular tube of 10×30 mm^2 cross-section viewed through the 30 mm side. No disturbance plate is adapted at the sharp edged tube entrance. The Reynolds number is 3200 at a flow temperature of 18.5°C. The 2.0 mm cylindrical probe is situated 1.60 m from the tube entrance and is inserted to various depths into the flow.

a, The probe is inserted about 0.7 mm; *b*, 1.4 mm; *c*, 3.5 mm; *d*, 8.5 mm; *e*, the probe is inserted to the middle of the tube (the same position as in Fig. 3.6*c*); *f*, the same flow as in picture *e* but viewed about 7 cm downstream of that picture.

the whole length of the probe. The increased velocity causes an increase of the rate of shear from the probe tip until some distance upstream, while downstream of the probe there is a region of apparently lower shear stresses. This shadowed flow region caused by the probe certainly does not mean laminar flow of low rates of shear but is due to cylindrical vortices initiated be the probe and rolling along the tube in the perpendicular plane, increasing the rate of shear in the same plane, thus "stealing" optical activity from the view plane of the flow.

It seems reasonable that transition between lighter and darker parts of flow fields should proceed continuously both in the case of circular and of rectangular tubes. This state of matters was observed only at low rates of shear. At higher rates of shear the optical activation in many cases changes very abruptly although the rate of shear certainly changes continuously. The pictures in Fig. 3.7 might serve as an illustration of this peculiarity. In all these pictures the left half of the flow field possesses continuous rate of shear decreasing from a maximum next to the wall

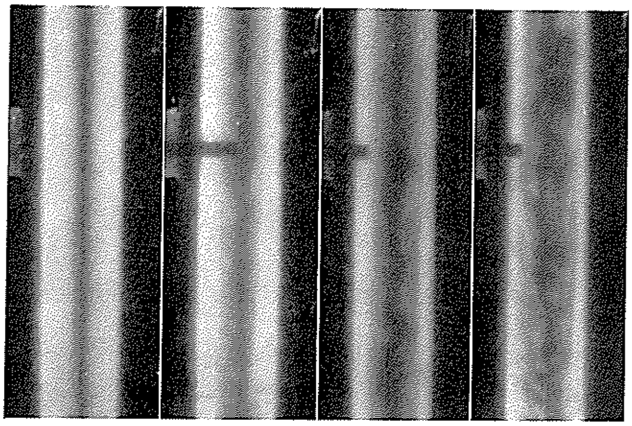

a b c d

Fig. 3.8. Flow of 2.5‰ bentonite sol through the rectangular plexiglass tube of 10 × 30 mm^2 cross-section viewed through the 10 mm side. The 2.0 mm cylindrical brass rod is inserted to various depths into the flow. No disturbance plate was adapted at the sharp edged tube entrance and the flow temperature was 19.0°C.

a, $R \approx 2600$. No probe is inserted into the flow in which appeared turbulent flashes with a moderate frequency. *b* and *c*, $R \approx 3200$. The probe is inserted 5 and 2 mm into the continuous turbulent flow. *d*, $R \approx 5100$. The probe is inserted to the same depth as in picture *c*.

to zero in the centre of the flow field. In spite of these circumstances the largest part of the flow field is evenly dark (indicating constant, almost zero rate of shear) broken by lighter streaks suggesting the presence of continuous turbulence rolling broadside on along the tube. In the neighbourhood of the left tube wall is visible an abrupt change to more luminous parts of the flow field, which should mean an almost discontinuous change to high rates of shear in the wall-near parts of the viewed flow field. Probably optical saturation phenomena are responsible for this misleading indication. A high degree of optical saturation might be expected to be dominant in flow planes perpendicular to the view plane and situated some distance from this wall. The saturation perhaps removes optical activity from the view plane though not close to the wall where the shear stresses in the perpendicular planes and in the view planes become comparable to each other, eliminating the saturation effect in the perpendicular planes and thus causing an abrupt change to luminosity in the view plane at a certain distance from the wall as shown in Fig. 3.7. In the actual case the broadside vorticity necessarily is destroyed in the neighbourhood of the wall and is replaced in the regions near the wall by vorticity in the view plane or "laminarity". (Such vorticity seems to be observable at the left wall in pictures *a* and *d*.) This means that a more abrupt change of the optical activity should appear in comparison to conditions exhibited by laminar flow as for instance illustrated by the pictures in Fig. 3.6.

The pictures of Fig. 3.8 show flow of the same bentonite sol as before but viewed through the 10 mm tube side at various Reynolds numbers. (It is to be noted that the printing process has been driven much harder for these pictures than for those shown in Figs. 3.5, 3.6 and 3.7. Otherwise the pictures in Fig. 3.8 would have been so luminous that scarcely any flow structure might have been observable. By increasing the exposure time for the photographic copies the flow texture has been brought out as shown in the pictures.)

Picture 3.8*a* shows a laminar interval of the flow at a Reynolds number of $R \approx 2600$ and consequently is to be compared to the pictures in Fig. 3.5 ($R \approx 2600$) and the pictures *c* and *d* Fig. 3.6 ($R \approx 2700$). The pictures 3.8*b* and *c* show the flow pattern of the same continuous turbulent flow at $R \approx 3200$ which is shown earlier in Fig. 3.7. The conclusion that the turbulent flow pictured in Fig. 3.7 consists of mainly two-dimensional vorticity rolling broadside on along the tube is also supported by the appearance of the flow texture shown in Fig. 3.8*b* and *c*. The characteristic features of the pattern shown in these pictures differ from each other although there is no change in the outer flow conditions. Such behaviour has occasionally been observed in several flow experiments.

Picture 3.8*d* shows the turbulence texture at $R \approx 5100$ and might be interpreted to exhibit about the same type of flow pattern as shown in picture *c*.

No effect of the 2.0 mm rod inserted into the flow can be traced in the pictures of Fig. 3.8 which however, does not mean that the flow in reality is unaffected by the probe.

Practical reasons prevented the study of the probe disturbances from a direction parallel to the probe axis as illustrated by Fig. 3.1*c* and *f* in the case of flow in a cylindrical tube.

Flow through a rectangular tube carrying regularly arranged roughness elements along one wall

In these experiments the cross-section of the 10×30 mm^2 rectangular channel was changed to 10×23 mm^2 by mounting a plexiglass panel along one of the 10 mm tube walls. The hydraulic diameter of this cross-section is $d = 14$ mm. Beginning at a distance of 1.30 m from the tube inlet the panel carried roughness elements consisting of 0.35 mm thick rectangular brass plates placed perpendicular to the flow direction spanning over one of the 10 mm sides of the tube and protruding 1.8 mm outside of the panel surface into the flow. The distance between neighbouring brass plates was 2.0 mm. The panel carried such brass plates to a distance of 0.1 m from the outlet end of the tube. No disturbance plate was adapted at the sharp-edged tube entrance in these experiments, which were performed with flow of both 1.9 and 5.0 ‰ bentonite sols. The flow was studied at two consecutive stations at 90 hydraulic diameters (1.30 m) and 121 diameters (1.70 m) distance from the tube entrance.

In Fig. 3.9 is shown the flow of the 5.0‰ bentonite sol at Stn. I where the smooth part of the panel changes to the rough part as viewed through the 25 mm tube side.

Picture *a* is taken during a laminar interval of the flow at a Reynolds number of $R \approx 1950$. Rare turbulent flashes were observed in this flow at the place of observation. In pictures *b*, *c* and *d* the Reynolds number is about 2600 with frequent flashes in the basic flow. Laminar intervals of the flow at $R \approx 2600$ looked the same as the laminar flow at $R \approx 1950$ shown in picture *a*. The flow pattern shown in pictures *b* and *c* might perhaps be considered as "half-turbulent" regions of the flow while picture *c* is thought to illustrate fully developed turbulence in the body of a flash. The vorticity of the flashes in the smooth part of the tube seems to be two-dimensional, rotating in planes perpendicular to the view plane.

The pictures show that the first roughness element (which abruptly contracts the

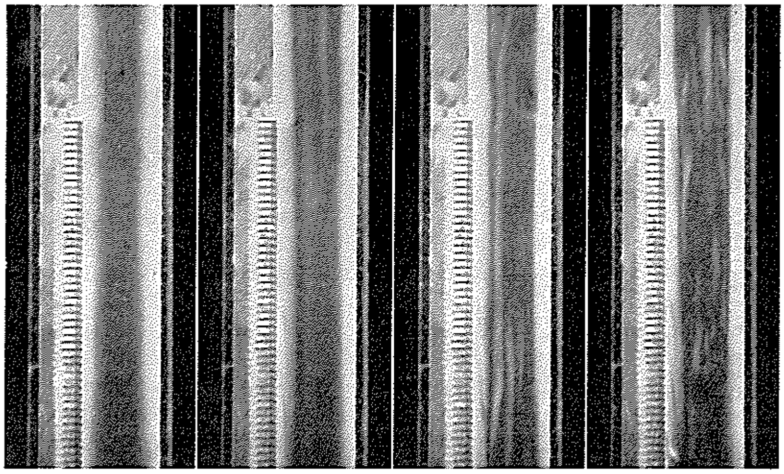

Fig. 3.9. Flow of 5.0‰ bentonite sol through the rectangular tube of cross-section $10 \times 23\ mm^2$ (hydraulic diameter $d = 14$ mm) in which the second part of one of the 10 mm walls is roughened, the rough part of the tube beginning at a location 1.30 m from the tube inlet. The regularly arranged roughness elements consist of 0.35 mm thick brass plates spanning over the whole 10 mm wall. They protrude 1.8 mm into the flow and the distance between neighbouring plates is 2.0 mm. No disturbance plate was adapted at the tube entrance and the flow temperature was 20.7°C. These pictures show the flow at the location where the roughened part of the tube begins.

a, $R \approx 1950$. The picture is taken during a laminar interval. Rare turbulent flashes appeared at the place of observation. *b*, *c* and *d*, $R \approx 2600$. Parts of turbulent flashes of various intensity. Frequent turbulent flashes appeared in the basic flow.

flow cross-section) acts as an origin to a stationary disturbance of increased circulation, which visually seems to dissipate into faster moving regions of the flow along a boundary looking like a parabola and disappearing downstream. At least up to Reynolds numbers of $R \approx 2600$ this disturbance was never observed to cause breakdown of the laminar flow.

In the pictures *b*, *c* and *d*, downstream of the stationary vorticity, can be seen similar but non-stationary vorticity regions moving downstream by the action of the faster moving parts of the flow. These disturbances are the last appearances of tails of turbulent flashes which proceed with a speed lower than other parts of the flashes.

Fig. 3.10 shows photographs of the same flow ($R \approx 2600$) at Stn. II about 30 hydraulic diameters (0.40 m) downstream of Stn. I. Picture *a* shows that the laminar flow is not disturbed by the regularly arranged protuberances. The velocity distribution of the laminar flow as shown both in Fig. 3.9*a* and Fig. 3.10*a* seems to be uninfluenced by the presence of the roughness elements (except the first brass plate initiating the stationary disturbance reported above). This implies that either the flow velocity cannot be zero at the tip of the roughness elements or the tip of each brass plate must be the origin to a stationary vorticity, which does not disturb the laminar flow pattern in the main. The photographs *a* and *b* in Fig. 3.11 actually seem to confirm both possibilities to be true. This state of matters also implies that stationary

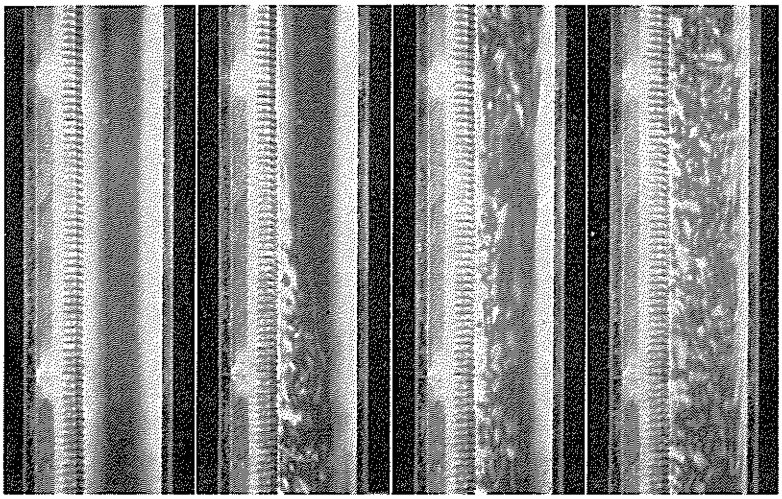

Fig. 3.10. Flow of 5 ‰ bentonite sol through the artificially roughened rectangular tube of cross-section 10×23 mm^2 (see text to Fig. 3.9) at a distance 0.40 m downstream of the location where the roughened part of the tube wall begins. The Reynolds number is 2600 at a flow temperature of 20.4°C. No disturbance plate was adapted at the tube inlet and frequent turbulent streaks appeared in the flow at the place of observation.

a View of a laminar interval of the flow.
b The tail of a turbulent streak passing by.
c The tail of a turbulent streak broken off by the front of another streak just arriving into the viewed flow field.
d Turbulence-structure in the body of a turbulent streak elongating itself as it travels along the rough tube wall.

vorticity must be present in the flow space between each pair of roughness elements in full accordance with the flow pattern exhibited by all the photographs in Figs. 3.9, 3.10 and 3.11.

The turbulent flashes emanating from the tube entrance usually were rather short when they arrived at the rough part of the tube. However, they were elongated to turbulent streaks when observed at Stn. II after 30 diameters (0.40 m) travel by the action of the rough tube wall. There is a continuous generation of turbulence by the action of the primary turbulent fluctuations in a flash breaking through the regular flow pattern along the rough surface, making each roughness element act as a disturbance generator casting off new disturbances into the flow. As, however, the flow velocity close to the rough surface is less than the mean velocity, the turbulent fluctuations generated along the rough wall will be delayed in comparison to more central parts of the flash. Since the disturbances cast off by the roughness elements continuously dissipate into the flow over the whole cross-section, the flash is continuously elongated to a turbulent streak as it travels along the tube. This process is illustrated by Fig. 3.10*b* showing the last part of a turbulent streak just passed by. Picture *c* shows the tail of a turbulent train passing by, and the front of another flash arriving into the view field. In picture *d* is shown the turbulent flow pattern in the main body

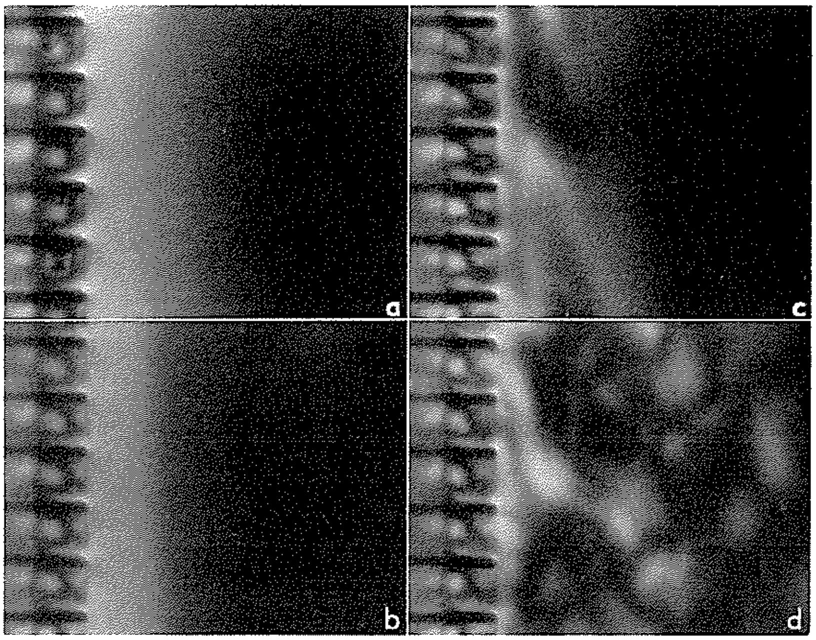

Fig. 3.11. "Close up" photographs of flow of 5‰ bentonite sol through the artificially roughened rectangular tube (see text to Fig. 3.9) of cross-section 10 × 23 mm². These pictures are obtained at the same location as those shown in Fig. 3.10. No disturbance plate was adapted and the flow temperature was 20.2°C.

a, $R \approx 1900$. Purely laminar flow. *b*, *c* and *d*, $R \approx 2600$. Picture *b* is taken during a laminar interval in the flow, while picture *c* shows two vortices forming a part of the tail of a turbulent streak. Picture *d* is taken during the passage of the body of a turbulent streak and shows two quite large eddies rolling along the roughened tube wall.

of a turbulent streak. It is interesting to compare the difference in the character of the turbulent fluctuations as viewed in Fig. 3.9*d* and Fig. 3.10*d*. The mainly two-dimensional turbulence exhibited by picture 3.9*d* has changed character and orientation in picture 3.10*d*, after traveling 30 diameters along the tube. However, the turbulent fluctuations decrease their intensity with increasing distances from the rough wall. Close to the smooth tube wall (opposite to the rough wall) the flow pattern in picture 3.10*d* looks almost the same as the two-dimensional vorticity exhibited in Fig. 3.9*d*. Evidently the smooth tube wall is unable to maintain the turbulent fluctuations agitated by the rough wall..

At Reynolds numbers of $R \approx 1900$ turbulent flashes sometimes were observed to arrive at the rough part of the tube at Stn. I but vanished before they reached Stn. II. This implies that even when the wall is very rough, it takes a least necessary disturbance level to break up the steady flow pattern close to the rough wall and thus turn the protuberances to active disturbance elements.

In Fig. 3.11 are shown "close up" photographs of the flow along the roughness elements at Stn. II. Picture 3.11 *a* shows purely laminar flow at a Reynolds number of $R \approx 1900$. The pictures *b*, *c* and *d* show the flow at the same Reynolds number $R \approx$

2600 pictured in Fig. 3.10. Picture b is taken during a laminar interval of the flow while picture c shows the flow character along the brass plates during the passage of the last part of the tail of a turbulent streak. Picture d is taken during the passage of the main body of a turbulent streak.

Comparing the pictures a and b we note the same saturation effect in picture b as discussed in the previous section. Both pictures also show the presence of vorticity giving the impression of two anti-rotational whirls in the interspace between each pair of brass plates. (In picture a also some air bubbles show up. These very thin bubbles are sticking between the panel and the tube wall. They did not disturb the studied flow and travelled slowly upwards.) The flow pattern of the vorticity between the roughness elements is strongly distorted when the plates act as disturbing elements. This is shown in pictures c and d. In picture d a disturbance is cast off into the flow from the interspace between the two brass plates situated highest upstream in the picture. This disturbance seems to form a part of a rather large whirl visible in the lower left corner of the photograph. Another discrete vortex of the same size seems to follow after the first one as shown in the same picture. The general impression is that there is a row of whirls rolling along the rough tube wall, disturbing the flow over the whole cross-section by direct mechancial action and diffusion effects. A similar interpretation is valid also for picture c in which two discrete eddies can be distinguished, forming a part of the tail of a turbulent streak.

Observations made on flow of the 1.9‰ bentonite sol are in every respect equivalent with those reported here for flow of the 5.0‰ bentonite sol, only that the photographs of the flow of the 1.9‰ sol are not so clear as those shown above for flow of the 5.0‰ sol.

SUMMARY

The development of disturbances caused by single obstacles protruding into flow of liquids in smooth tubes of circular and rectangular cross-sections has been examined by use of the stream bi-refringence method. The experiments have shown that primary induced disturbances have to distend into contact with the tube walls and then have to travel an additional distance in contact with the walls before selfmaintaining (real) turbulence is sprung into existence. Transition seems always to be characterized by the birth and maintenance of turbulent flashes as first observed by Reynolds at low levels of entrance disturbance and later observed by Binnie also at high disturbance levels. In the latter case the flashes travel with unaltered dimensions and constant speed of about the same value as the mean flow velocity. In its simplest form, a turbulent flash seems to consist of a torus whirl composed of a wide spectrum of smaller highly energetic eddies, thus differing from the decaying primary disturbances which do not exhibit the very intensive small scale structure possessed by the turbulent flashes.

Reynolds' assumption that breakdown of steady flow at any flow velocity occurs more readily for large disturbances than for smaller ones and also that the necessary disturbance level to cause breakdown of steady flow decreases with increasing flow velocity have been confirmed by the present experiments.

The experiments indicate that real turbulence—both in flashes and in continuous turbulent regions—is maintained by direct action of the bounding walls.

A certain type of spiral motion mentioned earlier by other authors and considered to have a special meaning in connection with the transition process, is shown to be agitated solely by the action of the tip of thin probes protruding into laminar flow. A simple qualitative explanation of the initiation of this type of flow is presented.

Finally, the effect of regularly arranged roughness elements (brass plates) along one wall in a rectangular tube has been studied. In each interspace between the plates regular vortices are formed but the laminar flow outside the plates is not disturbed and even the velocity distribution outside the regularly arranged brass plates seems to be unaffected by the presence of these plates.

Turbulent fluctuations, emanating from the tube entrance and arriving at the rough wall, mostly break up the regular flow pattern making each brass plate into a disturbance generator continuously casting off new turbulence into the flow, the turbulence spreading over all the flow cross-section of the tube. The generation of new turbulence takes place in flow layers where the velocity is less than the mean flow velocity of the turbulent flow parts. In this manner the flashes continuously elongate themselves forming turbulent streaks as they proceed along the tube.

At low Reynolds numbers it was observed that turbulent flashes arriving at the rough part of the tube might vanish completely after travelling a limited distance.

During the examination of the presented photographs, attention is drawn to complications and limitations that must be considered in evaluating observations performed by means of the stream double-refraction method in order to avoid misinterpretations.

4. Simultaneous observations of the transition process in liquid flow at various pairs of locations along long cylindrical tubes

Mention was previously made of the fading of turbulent fluctuations within the transition region of tube flow of bentonite sols, provided the concentration was not less than 2.5 ‰, while the damping effect seemed to disappear already at quite low Reynolds numbers in flow of bentonite sols of lower concentration. However, the pronounced irregularity of the appearance and behaviour of the turbulent flashes suggested that great advantages would be gained by recording simultaneous observations of tube flow at two or preferably at several locations along tubes considerably longer than those hitherto used. For this purpose an apparatus was constructed in which 12.5 m long experimental tubes were to be used. T. Thedéen assisted in the construction of the main apparatus, which is sketched in Fig. 4.1. The photograph of Fig. 4.2 shows the complete design together with all the measuring equipment used in the experiments.

Experimental procedure

Liquid is sucked from the supply reservoir 1 (see Fig. 4.1) by the circulation pump 2, which is run at constant speed. Depending on the adjustment of the three-way regulation cock 12, parts of the liquid are brought back to the reservoir by the short circuit pipe, while the rest of the liquid is pumped through the rubber hose 9 into the levelling tank 3. The air pressure in the container 3 was kept around 30000 N/m^2 (0.3 bar) above the surrounding atmospheric pressure, within a variation of about 15 %. The liquid is forced through the experiment tube 5 by the compressed air in the container 3. The flow velocity in the tube is controlled by means of the regulation cock 13 through which the liquid passes back to the reservoir 1, its interior open to the atmospheric pressure.

It was possible to obtain stationary flow conditions at any desired velocity through the test tubes by adjusting the regulation cocks 12 and 13 relative to each other taking account of the prevailing air pressure in the levelling tank 3, the liquid level in which being kept almost constant.

The rate of flow was continuously recorded by means of an orifice plate 7 connected to a strain-gauge pressure transmitter 8 which was electrically connected to a recording potentiometer and a feeding battery via a balancing unit. A slight temperature drift of the transmitter was easily compensated for by small adjustments of the balancing unit.

Calibration of the velocity recording device was made on several occasions during the experimental period. The first series of calibration measurements was performed by mounting the orifice plate fitment in the previously used flow apparatus (described in Part 2) measuring the discharge of liquid per time unit at constant deflection of the recorder pen, the calibration values being determined by means of the

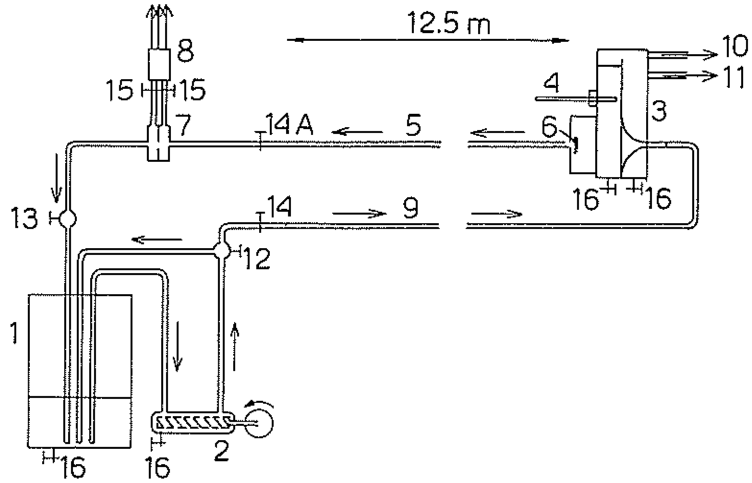

Fig. 4.1. Outline of the flow apparatus.

1 Liquid supply; the container is open to the atmospheric pressure
2 Circulation pump
3 Levelling tank
4 Thermometer
5 12.5 m long experiment tube
6 Disturbance plate, its distance from the tube inlet being variable from zero to 15 mm
7 Orifice plate with housing
8 Strain-gauge pressure transmitter
9 Rubber hose
10 Connection to a reduction valve of a steel flask containing compressed air
11 Connection to an open manometer
12 Three-way regulation cock
13 Regulation cock
14 Plug cocks
15 Cocks
16 Drainage cocks

measuring glass and the chronometer used before (see pp. 40–41 in Part 2). All the other calibration series were performed by emptying the filled liquid container 3 in Fig. 4.1, observing the time necessary to let the liquid surface drop between marks, representing known liquid volumes, at constant rates of flow. There is good agreement between the calibration values obtained from the various series of measurements. The values of the first and last series of calibration measurements, the time lapse between those being about one year, are shown in the calibration diagram of Fig. 4.3, the confirmative intermediate calibration series being omitted from the diagram.

Permanent records of flow disturbances, simultaneously at two locations, along the experiment tube were secured by means of two optic-electronic devices, based on the same principle as described by Binnie and Fowler 1947. Each device consisted of a point lamp, its light successively passing through a condenser lens of 10 mm diameter, a diaphragm of 1 mm opening and a polarizer. The polarized light beam then passed through the experiment tube and an analyzer, finally hitting the photocathode of a nine-stage photo-multiplier. P. Mitlid and A. Söderholm advised about the electronic design and A. Ramgard, who very capably assisted in the performance of all the experiments reported in this part of the work, undertook the practical construction of those apparatus.

The output signals from the optic-electronic devices were fed separately into the channels of a double beam cathode-ray oscilloscope equipped with a continuously recording camera.

Fig. 4.2. Photograph of the complete experimental equipment including also measuring components used for pressure drop measurements reported in Part 5 of the paper.

The levelling tank can be seen at the end of the bench which is fastened to the wall and which carries the 12.5 m long experiment tube. In the centre of the picture is shown the double-beam oscilloscope adapted with the continuously recording camera. High to the left at the wall is seen the strain-gauge pressure transmitter (velocity recorder), which is connected to the potentiometer recorder visible in the nearest window niche. The equipment placed in this niche includes balancing units for both the velocity recorder and the pressure transmitters, by which pressure drop measurements were performed (reported in Part 5), as also an accumulator for the velocity recorder and a power unit for feeding the pressure drop transmitters with constant voltage. The five pressure drop transmitters are mounted along the wall above the bench on which can be seen the two black optic-electronic devices connected to the oscilloscope via separate amplifiers. The supply container can be seen immediately behind the trolley which carries the galvanometer oscillograph, which is connected to the pressure drop transmitters. Beside the supply container we also see the circulation pump.

Photograph taken by Mr. Per Engström, *Aeronautics Lab.*, *KTH.*

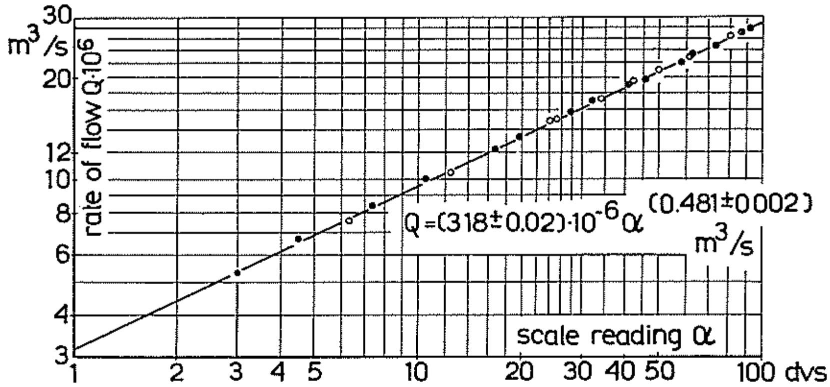

Fig. 4.3. Calibration diagram of the velocity (rate of flow) recording equipment. The dots represent calibration values obtained in March 1954, while the circles represent values obtained in April 1955.

At the time, records could not be obtained for more than two stations simultaneously, owing to the limited measuring equipment available.

The only jointless, transparent tubes of the desired length obtainable within a reasonable time were made of cellulose acetate-butyrate. Four tubes of about 6, 8, 10 and 12 mm inner diameter were procured and calibrated by filling with distilled water at room temperature, the tube diameter being determined sectionwise by subsequently tapping off the water, each time measuring the water volume by means of a calibrated burette. The lengths of the calibration sections were 1 m for the 6 mm; 0.8 m for the 8 mm; 0.5 m for the 10 mm and 0.4 m for the 12 mm tube. Fig. 4.4 shows the results of the tube calibrations. Each point represents the mean diameter of a tube section. Two series of calibrations were obtained for each of the tubes except the 12 mm tube for which only one series of calibration measurements was made. There is a shift of the calibration sections of the 8 and 10 mm tubes, while each dot for the 6 mm tube represents two calibrations, showing the high reproducibility of these calibration measurements. The accuracy of each volume determination is better than 0.2 % (see measurements reported in Part 2, pp. 30 and 45) while the length of each tube section is accurate within 0.2 %, so that the error in any of the given mean diameter values is estimated not to exceed 0.2 %.

The total mean diameter of each tube is determined both by calculating the arithmetic mean value of the diameter values of the calibration sections of the tube and by measuring the total water volume collected from the calibration sections using a larger measuring glass. Surprisingly good agreement was obtained between the total mean diameter values thus determined, which are 6.01; 8.18; 10.31 and 12.31 mm with an estimated accuracy of better than 0.4 % as recorded in Fig. 4.4. The figure shows that the mean diameter values of the various sections of each tube vary considerably relative to each other. In addition, still larger variations might be expected for local diameter values. These variations, however, seem not to have been crucial with respect to the results of the flow experiments.

In Fig. 4.5 some micrographs show the appearance of the inner surfaces of the tubes. It is to be noted that the tubes, except the 10.31 mm one, are made by the same manufacturer.

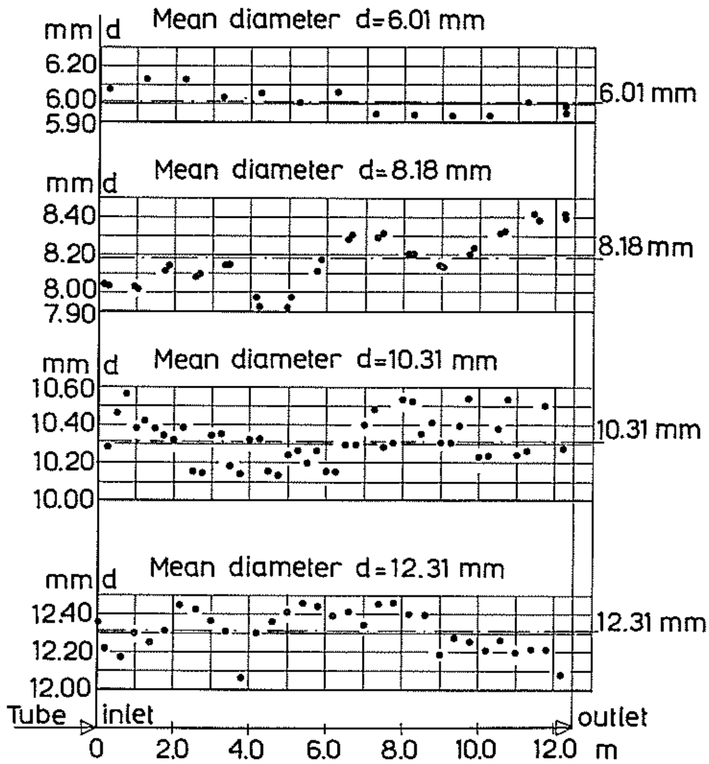

Fig. 4.4. Diameter values of the four experiment tubes. Each dot represents two measurements of the sections of the 6.01 mm tube. Two series of measurements were made of the tubes except the 12.31 mm tube which was calibrated only once.

The experiment tubes exhibited permanent polarizing effects which was of noticeable disadvantage. This quality prevented the polaroid plates from being adjusted to light extinction for the liquid at rest in the tubes, because in such a case no sensitivity at all was obtained for the stream double-refraction effects. At each observational location it was necessary to search for the orientation of the polaroid plates, relative to each other and the tube, which gave the maximum sensitivity for the turbulent fluctuations of the flow, letting through considerable quantities of light also when the liquid was at rest. The strong general background light, brought about by this arrangement, drowned the variations of the output signals due to variations of the rate of flow. Consequently, the records obtained inform only about disturbances of turbulent fluctuations appearing in the flow but not about the prevailing rate of flow.

Tubes made of optically neutral materials, as for instance such plexiglass tubes as were used in the previously reported experiments (Parts 2 and 3), would have implied great advantages regarding the possibilities of the experimental technique used.

At the beginning of the experiments the tubes were furnished with parallelepipedic

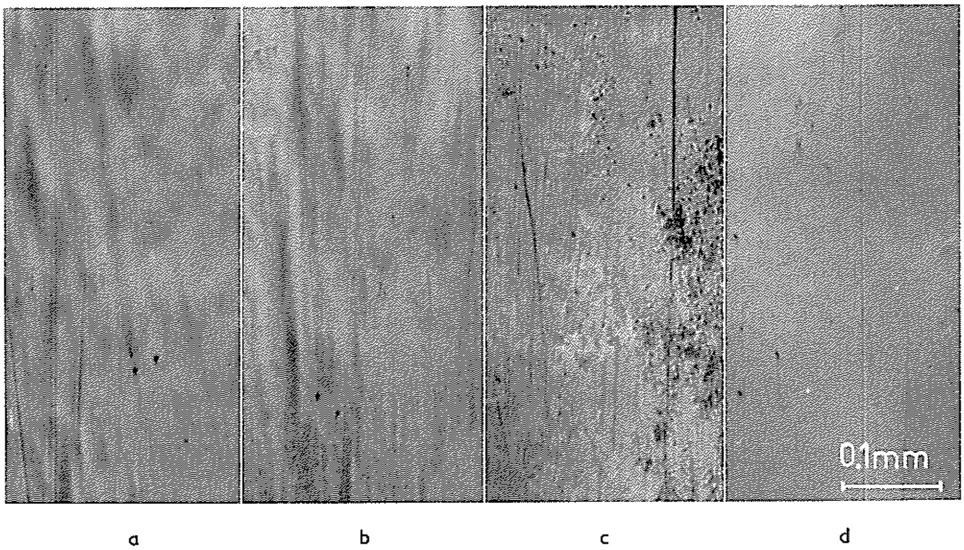

Fig. 4.5. The appearance of the tube surfaces of the experiment tubes.

a, 12.31 mm tube. *b*, 8.18 mm tube. *c*, 10.31 mm tube. (The black stains visible in this picture most likely are due to dried bentonite, hard to remove from the surface.) *d*, 6.01 mm tube.

The surface samples of the tubes were taken from pieces of the tubes never used in the experiments except for the sample of the 10.31 mm tube.

plexiglass cuvettes filled with water, with the purpose of neutralizing the lens effects of the liquid-filled tubes. This arrangement, however, soon proved superfluous provided quite heavy mechanical tube vibrations were avoided. Tests showed that tube vibrations in the absence of cuvettes were easily distinguished from disturbances appearing in the flow, making these cuvettes of no use.

The tube inlets were slightly rounded and the entry disturbances were initiated by a disturbance plate, its distance from the tube mouth being variable from zero to about 15 mm. (About the function of the disturbance plate see previous parts of the present work or Schiller 1921.)

The bentonite sols used in the experiments were of 1.33; 1.17; 1.02; 0.68 and 0.40‰ concentration, these values being correct within 1 % (see Part 1, pp. 16–17).

The viscosity of the sols was determined according to statements given in Part 1 of the paper.

The largest possible error in the rate of flow is estimated not to exceed 2 % at 4 divisions reading on the recording instrument, decreasing to about 1.1 % at full instrument deflection. The highly fluctuating local diameter values of the tubes render the estimated error of each tube's mean diameter quite problematic. If account is also taken of the conflicting situation as regards the concept of viscosity (see Part 1) it is evident that any estimation of the absolute error in the Reynolds numbers would be questionable. However, relative to each other and ordinary experiments reported in the literature the error in the Reynolds numbers of the present experiments probably does not exceed 3 %.

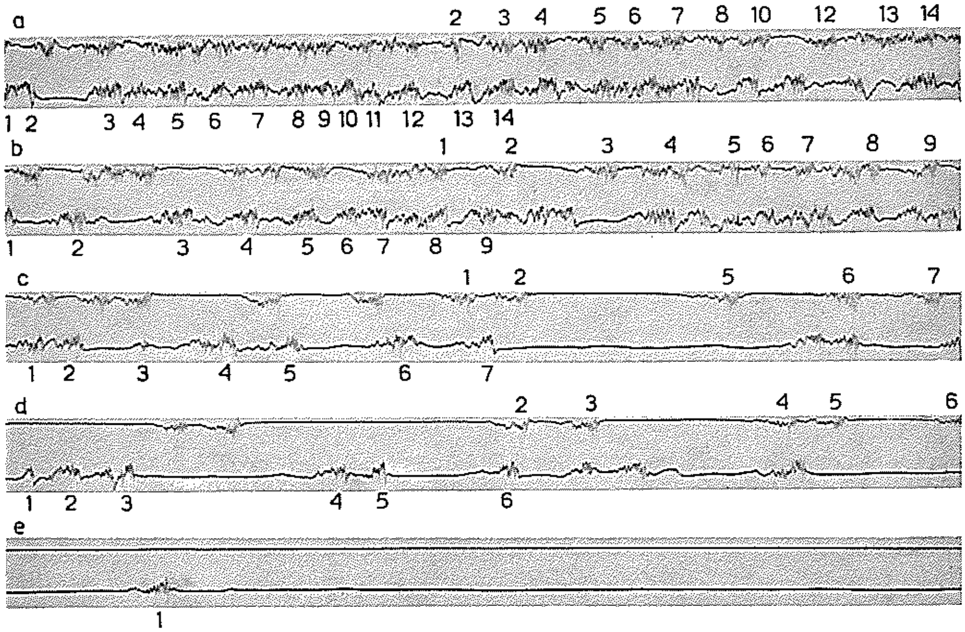

Fig. 4.6. Typical oscillograms obtained for flow of 1.02 ‰ (per mille) bentonite sol through the 10.31 mm tube with the disturbance plate situated 0.25 mm in front of the tube inlet. The lower trace in each record is transmitted by Stn. I situated 1.50 m from the tube inlet while the upper trace is due to Stn. II situated 3.00 m further downstream. The Reynolds numbers are: *a*, $R \approx$ 2490; *b*, 2480; *c*, 2350; *d*, 2280; *e*, 2110.

Development of turbulent disturbances in flow of bentonite sols of various concentrations

Flow of various bentonite sols through the 10.31 mm tube was investigated in order to trace possible variations of the flow behaviour depending on variations in the bentonite concentration within the interval 1.33–0.40 ‰. This investigation is a direct continuation of previously reported experiments carried out on flow of bentonite sols of higher concentrations.

The two optic-electronic devices were situated at distances of 1.50 m (Stn. I) and 4.50 or alternatively 11.90 m (Stn. II) from the tube inlet. The disturbance plate was adjusted at a distance of 0.25 mm in front of the tube inlet.

Typical oscillograms recorded for flow of the 1.02 ‰ bentonite sol are shown in Figs. 4.6 and 4.7 the lower traces being transmitted by Stn. I, while the upper traces are those of Stn. II situated 3.00 m downstream of Stn. I in Fig. 4.6 and 10.40 m in Fig. 4.7. The total length of the film strips reproduced here corresponds to a time interval of about 24 s which is only the shorter part of the original records which cover ranges from 60 to 200 s at a time-scale of about 0.080 s/mm. In Fig. 4.7 the oscillogram traces transmitted by Stn. II have been shifted to the left, in each case a distance corresponding to the average time interval necessary for the flashes to travel from Stn. I to Stn. II. Thus the same flashes, observed at the two stations,

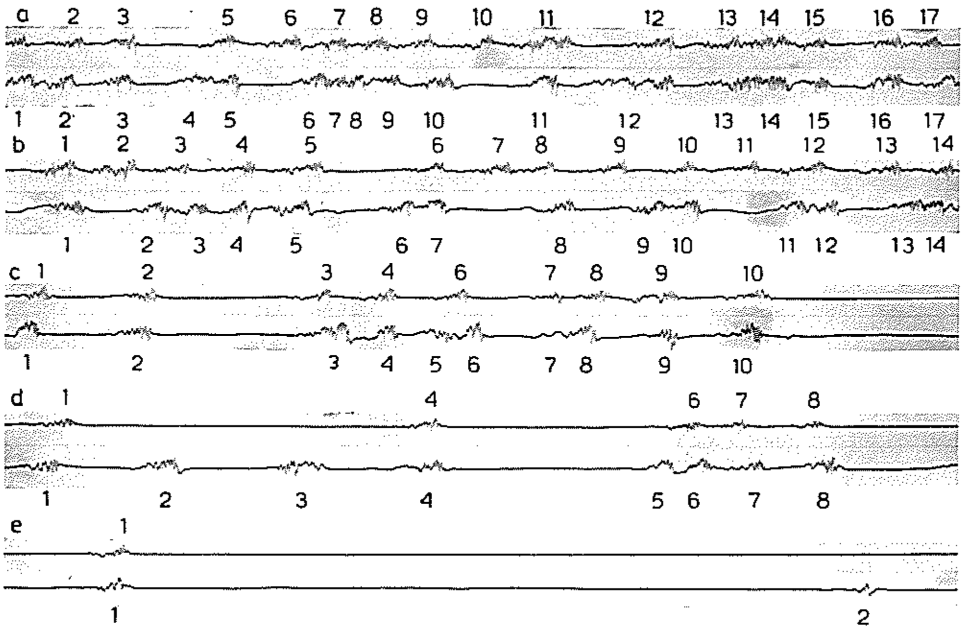

Fig. 4.7. Oscillograms obtained under the same circumstances as those of Fig. 4.6 only that Stn. II was moved to a position 10.40 m downstream of Stn. I and that for lack of space the oscillograph traces in each case are shifted a distance equal to the time necessary for the flashes to travel from Stn. I to Stn. II. The Reynolds numbers are: *a*, $R \approx 2430$; *b*, 2370; *c*, 2320; *d*, 2260; *e*, 2150.

approximately match each other in the records of Fig. 4.7, but owing to the varying flash velocities the positions do not agree perfectly. For the purpose of identification the flashes are numbered and we see that up to Reynolds numbers of $R = 2350$ turbulent flashes often disappear while travelling along the tube. Occasionally the identifications might seem questionable on the short film strips shown in these pictures, but up to Reynolds numbers of $R = 2400$ the identifications are quite reliable when examining the complete records. Above this Reynolds number groups of flashes begin to appear, in which the single units often cannot be distinguished at Stn. I, but which spread out to a discrete number of flashes when passing Stn. II. At still higher Reynolds numbers there appear turbulent streaks making such an identification meaningless.

It is clearly observed that the damping effect of the turbulent fluctuations observed at lower Reynolds number in the flow, represented by Figs. 4.6 and 4.7, disappears at Reynolds numbers around 2400, where even an increase of the turbulent regions might be noted. On the other hand, flow disturbances, even at quite high Reynolds numbers, were never observed to appear unless as developed from entrance disturbances. This statement is based on observations that no flow disturbances ever were observed at Stn. II without a primary disturbance first being observed at Stn. I, independent of the position of the stations along the 12.5 m long test tubes. This implies a confirmation of the observations on flow in shorter tubes reported earlier and is valid for flow of all the bentonite sols used.

Table 4.1. Flow data obtained for flow of various bentonite sols through a 10.31 mm tube with a disturbance plate situated 0.25 mm in front of the tube inlet.

Q = rate of flow, t = temperature, $n_1 = n_2$ = flash frequency recorded at Stn. I (situated 1.50 m from the tube inlet) and Stn. II respectively. $U_{F\,\mathrm{tail}}$ = velocity of the aft end of turbulent flashes, $U_{F\,\mathrm{front}}$ = velocity of the fore end of the flashes.

1.33 ‰					1.17 ‰					1.02 ‰					0.68 ‰					0.40 ‰					
$Q \cdot 10^6$ m³/s	t °C	$n_1 \cdot 100$, 1/s	$n_2 \cdot 100$, 1/s	U_F, tail m/s	$Q \cdot 10^6$ m³/s	t °C	$n_1 \cdot 100$, 1/s	$n_2 \cdot 100$, 1/s	U_F, tail m/s	$Q \cdot 10^6$ m³/s	t °C	$n_1 \cdot 100$, 1/s	$n_2 \cdot 100$, 1/s	U_F, tail m/s	$Q \cdot 10^6$ m³/s	t °C	$n_1 \cdot 100$, 1/s	$n_2 \cdot 100$, 1/s	U_F, tail m/s	$Q \cdot 10^6$ m³/s	t °C	$n_1 \cdot 100$, 1/s	$n_2 \cdot 100$, 1/s	U_F, tail m/s	U_F, front m/s
Stn. II at 4.50 m from the tube inlet																									
26.0	17.8				25.3	17.1				25.0	14.7				26.0	16.3				22.7	17.5				
25.2	17.8				24.4	17.0			0.265	24.8	14.8	72	72	0.280	25.5	15.6									
24.4	17.7				23.8	16.9	78	73	0.256	24.2	15.0	60	55		25.0	15.7	107	97	0.286	22.3	17.5				
23.8	17.8	79	79	0.256	23.2	17.0	52	51		23.4	15.1	47	38	0.270	24.2	15.8	86	82		21.7	17.6	69	74	0.233	
23.2	17.8	78	75	0.252	22.7	17.2	40	40		23.0	15.2	33	25		23.3	15.9	72	66	0.275	21.2	17.6	47	44		
22.7	18.0	52	48		22.2	17.3	42	35	0.248	22.5	15.3	28	25		22.8	16.0	52	49		20.6	17.7	37	32	0.227	
22.2	18.0	43	41		21.6	17.5	14	10		21.9	15.6	17	16	0.261	22.2	16.1	40	32	0.265	20.0	17.7	24	21		
21.7	17.8	27	22	0.244	21.4	17.6	10	10		21.5	15.7	9	5		21.6	16.1	17	13		19.6	17.7	8	6		
21.2	17.8	21	17		20.9	17.6	17	10	0.240	21.1	15.7	3	3		21.0	16.2	13	11		19.4	17.9	15	15	0.222	
20.8	17.8	6	6		20.4	17.7	6	3	0.236	20.6	15.8	4	1	0.256	20.6	16.2	5	4	0.256	19.1	17.8	9	8	0.219	
20.3	17.9	5	3	0.236																					
Stn. II at 11.90 m from the tube inlet																									
25.9	17.6				24.7	17.5				24.9	16.1				24.8	15.5	100	91		24.4	17.4				
25.1	16.8				23.9	17.6				24.3	16.1				24.2	15.3	74	74	0.280	23.5	17.4				
24.4	16.8				23.2	17.7	70	70		23.5	16.2	72	70	0.254	23.7	15.6	68	64		23.0	17.4				
23.6	16.9	72	72	0.252	22.7	17.8	58	53	0.248	22.9	16.3	61	63		23.1	15.7	58	51		22.3	17.5	78	78		
23.0	17.1	40	39	0.251	22.1	17.9	36	35	0.245	22.3	16.4	32	27	0.248	22.5	15.8	37	32	0.259	21.8	17.6	67	69	0.232	0.239
22.3	17.2	31	26		21.7	18.4	28	26	0.238	21.8	16.5	18	13		22.0	15.9	21	18		21.3	17.6	52	52	0.230	0.235
21.9	17.2	21	19		21.6	18.0	38	35		21.5	16.9	29	17	0.239	21.4	16.0	7	5	0.251	20.7	17.6	34	36		
21.6	17.3	12	11	0.241	21.2	18.0	16	14	0.239	21.4	16.6	19	13	0.242	20.8	16.2	7	3		20.7	17.0	18	18		
21.1	17.3	5	2	0.243	20.8	18.2	12	10	0.239	20.9	16.7	10	8	0.239	20.1	16.3	3	1	0.241	20.2	17.0	12	12	0.231	0.231
20.6	17.2	6	5		20.5	18.3	14	14		20.7	16.6	13	5							20.1	17.4	23	18	0.223	0.228
20.2	17.2	0	0		20.0	18.3	6	5		20.5	16.7	6	1	0.234						19.9	16.9	11	8	0.228	0.228
19.9	17.4	4	3	0.236	19.5	18.4	4	3	0.230	20.0	16.8	1	0	—						19.3	16.9	4	1	0.224	0.224
19.5	17.5	0	0	—						19.6	16.9	1	0	—						18.9	17.0	1	1	0.221	0.221
																				18.5	17.3	0	0	—	—

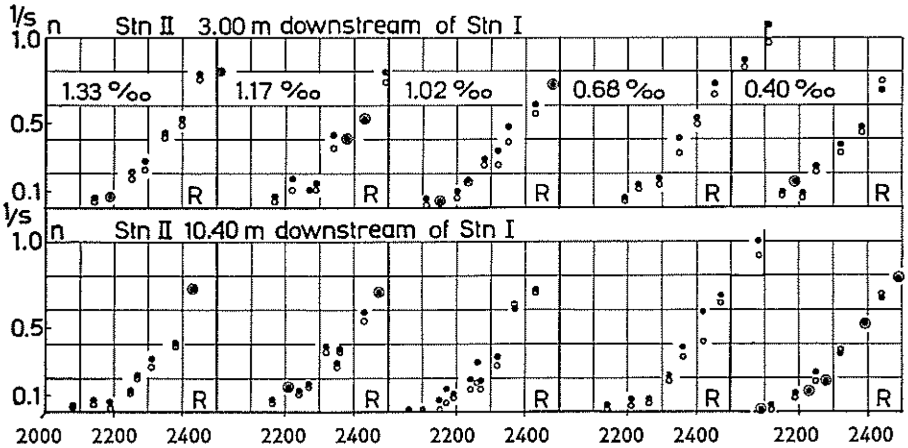

Fig. 4.8. Diagrams showing development of the flash frequency during 3.00 m and 10.40 m long passages through the 10.31 mm tube as a function of the Reynolds number in flow of bentonite sols of various concentration. The disturbance plate was adapted at 0.25 mm distance from the tube inlet. Dots represent the number of flashes per unit time recorded at Stn. I while circles represent those appearing at Stn. II.

The primary numerical data of the recorded observations are reported in Table 4.1 where Q = rate of flow, t = temperature, $n_1 = n_2$ = number of flashes per unit time appearing at Stn. I respectively Stn. II, U_F = mean speed of the flashes. In each record the flash frequencies n_1 and n_2 are counted on strip lengths equal to each other but shifted a length corresponding to the time interval determined necessary for the flashes to travel the distance between the Stns. I and II. The variation of the flash velocity in each record in no case was observed larger but mostly less than 4 %.

Fig. 4.8 illustrates the appearance of flashes for flow of the various bentonite sols through the 10.31 mm tube at the two locations of Stn. II as read from Table 4.1. The Stn. I records are marked with dots while the records of Stn. II are marked with circles. No systematic difference in the appearance of flashes due to varying bentonite concentration can be traced by the records in the figure. This suggests that pure water ought to behave in the same manner as the bentonite sols provided that the chosen method for defining the viscosity of the sols is appropriate in evaluating data of observations regarding the transition phenomenon.

The lowest Reynolds number recorded, at which turbulent flashes ever appeared in the experiments, is $R \approx 2060$ observed for flow of the 1.02 ‰. The next lowest values being $R \approx 2080$ and 2090 observed for flow of 1.33 and 0.40 ‰ sols respectively. These R-values agree quite well with those obtained for flow of 1.10 and 5.80 ‰ bentonite sols through a 10.70 mm plexiglass tube in experiments performed previously. (See Part 2 pp. 47–48.) The static pressure head at the tube entrance in the previously reported experiments never exceeded about 1000 N/m^2 (0.01 bar) while in the present experiments this pressure was kept around 30000 N/m^2 (0.3 bar). This state of affairs indicates that the pressure head at the tube entrance is of minor importance with respect to the appearance of turbulence in the case of high disturbance level of the entry flow, though it was found to be important in the case of low-disturbed entrance flow conditions (see Part 2, pp. 39–40).

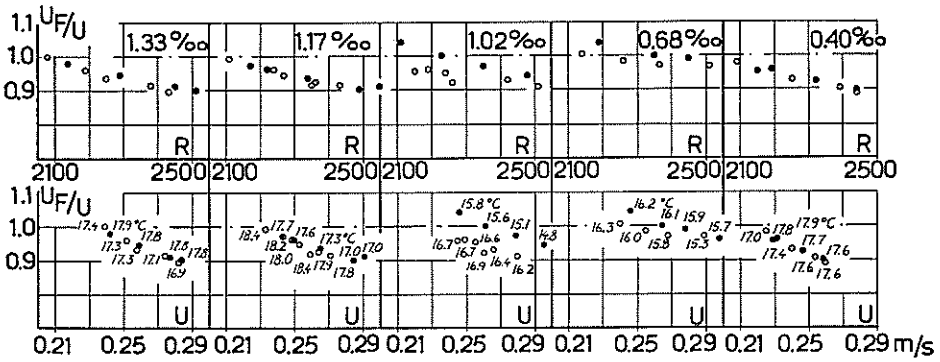

Fig. 4.9. The relative flash velocity U_F/U as a function of the Reynolds number R, and the mean flow velocity U under the same flow conditions as described in connection with Fig. 4.8. U_F = the velocity of the aft end of the turbulent flashes.

According to Fig. 4.8 there exist random damping effects of the turbulent flashes up to Reynolds numbers of 2300–2500. The extension of the travelling distance for the flashes from 3.0 to 10.4 m does not induce any noticeable effect of the number of fading flashes relative to the total number, although the irregular behaviour of the disturbances prevents any definitive judgement in this respect. The experiences suggest, however, that there does not exist any definite limit of the Reynolds number above which there is no damping effect of the turbulent fluctuations. On the other hand no systematic damping effect of the flashes is observed even at the Reynolds numbers where long ranging flashes first appear.

In Fig. 4.9 is shown the quotient between the flash velocity U_F and the mean flow velocity U plotted against both the Reynolds number R and the mean flow velocity U for the various bentonite sols. Evidently the flashes travel with velocity values around the mean flow velocity. It is to be noted that the relative flash velocity values plotted in Fig. 4.9 are referred to the aft end of the flashes. Above Reynolds numbers of about 2400, single flashes are observed to extend their lengths and also to split into several units, the front velocity of the flashes beginning to increase relative to the velocity of the aft end of the flashes.

By comparison of the diagrams in Fig. 4.9 it appears that the U_F/U values are more consistently related to the Reynolds number than to the mean flow velocity. It is, however, peculiar that the relative velocities obtained for the flashes in flow of the 1.02 and 0.68 bentonite sols in some cases appear higher than the flash velocities according to the other diagrams. I have not been able to unveil measuring errors which possibly could explain those deviations. For the present this peculiarity cannot be analyzed but has to be left open for further inquiry.

Development of disturbances in flow of 0.40 ‰ bentonite sol through cylindrical tubes of various diameters

Previously, it was reported (Part 2) that turbulence appeared at lower Reynolds numbers in flow through wider tubes than in narrower ones. The present experiments were undertaken as a direct continuation of those. The investigation was carried out

Table 4.2. The same flow data as those in Table 4.1 but for tubes of other diameters.

	6.01 mm tube. Stn. I located 0.93 m from the tube inlet						8.18 mm tube. Stn. I located 1.21 m from the tube inlet						12.31 mm tube. Stn. I located 1.78 m from the tube inlet					
	$Q \cdot 10^6$ m³/s	t °C	$100\,n_1$ 1/s	$100\,n_2$ 1/s	U_F tail m/s	U_F front m/s	$Q \cdot 10^6$ m³/s	t °C	$100\,n_1$ 1/s	$100\,n_2$ 1/s	U_F tail m/s	U_F front m/s	$Q \cdot 10^6$ m³/s	t °C	$100\,n_1$ 1/s	$100\,n_2$ 1/s	U_F tail m/s	U_F front m/s
	Stn. II 1.80 m from Stn. I						Stn. II 2.40 m from Stn. I						Stn. II 1.82 m from Stn. I					
1	13.3	18.4					18.6	18.6					28.3	19.2				
	12.9	18.4					18.0	18.7					26.7	19.1				
	12.6	18.5	(200)	(200)	0.396		17.4	18.8	?	?	0.301		26.0	19.0	61	64	0.196	
	12.4	19.1	183	183	0.388		16.9	18.8	50	72	0.295		25.3	18.9	43	46	0.192	
	12.2	18.6	150	150	0.388		16.3	19.1	29	28	0.287		24.8	18.8	23	28	0.186	
	11.9	18.6	91	88	0.388		15.8	19.2	15	16	0.279		24.3	18.6	15	17	0.184	
	11.5	18.7	55	48	0.381		15.2	19.2	7	7	0.274		23.7	18.5	5	5	0.183	
	11.2	18.8	17	12	0.381		14.6	19.3	2	2	0.271		23.1	18.3	2	2	0.182	
	10.7	18.9	12	7	0.375								22.8	18.2	0	0	—	
	10.5	19.0	0	0	—													
	Stn. II 3.52 m from Stn. I						Stn. II 3.29 m from Stn. I						Stn. II 3.57 m from Stn. I					
2	13.3	19.3					18.4	19.4					26.7	18.2				
	12.9	|					17.7	|					25.9	17.7				
	12.6	19.3					17.1	|	97	∞	0.292		25.5	17.9				
	12.2	19.4	(140)	(137)	0.378		16.5	19.4	38	39	0.286		24.8	18.0	39	47	0.192	
	11.8	|	141	134	0.366		16.0	19.5	19	21	0.282		24.3	18.2	34	38	0.192	
	11.5	19.4	91	81	0.366		15.5	19.5	6	6	0.276		23.8	18.2	8	8	0.188	
	11.2	19.5	58	45	0.360		15.0	19.6	2	2	0.271		23.4	18.3	18	20	0.187	
	10.8	|	25	15	0.360		14.5	19.6	0	0	—		22.9	18.4	3	3	0.183	
	10.5	19.5	5	2	0.357								22.5	18.5	7	8	0.181	
	10.2	19.6	8	1	0.351								22.2	18.6	2	3	0.178	

	Stn. II 6.21 m from Stn. I						Stn. II 8.25 m from Stn. I						Stn. II 6.14 m from Stn. I					
	13.5	17.3					18.7	19.6					28.8	18.1				
	13.1	17.4					18.1	19.6					27.0	18.3				
	12.9	17.6					18.0	19.7					25.6	18.8				
	12.6	17.8	(174)	(179)	0.390		17.6						24.3	19.4	49	51	0.189	
3	12.2	17.9	123	121	0.390		17.1						23.7	19.6	24	26	0.189	
	11.8	18.0	77	69	0.380		16.6		74	89	0.282		23.2	19.8	14	14	0.187	
	11.5	18.1	46	43	0.380		16.1		20	28	0.277		22.8	19.8	21	23	0.184	
	11.1	18.4	22	14	0.371		15.5		5	5	0.271		22.4	19.9	14	13	0.180	
	11.0	18.2	19	12	0.371		15.0		1	0	—		22.0	19.9	5	0	—	
	10.7	18.5	8	1	0.379		14.3	19.7	0	0	—		21.9	20.0	8	6	0.183	

	Stn. II 10.89 m from Stn. I						Stn. II 10.69 m from Stn. I						Stn. II 10.47 m from Stn. I					
	13.1	18.0					19.2	18.4					28.4	20.2				
	12.3	18.4	(161)	(171)	0.382	(0.389)	18.0	18.5					27.0	20.1				
	12.2	19.4	(227)	(230)			17.5	18.6	101	129			26.0	19.9				
	12.0	18.6	132	134	0.376	0.380	17.1	18.7	65	99	0.287	0.300	25.2					
	11.7	19.0	132	124			16.6	18.8	48	69	0.281	0.292	24.6				0.190	0.199
4	11.6	18.8	70	67	0.371	0.374	16.0	18.9	25	28	0.276	0.278	23.8	19.9	35	33	0.187	0.189
	11.2	18.9	51	44	0.366	0.367	15.8	19.0	8	8	0.274	0.275	23.2	20.0	28	30	0.185	0.186
	11.0	19.3	47	38	0.361	0.365	15.6		5	5	0.274	0.274	22.8	19.9	22	18	0.182	0.183
	10.8	19.0	17	12	0.361	0.361	15.2	19.0	1	1	0.270	0.272	22.5	19.9	3	3	0.181	0.182
	10.4	19.1	8	2	0.357	0.359	14.8	19.1	3	3	0.260	0.260	21.8	19.8	8	5	0.180	0.180

	Stn. II 10.97 m from Stn. I						Stn. II 10.69 m from Stn. I					
	14.7	18.5					19.5	16.8				
	13.6						18.7	17.1				
	13.2	18.5					18.1	17.2				
	12.9	18.6					17.6	17.3				
5	12.3	18.7	(167)	(197)	0.387	0.401	17.1	17.4	77	104	0.293	0.302
	11.8	18.7	76	70	0.376	0.378	16.5	17.5	27	29	0.285	0.288
	11.4	18.8	48	39	0.371	0.372	15.7	17.6	7	7	0.279	0.280
	10.9	18.9	18	15	0.366	0.366	15.3	17.7	5	3	0.276	0.276
	10.5	19.0	6	4	0.357	0.358	14.8	17.8	0	0	—	—

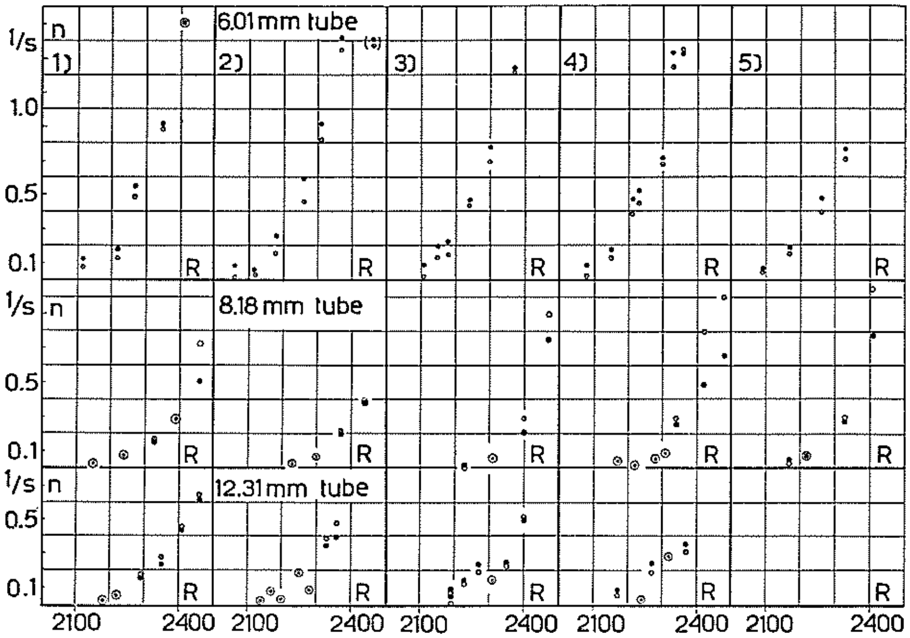

Fig. 4.10. The development of the flash frequency during various tube passages (see Table 4.2) for flow of 0.40‰ bentonite sol. In each case the disturbance plate was situated 0.25 mm from the tube inlet. Dots represent the flash frequency at Stn. I and circles that at Stn. II.

on flow of the 0.40‰ bentonite sol as being closest to pure water, even though the experiments of the previous section indicated no observable influence on the transition process by the presence of bentonite, when the concentration was below 1.3‰.

The measurements were carried out in the same way as those described in the preceding section, by use of the 6.01; 8.18 and 12.31 mm tubes (see Figs. 4.4 and 4.5). Stn. I was placed respectively 0.93 m (155 tube diameters d); 1.21 m (148d) and 1.78 m (145d) from the tube entrance, while Stn. II was located at four positions along each tube as shown in Table 4.2 which contains the recorded flow data, showing the development of the turbulent flashes as they travel along the tubes. In Fig. 4.10 dots represent the flash frequencies at Stn. I, while circles indicate the corresponding flash frequencies at Stn. II as read from Table 4.2.

The records of Figs. 4.8 and 4.10 show that the first turbulent flashes appear at a Reynolds number $R \approx 2000$–2050 in flow through the 6.01 and 10.31 mm tubes, whereas no flashes were observed to appear below Reynolds numbers of $R \approx 2140$ for flow in the 8.18 or 12.31 mm tubes while general turbulence established itself at Stn. I in the flow through all the tubes at a Reynolds number of about 2700–2900. No systematic relations between tube diameter and the appearance of turbulence were obtained in these experiments in contradistinction to those reported in Part 1.

Also the records of Fig. 4.10 do not indicate any systematic damping effect of the flashes as depending on the travelling distances, thus confirming the observations reported in the previous section for flow through the 10.31 mm tube. It is, however, remarkable to note the characteristic difference of the damping effect of the turbulent

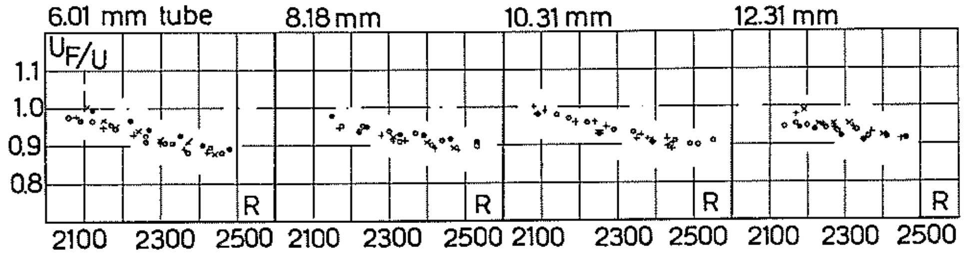

Fig. 4.11. The relative flash velocity U_F/U as a function of the Reynolds number in flow of 0.40 ‰ bentonite sol for various tube passages under the same conditions as described in connection with the Figs. 4.8 and 4.10. (The diagram for flow through the 10.31 mm tube also contains the flash velocity values in flow of 1.33 and 1.17 ‰ bentonite sols as shown in Fig. 4.9.)

flashes when the records of the flow through the 6 and 10 mm tubes are compared with those of the 8 and 12 mm tubes if we also consider the appearance of the tube surfaces shown in Fig. 4.5. Evidently the damping factor is most active in the flow through the 6.01 mm tube while the damping effect is not quite so pronounced for flow in the 10.31 mm tube. However, in the flow through the 8.18 mm and 12.31 mm tubes scarcely any damping effect at all is to be observed. Instead there is mostly to be noted an increase of the number of turbulent flashes implying that single flashes might develop to several units as they travel along the tube, even at quite moderate Reynolds numbers ($R \approx 2200$). This behaviour has a very important bearing on the turbulence maintaining processes if we consider the rough appearance of the 8 and 12 mm tube surfaces as compared to the relative smoothness of the 6 and 10 mm tubes (all these tubes are to be classified as "technically smooth"). Here it should be remarked that an increase of the number of flashes does not mean that new flashes spontaneously spring into existence by themselves during the flow tube passage. Instead it is found that new flashes appear as the result of flash fronts travelling faster than the tails. In this way a flash might extend itself during the tube passage, but instead of forming a continuous turbulent streak it splits into two or more flash units. This behaviour was, however, observed only at high levels of entrance disturbances. In case of low disturbance levels of the entrance flow, so that flashes appear first at higher Reynolds numbers, they do not split into several units when extending their lengths, but form continuous turbulent streaks.

Here I want to remind of similar observations reported in Part 2, where the damping effect of turbulent flashes in flow of 1.6 ‰ bentonite sol through a 6.55 mm tube ceased at a Reynolds number of $R \approx 2200$, the surface of the technically smooth tube being "very rough" as shown in Fig. 2.2, while a distinct damping effect was observed even at quite high Reynolds numbers in flow through a smoother 10.70 mm tube, although at the time this effect could not be excluded as due only to the high bentonite concentration (5.8 ‰) of the sol used in that series of observations. The variation of the damping effect of the turbulent flashes with variation of the roughness grade, even of technically smooth tubes, might account for some variations of the "critical" Reynolds number determined by means of pressure drop measurements performed by various authors.

In Fig. 4.11 is plotted the quotient U_F/U, U_F being the velocity of the aft end of the flashes, versus the Reynolds number R according to data given in Tables 4.1

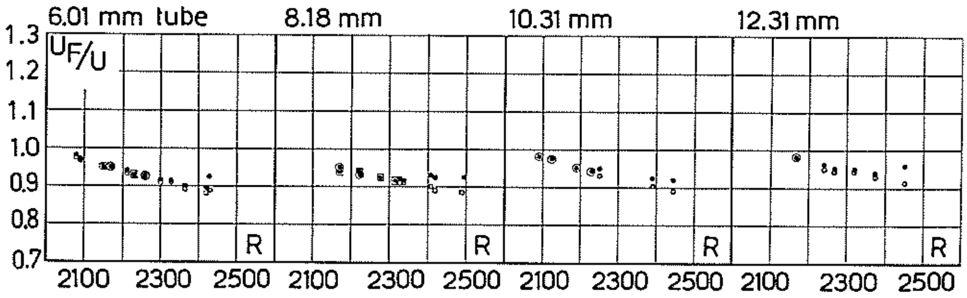

Fig. 4.12. Comparison between the relative velocity of the fore and aft ends of turbulent flashes in flow of 0.40‰ bentonite sol under the same flow conditions as described in connection with Fig. 4.11. U_F = flash velocity, U = mean flow velocity. Filled dots represent front velocities while open dots represent tail velocities.

and 4.2. The data reported for the 10.31 mm tube in Fig. 4.11 (Table 4.1) include the flash velocity in flow of the bentonite sols of 1.33, 1.17 and 0.40‰ concentration shown previously in Fig. 4.9.

The reported observations suggest that the quotient U_F/U (aft end of the flashes) versus the Reynolds number R in the main is independent of microscopic variations of the surface roughnesses (technically smooth tubes) as well as of the concentration of the bentonite sols (for concentrations less than 1.33‰).

In Fig. 4.12 is plotted the quotient U_F/U versus the Reynolds number both for the fore and aft ends of the flashes in flow of 0.40‰ bentonite sol through the various tubes in accordance with primary data reported in the Tables 4.1 and 4.2. The purpose was to determine the variation of the front velocity relative to the velocity of the aft end of the flashes. As the records clearly showed that any difference should be quite low, the investigation was carried out only on the longest measuring distances.

We see in the diagrams of Fig. 4.12 (filled dots and squares represent the front velocity) that in comparison to the tail velocity a noticeable increase of the front velocity appears above Reynolds numbers of $R \approx 2300$–2400 while no distinct difference is observable at lower Reynolds numbers. The flash development at higher Reynolds numbers cannot be read from the records reported in Tables 4.1 and 4.2.

The front and tail velocities of turbulent disturbances at higher Reynolds number

For this purpose the inlet end of the 6.01 mm tube was formed to the shape of a trumpet mouth by use of a brass form and hot water. The trumpet shown in Fig. 4.13*a*, was situated within the levelling container 3 in Fig. 4.1 and the disturbance plate was removed. By this arrangement the entrance disturbance level decreased and no flashes appeared in the flow (0.40‰ bentonite sol) below Reynolds numbers of $R \approx 2700$. Stn. I was situated 0.89 m from the inlet of the tube mouth and Stn. II was situated 8.50 m downstream of Stn. I.

In Fig. 4.14 is shown a part of a typical record obtained under the present circumstances at a Reynolds number of $R \approx 2860$. The upper trace is due to Stn. I while the lower trace belongs to Stn. II. The record shows the elongation of an originally

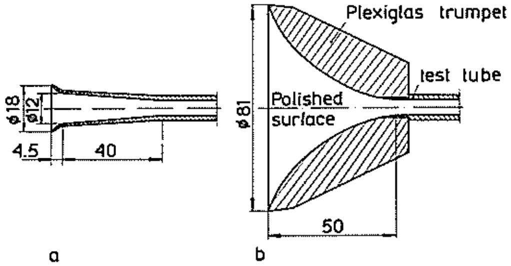

Fig. 4.13. Two inlet trumpets to the 6.01 mm tube designed with the purpose of avoiding entry flow disturbances. The trumpet in figure *a* proved more efficient, suppressing turbulence up to Reynolds numbers $R \approx 2650$, whereas turbulent flashes appeared already at $R \approx 2370$, when the tube was equipped with the trumpet shown in figure *b*.

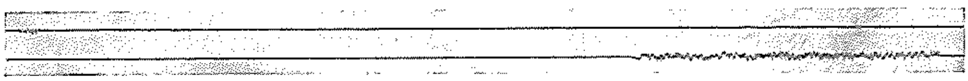

Fig. 4.14. Oscillogram showing the elongation of a flash forming a turbulent streak in flow of 0.40‰ bentonite sol during an 8.50 m long passage through the 6.01 mm tube equipped with the trumpet shaped inlet shown in Fig. 4.13*a* and with the disturbance plate removed. The Reynolds number of this flow is $R \approx 2860$ at a temperature of 18.0°C. The mean flow velocity is 0.52 m/s, the velocity of the flash front 0.60 m/s, and the velocity of the tail of the flash is 0.42 m/s.

short flash in forming a turbulent streak similar to the development of turbulent flashes along the regularly, artificially roughened tube surface reported in Part 3 of the paper. In the record of Fig. 4.14 the front velocity of the flash is evaluated to be 0.60 m/s while its aft velocity is 0.42 m/s at a mean flow velocity of 0.52 m/s.

The results of the experiments are recorded in Table 4.3 and are illustrated in the diagrams *a* and *b* of Fig. 4.15, which also contains the data obtained of the flash

Table 4.3. Determination of the velocity of the fore and aft ends of turbulent regions in flow of 0.40‰ bentonite sol through the 6.01 mm tube equipped with the trumpet-shaped inlet shown in Fig. 4.13*a*.

$Q \cdot 10^6$ m³/s	t °C	$\nu \cdot 10^6$ m²/s	R	U m/s	U_F front m/s	U_F tail m/s
13.7	17.4	1.105	2630	0.483	no turbulence	
14.4	17.5	1.101	2770	0.508	0.570	0.421
15.8	17.5	1.101	3040	0.557	0.675	0.438
16.8	17.7	1.096	3250	0.592	overlapping turb. regions	
13.9	18.0	1.088	2700	0.490	0.515	0.408
14.2	18.0	1.088	2760	0.501	0.553	0.413
14.7	18.0	1.088	2860	0.518	0.596	0.419
15.3	18.1	1.085	2990	0.539	0.643	0.426
15.6	18.2	1.083	3050	0.550	0.680	0.433
16.0	18.2	1.083	3130	0.564	0.707	0.440
16.2	18.2	1.083	3170	0.571	0.727	0.444

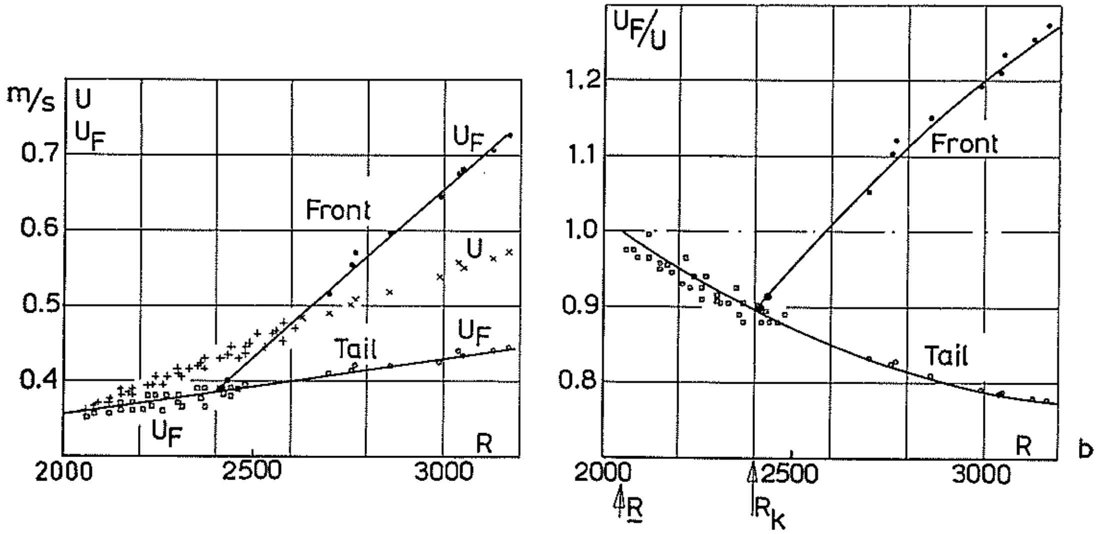

Fig. 4.15. The velocity U_F of the fore and aft ends of turbulent disturbances in flow of 0.40‰ bentonite sol of the mean flow velocity U through the 6.01 mm tube, the travelling distance being 8.50 m. Flow conditions described in connection with Fig. 4.14. Black dots represent the velocities obtained for the fore end of the flashes and circles the corresponding velocities of their aft end. Around the flow region $\underline{R} > R > R_k$ the flash tail velocity is marked by open squares. The mean flow velocity U of each test run is marked by a cross.

velocity, in flow of highly disturbed entrance flow conditions, previously shown in Figs. 4.11 and 4.12.

There appear almost rectilinear relations between the velocities U_F of the flash fronts and tails and the Reynolds number R according to Fig. 4.15*a*. However, the limitation of the temperature range of the experiments prevents any judgment in this matter. We see from the diagrams in Fig. 4.15*b* that the values obtained of the tail velocity at higher Reynolds numbers form a smooth continuation of the velocity values previously obtained for flashes at lower Reynolds numbers under highly disturbed entrance flow conditions.

According to Fig. 4.15 flashes appear at a lowest possible Reynolds number at which the flash velocity U_F is about the same as the mean flow velocity U, which velocity it does not seem to exceed. This Reynolds number, at which the first self-maintaining flashes appear, was previously (Part 2) symbolized by $\underline{R}$, which according to the interpretation of Fig. 4.15 in the present case should have the value $\underline{R} \approx 2050$ which value agrees with direct observations reported on p. 88. Above the $\underline{R}$ value is a region in which the flashes proceed with, in general, unaltered dimensions at decreasing relative velocity U_F/U. After exceeding certain Reynolds numbers, however, the fronts of the turbulent disturbances begin to travel faster than their aft parts, elongating themselves as they proceed along the tube. This process means a continuous generation of new turbulence causing an increase of the energy dissipation in the flow. The Reynolds number at which this development of the turbulent disturbances sets in seems to have approximately the same value as the generally adopted critical Reynolds number R_k, at which is observed an increase of the pressure drop for flow in tubes and channels. It is interesting to note that the elongation of turbulent streaks in flow of water through tubes at high Reynolds numbers was reported already by Prandtl-Tietjens in their *Hydro- und Aeromechanik* (1931, Vol. II, p. 40):

"Dieser 'Turbulenzpropfen' schiebt sich dann durch das Rohr, wobei das stromabwärts befindliche Ende etwa mit der durchschnittlichen Geschwindigkeit $\bar{u}$, das stromaufwärts befindliche Ende mit geringerer Geschwindigkeit durch das Rohr fliesst. An diesem Ende bauen sich nämlich dauernd neue Turbulenzgebiete an, so dass der turbulent strömende Teil beim Durchfliessen des Rohres allmählich grösser wird."

Evidently, the Prandtl–Tietjens' estimation of the front and tail velocities of the turbulent flashes does not agree with the values determined in the present experiments, which discrepancy, however, very well is to be explained as due to their very primitive method of measurements and perhaps also by the fact that they used a glass tube which certainly possessed smoother surfaces than the plastic tubes used in the present experiments.

Here is also the place to confirm the Prandtl–Tietjens' report of pulsating flow at high Reynolds numbers as being due to the elongation of turbulent flashes during the tube passage increasing the pressure drop and decreasing the rate of flow so that the formation of new flashes is prevented until the turbulent flow region begins to leave the tube through the outlet end. Then the rate of flow again begins to increase until a new flash appears, repeating the same flow cycle. This phenomenon was frequently observed during the present experiments. The flow pulsations decrease in magnitude and increase in frequency according as the number of turbulent disturbances increases with increasing Reynolds numbers of the flow, provided the inlet flow conditions are unaltered. The intermittent appearance of the turbulent disturbances within any transition regions is, however, preserved even in the case of constant rates of flow, as also was observed already by Reynolds 1883 and later (on flow of air) by J. Rotta 1956.

The experiments reported in this and the previous sections evidently seem to indicate that even microscopic surface roughnesses of the tube walls should be of major importance with respect to the turbulence maintaining processes. However, the experiments further suggest that some other quite unknown factors might be of importance, at least in connection with the maintaining processes of turbulent flashes in the flow regions $\underline{R} < R < R_k$, where the flashes proceed with, in the main, unaltered lengths.

Allowing a long enough travelling distance from the tube entrance it would seem likely that continuous turbulence should establish itself sooner or later in the flow as soon as the Reynolds number $R \geq R_k$ provided turbulent flashes ever appear. Taking account of the observations of the development of single turbulent streaks and flashes into several discrete flash units, that takes place around the R_k value, it appears, however, that continuous turbulence will not establish itself anywhere in the tube, however long development lengths are allowed for, unless $R > \bar{R}_k$ where $\bar{R}_k$ is the upper critical Reynolds number, above which each turbulent flash begins to elongate itself, as it travels, without splitting into several units ($R_k < \bar{R}_k$).

The experiments show that in the case of low disturbance levels at the tube inlet, the disturbance vortices might break down to turbulent flashes at higher Reynolds numbers rather far downstream from the tube inlet. Provided $R > \bar{R}_k$ each turbulent flash elongates itself as it travels downstream and if the tube is long enough and the disturbances follow each other closely enough, continuous turbulence will appear sooner or later in the tube. We thus understand that even when turbulent flashes do not appear near the tube entry unless $R \gg \bar{R}_k$, as in the present case, pressure drop experiments performed on test sections of a suitable long tube and situated at increasing distances from the tube inlet, would indicate decreasing R_k values, and if extrapolated, perhaps tending towards the actual R_k value for flow of high entry disturbance level through the same tube. This state of matters explains the experimental results due to Schiller 1924 according to which there was a tendency to approach the R_k value of "fully" disturbed entrance flow, even in the case of flow of low entrance disturbance levels, by increasing the entry lengths.

Further determinations of the front velocity of turbulent regions

The front velocity of turbulent regions was also determined on flow of 0.40‰ bentonite sol through the 8.18 mm tube but this time by instantaneous opening of the—for a moment closed—cock 14*A* in Fig. 4.1, at various preadjusted flow velocities, measuring the time necessary for the turbulence front to travel from Stn. I (placed 1.22 m from the tube inlet which was furnished with the disturbance plate) to Stn. II placed alternatively at 0.50; 0.89; 1.70 and 2.40 m distance from Stn. I.

The records of Fig. 4.16 illustrate such starting processes for flow of 0.40 ‰ bentonite sol through the 6.01 mm tube and the progress of the disturbance front, the upper traces representing Stn. I and the lower Stn. II. Stn. I was placed 0.90 m from the tube inlet. In record *a* the Reynolds number is $R \approx 3960$ ($t = 19.3$°C), Stn. II being placed 10.92 m downstream of Stn. I. The Reynolds number is $R \approx 2280$ ($t = 19.1$°C) in record *b* and Stn. II was located 1.90 m downstream of Stn. I while corresponding data for record *c* are $R \approx 2060$ ($t = 19.6$°C), Stn. II 3.52 m downstream of Stn. I. It is to be noted that the initial disturbance in record *c* disappeared completely although in later parts of the same record there occur spontaneous flashes, which do not disappear within the distance observed. The wavy deflections of the oscillograph traces appearing in the beginning of the records are due to an oscillation caused by the instantaneous opening of the cock 14*A*. Such oscillations, possibly gravitational, were observed to travel several cycles forward and back in the liquid filled tubes after turning off the flow instantaneously by means of the cock 14*A*. Evidently, the records indicate that there does not occur breakdown of the laminar flow in the initial period during development of the parabolic velocity profile which might have been expected if the instability theory of small oscillations should be valid.

Immediately after the start, the velocity recorder indicated high rates of flow which gradually decreased with the progress of the disturbance front along the tube, approaching the stationary value when all the tube was filled with disturbed flow, corresponding to the actual state of equilibrium.

In Fig. 4.17 *a–d* are shown the results obtained from the measurements of the front velocity of the turbulent disturbances at various Reynolds numbers. Also the mean flow velocity U and its maximal value $2U$ (parabolic velocity profile assumed) are given in the diagrams. Each mean flow velocity is calculated from the arithmetic mean value of the rate of flow recorded during the corresponding time interval necessary for the disturbance front to cover the distance from Stn. I to Stn. II. (Also the Reynolds numbers are calculated on those mean flow values.) The height of the

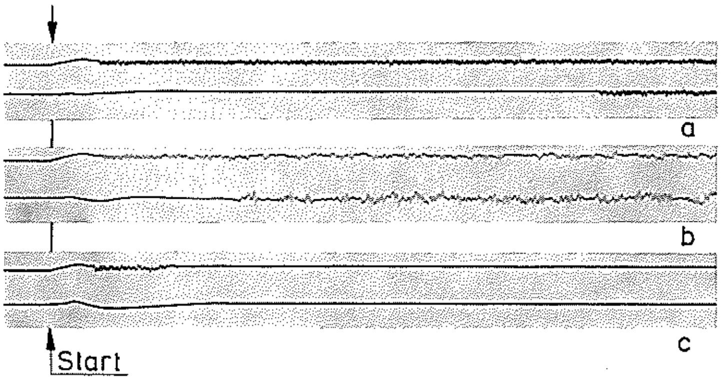

Fig. 4.16. Flow records obtained by instantaneous starting of the flow of 0.40‰ bentonite so through the 6.01 mm tube. The upper trace in each record is transmitted by Stn. I situated 0.90 m from the tube inlet while the lower trace is transmitted by Stn. II situated (*a*) 10.92 m downstream of Stn. I at a Reynolds number of $R \approx 3960$; (*b*) 1.80 m downstream of Stn. I, $R \approx 2480$; (*c*) 3.52 m downstream of Stn. I, $R \approx 2060$. The disturbance plate was situated 0.25 mm in front of the tube inlet.

bars in Figs 4.17 indicate the number of observations of each disturbance velocity. The widths of the bars indicate the uncertainty in the accuracy of the velocity values determined. The diagrams show that the disturbance fronts proceed with irregular velocities and further that this irregularity increases with decreasing Reynolds numbers. The disturbance velocity was never observed to approach the maximum velocity of the flow and further is noted that the disturbances often disappeared during the tube passage when the front velocity was some amount below the mean flow velocity. According to the diagrams, increasing travelling distances imply less spreading of the velocity values. This might be due to the fading away of slow initial disturbances during the passage of longer distances while such disturbances might be recorded when Stn. II is placed not too far from Stn. I.

The mean values of the front velocities of the turbulent regions shown in the diagrams of Fig. 4.17 are transformed in Fig. 4.18 to show the front velocity of the turbulent disturbances as a function of the Reynolds number. There is also shown a curve representing the velocity of the aft end of flashes in flow through the same 8.18 mm tube according to Fig. 4.11. In Fig. 4.18 is noticeable a remarkably wide spreading of the front velocity of the turbulent regions when compared to the determinations presented previously. The front velocity values situated below the solid curve (which represents the flash tail velocities, according to Fig. 4.11) are readily explained as obtained for slow moving entrance disturbances that disappear during the tube passage (see Fig. 4.16*c*) and are not compatible with the behaviour of selfmaintaining turbulent flashes. These extremely low front velocities were observed only for the two shortest measuring distances where the front velocity values obtained, according to Fig. 4.17*a*, *b*, show a higher degree of spreading than the velocities recorded for the longer travelling distances as shown in Fig. 4.17*c*, *d*. In the main these observations confirm the results obtained for flow through the 6 mm tube as reported in Fig. 4.15 though the R_k value (at which the flash fronts begin to travel faster than the tails) for flow through the 8 mm tube rather tends towards $R_k \approx 2200$ than to the value $R_k \approx 2400$ obtained for flow through the smoother 6 mm tube.

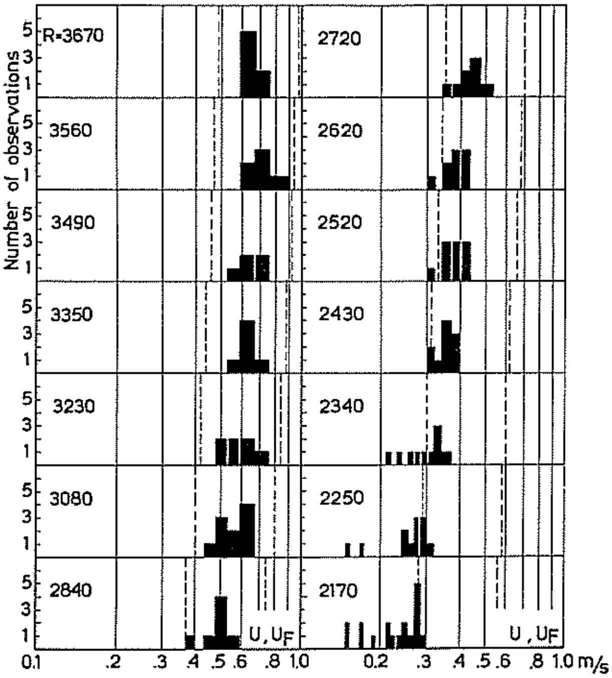

Fig. 4.17*a*. Determination of the front velocity of turbulent regions in flow of 0.40 ‰ bentonite sol through the 8.18 mm tube with the disturbance plate situated 0.25 mm in front of the tube inlet. The flow was started by instantaneous opening of the plugcock 14*A* in Fig. 4.1. The time necessary for the turbulent flow front to travel from Stn. I, situated 1.22 m (149 tube diameters) from the tube inlet, to Stn. II, situated 0.50 m further downstream, was measured by watching the signal outputs on the oscilloscope screen, while the rate of flow was recorded during the same time period. The liquid temperature varied from 18.0 to 19.5°C during this series of measurements.

The mean flow velocity U and its double value (parabolic velocity profile assumed) are indicated by dotted vertical lines. The height of each bar in the diagrams indicates the number of observations made of the corresponding front velocity U_F of turbulent flow regions, while the width of each bar indicates the uncertainty in the velocity determination. Logarithmic velocity axis.

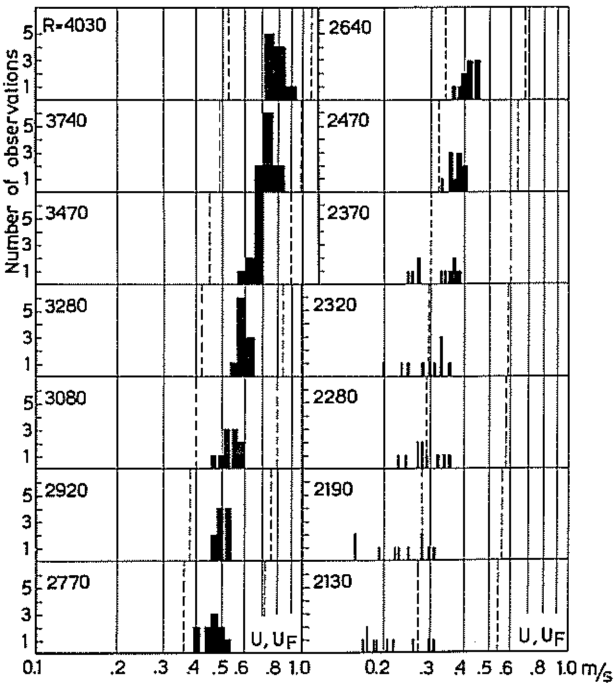

Fig. 4.17*b*. Same as in Fig. 4.17*a* except that Stn. II was placed 0.89 m downstream of Stn. I. Temperature range: 18.4→20.2°C.

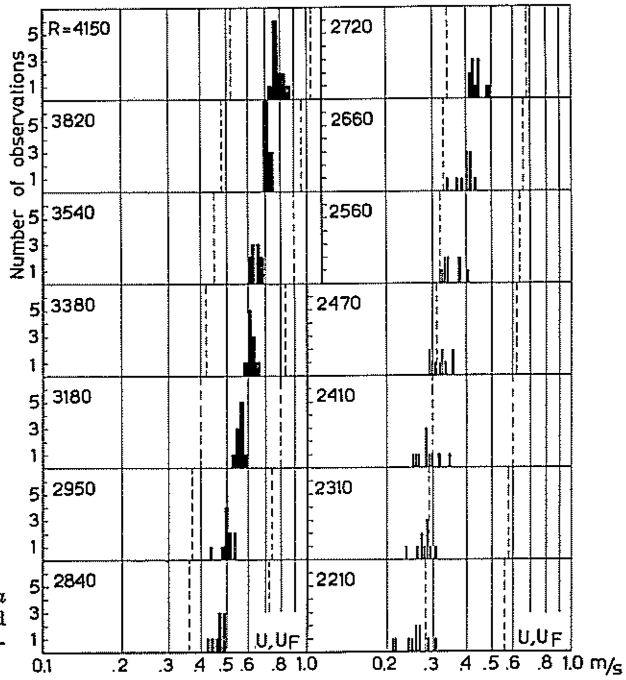

Fig. 4.17*c*. Same as in Fig. 4.17*a* except that Stn. II was placed 1.70 m downstream of Stn. 1. Temperature range: 19.9→20.7°C.

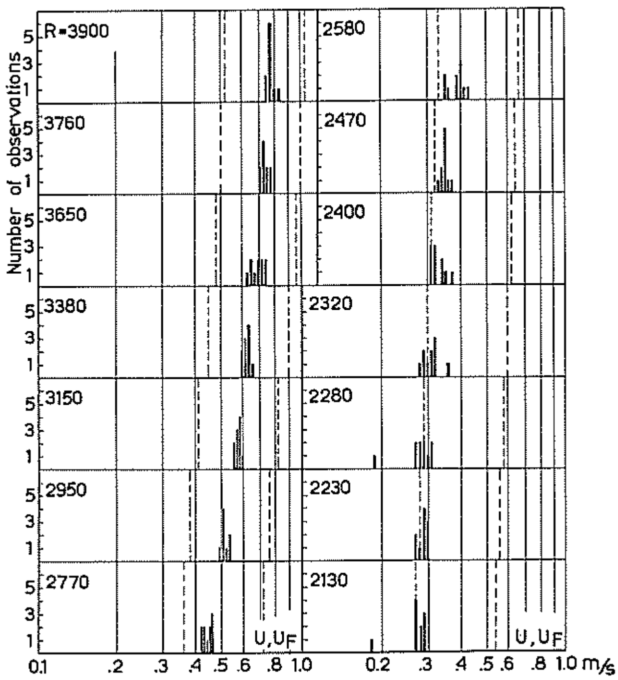

Fig. 4.17*d*. Same as in Fig. 4.17*a* except that Stn. II was placed 2.40 m downstream of Stn. I. Temperature range: 18.1→20.0°C.

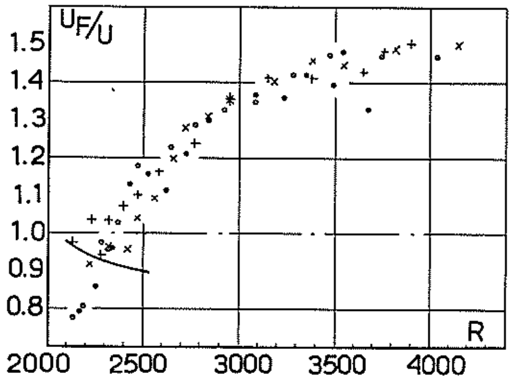

Fig. 4.18. The diagrams of Fig. 4.17*a–d* inverted to show the relative disturbance front velocity U_F/U (U_F = front velocity; U = mean flow velocity) as function of the Reynolds number R. The solid drawn curve represents the corresponding velocities of the aft end of turbulent flashes as shown in Fig. 4.11 for flow through the same 8.18 mm tube.

The wide spreading of the velocity data for flow through the 8 mm tube as compared to the well collected data of the flow through the 6 mm tube might be interpreted as due to the forced agitation of the turbulence by the instantaneous starting of the flow in the former case while in the latter case the turbulent regions appear spontaneously.

From the observations reported we conclude that the disturbance front velocity only asymptotically might approach twice the value of the mean flow velocity, which is the maximum velocity of the parabolic velocity distribution. This state of matters implies that, at any R value, some fluid loses its turbulence at the fore end of turbulent regions while at the aft end laminar flow becomes turbulent. This process is specially pronounced in the region $\underline{R} < R < R_k$, where the flashes proceed with unaltered lengths at velocities lower than the mean flow velocity.

I cannot see any other reasonable explanation of the experimental indications described than that the turbulence maintaining processes at least to some extent must depend on wall effects (see pp. 88–89) as was also indicated by the experiments reported in Part 3 of this paper. It is, however, to be pointed out that this interpretation is not quite in agreement with the viscous layer hypothesis.

Some special experimental observations

In experiments recorded in Fig. 4.15 no turbulent disturbances at all were observed up to Reynolds numbers of $R \approx 2650$ by using the trumpet shaped tube inlet of the 6 mm tube shown in Fig. 4.13*a*. Mr. Ramgard, when assisting in the experiments, proposed a "better" shaped tube inlet with the purpose of obtaining still higher Reynolds numbers without the appearance of turbulent disturbances. He was given a free hand to make a most favourably shaped tube inlet, and produced the plexiglass trumpet shown in Fig. 4.13*b* with carefully polished surfaces. In spite of these efforts turbulent flashes appeared in the flow already at Reynolds numbers of $R \approx 2370$, which, if we consider the shape of the tube inlet, implies a confirmation of earlier statements that laminar separation and flow contraction with the subsequent formation of vortices at the tube inlet might be one primary cause of the initiation of turbulence.

It is noteworthy that the $\underline{R}$ values for flow in the 8.18 and 12.31 mm tubes are distinctly higher than those obtained for the 6.01 and 10.31 mm tubes. This might be accidental, but a possible explanation is that the "rough" surfaces of the 8.18 and 12.31 mm tubes increase the wetted perimeter relative to the smoother surfaces of the 6.01 and 10.31 mm tubes. It seems likely that such an increase of the wetted perimeter should have a suppressing effect on the flow separation at the tube inlet while on the other hand an increase of the roughness grade also ought to lessen the damping effects of once initiated turbulent disturbances in full agreement with the observations made.

There still remains the problem whether only surface roughnesses of the tubes are crucial with respect to the maintenance of the turbulent flashes in the regions $\underline{R} < R < R_k$ or if other wall effects or quite other causes might be traced. An attempt to study this problem was made by observing the development of turbulent disturbances in tube flow agitated by a probe inserted in the flow as compared to the same flow in absence of the probe.

A cylindrical brass probe of 1 mm diameter could be inserted and removed, from the flow of 0.40‰ bentonite sol through the 8.18 mm tube, along a tube diameter at a distance of 1.13 m from the tube inlet (the disturbance plate was situated at 0.25 mm distance in front of the tube inlet). Stn. I was located 0.09 m downstream of the probe and Stn. II 10.63 m downstream of Stn. I. After establishment of stationary flow conditions at each rate of flow, records were obtained with and without the probe inserted into the flow. Fig. 4.19 shows the records when no probe was inserted into the flow. The upper traces are those from Stn. I and the lower ones are those from Stn. II, in each case shifted a distance corresponding to the time necessary for the turbulent disturbances to travel from Stn. I to Stn. II.

In Fig. 4.20 we observe that the flow 0.09 m downstream of the inserted probe appears fully turbulent at all the Reynolds numbers recorded. There is also to be observed a tendency of group formation in the continuous turbulent flow even at quite high Reynolds numbers at large distances from the origin of the disturbances. In Fig. 4.19 there is quite a similarity between the traces from Stn. I and Stn. II, indicating equilibrium flow conditions, but we also see that the traces of Stn. II in Fig. 4.20 look very similar to those of Fig. 4.19, indicating that the fully disturbed flow pattern close to the probe develops towards certain equilibrium states, which in the main seem to be determined by the general flow conditions.

In the records *e* ($R \approx 2350$) and *f* ($R \approx 2260$) of Fig. 4.19 is observed how some flashes have parted into several units after travelling the distance between Stn. I and Stn. II. This state of matters might be interpreted as a tendency to increasing turbulence by the action of the surface roughnesses. However, corresponding records of Fig. 4.20 show a decrease from continuous disturbed flow to approximately the same equilibrium state, as in the records of Fig. 4.19, of some few turbulent flashes per unit time. This state of matter suggests that besides the surfaces roughnesses or other wall effects the presence of some kind of various grades of response effects or dispositions within the liquid are necessary for the release and maintenance of turbulent flashes in liquid flow. In fact, the experiments have given me an impression that there is a certain similarity between the initiation and maintenance of turbulent flashes in viscous flow and the appearance of cavitation in liquids, both phenomena partly depending on the presence of some as yet unknown nuclei.

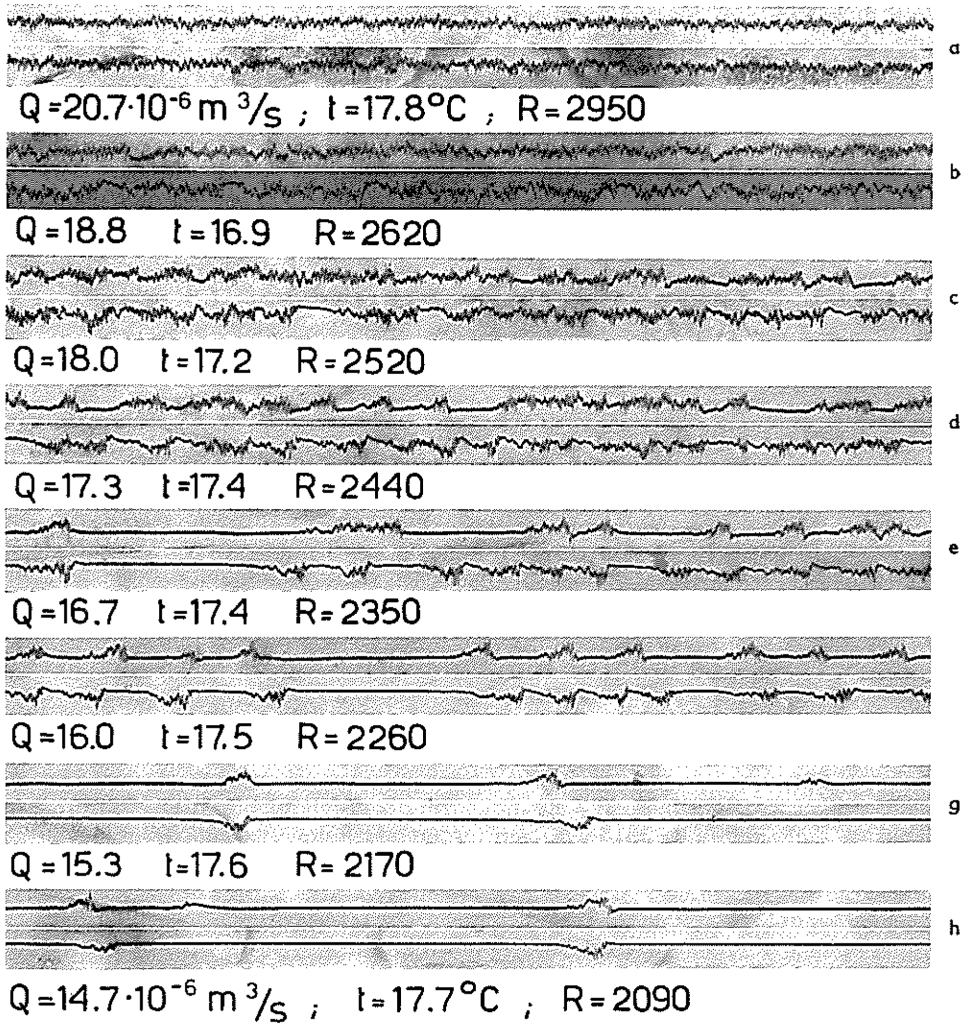

Fig. 4.19. Flow of 0.40‰ bentonite sol through the 8.18 mm tube, the upper trace being transmitted by Stn. I, situated 1.22 m from the tube inlet, while the lower trace is transmitted by Stn. II, situated 10.63 m further downstream. The disturbance plate is mounted 0.25 mm in front of the tube inlet. The traces of each record have been shifted lengths corresponding to the time interval necessary for the disturbance fronts to proceed from Stn. I to Stn. II.

SUMMARY

Experiments are described in which have been recorded observations of the development of turbulent flow disturbances at two stations simultaneously along rather long test tubes.

The experiments show that turbulent flashes to some extent might fade away during the tube passage for flow within a region $\underline{R} < R < R_k$, where $\underline{R}$ in each case is the lowest Reynolds number at which spontaneous turbulent flashes ever appear at larger distances from the tube inlet

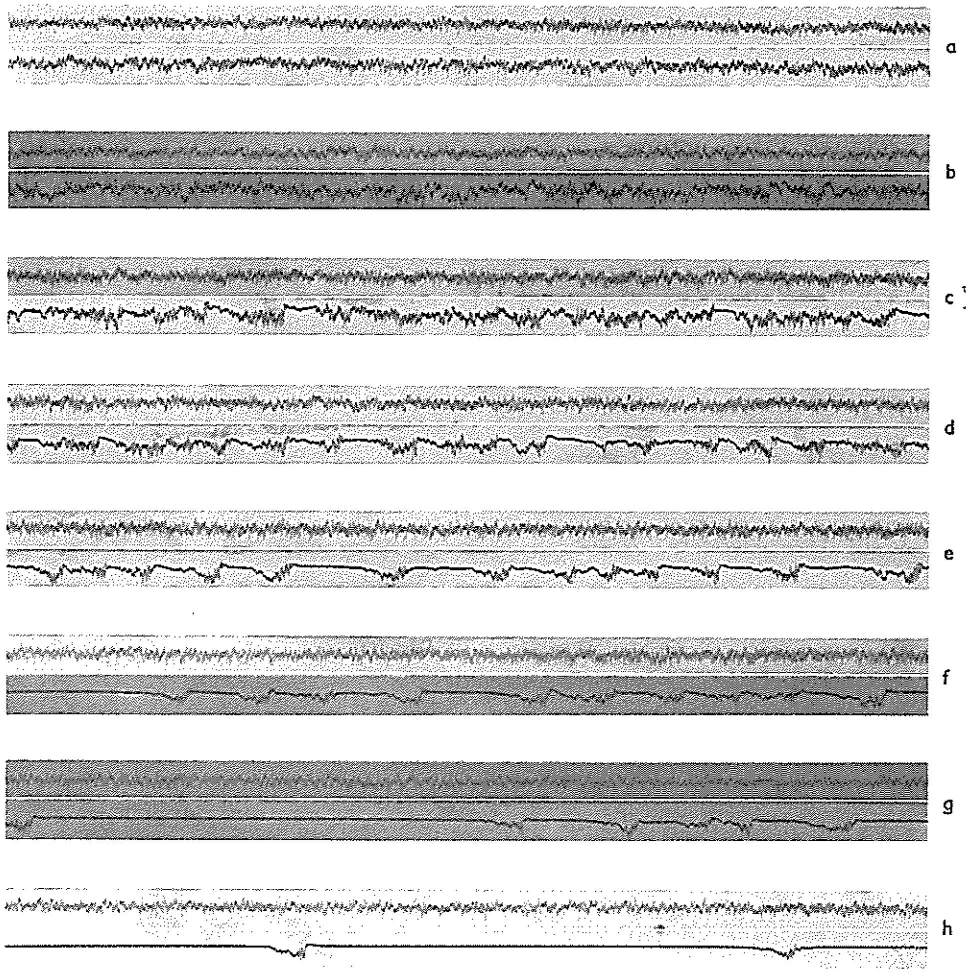

Fig. 4.20. The same flow as shown in Fig 4.19 except that a cylindrical brass pin of 1.0 mm diameter is inserted along a whole tube diameter located 0.09 m upstream of Stn. I.

and R_k is the Reynolds number at which the flashes begin to multiply during their travel through the tube, the net effect being an elongation of each original turbulent flash.

The value of the "critical" Reynolds number R_k appears to depend on the roughness grade of the tube surfaces even in the case of technically smooth tubes and agrees approximately with the "critical" Reynolds numbers at which is observed an "instantaneous" increase of the flow resistance coefficient according to several determinations of the pressure drop along tubes reported in the literature.

In the region $\underline{R} < R < R_k$ the turbulent flashes in the main proceed with unaltered lengths. Around the Reynolds number $\underline{R}$ the velocity of the flashes is about the same as the mean flow velocity. The velocity of the flashes relative to the mean flow velocity, however, decreases with increasing Reynolds numbers until the R_k value is approached. On further increasing the Reynolds number, the relative velocity of the fore end of the turbulent flow regions begins to increase noticeably while the relative velocity of their aft end proceeds to decrease in the same manner as before.

The upper critical Reynolds number $\bar{R}_k$ ($> R_k$) is the Reynolds number where each turbulent flash elongates itself continuously, without splitting, as it travels through the tube. When $R > \bar{R}_k$ and provided turbulent flashes actually occur, then, the flow will become fully turbulent at tube sections situated far enough from the tube inlet.

We understand that since the damping effect of the turbulent flashes within the flow region $R < R_k$ depends on the roughness grade of the "smooth" tube surfaces, these microscopic roughnesses ought to be of importance also with respect to the turbulence maintaining processes in the flow region $R > R_k$. The conclusion that wall effects are important for the turbulence maintaining processes is also supported by the fact that laminar flow becomes turbulent at the aft end of the turbulent regions while turbulent flow becomes laminar at their fore end. Whether other wall effects or perhaps quite other causes also are responsible for the maintenance of turbulent flashes or of continuous turbulent flow cannot be decided as yet although the experiments have given the impression that also some response effects or dispositions within the liquid seem to be important with respect to the release and maintenance of the turbulent flashes.

5. Studies on the onset of turbulence in liquid flow by means of simultaneous pressure drop measurements at several locations along long cylindrical tubes

These experiments were performed as a direct continuation of the optically recorded observations reported in the previous part of the paper. The main purpose of the experiments was to decide for certain whether the flow characteristics observed for flow of bentonite sols would be valid also for flow of distilled water. Also it was desirable to find out whether further information regarding the characteristics of tube flow could not be obtained by simultaneous recording of the pressure drop of the flow at several locations along the tube by use of strain-gauge pressure transmitters.

Experimental equipment

The experiments were carried out on the same premises as before, using the flow apparatus outlined in Fig. 4.1, the measuring equipment completed with several items as already indicated in Fig. 4.2.

The measurements were performed on flow of 1.02 ‰ (per mille) bentonite sol and on flow of distilled water through the 8.18 mm and 10.31 mm tubes along 5 measuring sections each of 0.5 m length situated as shown in Fig. 5.1. This figure also informs about the local as well as the mean diameter values of each measuring section.

Arne Söderholm at the *Aeronautics Lab. KTH* undertook the delicate work of constructing pressure transmitters sensitive enough to admit recording of the estimated pressure differences. The measuring equipment further consisted of a multichannel galvanometer oscillograph equipped with suitable galvanometers; a stabilizing device, feeding the transmitters with constant voltage via a 6-channel balancing unit. Use was also made of the previously described instrument components for continuously recording the rate of flow, as well as the equipment for optic-electronic recording of the flow characteristics of bentonite sols, the latter equipment being used simultaneously with the pressure drop recording device when studying the flow of the 1.02 ‰ bentonite sol.

Calibration

Fig. 5.2 shows the arrangement according to which the pressure transmitters were calibrated. The most troublesome task in handling the transmitters was that of filling them with distilled water without destroying the strain-gauge wires. The highest permissible pressure difference over the transmitters was only about 500 N/m^2. It was of importance to ensure that no air bubbles remained in the transmitters or in their feeding lines, as otherwise capillary forces probably would dominate over regular pressure differences caused by the flow. At least in one case such capillary forces actually proved so strong that they destroyed the strain-wires of one transmitter.

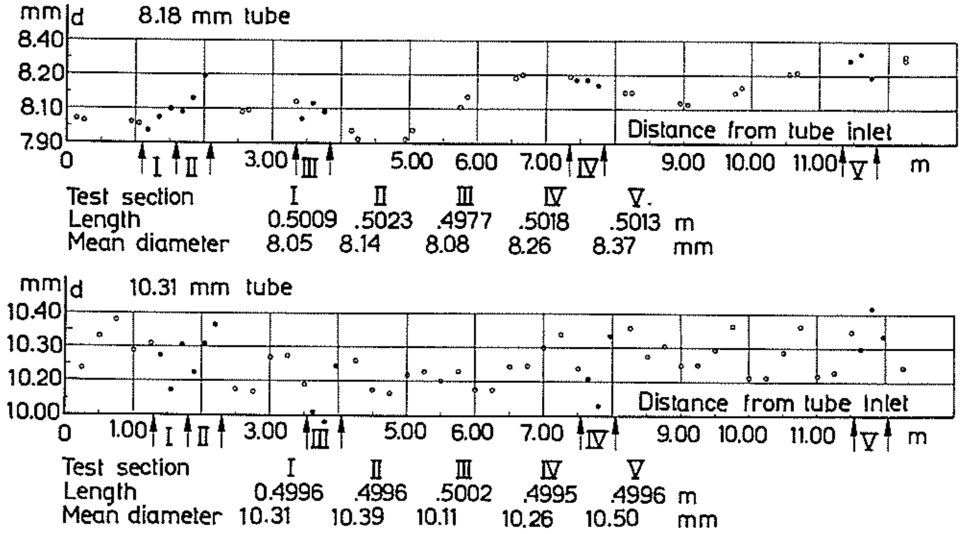

Fig. 5.1. Dimensions of the various measuring sections of the two tubes used for pressure drop measurements of flow of distilled water and on flow of 1.02‰ bentonite sol.

The calibration manometer tubes were thoroughly cleaned in chromium bisulphite and rinsed in distilled water. They were then treated with a siloxane liquid[1] in order to neutralize disturbing capillary actions on the manometer levels (see for instance L. A. Spitse and D. O. Richards 1947).

Prior to the filling of the pressure transmitters with water, a droplet of photographic wetting agent was introduced into each of the two pressure chambers of each transmitter in order to make the filling process easier. In each case this process was started by applying a small overpressure in the water-filled levelling container and experiment tube (see Fig. 4.1, p. 76), the latter being properly connected to each of the transmitters. When doing this, all the cocks shown in Fig. 5.2, except those marked 6 *a* and *b*, were open. Then, by carefully opening the cock 6 *b* the water was allowed slowly to rise to the level of the branch point B, the liquid level in the manometer tube 2 *b* rising to the same height. After closing the cock 6 *b*, the process then was repeated for branch A by opening the cock 6 *a*, the liquid level in the feeding line passing the branch point A, filling the short circuit connection leading to branch point B, which was situated higher than A. From then on the liquid levels in all the branches were allowed to rise through at the same low speed as before. Some time after the water began to drain out through the bleed cocks 3 of the pressure transmitter the cocks 5, leading to the manometer tubes, were closed, and then also cock 3 *b* was closed thus allowing water to drain only through the cock 3 *a* until it was considered that all air was removed from branch A. After closing the cock 3 *a*, cock 3 *b* was opened and the same process was repeated for branch B.

During the filling process each pressure transmitter was connected to a light-spot galvanometer and an electric battery via a balancing unit for continuous control that allowable stress limits of the measuring elements were not exceeded.

[1] DC 1107. *Dow Corning Company*, Midland, Mich. U.S.A.

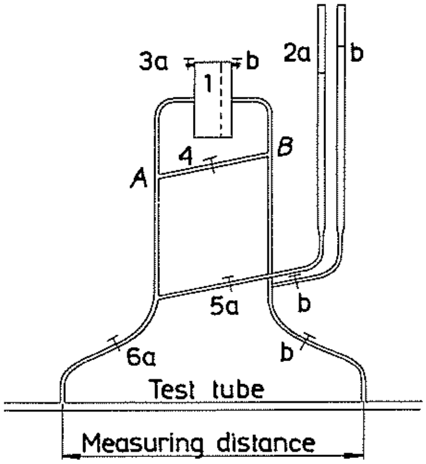

Fig. 5.2. Arrangement of pressure transmitters for calibration and pressure drop measurements.

1 Pressure transmitter
2 Calibration manometer tubes
3 Bleed cocks
4 Short circuit cock
5 Calibration manometer tube cocks
6 Main cocks.

In several cases the above water filling process had to be repeated and modified owing to the presence of small air bubbles sticking to the walls on various locations of the pressure transmitter circuits.

After the filling process appeared to have been satisfactorily performed, the cocks $6a$ and b were closed and the cocks $5a$ and b, leading to the manometer tubes, were opened.

Calibration of the pressure transmitters was prepared for by applying a moderate over-pressure in the levelling container and breaking the short circuit AB in Fig. 5.2 by closing cock 4. Then the cock $6b$ was carefully opened to let the water level in manometer tube $2b$ rise to the desired height above the water level in manometer tube $2a$, at which height the cock $6b$ was turned off. The difference between the water levels in the two manometer tubes was read by means of a cathetometer equipped with a horizontal spirit level. The errors in the cathetometer readings were estimated not to exceed ± 0.005 mm. The deflection of the corresponding oscillograph galvanometer at the chosen reference voltage (10.80 V), received from the constant voltage device via the selected balancing channel, was read directly or recorded on the oscillograph paper. Calibration values were obtained at suitable intervals of the manometer levels up to the maximum presure difference allowed. The calibration cycle then was proceeded in the reverse order by successively lowering the water level in manometer tube $2b$ by opening the cock $6b$ with no over-pressure in the levelling container (No. 3 in Fig. 4.1).

The temperature of the liquid was read for each series of calibration measurements.

The water surfaces in the siloxane treated manometer tubes (of 12 mm diameter) did not show any meniscus but were beautifully plane as intended. It was expected that this would imply neutralization of disturbing capillary effects. The result, however, was very disappointing. It soon appeared that, even in the absence of a

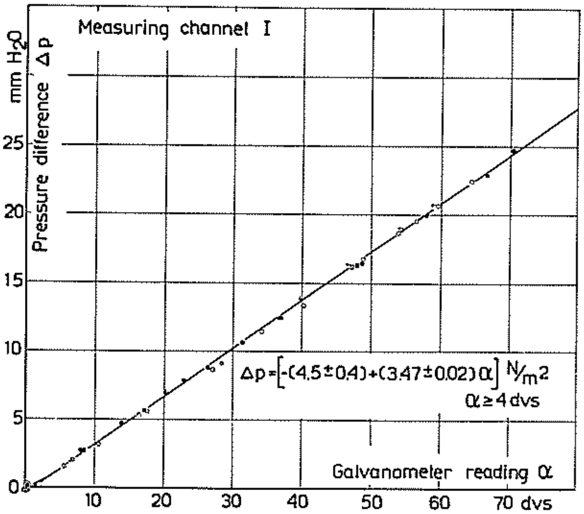

Fig. 5.3 *a.*

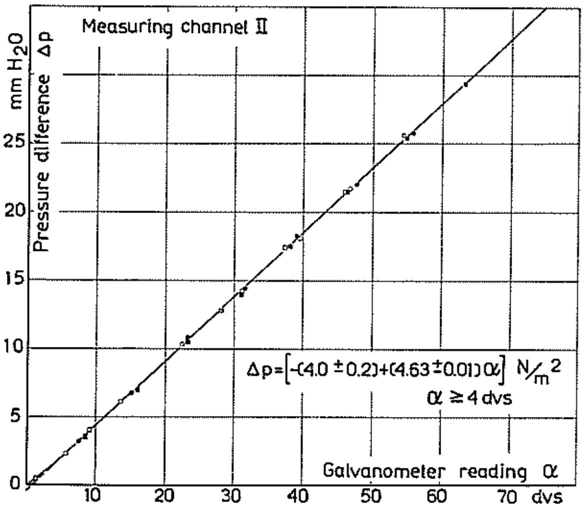

Fig. 5.3 *b.*

Fig. 5.3. Calibration diagrams and calibration formulae of the various measuring channels including the quadratic mean errors of the calibration constants.

meniscus, strong capillary forces were active in the manometer tubes. This capillary action was observed as discontinuous changes of the manometer levels, instead of smooth changes, for continuous alteration of the pressure difference between the manometer tubes. The net effect was a shift of calibration values obtained in calibration series of increasing and decreasing pressure difference respectively.

By adding a droplet of photographic wetting agent in each of the manometer tubes the shift of the calibration values as well as the discontinuous changes of the manometer levels almost completely were eliminated though at the same time a tendency to meniscus formation was also observed.

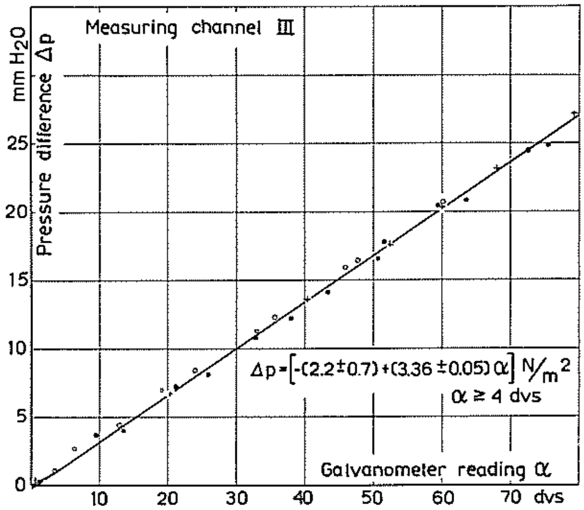

Fig. 5.3 *c*.

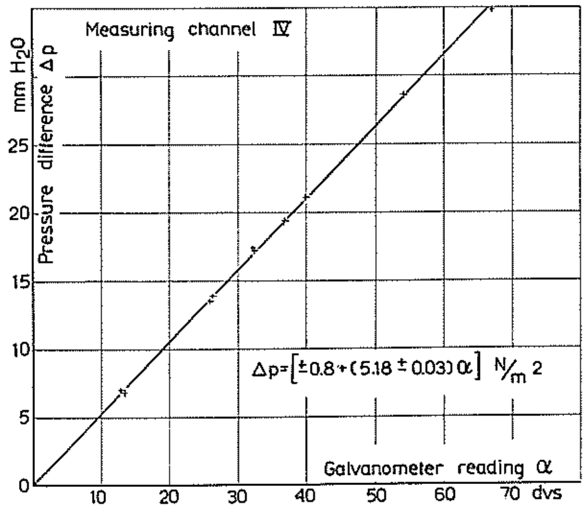

Fig. 5.3 *d*.

In Figs. 5.3*a–e* are shown the calibration values obtained for the five measuring channels used.

The diagrams indicate rectilinear relations between pressure difference Δp and galvanometer deflection α except for very small values of Δp and α. The least sensitive channel (no. IV), however, appears to have rectilinear relations over all the measuring range.

According to Mr. Söderholm, who constructed the pressure transmitters, the rectilinear relations were to be predicted, while the deviation from the rectilinearity for small measuring values could not be fully explained, although it was in line with

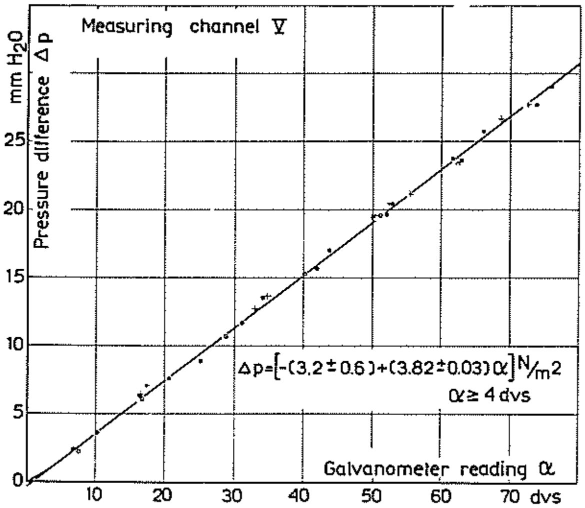

Fig. 5.3 *e*.

his previous experiences. On the other hand, repeated tests showed that the galvanometer deflection possessed a stable zero point for zero pressure difference.

The calibration formulae given in the diagrams are obtained in accordance with the method of least squares and the errors indicated are the quadratic mean errors of the calibration constants.

Experimental procedure

The starting of a series of pressure drop measurements was prepared for by first closing the manometer tube cocks 5 (see Fig. 5.2) and then opening the connection cocks 6 under low over-pressure in the levelling container 3 (see Fig. 4.1) about equal to the static pressure head of the water columns in the transmitter circuits. After these preparations the air pressure in the levelling container was increased to the working pressure and the short circuit cock 4 (in Fig. 5.2) was closed. The flow circulation through the experiment tube then was started by opening the plug cocks 14 (in Fig. 4.1) and the desired rate of flow under stationary flow conditions was adjusted by means of the regulation cocks 12 and 13 (in Fig. 4.1).

Repeated test runs at low and high rates of flow showed that the transmitter zero point was quite stable apart from a temperature drift which was quite large for the transmitters II and V. The temperature drift of each transmitter, however, could easily be compensated for by adjusting the corresponding balancing unit.

Actually the temperature drift of the pressure transmitter II gradually became so large that the strain wires were destroyed when one series of measurements remained to be performed. The strain wires of transmitter IV on the other hand, were accidentally destroyed after completing several series of calibrations prior to the pressure drop experiments. This is the reason why only one calibration series is recorded in Fig. 5.3*d* for this measuring channel. Several reasons prevented extra calibrations from being performed on this transmitter.

The method of measurement adopted proved quite satisfactory, implying considerable advantages over conventional methods of reading the height of free liquid surfaces of ordinary liquid manometers. A special advantage appears to be the very small displacements of liquid within the transmitters even for comparativley large variations of the pressure difference (less than 0.1 cm^3 when the pressure difference varied from zero to the maximum value applied (200 N/m^2) or vice versa). Thus the investigated flow is not disturbed to the same extent as by ordinary manometers which pump large liquid volumes to and from the experiment tube when the flow is in the transition region where turbulent regions alternate with laminar intervals.

Observations of the appearance of flashes according to synchronized pressure drop and optic-electronic records

One cannot exclude the possibility that important but unknown flow characteristics, to which a certain measuring method might be insensitive, could remain undetected, if only that very technique of observation was used. However, if the appearance of flow characteristics, as recorded by the optic-electronic method, should coincide with those recorded when using pressure drop transmitters the reliability of observations made by means of either method should greatly increase. For the purpose of such coincidence measurements synchronized optic-electronic and pressure drop observations were performed on flow of the 1.02 ‰ bentonite sol through the 8.18 mm tube. The two optic-electronic devices were situated at the middle of the measuring sections I and V of the tube and were connected to the recording double-beam oscilloscope in the same manner as described in Part 4.

In these experiments the disturbance plate (see Schiller 1921 or previous parts of the present paper) was located 0.25 mm in front of the tube inlet, thus securing high disturbance level of the entrance flow.

The experiments indicated full coincidence between the two methods of observation. Each time a flash appeared on the oscillogram as transmitted by the optic-electronic devices at the measuring sections I and V a crest appeared on the corresponding oscillograph traces due to the pressure transmitter channels I and V.

When viewing the galvanometer deflections on the oscillograph screen the tube passage of each individual flash could be followed as it approached the various measuring sections, provided the flashes did not follow each other so closely that a new flash entered a measuring section before the previous flash had left the same section.

It was observed that the oscillograph galvanometer traces, representing "laminar" flow, often showed a vague wavy form, which pattern was often also observed on records transmitted by the optic-electronic devices reported in this and the previous part of the paper. The waviness, however, was always observed to become smaller and disappear with increasing distances from the tube inlet. Only provided high disturbance levels were secured to the entry flow was such waviness observed at low Reynolds numbers while high Reynolds numbers were necessary for the appearance of waviness in records of flow of low entrance disturbance level. Thus it appears that the waviness of the oscillograph traces should be due to entrance disturbance vortices which by themselves are damped but which in some cases might change spontaneously into turbulent flashes as described in Part 2 of the paper.

A typical pressure drop record is shown in Fig. 5.4 which illustrates the appearance of two turbulent flashes in flow of the 1.02 ‰ bentonite sol at a Reynolds number of

$R \approx 2320$. During the tube passage each of the two flashes develops into a pair of flashes as indicated by the synchronized optic-electronic record shown below the pressure drop record. (It should be remembered that the optic-electronic traces correspond to the pressure drop traces I and V.)

We see that the pressure drop crests obtained for the measuring sections I and III appear "plain" and that the optical record indicates that these crests represent single flashes appearing in measuring section I. However, the pressure drop crests representing the same flashes when passing test sections IV and V appear elongated with an extra hump in the middle. Considering the indications of the optical record we understand that this extra hump probably is due to both flashes of each pair being contained for a short while within measuring sections IV and V respectively. We conclude that for each time interval during which a flash is completely contained within a measuring section there appears to be recorded an—at least approximately—constant extra pressure drop. Consequently, if a second flash arrives into a measuring section before the previous one has begun to leave the same section, the recorded extra pressure drop ought to increase to the sum of the extra pressure drops caused by each flash separately. The records obtained in the main confirm this state of matters.

The pressure transmitter II was not in workable condition during this set of experiments (the experiments are not reported in chronological order) and so only four pressure drop traces were recorded as shown in Fig. 5.4. The galvanometer zero lines (zero flow velocity in the experiment tube) were in each case recorded before and after each record. Straight lines connecting the zero lines are drawn dotted in the record of Fig. 5.4.

The film speeds of the pressure drop records and the optical records were not the same, which means that the two oscillograms of each synchronized pair of records over any time interval are of different lengths. In Fig. 5.4 a photographic scale reduction has been made so as to make the two records equal in length. They represent a time interval of 48.0 s.

We understand from Fig. 5.4 that individual flashes—as previously hinted—cannot be distinguished with use of the pressure drop method if they appear with such short intervals that a second flash enters a measuring section before the nearest flash ahead has left the same section. It might, however, be concluded that the adopted method of pressure drop measurements is well suited as a complementary method to the stream bi-refringence technique for investigation of various fluid flow phenomena.

Quantitative observations of the flow of 1.02 ‰ bentonite sol through the 8.18 mm tube

As long as the flow is purely laminar there is no problem as to how to evaluate the pressure drop records obtained by means of pressure transmitters. However, when flashes appear it must be decided over which time interval the mean pressure drop is to be read.

When using the conventional method of pressure drop measurements by reading the levels of a liquid manometer, the jumps of the manometer levels due to less frequent flashes certainly are neglected. On the other hand, when the flashes appear above some frequency at the same time as their energy transposition increases, the manometer levels will develop strong oscillations which in turn must cause additional

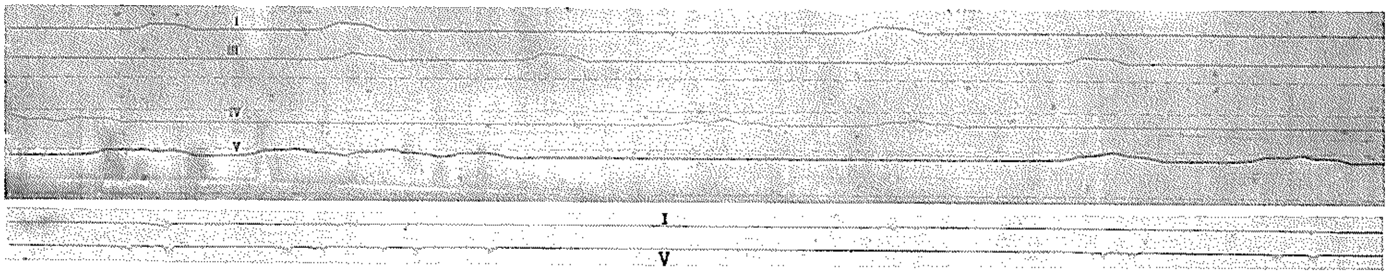

Fig. 5.4. The appearance of turbulent flashes in flow of 1.02‰ bentonite sol through the 8.18 mm tube at a Reynolds number of $R \approx 2320$ under highly disturbed entrance flow conditions according to parts of both a pressure drop record and a "visual" record, their recording processes being synchronized with each other. The numbering of the pressure drop traces refers to the corresponding measuring sections of the tube according to Fig. 5.1.

The "visual" record is transmitted by two optic-electronic devices (according to the technique described in Part 4 of the paper) situated in the middle of the measuring sections I and V respectively. Consequently, the traces of this record are to be compared to the traces I and V of the pressure drop record.

The two original record strips are of unequal length but have been reduced to about the same length by proper scale reduction. They represent a time interval of 48.0 s. The zero pressure drop traces of the galvanometers are drawn dotted in the record.

disturbances of the investigated flow with an additional pressure drop as the result. In this manner the conventional method of measurements apparently might indicate an almost instantaneous onset of turbulence although the true transition process follows another course. A more continuous change between laminar and turbulent flow would probably be the result when the transition process is investigated by means of pressure transmitters admitting only very small liquid volumes through the transmitter connections to the experiment tube even at quite large fluctuations of the pressure drop.

In the present experiments the mean pressure drop is read over a time interval approximatively equal to the time lapse between two consecutive flashes at the lowest Reynolds number at which flashes ever appeared.

The results obtained from the four measuring sections for flow of highly disturbed entrance flow conditions (the disturbance plate situated 0.25 mm in front of the tube inlet) are reported in Table 5.1. The galvanometer deflections given for "laminar" parts and parts of fully developed continuous turbulence according to the records, are read directly from the oscillograms while those given for parts of intermittent turbulence are the mean galvanometer deflections, calculated from the integrated oscillogram surfaces. The integrations have been made by means of a standard roller planimeter, commonly used in ship drafting.

The galvanometer deflections α are corrected with respect to the slightly varying feed voltage U (α is a rectilinear function of U). The Reynolds numbers are calculated by use of the kinematic viscosity values ν according to formula (1.6) (see Part 1, p. 28) and of the total mean diameter value ($d = 8.18$ mm) of the tube.

Apparent values of the dynamic viscosity μ are determined by applying formula (2.1) (see Part 2, p. 44) to the experimental data. The apparent viscosity values determined at various temperatures are transformed to 20°C reference temperature in Table 5.1 under the assumption that relations between temperature and viscosity of water are correct as given by Bingham and Jackson 1918 (see Part 1, pp. 10–11). The table also contains the mean viscosity values at 20°C and the mean square error of each mean value, even though it is realized that the estimation of the statistical error scarcely could be correct with only four individual values to each mean value.

We observe quite a wide systematic spreading of the viscosity values due to the various measuring channels. This spreading might perhaps be explainable in terms of the accuracy of the pressure transmitter calibrations; also diameter variations of the various test sections could be responsible for this, although the latter possibility is less probable

The diagrams of Fig. 5.5 show the estimated maximum relative (probable) errors of the viscosity values for each of the measuring channels as a function of the rate of flow. These errors involve possible errors of length and diameter of each test section and of the record readings, as well as the probable errors of the calibration constants of each measuring channel (see Fig. 5.3*a–e*). The errors of the rate of flow Q are not included in these diagrams but are shown separately in an extra diagram of Fig. 5.5. The total relative errors of the apparent viscosity values will thus be obtained by simple addition of the relative error of the rate of flow with the corresponding relative error of the measuring channel in question according to the diagrams in Fig. 5.5.

If we apply the relative errors of μ given in Fig. 5.5 we observe that the limits of the obtained apparent viscosity values due to the various sections in some cases will not overlap each other but a discrepancy of 2–4 % might remain. (The error of the

Table 5.1. Primary experimental data and apparent dynamic viscosity values determined therefrom, obtained on flow of 1.02 ‰ bentonite sol through the 8.18 mm tube, as measured over various measuring sections of the tube.

In these experiments highly disturbed entrance flow conditions were secured by the presence of a disturbance plate at 0.25 mm distance from the tube inlet. Q = rate of flow; R = Reynolds numbers calculated by use of the μ_∞ values and the total mean diameter of the tube 8.18 mm; (μ_∞ = standard dynamic viscosity derived from formula (1.6) in Part 1 of the paper (p. 28)); U = feed voltage of the pressure transmitters; $\Delta\mu$ = mean square error of the arithmetic mean value of each series of apparent dynamic viscosity values at 20°C. The oscillograph galvanometer deflections determining the pressure drop are corrected as to the calibration feed voltage U = 10.80 V.

$Q \cdot 10^6$	Temp.	R	U	Galvanometer deflection for pressure drop over various measuring sections Scale divisions				Apparent dynamic viscosity $\mu \cdot 10^3$ reduced to 20°C reference temperature kg/ms				Mean value $\mu \cdot 10^3$ at 20°C	$\pm\Delta\mu \cdot 10^3$
m³/s	°C		V	I	III	IV	V	I	III	IV	V	kg/ms	kg/ms
4.20	15.6	540	10.81	7.0	7.2	3.9	5.2	0.87	0.98	0.98	0.86	0.95	0.04
6.86		880		11.3	11.5	6.3	8.9	0.93	0.99	0.97	0.97	0.97	0.01
8.40	15.6	1080		13.9	14.3	7.8	11.0	0.96	1.02	0.98	0.99	0.99	0.01
9.96	15.7	1280		16.2	17.0	9.0	12.8	0.96	1.04	0.96	0.99	0.99	0.02
11.28	15.8	1460		17.9	19.2	10.2	14.4	0.95	1.04	0.96	0.99	0.98	
12.38	15.9	1600		19.8	21.2	11.2	15.9	0.96	1.05	0.96	1.01	1.00	
13.42	16.0	1740		21.5	22.9	12.3	17.2	0.97	1.06	0.98	1.01	1.01	
14.24	16.2	1860		22.6	24.3	12.9	18.0	0.97	1.06	0.97	1.01	1.00	
14.33	16.3	1880		22.7	24.4	13.0	18.2	0.97	1.06	0.98	1.01	1.01	
15.2	16.4	2000		24.3	26.2	14.1	19.7	0.99	1.08	1.00	1.04	1.03	
16.1	16.5	2110		25.2	27.6	14.6	20.5	0.97	1.08	0.98	1.03	1.01	
16.7	16.6	2200		26.4 26.5	28.7 28.8	15.4 15.4	21.5 21.6	0.99 0.99	1.08 1.10	1.00 1.00	1.04 1.05	1.03 1.04	0.03
17.1	16.7	2270	10.81	27.5 27.9	29.6 30.4	16.0 16.2	22.0 22.5	1.01 1.02	1.10 1.13	1.02 1.03	1.05 1.07	1.05 1.06	0.03
17.3	17.2	2320	10.80	27.5 28.2	29.5 30.3	16.6 16.6	21.1 23.0	1.01 1.04	1.09 1.12	1.02 1.06	1.05 1.10	1.04 1.08	0.02
17.5	17.4	2360	10.79	28.4 29.5	30.1 31.5	16.2 17.1	22.6 24.9	1.04 1.08	1.11 1.16	1.02 1.08	1.07 1.18	1.06 1.13	0.02 0.03
18.1	17.4	2480	10.78	29.1 31.9	31.9 36.2	16.6 19.9	23.3 25.5	1.03 1.13	1.14 1.30	1.01 1.22	1.07 1.17	1.06 1.20	0.03 0.04
18.5	17.5	2500	10.77	30.5 34.4	32.7 40.2	17.7 22.4	25.1 32.7	1.06 1.20	1.15 1.41	1.06 1.34	1.13 1.49	1.10 1.36	0.02 0.06
18.8		2550		41.2	46.5	25.6	34.0	1.43	1.61	1.51	1.52	1.52	0.04
19.2	17.5	2600		44.1	48.6	26.6	36.4	1.50	1.65	1.54	1.60	1.57	0.04
19.6	17.6	2650		49.0	52.4	29.0	38.5	1.64	1.75	1.64	1.66	1.67	0.03
19.6		2650		44.2	49.9	27.3	37.0	1.47	1.66	1.55	1.58	1.57	0.04
20.1		2720		53.3	54.5	30.3	40.4	1.74	1.78	1.69	1.70	1.73	0.02
20.7		2800		57.6	59.5	34.2	44.5	1.83	1.88	1.84	1.83	1.84	0.01
21.3		2880		59.5	63.0	35.3	46.6	1.84	1.94	1.84	1.86	1.87	0.02
21.8	17.6	2950	10.77	63.5	65.5	37.1	48.9	1.92	1.97	1.89	1.91	1.92	0.02

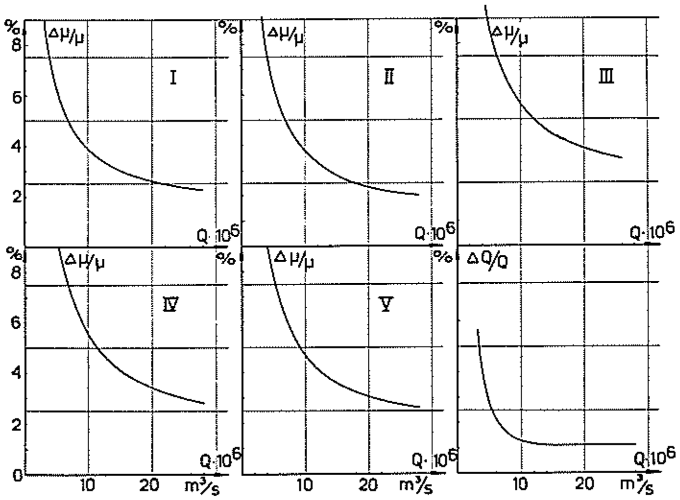

Fig. 5.5. Estimated maximum probable error, $\Delta\mu/\mu$, of individual viscosity values, determined on flow through the 8.18 mm tube, related to the rate of flow, Q. The total relative error of each μ value is received by addition of the respective $\Delta\mu/\mu$ value with corresponding $\Delta Q/Q$ value, read from the last diagram in the figure.

rate of flow should not be considered in this connection as the rate of flow must necessarily be identical through all the measuring sections.) This state of matters might indicate the presence of unknown factors, either in the calibration process or in the flow experiments or in both. On the other hand, the deviations of the individual viscosity values from the corresponding mean values do not exceed about 5 % and here the mean square error and each individual viscosity error in general overlap each other or at least touch each other. We are thus able to place some confidence in the results obtained. This the more as the deviations decrease with increasing rate of flow within the turbulent region where the deviations of the individual values are very well overlapped by the measuring errors given in Fig. 5.5.

The apparent mean viscosity values at 20°C as given in Table 5.1 are shown in the diagram of Fig. 5.6. Black dots represent laminar flow and laminar flow intervals while open circles represent the total mean pressure drop including also turbulent flow regions. As should be the case, the diagram indicates a fully continuous transition between laminar and turbulent flow.

It is most remarkable to observe in Fig. 5.6 a distinct, almost rectilinear, increase of the apparent dynamic viscosity with increasing Reynolds numbers even within the purely laminar flow region. Although the viscosity values obtained from the various measuring sections are widely spread relative to each other this tendency is about the same for the μ values obtained from each of the four test sections, so an explanation in terms of the development of the velocity profile in the entry length of the tube is not appropriate. Furthermore, the entry length according to Boussinesq 1891

$$x = 0.06\, d \cdot R \qquad (d = \text{tube diameter; } R = \text{Reynolds number})$$

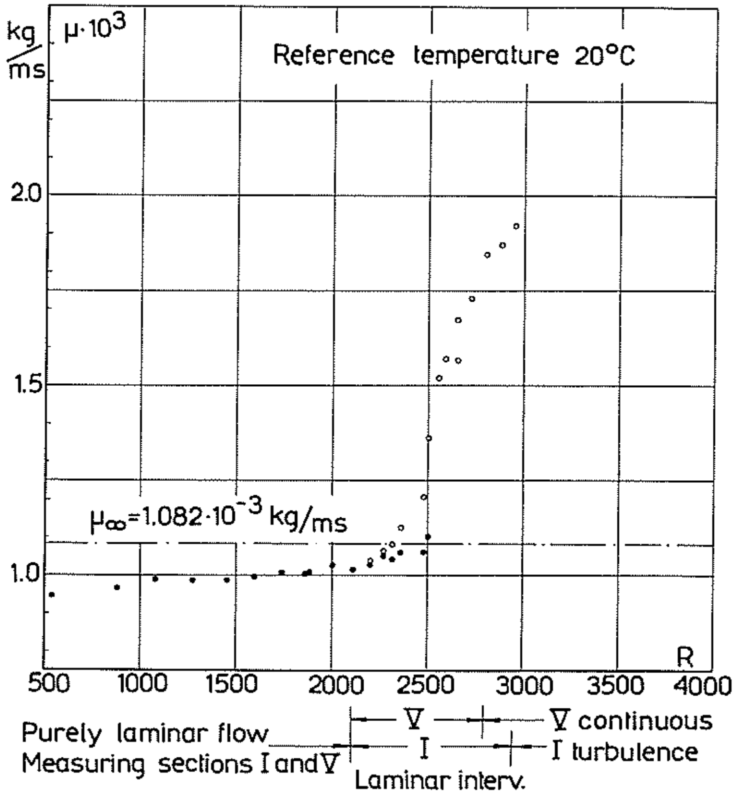

Fig. 5.6. Apparent dynamic viscosity μ of 1.02‰ bentonite sol, referred to 20°C reference temperature, related to the Reynolds number R. μ_∞ = standard value of the dynamic viscosity of 1.02‰ bentonite sol determined according to formulae (1.3) and(1.6) of Part 1 of the paper. The Reynolds number of the flow of each measuring point was determined by use of the standard viscosity value ν_∞ at the temperature in question.

●, laminar pressure drop; ○, turbulent mean pressure drop.

will be about 1.2 m for flow through the 8.18 mm tube at a Reynolds number of $R \approx 2500$. This entry length is about the same as that allowed for, to the first measuring section in the present experiments. Experiments due to Schiller 1921 indicate that the presence of a disturbance plate should not greatly affect the entrance length within which any influence on the pressure drop is observable, the entry length according to Schiller 1922 being less than half as long as that given by Boussinesq above.

We see in Fig. 5.6 that the viscosity values determined for the laminar flow increase from quite low magnitudes at low Reynolds numbers gradually approaching the μ_∞ value, calculated in accordance with formula (1.6) (Part 1, p. 28), in the neighbourhood of the "critical" Reynolds number, where the total pressure drop increases rapidly due to the appearance also of turbulent flow regions.

As yet I have not been able to explain away the obtained variation of μ with the Reynolds number R (laminar flow) as caused by measuring faults, and the tendencies

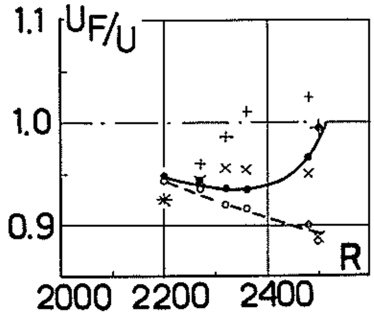

Fig. 5.7. Relative velocity U_F/U of fronts and tails of turbulent flow regions as related to the Reynolds number R in flow of 1.02‰ bentonite sol through the 8.18 mm tube. U = mean flow velocity; U_F = front or tail velocity of turbulent flow regions.

+ front velocity, × tail velocity } according to pressure drop records.
● front velocity, o tail velocity } according to optic-electronic records.

are too distinct and uniform to be ignored as accidental. Perhaps ideas developed in modern Rheology might suggest explanations to the observed peculiarities as already emphasized in Part 1 of the paper.

Both the pressure drop records and the optic-electronic records have also been used for evaluation of the velocities of the fore and aft ends of turbulent flow regions. The flash velocities are obtained from the pressure drop records by determination of the time interval during which it is observed how a flash, as represented by its pressure drop crest, enters (front velocity) and leaves (tail velocity) consecutive measuring distances. Table 5.2 contains the recorded velocity data according to both the optical and the pressure drop records as illustrated in Fig. 5.7. Unfortunately, the record speed regulator of the galvanometer oscillograph was not in perfect order during the experiments as can be seen in the "time scale" column of the table. (The time scale in each case was determined by measuring the time interval during which the film record was exposed.) This fault was not detected until the evaluation of the pressure drop records was undertaken about 1½ years after finishing the experiments. There is an increase of the record speed of about 40 % for the six records of Table 5.2 and, furthermore, the record speed was very irregular also within each record, which reveals itself as a varying intensity of the blackness of the record traces. This accounts for the very irregular spreading of the flash velocity values read from the pressure drop records in contradistinction to the continuously distributed velocity values read from the synchronized optical records, the record speed of which being constant within 1.5 % variation. The flash velocity plotted versus the Reynolds number according to the optical records, in the main confirms the results reported in the previous part of the paper, although the front velocity accidentally appears to increase relative to the tail velocity already at lower Reynolds numbers in the later experiments than in the corresponding earlier experiments.

The length of a single flash, in flow of the 1.02‰ bentonite sol through the 8.18 mm tube, over which its presence can be traced in one way or another, appears to be about 0.3–0.4 m while the part that contains "real" turbulence is limited within a

Table 5.2. Velocity data of turbulent flow regions in flow of 1.02 ‰ bentonite sol through the 8.18 mm tube according to both "visual" and pressure drop records.

U = mean flow velocity; R = Reynolds number (see text to Table 5.1); U_F = front or tail velocity of turbulent flow regions.

U	Temp.	R	Optical records						Pressure drop records							
			Time scale of the record	Record interval between fronts	Record interval between tails	Tube passage length	U_F/U front	U_F/U tail	Time scale of the record	Record interval between fronts	Record interval between tails	Tube passage length	U_F/U front	U_F/U tail	Mean U_F/U front	Mean U_F/U tail
m/s	°C		s/mm	mm	mm	m			s/mm	mm	mm	m				
0.318	16.6	2200	0.0804	426	428	10.26	0.947	0.943	0.0701	106 191 203	106 192 203	2.255 4.00 4.00	0.953 0.940 0.884	0.953 0.934 0.884	0.93	0.93
0.325	16.7	2270	0.0805	417^{+5}_{-4}	421^{+4}_{-5}	,,	0.945	0.935	0.0642	108^{+1}_{-2} 202^{+6}_{-4} 208^{+2}_{-4}	112^{+1}_{-4} 201^{+7}_{-5} 210^{+6}_{-5}	,,	1.006 0.948 0.923	0.969 0.954 0.914	0.96	0.95
0.329	17.2	2320	0.0800	416^{+7}_{-5}	424^{+6}_{-3}	,,	0.936	0.921	0.0577	116^{+4}_{-8} 214^{+12}_{-10} 222^{+4}_{-8}	120^{+6}_{-4} 221^{+4}_{-5} 226^{+5}_{-4}	,,	1.024 0.982 0.951	0.988 0.951 0.933	0.99	0.96
0.333	17.4	2360	0.0795	411^{+10}_{-8}	420^{+8}_{-11}	,,	0.937	0.916	0.0538	117^{+6}_{-7} 225^{+3}_{-8} 230^{+9}_{-20}	127^{+6}_{-3} 234 ± 8 243^{+9}_{-6}	,,	1.072 0.994 0.970	0.991 0.955 0.919	1.01	0.96
0.344	17.4	2480	0.0800	387^{+8}_{-10}	415 ± 1	,,	0.965	0.898	0.0498	120 ± 10 228^{+12}_{-11} 246^{+16}_{-11}	133^{+4}_{-9} 247 ± 5 253^{+3}_{-2}	,,	1.099 1.023 0.948	0.988 0.945 0.922	1.02	0.95
0.352	17.5	2500	0.0798	367^{+1}_{-2}	413 ± 0	,,	0.994	0.884	0.0496	127 ± 10 227 ± 2 240 ± 6	141^{+6}_{-5} 260^{+3}_{-4} 264^{+1}_{-2}	,,	1.020 1.009 0.955	0.912 0.884 0.869	0.99	0.89

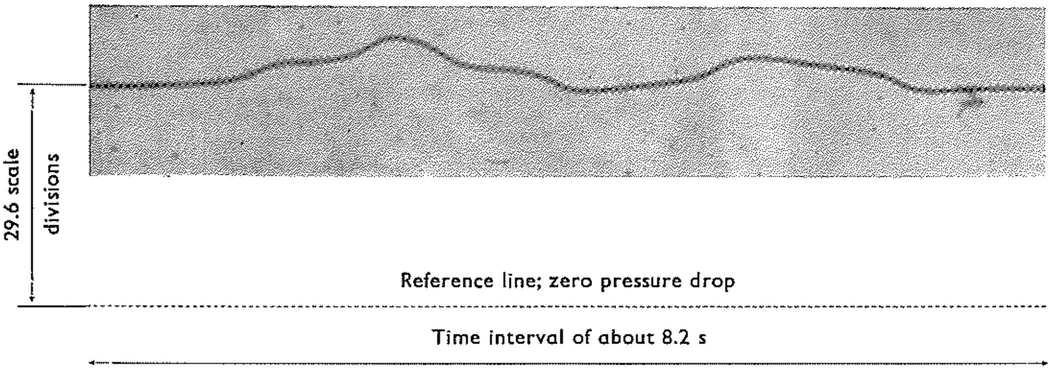

Fig. 5.8. Part of a pressure drop record of original size showing the appearance of a pair of flashes followed by a single flash in flow of 1.02 ‰ bentonite sol through the 8.18 mm tube at measuring section III. The Reynolds number is about $R \approx 2270$ and the flow is highly disturbed at the tube entrance.

length of about 0.1 m, its turbulence, however, being by no means homogeneous either along its length or along its radial dimensions.

An approximately constant additional pressure drop appears as long as the whole energy-containing parts of a flash are situated within a measuring section. In the long run, however, its strength seems to vary during the tube passage according to how the regeneration process develops. The two flashes in the records of Fig. 5.4 ($R \approx 2320$), each of them developing to a pair of flashes, are a good demonstration of the discrete energy distribution of flashes. The flashes are single when passing the measuring sections I and III, and here the amount of energy of each flash is represented by a discrete pressure drop of 6 and 10 N/m^2 respectively for the first flash and 10 and 12 N/m^2 respectively for the second one. In trace IV each of the two flashes has parted into two units and, as far as can be judged from the records, each pair of flashes is completely contained within the measuring section IV for some moments. The first pair of flashes is represented by the discrete additional pressure drops of around 9 and 9 N/m^2, while the maximum height of the middle of the pressure drop crest corresponds to a pressure drop of about 19 N/m^2, which is about the sum of the extra pressure drops caused by each flash. Still better agreement is obtained for the second pair of flashes, the extra pressure drop of each flash being about 11 and 7 N/m^2 respectively, while the maximum extra pressure drop is evaluated to be about 18 N/m^2.

When passing measuring section V the individual flashes of each pair have parted so far from each other that the first flash has begun to leave the test section before the second one has completely arrived into it. Consequently, the maximum extra pressure drop recorded is less than the sum of the pressure drops caused by the individual units.

For the sake of illustration there is also shown a strip of a pressure drop record of original size in Fig. 5.8. The record shows a pair of flashes together with a single one appearing at a Reynolds number of $R \approx 2270$ as transmitted from measuring section III. Both flashes of the pair appear to be completely contained for some mo-

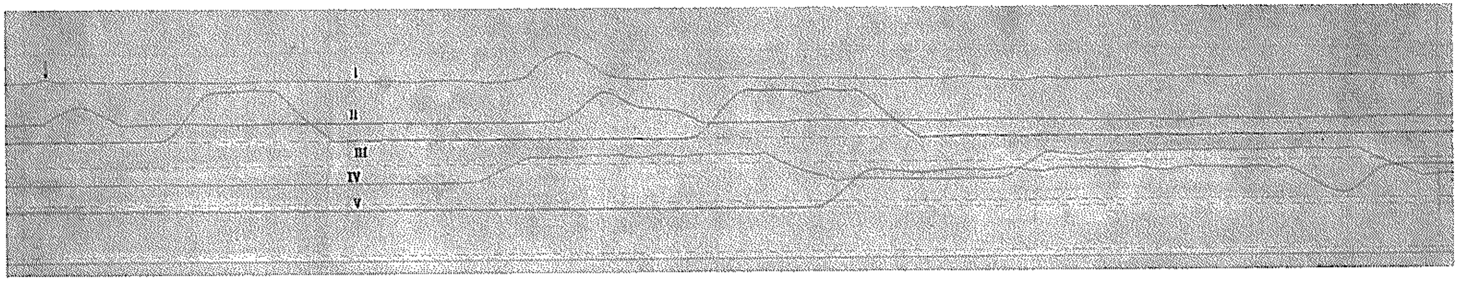

Fig. 5.9. Pressure drop record showing the formation and development of turbulent flow regions in flow of distilled water through the 8.18 mm tube at the Reynolds number $R \approx 3180$ in the case of low disturbance level of the inlet flow. The arrow, drawn in the record, points out the first signs of an instantaneous formation of turbulence to take place in measuring section I of the tube. Each trace is numbered with a Roman figure which refers the trace as being obtained over the corresponding measuring section of the tube (see Figs 5.1 and 5.2). The length of the record strip corresponds to a time interval of about 37.0 s.

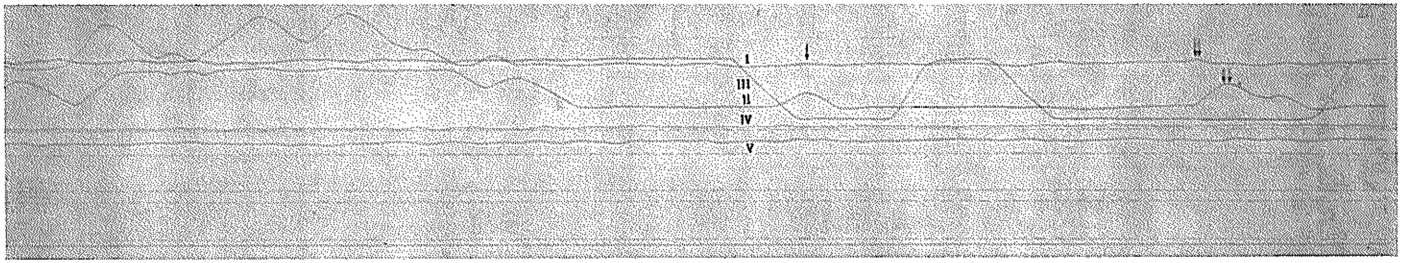

Fig. 5.10. Pressure drop record showing the formation and development of turbulent flow regions in flow of distilled water through the 8.18 mm tube at a Reynolds number of $R \approx 3480$ in the case of low disturbance level of the inlet flow. The single arrow, drawn in the record, points out the birth of a turbulent flow region within measuring section II without any extra signs of this formation being observable in measuring section I. The double arrow, drawn later in the record, points out a similar transition that takes place in measuring section I. The zero pressure drop lines of the oscillograph galvanometers are drawn dotted in the records. The length of the record strip corresponds to a recording time interval of about 32.6 s.

Table 5.3. Primary experimental data and therefrom determined apparent dynamic disturbed

For detailed notations

$Q \cdot 10^6$	Temp.	R	U	Galvanometer deflection for pressure drop over various measuring sections Scale divisions									
m^3/s	°C		V	I		II		III		IV		V	
4.42	15.6	610	10.80	6.6		4.3		6.6		3.3		5.0	
7.00	15.5	970		10.7		7.1		10.8		6.0		8.1	
8.50	15.6	1180		12.6		8.4		13.5		7.4		9.8	
10.03	15.6	1390		14.6		9.8		16.4		8.2		11.3	
11.22	15.8	1560	10.81	16.6		11.2		17.9		9.1		12.9	
12.45	16.0	1740		18.3		12.4		19.6		10.3		14.3	
13.42	16.3	1890		19.4		13.1		21.1		11.0		15.7	
14.33	16.4	2030		21.2		14.4		22.7		11.9		16.5	
15.1	16.4	2140	10.82	22.7	23.0	15.2	15.4	24.4	24.7	12.6	12.8	17.4	17.6
15.8	16.6	2250		24.0	24.9	16.2	17.0	25.9	27.0	13.8	14.4	18.7	19.4
16.6	16.7	2370		24.9	27.7	17.3	19.3	27.0	30.7	14.8	17.0	19.9	23.2
16.9	16.7	2410		25.3	30.0	17.7	21.3	27.8	33.6	14.7	18.6	19.8	25.3
17.5	16.8	2500	10.83	26.5	36.2	18.6	23.8		38.7		21.7		28.5
18.0	16.8	2570			42.4		29.2		45.4		24.2		31.7
19.0	16.9	2720			46.1		32.4		48.8		27.4		35.7
19.7	17.0	2830			51.6		35.8		53.8		28.9		39.6
20.6	17.0	2960	10.84		55.8		38.2		58.0		31.9		43.1
21.4	17.1	3080			61.3		42.2		63.7		35.1		47.7
22.5	17.2	3250			67.1		45.7		70.4		39.0		52.5
21.9	17.2	3160			63.6		44.5		67.3		36.5		49.4
20.2	17.3	2920	10.85		54.2		37.3		56.3		30.6		40.9
18.5		2680			42.4		30.3		45.8		24.5		33.9
17.8		2580		27.8	36.9		26.5		42.7		23.5		30.8
17.1		2470			30.9		22.9		36.9		19.7		27.0
16.1	17.3	2330	10.86	24.4	25.7	17.0	17.9	26.9	28.1	14.9	15.7	18.7	19.9

ments within the measuring section. Also here the sum of the pressure drops of the individual flashes 10 and 7 N/m^2 respectively is about equal to the maximum extra pressure drop recorded, which is about 20 N/m^2.

It is emphasised that the experiments in their present shape are not very well suited for determination of the energy transposition of turbulent flashes, which subject has to be left for future investigations.

Quantitative observations on flow of distilled water through the 8.18 mm tube

The experiments and their evaluation were performed in the same manner as described in the previous section for flow of the 1.02‰ bentonite sol, omitting the optical parts. Two series of measurements were obtained. In one series the disturbance plate was situated at 0.25 mm distance from the tube inlet, while in the second series this distance was increased to 15 mm.

In the first series of experiments the pressure drop records in the main show up the same characteristic features as are known from the records of Figs. 5.4 and 5.8, viscosity values of flow of distilled water through the 8.18 mm tube during highly entry flow.

see text to Table 5.1.

Apparent dynamic viscosity $\mu \cdot 10^3$ reduced to 20°C reference temperature kg/ms										Mean value $\mu \cdot 10^3$ at 20°C kg/ms		$\pm \Delta\mu \cdot 10^3$ kg/ms	
I		II		III		IV		V					
0.77		0.69		0.85		0.79		0.77		0.77		0.03	
0.86		0.79		0.91		0.91		0.85		0.86		0.02	
0.85		0.79		0.95		0.92		0.86		0.87		0.03	
0.85		0.79		0.99		0.86		0.86		0.87		0.03	
0.88		0.82		0.97		0.86		0.89		0.88		0.03	
0.88		0.83		0.97		0.88		0.90		0.89		0.02	
0.88		0.83		0.98		0.88		0.93		0.90		0.03	
0.91		0.86		0.99		0.90		0.92		0.91		0.02	
0.93	0.94	0.86	0.87	1.01	1.02	0.90	0.91	0.92	0.93	0.92	0.94	0.02	0.03
0.94	0.98	0.89	0.93	1.03	1.08	0.95	0.99	0.95	0.99	0.95	0.99	0.03	
0.94	1.05	0.91	1.02	1.03	1.18	0.97	1.12	0.97	1.14	0.96	1.10	0.02	
0.93	1.12	0.91	1.11	1.04	1.27	0.94	1.20	0.95	1.22	0.96	1.18	0.02	
0.95	1.32	0.93	1.21		1.42		1.36		1.35	(0.94)	1.33		
	1.51		1.45		1.62		1.47		1.46		1.50		0.03
	1.56		1.53		1.65		1.58		1.56		1.58		0.02
	1.70		1.64		1.76		1.61		1.68		1.68		0.03
	1.76		1.67		1.82		1.70		1.76		1.74		
	1.87		1.79		1.93		1.81		1.88		1.86		
	1.95		1.85		2.04		1.92		1.97		1.95		
	1.90		1.85		2.00		1.84		1.91		1.90		
	1.76		1.68		1.82		1.68		1.71		1.73		
	1.49		1.49		1.61		1.47		1.54		1.52		0.03
1.00	1.34		1.35		1.56		1.47		1.45	(1.00)	1.44		0.04
	1.16		1.20		1.40		1.28		1.32		1.27		0.04
0.96	1.02	0.94	0.99	1.08	1.13	1.03	1.08	0.96	1.02	0.99	1 05	0.03	0.02

obtained for flow of the 1.02 ‰ bentonite sol. This part of the experiments does not need a further explanation, the evaluations being reported in Table 5.3 in the same manner as those in Table 5.1.

When the disturbance plate was situated 15 mm from the rounded tube inlet, turbulence did not appear at Reynolds numbers below $R \approx 2740$. The record of Fig. 5.9 shows the appearance and development of two turbulent flow regions travelling along the tube at a Reynolds number of $R \approx 3180$. We see—or at least it is visible in the original records—that the parts of the traces I, II and III representing "laminar" flow are not perfectly straight, but possess a slightly wavy pattern, the waviness being most pronounced in the traces I and II, although it is distinguishable also in trace III. This waviness appears to be due to entry disturbance vortices which roll along the tube walls and which fade out sooner or later unless, by the action of some unknown factors, they spontaneously transform into turbulent flashes. According to the record, such a whip-like transformation has taken place in the measuring section I, the moment of birth indicated by an arrow. When comparing the traces I and II, their measuring sections being in suit (see Fig. 5.1), we observe the very fast development of the turbulent "spot" during its initial stage, both with respect to its dimensions

Table 5.4. Primary experimental data and apparent dynamic viscosity

Low disturbance level of the entry flow was arranged for by locating the disturbance plate

$Q \cdot 10^6$	Temp.	R	U	Galvanometer deflection for pressure drop over various measuring sections Scale divisions								
m³/s	°C		V	I	II		III		IV		V	
4.61	17.5	670	10.81	6.6	4.4		6.6		3.4		4.9	
6.94	17.5	1010		9.8	6.7		10.2		5.7		7.6	
8.72	17.6	1270		12.5	8.3		13.0		7.1		9.5	
10.08	17.6	1470		14.2	9.5		15.2		8.1		11.0	
11.34	17.7	1660		16.1	10.8		17.3		9.3		12.5	
12.38	17.8	1810		17.5	11.8		18.8		10.3		13.7	
13.42	18.0	1980		19.1	12.8		20.4		11.2		14.9	
14.35	18.1	2120		20.4	14.0		21.9		12.0		15.9	
15.3	18.2	2260		21.8	14.8		23.7		12.8		17.0	
16.1	18.3	2390		23.1	15.8		25.0		13.7		17.9	
16.9	18.4	2510		24.5	17.0		26.3		14.5		18.9	
17.7	18.5	2640		25.8	17.7		27.7		15.0		19.9	
18.4	18.5	2740		27.0	18.5		28.9		15.7		20.8	
19.1	18.5	2850		28.3	19.6		30.4		16.4		21.7	
19.6	18.6	2930		29.4	20.3	34.7	31.5	52.6	17.0	28.7	22.7	38.9
20.3		3030		30.8	20.8		32.3	55.5	17.5	30.6	23.3	41.6
20.8		3110		31.9	21.7		33.4	58.4	18.1	32.1	23.7	43.1
21.3		3180		32.4	23.2		35.0	61.7	18.9	33.7	25.0	46.1
22.0		3290		34.1	23.9		36.5	65.9	19.9	35.3	26.0	49.2
22.3		3330		35.6	25.0	44.6	38.3	68.8		39.0		51.4
23.3		3480		37.4	27.0	49.2	41.0	75.3		42.3		56.2
24.2		3620		39.0	29.4	53.6		81.4		46.3		63.6
25.5	18.6	3810	10.81			59.1		89.9		51.4		67.5

and to its magnitude in energy transposition. When this turbulent region reaches the measuring section III it has considerably elongated itself, but we also see that its pressure drop crest has got a flattened "roof", its height corresponding to the equilibrium pressure drop as determined by the prevailing flow conditions. The same conclusions hold for the second turbulent region, shown by the record of Fig. 5.9, and which evidently is formed in the entry length of the tube, prior to the measuring section I. The turbulent regions have further elongated themselves, when reaching measuring section IV, as it appears, at constant rate of extension. At measuring section V the front of the second turbulent region has just overtaken the tail of the first one, so that there remains only a depression of the turbulent pressure drop trace as the result of the further extension of the two turbulent flow regions.

In Fig. 5.10 is shown a similar pressure drop record of flow at a Reynolds number of $R \approx 3480$. In the first part of the record we observe the appearance of rather large turbulent disturbances, which develop to equilibrium pressure drop already in measuring section II. However, there is also to be observed the formation and growth of a turbulent spot in section II, without any sign of this transformation being observable in the trace transmitted from section I. The single arrow shown in the record indicates the first appearance of this turbulent region. The double arrow shown later in the same record points out a similar flash-like formation of turbulence. In this determined on flow of distilled water through the 8.18 mm tube.

at a distance of 15 mm from the tube inlet. For detailed notations see text to Table 5.1.

Apparent dynamic viscosity $\mu \cdot 10^3$ reduced to 20°C reference temperature kg/ms									Mean value $\mu \cdot 10^3$ at 20°C kg/ms		$\pm \Delta\mu \cdot 10^3$ kg/ms	
I	II		III		IV		V					
0.77	0.68		0.85		0.82		0.76		0.78		0.03	
0.82	0.78		0.91		0.91		0.84		0.85			
0.86	0.80		0.94		0.91		0.86		0.87			
0.86	0.81		0.96		0.90		0.87		0.88			
0.88	0.82		0.98		0.91		0.89		0.90			
0.89	0.83		0.98		0.93		0.90		0.91		0.03	
0.90	0.84		0.98		0.94		0.92		0.92		0.02	
0.91	0.87		0.99		0.94		0.92		0.93			
0.92	0.87		1.00		0.94		0.93		0.93			
0.92	0.88		1.02		0.96		0.93		0.94			
0.94	0.91		1.03		0.97		0.94		0.96			
0.95	0.91		1.04		0.96		0.95		0.96			
0.96	0.92		1.04		0.97		0.96		0.97			
0.97	0.94		1.06		0.98		0.97		0.98			
0.99	0.95	1.66	1.07	1.80	0.99	1.67	0.99	1.72	1.00	1.71		0.03
1.00	0.94		1.06	1.84	0.98	1.72	0.98	1.78	0.99	1.78		0.04
1.02	0.96		1.07	1.89	0.99	1.76	0.98	1.80	1.00	1.82		0.04
1.01	1.00		1.10	1.95	1.01	1.81	1.01	1.89	1.03	1.88		0.04
1.03	1.01		1.11	2.02	1.03	1.83	1.02	1.95	1.04	1.93	0.02	0.06
1.06	1.04	1.88	1.15	2.08		1.99		2.01		1.99		0.04
1.07	1.08	1.99	1.18	2.18		2.07		2.11		2.09		0.04
1.07	1.13	2.09		2.27		2.18		2.30		2.21		0.05
		2.19		2.38		2.30		2.32		2.30		0.04

case, however, the formation is observed as started in section I. In section III there still appear "laminar" intervals, in the flow, but already in section IV the turbulent flow regions overlap each other, forming continuous turbulence, which never was observed to be broken off by "laminarity".

It is to be noticed that also in the case of highly disturbed entrance flow conditions (the disturbance plate situated 0.25 mm in front of the tube inlet) strong irregular fluctuations of the pressure drops are observed in the upper transition region of the flow at the measuring sections I and II. These fluctuations decrease with the travelling distance towards the actual state of equilibrium, which mostly appears to be fully developed at measuring sections IV and V, their turbulent pressure drop fluctuations being rather small.

From the above statements we understand that the average total pressure drop, integrated over extended time intervals over various measuring sections of any tube, would indicate turbulent equilibrium state at Reynolds numbers which are the higher the nearer to the tube inlet the measuring section is situated. This interpretation coincides with similar statements made in Part 4 of the paper, based on optic-electronic observations of flow of 0.40 ‰ bentonite sol through the same and other tubes.

However, I want to point out that the above conclusions in general are not valid for flow within certain "lengths of accumulation", this length in the main being determined by the disturbance level of the inlet flow although other factors also probably might be important in this respect, as for instance the surface properties of the tube walls. Within the length of accumulation the given description of the flow characteristics and their meaning has to be modified in several respects. Some of those modifications are elucidated in Part 2 of the present paper.

It is now possible properly to co-ordinate the present investigations with those according to Schiller 1924. The preceding analysis shows that the observed increase of the pressure drop with increasing entry lengths at the same Reynolds number for flow through the same tube does not mean a decrease of the "critical" Reynolds number towards a "lower critical" Reynolds number $R_k = 2320$ with increasing entry lengths as was concluded by Professor Schiller. On the contrary, quite high Reynolds numbers, mainly determined by the inflow conditions, might be obtained without any turbulence appearing in the flow, independent of the entry lengths allowed for.

Table 5.4 contains the flow data recorded for flow of low entrance disturbance level. The apparent dynamic viscosity of each turbulent flow is calculated by use of the total equilibrium pressure drop determined. No average values determined by integration over extended time intervals have been used in the calculations, such mean values being of no significance whatsoever. Furthermore, the chosen method of evaluation makes the data in the Tables 5.3 and 5.4 compatible with each other, so that they can be collected in the same diagram as shown in Fig. 5.11.

We observe the same systematic spreading of the apparent viscosity values for flow of distilled water according to Tables 5.3 and 5.4, as was noted for flow of the 1.02‰ bentonite sol according to Table 5.1. The values determined through measuring channel II, which was not operating during the experiments reported in the previous section, appear quite low, in the same manner as the values according to channel III are rather high in comparison to the corresponding values due to the other measuring channels. The deviations decrease as the apparent viscosity values determined increase, a tendency that was observed also for flow of the 1.02 ‰ bentonite sol. The maximum probable error of each μ value is given by the diagrams of Fig. 5.5 and the discussion regarding the validity and accuracy of the results, which was kept in connection with this figure is applicable also with respect to the present viscosity values obtained for flow of distilled water.

According to the records of the experiments with low disturbance level of the inlet flow, the velocities of the turbulent flow regions when passing from section I to section II deviate considerably from the velocities obtained for passages between the later sections. This deviation depends mainly on the flash-like formation of the turbulence, implying a very fast growth of the turbulent regions during their initial stage at high Reynolds numbers.

Fig. 5.11 shows that there is good agreement between the apparent μ values from Table 5.3 and those of Table 5.4, the values of Table 5.4 implying a confirmative extension towards higher Reynolds numbers.

There is a close resemblance between the flow data obtained for flow of 1.02‰ bentonite sol, as shown in Fig. 5.6, and those for flow of distilled water according to Fig. 5.11. In both cases the dynamic viscosity μ for laminar flow increases with increasing Reynolds number R with about the same constant rate of change, the μ values being smaller than the respective μ_∞ values at 20°C with about the same amount and in both cases approaching the μ_∞ values at a Reynolds number of about $R \approx 2700$-3000. (When making this comparison, we have to bear in mind that pressure transmitter II, which systematically indicated rather low μ values as compared

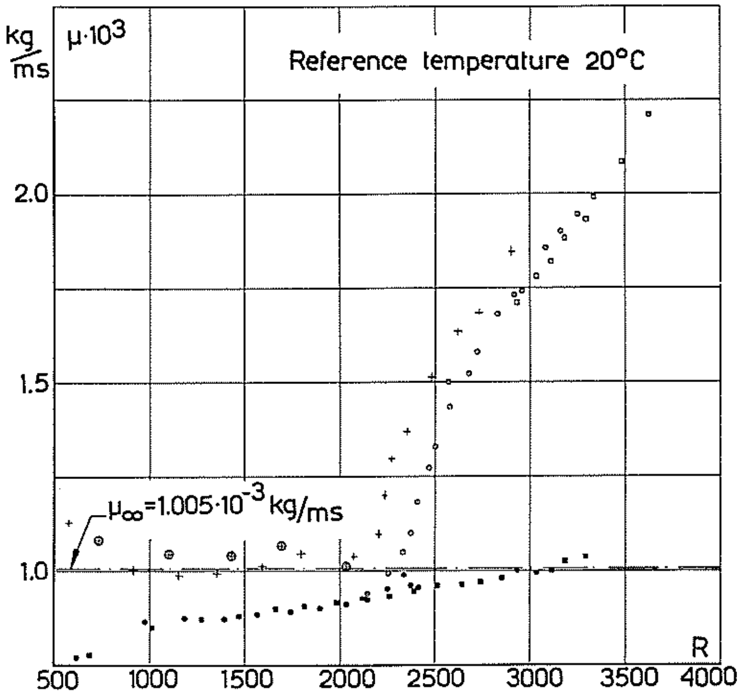

Fig. 5.11. Apparent dynamic viscosity μ of distilled water at 20°C as related to the Reynolds number R according to Tables 5.3 and 5.4. Also the standard dynamic viscosity value μ_∞ of water at 20°C according to Bingham and Jackson 1918 is given in the diagram as well as some apparent dynamic viscosity values evaluated from Reynolds' primary experimental data on flow of tap water through a cylindrical lead pipe of diameter 6.15 mm.

The R value of each measuring point in the diagram is calculated by use of the standard kinematic viscosity value ν_∞ of water at the flow temperature in question, as given by the authors cited above.

● laminar pressure drop
○ turbulent mean pressure drop } Disturbance plate situated 0.25 mm from the tube inlet

▪ laminar pressure drop
□ turbulent equilibrium pressure drop } Disturbance plate situated 15 mm from the tube inlet

+
⊕ } Mean pressure drop according to Reynolds (1883 Tables III and IV). High disturbance level of the entry flow.

to the other transmitters, was out of operation when determining the data of Fig. 5.6.)

Fig. 5.11 also contains viscosity data evaluated from Professor Reynolds' pressure drop measurements on flow of tap water through a 4.88 m long cylindrical lead pipe of 6.15 mm diameter. The entry length was 2.93 m and the measuring section was 1.52 m long. The viscosity values given are those according to Table IV and those of the laminar flow region reported in Table III of Reynolds' paper 1883 the values being reduced to 20°C temperature.

Although the viscosity values due to Reynolds appear quite spread within the laminar flow region, they agree in the main with the standard value indicated in

Table 5.5. Velocity data of turbulent flow regions in flow of distilled water through the 8.18 mm tube according to pressure drop records.

For further information see text to Table 5.2.

U m/s	Temp. °C	R	Time scale of the record s/mm	Record interval between fronts mm	Record interval between tails mm	Tube passage length m	U_F front m/s	U_F tail m/s	Mean U_F/U front	Mean U_F/U tail
0.287	16.4	2140	0.0712	26 ± 3 81 ± 1 201^{+3}_{-5} 209 ± 3	24 ± 1 85^{+2}_{-1} 200 ± 3 210 ± 3	0.50 1.75 4.00 4.00	0.272 0.305 0.280 0.269	0.289 0.288 0.281 0.268	0.98	0.98
0.301	16.6	2250	0.0657	24^{+4}_{-3} 92^{+7}_{-5} 219^{+7}_{-4} 222 ± 10	26^{+2}_{-1} 93^{+4}_{-3} 218^{+5}_{-7} 226^{+3}_{-7}	”	0.316 0.290 0.278 0.274	0.289 0.287 0.280 0.270	0.96	0.94
0.316	16.7	2370	0.0612	26^{+4}_{-7} 93^{+3}_{-8} 223^{+7}_{-12} 229^{+5}_{-6}	28 ± 2 98 ± 3 228^{+6}_{-7} 237^{+6}_{-8}	”	0.314 0.308 0.294 0.285	0.294 0.293 0.287 0.275	0.95	0.91
0.322	16.7	2410	0.0573	29^{+4}_{-5} 95 ± 9 230^{+10}_{-12} 242	30 ± 3 104 ± 4 241^{+7}_{-5} 242	”	0.303 0.323 0.303 0.288	0.292 0.295 0.289 0.288	0.94	0.90
0.333	16.8	2500	0.0543	26^{+2}_{-4}	31^{+1}_{-2}	”	(0.357)	(0.296)	(1.04)	(0.87)
0.306	16.8	2330	0.0378	43 ± 8 159^{+8}_{-9} 376^{+21}_{-12} 392^{+19}_{-22}	46^{+6}_{-3} 164^{+4}_{-6} 385^{+7}_{-15} 397^{+8}_{-9}	”	0.313 0.292 0.282 0.270	0.286 0.283 0.276 0.267	0.94	0.91
0.373	18.6	2930	0.0574	17 65 153 160	25 98 222 234	”	(0.510) 0.469 0.456 0.436	(0.347) 0.311 0.314 0.298	1.22	0.83

Table 5.5 (*continued*)

U m/s	Temp. °C	R	Time scale of the record s/mm	Record interval between fronts mm	Record interval between tails mm	Tube passage length m	U_F front m/s	U_F tail m/s	Mean U_F/U front	Mean U_F/U tail
0.386	18.6	3030	0.0532	15 66 155 ± 9 167^{+1}_{-2}	28 101^{+1}_{-2} 237^{+2}_{-3} 249 ± 0	0.50 1.75 4.00 4.00	(0.625) 0.499 0.485 0.451	(0.336) 0.327 0.318 0.302	1.24	0.82
0.396	,,	3110	0.0496	11 71 164 182	32 111 258 272	,,	(0.909) 0.497 0.492 0.443	(0.314) 0.318 0.313 0.297	1.20	0.78
0.405	,,	3180	0.0464	8^{+9}_{-4} 71^{+7}_{-1} 170^{+1}_{-3} 184 ± 9	27^{+7}_{-9} 119^{+2}_{-3} 276 ± 1 294	,,	(1.316) 0.529 0.509 0.469	(0.394) 0.318 0.313 0.293	1.24	0.76
0.419	,,	3290	0.0439	13^{+17}_{-9} 67^{+2}_{-3} 162 ± 3 174^{+9}_{-10}	44^{+15}_{-10} 122^{+3}_{-4} 281 ± 4 301^{+4}_{-6}	,,	(1.351) 0.599 0.562 0.524	(0.313) 0.328 0.324 0.303	1.34	0.76
0.424	,,	3330	0.0423	9^{+12}_{-6} 71^{+3}_{-4}	31^{+8}_{-17} 128 ± 5	,,	(1.316) 0.587	(0.379) 0.324	(1.32)	(0.74)
0.443	,,	3480	0.0410	9 67	32^{+4}_{-11} 129^{+7}_{-5}	,,	(1.351) 0.639	(0.382) 0.331	(1.37)	(0.72)

the figure ($\mu = \mu_\infty = 1.005 \cdot 10^3$ kg/ms). They evidently do not confirm the well collected data of the present pressure transmitter experiments but, on the other hand, they show a resemblance to values determined in some of the series of measurements shown in Figs. 2.10; 2.11 and 2.12 in Part 2 of the present paper. The discrepancies do not mean that the pressure transmitter measurements necessarily should be faulty. Of course, improved pressure transmitter measurements must be undertaken in the future in order to decide about the reliability of the results obtained. It is, however,

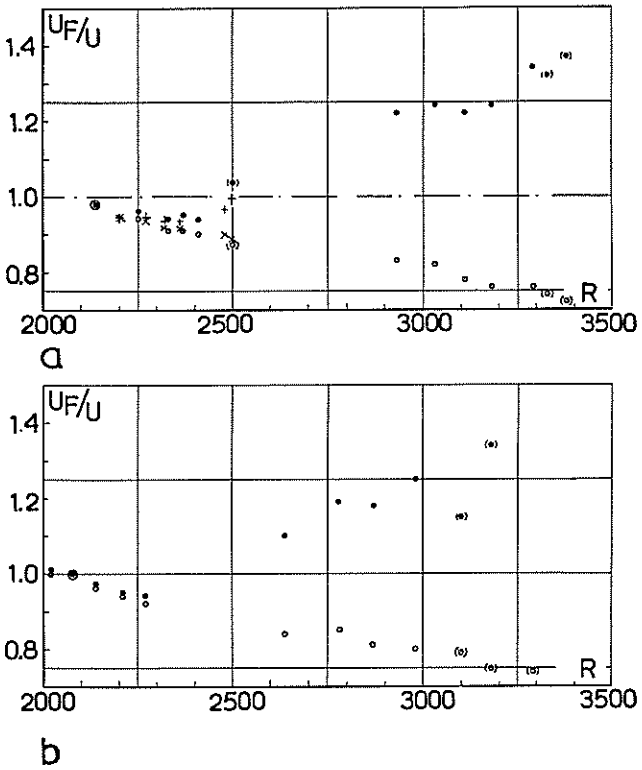

Fig. 5.12. Relative velocity U_F/U of fore and aft ends of turbulent flow regions in flow of distilled water through (*a*) the 8.18 mm tube, (*b*) the 10.31 mm tube related to Reynolds number R according to pressure drop records evaluated in Tables 5.5 and 5.8.

Fig. 5.12*a* also shows the velocities of turbulent regions in flow of 1.02‰ bentonite sol through the 8.18 mm tube as determined by means of "visual" records (see Fig. 5.7) for comparison purposes.

U = mean flow velocity; U_F = velocity of fore or aft ends of turbulent regions.

● front velocity according to pressure drop records
o tail velocity according to pressure drop records
+ front velocity according to "visual" records
× tail velocity according to "visual" records.

to be noted that the present measurements have resulted in mean values obtained over several test sections simultaneously and that rheologic properties of the liquids might be responsible for the discrepancies. For instance, there are no free liquid surfaces in the pressure transmitters, and there are only very small volume displacements for pressure drop variations in contradistinction to what is the case for ordinary liquid manometers, of what importance that now might be.

It is not necessary specially to point out that there is a gradual transition between "laminar" and turbulent flow of distilled water according to Fig. 5.11, as was previously found to be the case for flow of bentonite sols. The experiments indicate that there are no qualitative differences between flow of distilled water and flow of bentonite sols, at least not for sols of low concentration. This fact is further confirmed when considering also the relative velocity of the fore and aft ends of turbulent regions as shown in Fig. 5.12*a* according to data given in Table 5.5 read from the pressure drop oscillograph records.

In spite of the rather uneven recording speed of the galvanometer oscillograph, the velocity data obtained appear not too widely spread. For comparison Fig. 5.12*a* also contains the velocity values of turbulent regions in the flow of 1.02‰ bentonite sol determined by means of the optic-electronic method as reported in Table 5.2. There is quite good agreement between the velocity values obtained for the turbulent disturbances appearing in flow of the two liquids investigated.

The extra pressure drop caused by a single flash situated completely within each measuring section was evaluated to be about 7 N/m^2 varying about 50 % during the tube passage at a Reynolds number of $R \approx 2140$, the laminar pressure drop being about 70 N/m^2. At $R \approx 2250$ the flash pressure drop was about 9 N/m^2, while the laminar pressure drop was about 75 N/m^2. At a Reynolds' number of $R \approx 2370$ the concept of single flashes lost its meaning, as here the flashes began to extend their dimensions or began to split into several units overlapping each other, as they travelled along the tube.

During the above experiments there was never observed the fading out of a flash during its tube passage. This statement is in agreement with observations of flow of bentonite sols through the same 8.18 mm tube as reported in Part 4 of the paper.

Quantitive observations on flow of distilled water through the 10.31 mm tube

The purpose of these complementary tests was to decide whether a change of the diameter would affect any of the flow phenomena reported in the previous section.

Also here two series of records were obtained with the disturbance plate situated 0.25 mm and 15 mm respectively from the tube inlet. The Tables 5.6 and 5.7 contain the individual values of the apparent dynamic viscosity due to the various measuring channels as also the corresponding mean values, shown in Fig. 5.13.

There is a substantial increase of the spreading of the individual apparent viscosity values relative to each other as well as of their mean values, determined on flow of water through the 10.31 mm tube when compared to those determined on flow through the 8.18 mm tube. This state of matters is quite natural, if we consider the maximum probable errors according to Fig. 5.14 (estimated for flow through the 10.31 mm tube), which are about twice as large as corresponding errors due to Fig. 5.5 (estimated for flow through the 8.18 mm tube). (The errors are related, roughly, to the fourth power of the tube diameter.)

The records and results obtained do not need further comments, but verify the experiments on flow through the 8.18 mm tube in every respect. Even in the laminar flow region the absolute magnitude of the apparent values determined and their rate of change as related to the Reynolds number agree surprisingly well according to the Figs. 5.11 and 5.13. This state of matters increases the trustworthiness of the results obtained as the pressure drop over the measuring sections of the 10.31 mm tube is only about half that over the measuring sections of the 8.18 mm tube at corresponding Reynolds numbers of the flow.

Of course, new experiments must be undertaken for control and extension of the present experiments. At the time, however, I cannot see how to explain the flow char-

Table 5.6. Primary experimental data and apparent viscosity values determined for level of the

Further information is given

$Q \cdot 10^6$ m³/s	Temp. °C	R	U V	Galvanometer deflection for pressure drop over various measuring sections Scale divisions: I		II		III		IV		V	
8.50	14.9	920	10.82	5.4		3.6		5.8		3.2		4.2	
11.55	15.1	1250		7.1		4.5		7.5		4.2		5.6	
13.88	15.3	1510		8.6		5.2		9.2		5.1		6.5	
15.4	15.4	1680		9.5		6.1		10.7		5.5		7.3	
17.2	15.6	1890		11.2		6.9		12.1		5.9		8.2	
18.3	15.8	2020		12.0	12.3	7.2	7.4	12.6	12.8	6.4	6.5	8.8	9.4
18.7	16.0	2080		12.1	12.5	7.0	7.4	12.6	13.0	6.4	6.6	8.7	9.2
19.2	16.1	2140		12.9	13.7	7.4	8.2	13.1	13.9	6.7	7.3	8.9	9.9
19.8	16.2	2210		13.0	14.0	7.5	8.5	13.3	14.1	6.9	7.3	9.3	10.4
20.3	16.3	2270		13.1	14.7	7.3	9.7	13.9	15.8	6.9	8.7	9.8	12.4
21.1	16.3	2360			15.5		10.9		17.3		9.1		13.4
21.7	16.4	2430			19.2		11.9		19.7		9.8		14.5
22.2	16.4	2490			20.4		13.1		21.7		10.4		16.6
22.8	16.5	2560			22.6		15.0		23.5		11.7		18.6
23.5	16.6	2650			23.7		15.1		24.4		11.5		19.4
24.1	16.6	2720			25.4		17.3		26.0		12.8		20.0
6.30	15.3	690		4.1		2.4		4.6		2.0		3.2	
10.15	15.5	1110		6.3		4.2		6.8		3.4		4.9	
12.72	15.7	1400		7.4		4.7		8.2		4.3		6.1	
14.66	16.1	1630		8.9		5.6		9.7		4.9		7.0	
16.1	16.3	1800		10.8		6.1		10.6		5.7		7.5	
25.3	16.6	2850			28.3		18.4		29.6		15.3		22.9
27.2	16.7	3080	10.82		33.4		22.4		35.4		18.1		16.7

Table 5.7. Primary experimental data and apparent viscosity values determined for flow flow was

For further details

$Q \cdot 10^6$ m³/s	Temp. °C	R	U V	Galvanometer deflection for pressure drop over various measuring sections Scale divisions: I		II		III		IV		V	
9.11	15.2	990	10.82	5.6		3.4		6.6		3.0		4.2	
11.22	15.2	1220		6.9		4.3		8.0		3.7		5.5	
13.12	15.3	1430		8.1		4.9		9.2		4.2		6.2	
14.62	15.4	1600		9.1		5.6		10.4		4.8		6.9	
16.1	15.5	1760		10.3		6.3		11.4		5.6		7.8	
17.3	15.6	1900		11.1		6.6		12.9		6.1		8.4	
18.5	15.8	2040		11.9		7.0		13.3		6.5		8.9	
19.6	15.9	2170		12.9		7.8		14.1		6.9		9.5	
20.2	16.0	2240		13.2		7.6		14.3		7.1		9.8	
20.7	16.2	2310		13.6		8.0		14.9		7.2		9.9	
21.6	16.4	2420		14.5		8.4		15.3		7.7		10.4	
22.5	16.6	2540		15.2		8.9		16.1		8.1		11.0	
23.3	16.7	2640		16.1		9.1		16.8		8.5	12.3	11.5	19.3
24.4	17.0	2780		16.5		9.6		17.6		9.1	13.9	11.9	21.7
25.1	17.1	2870		17.5		9.9		18.6	30.0	9.4	14.4	12.6	23.3
26.0	17.2	2980		17.8	29.1	10.3	20.7	19.3	30.5	9.8	16.0	12.9	24.2
26.9	17.4	3100		18.4	32.4	10.3	21.5		35.5		17.3		25.8
27.6	17.4	3180		19.2	34.1	11.0	22.9		36.5		18.5		27.1
28.5	17.5	3290	10.82	19,9	36.8	11.0	24.3		39.4		20.4		29.2

flow of distilled water through the 10.31 mm tube in the case of high disturbance entry flow.

in the text to Table 5.1.

Apparent dynamic viscosity $\mu \cdot 10^3$ reduced to 20°C reference temperature kg/ms										Mean value $\mu \cdot 10^3$ at 20°C kg/ms		$\pm \Delta\mu \cdot 10^3$ kg/ms	
I		II		III		IV		V					
0.815		0.750		0.920		0.934		0.793		0.84		0.03	
0.854		0.734		0.942		0.910		0.834		0.86		0.04	
0.897		0.738		0.943		0.920		0.827		0.87			
0.920		0.806		1.005		0.903		0.856		0.90			
0.993		0.830		1.027		0.867		0.871		0.92			
1.013	1.044	0.824	0.854	1.010	1.028	0.887	0.901	0.892	0.962	0.93	0.96		0.04
1.010	1.044	0.787	0.839	0.992	1.029	0.877	0.901	0.864	0.924	0.91	0.95	0.04	
1.058	1.127	0.821	0.919	1.013	1.078	0.894	0.973	0.866	0.975	0.93	1.01	0.05	
1.035	1.126	0.807	0.932	1.002	1.063	0.891	0.946	0.885	1.000	0.92	1.01	0.04	
1.021	1.158	0.767	1.049	1.023	1.173	0.873	1.016	0.914	1.186	0.92	1.12	0.05	0.04
	1.183		1.148		1.237		1.106		1.235		1.18		0.03
	1.450		1.229		1.381		1.164		1.315		1.31		0.05
	1.516		1.334		1.489		1.209		1.478		1.41		0.06
	1.647		1.505		1.582		1.327		1.629		1.54		0.06
	1.687		1.473		1.601		1.270		1.656		1.54		0.08
	1.769		1.662		1.667		1.375		1.667		1.63		0.07
0.760		0.575		0.961		0.798		0.759		0.77		0.06	
0.847		0.776		0.929		0.841		0.816		0.84		0.03	
0.832		0.720		0.920		0.855		0.846		0.84			
0.906		0.774		0.962		0.854		0.866		0.87			
0.950		0.783		0.967		0.908		0.859		0.89		0.03	
	1.883		1.688		1.813		1.565		1.826		1.76		0.06
	2.100		1.935		2.026		1.731		1.996		1.96		0.06

of distilled water through the 10.31 mm tube when low disturbance level of the entry arranged for.

see text to Table 5.4.

Apparent dynamic viscosity $\mu \cdot 10^3$ reduced to 20°C reference temperature kg/ms										Mean value $\mu \cdot 10^3$ at 20°C kg/ms		$\pm \Delta\mu \cdot 10^3$ kg/ms	
I		II		III		IV		V					
0.806		0.650		1.000		0.821		0.746		0.81		0.06	
0.851		0.720		1.000		0.825		0.841		0.85		0.05	
0.888		0.728		0.998		0.803		0.827		0.85		0.05	
0.915		0.765		1.023		0.825		0.846		0.88		0.05	
0.961		0.802		1.029		0.880		0.885		0.91		0.04	
0.978		0.789		1.092		0.891		0.898		0.93		0.05	
0.993		0.794		1.061		0.892		0.893		0.93		0.05	
1.031		0.847		1.068		0.894		0.910		0.95		0.04	
1.024		0.798		1.053		0.896		0.913		0.94		0.05	
1.040		0.828		1.077		0.891		0.907		0.95			
1.075		0.847		1.068		0.920		0.922		0.97			
1.091		0.868		1.088		0.935		0.943		0.99			
1.130		0.865		1.100		0.948	1.369	0.963	1.666	1.00	(1.52)		0.15
1.113		0.882		1.108		0.975	1.490	0.959	1.812	1.01	(1.65)		0.16
1.157		0.890		1.145	1.875	0.983	1.505	0.995	1.900	1.03	(1.76)		0.13
1.138	1.920	0.891	1.884	1.151	1.845	0.990	1.619	0.985	1.909	1.03	1.84	0.05	0.06
1.145	2.089	0.864	1.905		2.091		1.700		1.988	(1.01)	1.96	0.14	0.07
1.171	2.144	0.912	1.986		2.095		1.853		2.032	(1.04)	2.02	0.13	0.05
1.185	2.254	0.888	2.050		2.203		1.899		2.133	(1.04)	2.11	0.15	0.06

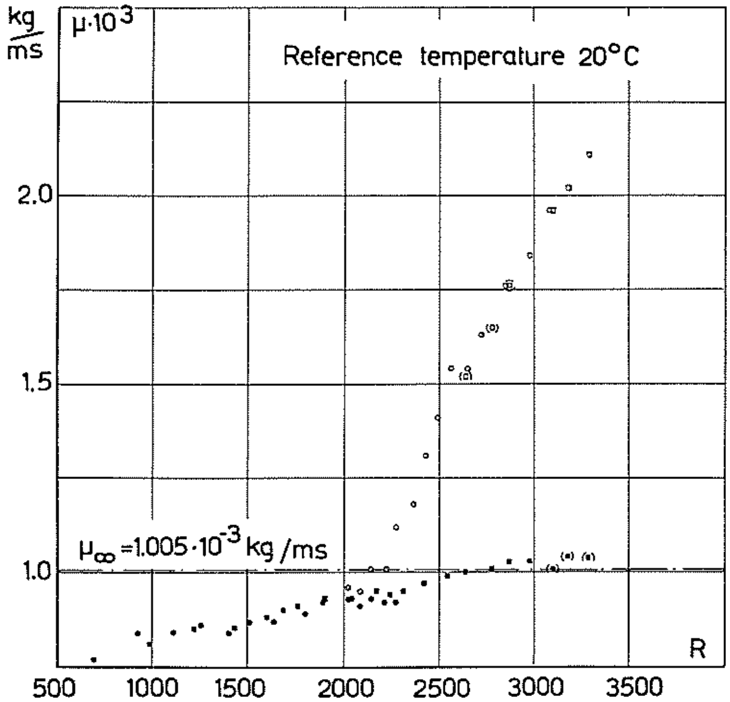

Fig. 5.13. Apparent dynamic viscosity μ of distilled water at 20°C related to Reynolds number R according to data of Tables 5.6 and 5.7. Detailed explanation of the diagram is found in the text to Fig. 5.11.

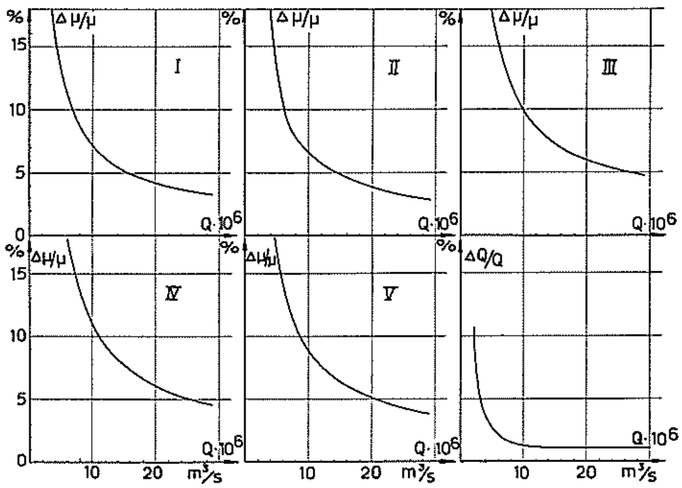

Fig. 5.14. Estimated maximum probable error, $\Delta\mu/\mu$, of individual viscosity values, determined on flow through the 10.31 mm tube, related to the rate of flow, Q. For further informations see text to Fig. 5.5.

Table 5.8. Velocity data of turbulent flow regions appearing in flow of distilled water through the 10.31 mm tube according to pressure drop records.

Detailed notations are given in the text to Table 5.2.

U m/s	Temp. °C	R	Time scale of the record s/mm	Record interval between fronts mm	Record interval between tails mm	Tube passage length m	U_F front m/s	U_F tail m/s	Mean U_F/U front	Mean U_F/U tail
0.219	15.8	2020	0.0708	31^{+3}_{-1} 110^{+10}_{-9} 259^{+1}_{-2} 257^{+15}_{-10}	32 ± 3 112^{+3}_{-4} 254^{+3}_{-4} 268 ± 12	0.50 1.75 4.00 4.00	(0.226) 0.225 0.218 0.220	0.221 0.222 0.222 0.211	1.01	1.00
0.224	16.0	2080	0.0648	31^{+7}_{-4} 115^{+13}_{-10} 280^{+10}_{-9} 279^{+13}_{-8}	34^{+3}_{-2} 119^{+6}_{-5} 278^{+9}_{-7} 287^{+9}_{-10}	,,	(0.250) 0.235 0.220 0.221	0.228 0.227 0.222 0.215	1.00	1.00
0.230	16.1	2140	0.0602	36^{+9}_{-5} 130 ± 6 302^{+6}_{-5} 299^{+11}_{-12}	38^{+1}_{-2} 129^{+6}_{-7} 302^{+6}_{-18} 308^{+6}_{-9}	,,	(0.228) 0.223 0.220 0.223	0.221 0.225 0.220 0.216	0.97	0.96
0.237	16.2	2210	0.0565	37^{+7}_{-9} 134^{+12}_{-11} 319^{+8}_{-10} 315^{+11}_{-15}	40^{+3}_{-2} 134^{+5}_{-3} 315^{+12}_{-14} 328^{+4}_{-3}	,,	(0.240) 0.231 0.222 0.225	0.220 0.231 0.225 0.216	0.95	0.94
0.243	16.3	2270	0.0535	35^{+7}_{-6} 142^{+3}_{-2} 323^{+5}_{-6} 336^{+4}_{-2}	42 ± 1 142 ± 4 332 ± 6 351 ± 3	,,	(0.269) 0.231 0.232 0.222	0.224 0.231 0.225 0.213	0.94	0.92
0.242	16.0	2240	0.0716	239 240	241 246	,,	0.234 0.232	0.232 0.227	(0.96)	(0.94)
0.279	16.7	2640	0.0551	26 94 229 273	35 134 306 313 ± 2	,,	(0.350) 0.338 0.317 0.266	(0.259) 0.237 0.237 0.232	1.10	0.84

Table 5.8 (*continued*)

U m/s	Temp. °C	R	Time scale of the record s/mm	Record interval between fronts mm	Record interval between tails mm	Tube passage length m	U_F front m/s	U_F tail m/s	Mean U_F/U front	Mean U_F/U tail
0.292	17.0	2780	0.0513	27^{+11}_{-6} 101^{+2}_{-1} 219^{+11}_{-14} 224	38 ± 1 135 ± 3 317 ± 7 320	0.50 1.75 4.00 4.00	(0.365) 0.337 0.356 0.348	(0.256) 0.253 0.246 0.244	1.19	0.85
0.301	17.1	2870	0.0502	25 100 235 213	37 151 314 330	,,	(0.398) 0.349 0.339 0.374	(0.273) 0.231 0.254 0.242	1.18	0.81
0.311	17.2	2980	0.0482	31 ± 10 96 ± 7 212 211 ± 4	40 ± 3 153^{+10}_{-12} 322 332	,,	(0.331) 0.378 0.391 0.394	(0.258) 0.237 0.258 0.250	1.25	0.80
0.322	17.4	3100	0.0444	30^{+4}_{-6}	42 ± 3	,,	0.382	0.272	1.15	(0.79)
0.331	17.4	3180	0.0450	24^{+4}_{-3}	42^{+2}_{-3}	,,	0.455	0.266	(1.34)	(0.75)
0.341	17.5	3290	0.0434	21^{+5}_{-7}	42 ± 1	,,	0.549	0.273	(1.57)	(0.74)

acteristics determined as due to accidental or systematic measuring errors. In this connection it must be repeated that concepts due to modern Rheology might provide the answers to what, according to Hydrodynamics, are anomalous flow phenomena.

In the pressure drop records of the flow of water through the 10.31 mm tube occasionally was observed the disappearance of turbulent flashes between the measuring sections I and III while no flash was observed to disappear further downstream. This implies a final verification of observations reported in Part 4 of the paper according to which no increase of the damping effect was observed, when the distance between the recording stations I and II was increased from about 300 to 870–1800 tube diameters, Stn. I situated 1.50 m downstream of the tube inlet. Further, the observations reported imply full agreement also with respect to the general damping effects on flashes observed, which, under the given conditions, were nonexistent for flow through the 8.18 mm tube also according to Part 4, while a slight damping effect was observed for turbulent flashes in flow through the 10.31 mm tube.

For flow of water through the 10.31 mm tube, the extra pressure drop caused by a single flash completely contained within a measuring section was about 5 N/m^2 at a Reynolds number of $R \approx 2020$, while the corresponding laminar pressure drop was 34 N/m^2. At the Reynolds number $R \approx 2140$ the flash pressure drop was about 8 N/m^2 and the laminar pressure drop was 36 N/m^2. Above the Reynolds number $R \approx 2250$ flashes began to split and extend themselves so that the concept of single flashes lost its meaning.

The velocity data of the turbulent flow regions are presented in Table 5.8 and are also shown diagrammatically in Fig. 5.12*b*. They imply a further confirmation of previous observations and do not need further comments.

SUMMARY

Pressure drop measurements on flow of distilled water and of 1.02‰ bentonite sol, through two 12.5 m long cylindrical, technically smooth, transparent plastic tubes of diameters 8.18 and 10.31 mm, have been carried out simultaneously over several 0.50 m long measuring sections at various locations along the tubes by use of recording strain-gauge pressure transmitters.

Pressure drop records obtained for flow of the 1.02‰ bentonite sol were synchronized with optic-electronic records. These co-ordinated observations mutually confirmed each other in every respect as regards the appearance of turbulence or disturbances in the flow. Single flashes, however, cannot be distinguished from each other by means of pressure drop experiments in case the flashes appear so close to each other that a preceding flash has not left the measuring section in question before a new one enters into it. On the other hand, the use of pressure transmitters, which allow only very small volume displacements for quite large pressure drop fluctuations, considerably increased the range of information regarding the transition process, so that also the energy transpositions could be investigated in certain connections under various flow conditions.

It was found that the apparent dynamic viscosity, determined on flow of 1.02‰ bentonite sol as well as on flow of distilled water, increased rectilinearily with increasing Reynolds numbers from rather low values, considerably lower than the standard viscosity value at a Reynolds number of $R \approx 500$ and exceeding the standard value at a Reynolds number of about $R \approx 2800$–3000. (The Reynolds numbers are calculated by use of the standard viscosity values.)

Each single turbulent flash was found to represent a discrete amount of energy transposition, which amount, however, might vary as the flash travels along the tube as depending on how known and unknown turbulence maintaining factors vary along the tube. The average energy transposition of the individual flashes increases very fast with increasing Reynolds numbers, while the "laminar" pressure drop increases at a much slower rate. Even so it was finally verified that transition between laminar and turbulent flow manifests itself as a fully continuous increase of the pressure drop with the Reynolds number. This means that the definition of the "critical" Reynolds number as connected to an instantaneous increase of the flow pressure drop is not adequate with true flow conditions. This the more as the present experiments in all respects

have confirmed statements given in the previous part of the paper, according to which the magnitude of the Reynolds numbers, at which transition gradually takes place, depends on several factors, as for instance the surface properties of the bounding walls. It is also to be mentioned that turbulent flashes, according to the pressure drop records, were observed to disappear in flow of distilled water through the 10.31 mm tube within the first 3.5 m of the tube, while no flashes were observed to disappear further downstream. Furthermore, no flashes at all were observed to disappear in flow through the 8.18 mm tube, the technically smooth surface of this tube being more rough than that of the 10.31 mm tube. (The observations reported refer only to flow in the tubes at distances farther than about 130 tube diameters from the inlet end.) This state of matters implies a confirmation of indications also reported in Part 4 of the paper.

6. Context of the present experimental findings in view of observations reported in the literature

During the progress of the study presented, new information has continuously been obtained on the various flow processes and it has often been necessary to modify previously made interpretations. Consequently it appeared desirable to finish the paper with a survey on the flow processes studied, considering the various aspects of the investigation in view of several findings reported in the literature.

Laminar flow and the concept of viscosity

The following synopsis on laminar flow deals mainly with measurements on the viscous properties of flow of water and mercury.

Present observations

The determination of the viscosity of water as reported in Part 5 of the paper gave results which deviate considerably from observations commonly assumed "normal". Not only that the viscosity, as determined at low flow velocities, appeared to be about 20 % lower than the corresponding standard value but also the viscosity showed an approximatively rectilinear increase with increasing flow velocity. According to current ideas such findings are inconceivable and I do not think that they are explicable even in terms of non-Newtonian behaviour of water predicted by advanced rheologists as Forslind 1952, 1953; F. S. Feates & J. G. Ives 1956 or Michel Lavergne & Walter Drost-Hansen 1956. The results obtained cannot in any case be explained from the point of view of the Eyring theory as presented by, for instance, J. O. Hirschfelder, C. F. Curtiss & R. B. Bird in their *Molecular Theory of Gases and Liquids* (1954, pp. 625–627).

Since I have as yet not been able to explain the anomalous results obtained as due either to systematic or to accidental errors, I have undertaken a review of some of the literature dealing with viscosity measurements of water and mercury in order to see whether large deviations from the standard values of viscosity possibly have been observed earlier. This study has proved most interesting and it appears that several, as it seems, unexceptionable determinations of the viscosity of both water and mercury have given results which deviate from the standard values to the same degree as have those of the present experiments.

A note on viscometry

Starting from the monographs on viscosity by Guy Barr 1931 and Marcel Brillouin 1907 one soon reaches the excellent review on the history, theory and determination of the viscosity of water by G. H. Knibbs 1895, 1896. As early as 1895 Knibbs (1895, p. 77) formulated the conflicting situation as regards the results of viscosity measurements of water as seen from the classical point of view: "Each observer's measurements are in general fairly consistent among themselves, but when compared with others, discrepancies are found ranging over somewhat wide limits. This is true, even where the schemes of observation have been identical: where they have differed the divergence of results is very marked."

In the second paper Knibbs (1896) stated that the great discrepancies were apparently not explained by possible errors of observation either of temperatures or efflux times or of the dimensions of the apparatus. He also concluded that determinations of the viscosity of water to the order of precision 0.1 % would involve an investigation of the cause of the large discrepancies. It is noteworthy that viscosity determinations of that order of accuracy are at present known with a discrepancy of 0.6 % between the results (Swindells, Coe & Godfrey 1952 on the one hand and Höppler 1952 on the other) without a reasonable explanation from the classical point of view, according to which water should be a Newtonian liquid.

Uncertainties in viscometry

It appears that the general discussion on the discrepancies in viscometry has diminished in intensity during the last 30 years although works on this subject have appeared now and then and even quite recently. The discussion has dealt mainly with the possibilities of slip between the bounding walls and the liquid tested and also with the problem of end corrections necessary to be applied when using the efflux method (flow through capillaries) as this is almost the only one used for "accurate" determination of the viscosity of liquids.

With respect to slip it is currently believed that if slipping occurs it must be of a negligible order of magnitude, even in the case of non-wetting wall-liquid combinations. This subject will not be taken up for discussion but reference is made to the works by Barr 1931 and Brillouin 1907 already cited and also to a comprehensive review given in Goldstein, *Modern Developments in Fluid Dynamics* (1938, vol. II, p. 676). However, in this connection it appears desirable to point out that Frances Richardson, J. K. Ferrel, H. A. Lamonds & K. O. Beatty 1955, using radio isotopes for studying the velocity distribution of laminar flow of water and glycerine through cylindrical tubes, reported some peculiar deviations from the parabolic velocity profile in the immediate vicinity of the tube wall. However, in a paper presented about a month later the same team, Beatty, Ferrel & Richardson 1955, reported the same, almost perfect parabolic velocity profile of the flow of glycerine to be valid as close as 0.15 mm from the tube wall, without mention of the deviations from the parabolic velocity distribution at distances closer than 0.15 mm to the tube wall as reported in their previous paper.

It is quite surprising to find that only some few investigations are reported in the literature in which direct attempts have been made to determine the laminar velocity distribution. The subject appears almost exhausted after mention of the works by Kohlrausch 1914, T. E. Stanton, Dorothy Marshal & C. N. Bryant 1920, J. Nikuradse 1931, R. R. Rothfus, C. C. Monrad & V. E. Senecal 1950 and Alexander Kolin 1953. However, only the experiments of Nikuradse and Kolin deal with liquid flow (water), while the other determinations are performed on flow of air. Kolin's method might be classified as a demonstration test which is not fit for any accurate determinations of the velocity distribution but which, however, on the whole was found to approach a parabola. Nikuradse's measurements, on the other hand, appear to have been published only as a short note in Prandtl-Tietjens, *Hydro- und Aeromechanik* (1931, vol. II, p. 28) where they are represented by smoothed curves lacking any experimental data. No velocity values are given for layers situated closer than 0.1 r (r = tube radius) from the tube wall, but until that distance, the measurements indicate a good verification of the parabolic velocity distribution. Nikuradse's corresponding measurements on turbulent pipe flow (Prandtl-Tietjens 1931, vol. II, p. 53) were reported as close as 0.02 r from the tube wall, so that one might wonder why no velocity data are given for the laminar flow at layers situated closer than 0.1 r to the wall. Here it is of interest to note that later measurements of the velocity profile of turbulent flow of water through cylindrical tubes, reported in detail by Nikuradse 1932, actually do indicate the occurrence of slip at the tube walls. These observations, however, and also those above according to Stanton, Marschal & Bryant 1920 and Rothfus, Monrad & Senecal 1950, are discussed later in this paper from another point of view. The paper by Kohlrausch 1914, already dealt with (pp. 37–38), is not significant in these connections and will not be considered further.

With the inclusion of the papers mentioned above it appears that as yet no satisfactory experimental information has been presented concerning the precise course of the laminar velocity profile in the proximity of the walls bounding the flow. This state of affairs might be understood if we consider the works published by J. D. Fry & A. M. Tyndall 1911 and Muriel Barker 1922 which show that measurements of low flow velocities close to rigid walls by the use of pitot tubes is quite a problem. It might be expected that such measurements would be troublesome with the use of any type of measuring probe, one important type of which is the hot-wire anemometer.

Also the problem of application of proper end corrections on viscosity measurements by means of the capillary method still appears to be open to inquiry. Reference can here be made to Swindells Coe & Godfrey 1952, Barr 1931, Emil Hatschek 1928, Brillouin 1907 and Knibbs 1895 and it is not necessary to present a discussion on this topic. Instead I shall direct attention to some reports on viscometry of water and mercury which appear to be of special interest with regard to the inquiry into the concept of viscosity.

Extreme values of the viscosity of water determined by means of the efflux method

According to Landolt-Börnstein, *Physikalisch-Chemische Tabellen* (5th ed., Hw. I, pp. 135–6; Eg. I, pp. 82–83) the viscosity values of distilled water at 20°C, as determined by various authors applying the efflux method by use of thin glass capillaries, appear to deviate from each other by as much as 1 % and at other temperatures the viscosity values determined deviate still more from each other as is demonstrated in a paper by Preston M. Kampmeyer 1952.

However, really great discrepancies of the order of 10 % or more have not been obtained so often and only when the tubes have not been made of glass and when their cross-dimensions have been larger than capillary size. Here note must be taken of the already quoted experiments of Schiller 1924 (see p. 10) in which was observed a 70 % fall of the "normal" laminar flow resistance coefficient of the flow of tap water, through a brass tube of 120 mm diameter, when a Reynolds number of about 10000 was exceeded, and Schiller stated that he could give no reasonable explanation of the deviations observed. Deviations in the opposite direction have been recently reported in a paper by Marion Brockman 1956.[1] In those experiments determination was made of the flow resistance coefficient on flow of tap water, in various test sections along an 8.5 m long tube which consisted of a 3 m long brass tube of 25.4 mm diameter followed by a 2.5 m long teflon tube of 24.5 mm diameter while the last part of the tubing was again a 3 m long brass tube of 25.4 mm diameter. The specific flow resistance in the first half of the first brass tube on the average exceeded the expected standard values by about 10 % while in the second half of the brass tube the deviation on the average had increased to 15 % or more. However, in the first part of the teflon tube (teflon is a very water-repellent material) the flow resistance exceeded the expected value by as much as 30 % while in the second half of that tube the deviation on the average had decreased to about 15 %. In the following brass tube the flow resistance values determined did not deviate so much from the expected ones except at a low Reynolds numbers where the deviations were about the same as or even exceeded those recorded at the measuring sections situated nearer the tube inlet. Brockman assumed that probably a swirl at the tube entry could be responsible for the deviations observed. This explanation appears not to be appropriate because if the entry disturbances had been so intensive that they influenced the "laminar flow resistance" then they certainly should cause transition to turbulence at a much lower Reynolds number than 4000, which was the lowest Reynolds number at which a rapid increase of the pressure drop in the measuring section situated farthest downstream of the tube inlet (entry length 271 tube diameters) was observed.

Extreme values of the viscosity of water determined by means of the Mallock-Couette apparatus

The Mallock–Couette apparatus consists in the main of two concentric cylinders of which one or both can be rotated around the common axis of symmetry, the test liquid being situated in the annular space between the cylinders. This type of flow is currently credited to M. M. Couette 1890 although two years before him, A. Mallock 1888/89 reported measurements of the viscosity of water and observations on the onset of turbulence in flow of water by use of such an experimental arrangement.

In Mallock's apparatus, the outer cylinder was rotated and the moment of force exerted on the inner cylinder was measured. The diameter of the inner cylinder was 46 mm and that of the outer one 50 mm while their height was about 110 mm. The viscosity values were determined by Mallock over a temperature interval from 0 to 45°C and agreed pretty well with those determined by Poiseuille 1840, 1841, (1846) but for a constant difference of about 3 %, by which amount the values due to Poiseuille exceeded those of Mallock. (Poiseuille performed his measurements by means of the efflux method, using glass capillaries.)

Some years later Mallock 1896 presented another report on viscosity measurements of water which he had performed by means of an inproved Mallock–Couette apparatus in which the outer rotating cylinder was interchangeable. Two outer

[1] I am indebted to Dr. Sune Berndt of the Aeronautical Research Institute, Stockholm, for drawing my attention to this paper.

cylinders of diameters 87 mm and 99 mm were employed. The diameter of the inner cylinder was 76 mm and its height 245 mm. Unexpectedly, the viscosity values determined by use of the smaller outer cylinder exceeded on the average the viscosity values due to the study of 1888/89 by about 30 % over all the temperature interval investigated while in the case of the larger cylinder the viscosity values determined exceeded the older ones on the average by as much as 100 %. Mallock was unable to explain these large discrepancies as being due to measuring errors. He carefully noted when transition from laminar to turbulent flow set in so that this possible cause of deviation is eliminated, and since the inner cylinder was at rest in these measurements, an initiation of "Taylor vortices" could not be an explanation of the deviations observed. (About 'Taylor vortices" see Taylor 1922/23 or Goldstein 1938, vol. I, pp. 196–7).

Mallock did not give any information about the material of the cylinders nor of the conditions of the cylinder surfaces.

C. Brodmann 1891 also employed a Mallock-Couette viscometer with rotating outer cylinder but with interchangeable inner cylinder in contradistinction to the arrangement used by Mallock. He also made viscosity measurements by means of two concentric spheres of which the inner sphere was bifilarly suspended while the outer one was rotated. The inner sphere was interchangeable. The spheres and cylinders were all made of brass. The wetted surfaces were gilt and polished and they were cleaned with caustic soda, alcohol and distilled water before starting each series of experiments.

The performance of the experiments with the sphere arrangement was varied by use of three inner spheres of diameters 30, 40 and 50 mm, while the diameter of the outer sphere was 60 mm. These measurements indicated that the viscosity of water increased with the rotational speed in agreement with observations reported by M. B. Elie 1882 who had applied the same technique of measurement. It appears that as yet no analysis has been published on the stability of this type of flow which was assumed laminar in Kirchhoff's treatment of the boundary problem (see e. g. Barr 1931, p. 217). Probably the observations reported by Brodmann and Elie could be due to the presence of secondary currents similar to the Taylor vortices which under certain circumstances might appear in the Mallock-Couette flow. Such an explanation is most likely because Brodmann's experiments with the Mallock-Couette apparatus did not indicate any apparent variation of viscosity with the rotational speed. (No secondary currents of the Taylor type can occur in the Mallock apparatus when the inner cylinder is kept at rest.).

Brodmann used three inner cylinders of diameters 29, 38 and 48 mm, their height being about 140 mm, while the diameter of the outer cylinder was 58 mm and its height about 170 mm. He observed increasing viscosity with increasing annular space as did Mallock in 1896. The viscosity values obtained by Brodmann were

$1.132 \cdot 10^{-3}$ kg/ms at	15.1 ± 0.2°C	(smallest cylinder)
1.114	15.05 ± 0.1	(medium cylinder)
1.049	15.0 ± 0.1	(largest cylinder)

These values should be compared with the standard viscosity value of water at 15.05°C which is $1.138{,}10^{-3}$ kg/ms. We observe, however, that there is a fair agreement bettween the viscosity values of distilled water obtained by Mallock 1888/89 and Brodmann 1891.

Extreme values of the viscosity of mercury determined by means of the efflux method

From the present point of view a most interesting paper on the viscosity of mercury was presented by G. Tamman & J. Hinnüber 1927. These authors determined the viscosity by measurement of the efflux of mercury through various metal capillaries. Mercury flowing through a 1.0 m long steel capillary of 1.06 mm diameter at a temperature of 13.5°C apparently possessed a viscosity which was about 2 % lower than the corresponding standard value determined by the use of thin glass capillaries. (See Landolt–Börnstein, 5th ed., Hw. I, p. 133, Eg. I, p. 81, Eg. II*a*, p. 104, Eg. III*a*, p. 168). When measuring the efflux through a 0.61 m long nickel capillary of 0.35 mm diameter at 9°C the obtained viscosity value exceeded the corresponding standard value by about 8 %. When the nickel capillary was replaced by a 1.0 m long copper capillary of 0.43 mm diameter, the clean inner surface of which was covered by the usual thin oxide layer, the apparent viscosity increased to about 22 % above the standard values. Tamman & Hinnüber continuously repeated their measurements of the efflux of mercury through the oxide coated copper capillary for about 72 hours without noticing any systematic change of the rate of flow. After removal of the oxide layer from the inner surfaces of the copper tube, continuously repeated measurements indicated a continuous increase of the viscosity with progressing amalgation of the tube walls. After 163 hours of measurement the apparent viscosity value had become about three times as large as the corresponding standard value. During the experiments with the copper capillary the temperature varied within the limits 10–7°C.

S. Erk 1928 and Eug. C. Bingham & Theod. R. Thompson 1928 objected to the observations of Tamman & Hinnüber quoted above. Erk supposed the anomalous results to be due to the onset of turbulence. We understand this to be a rather strained explanation since Erk himself, using standard viscosity values, estimated the Reynolds number of the various flow experiments to be 700–1000 (steel capillary), 140–250 (nickel capillary), and 250 (copper capillary). The unjustifiable in Erk's criticism has already been pointed out by Bingham & Thompson. Those authors merely directed their objections to the series of experiments with the copper tube in which the process of amalgation took place. They concluded that the decrease of fluidity was an indirect result of the very slight solubility of copper in mercury. "Differential solubility" was said to cause large crystals to build up on the capillary surface and interfere with the flow.

After studying Bingham & Thompson's paper which contains photographs of copper surfaces after 1 hour, 42 hours and 4 weeks duration of amalgating process, it appears unlikely to me that the observations of Tamman & Hinnüber could be explained solely as caused by mechanical action of the rough surfaces. In Part 3 of the present paper it is shown that even very great but regular roughness elements do not interfere with the flow very much as long as it is laminar, which was most likely the type of flow studied by Tamman & Hinnüber. The validity of their observations is further increased by their careful determination of the capillary diameters. They did not observe any change of the diameter values of the capillaries with the exception of a slight decrease of the diameter of the amalgated copper tube, the difference, however, being rather too small to explain the observed apparent decrease of fluidity. They also examined the tube surfaces by eye but they could find no substantial trace of mercury on any of the tube surfaces but for the amalgated one. The thin cover of mercury, causing the decrease of the diameter of the amalgated copper tube was, however, found to be a film of liquid structure that could be washed away. Finally they mentioned a comparison of the rate of flow of pure mercury through a glass capillary with that of mercury saturated with copper which indicated no substantial difference of the fluidity as being due to the dissolved copper.

It seems that the anomalous observations reported by Tamman & Hinnüber cannot be explained in terms of mechancial agitation of flow disturbances or turbulence or as an effect of dissolved copper in the mercury.

Conclusion

There are quite of few investigations reported in the literature which indicate inconsistent conditions with respect to the concept of viscosity. Such papers have been published by, for example, H. v. Helmholtz & G. v. Piotrowsky 1860, R. Ladenburg 1906, H. Glaser 1907, Charles E. Fawsitt 1907/08, J. Tausz & F. v. Kőrösy 1929, as well as by several other authors. It is, however, not my task to give a general survey on this subject. The papers quoted merely serve the purpose of illustrating that the anomalous results of the viscosity measurements reported in Part 5 of the paper are by no means singular in appearance. However, the increase of viscosity noted with increasing rate of flow seems to be quite an exceptional observation, because secondary currents are not likely to have occurred in this flow. I have found no paper in the literature reporting such a behaviour which could not be objected to as being caused by the presence of secondary currents (see for instance p. 141). Furthermore, in contradistinction to the present observations, experiments reported by Albert & Constance Griffiths 1920/21 and Albert Griffiths & P. C. Vincent 1925/26 on flow of water through thin glass capillaries at very low rates of shear indicated no systematic deviation from corresponding standard values obtained under normal rates of shear.

The continued study on the concept of viscosity presented in this part of the paper has not clarified but complicated the questions arising in Part 1. Unless the results of the several viscosity determinations reviewed should be explained as being caused by measuring errors, they confirm neither classical nor advanced ideas on the fluidity of liquids. In addition I have not managed to trace any systematic relationships between the anomalies observed. According to advanced ideas in Rheology (Part 1, pp. 9–11), the apparent viscosity of water, generally speaking, ought to decrease with increasing rate of shear, increasing cross-section of the flow and increasing water-repellency of the bounding walls. This behaviour might be true on its own but experimental results (for instance the works of Griffiths 1925/26, Brodmann 1891 and Brockman 1956 in the order mentioned) do not always seem to support the presumed scheme of flow.

Desisting from useless guesses at possible causes of the deviations noted, I wish to emphasize that we should not allow ourselves to put aside experimental results as being false just because they might not fit into some tractable hypothesis—unless, of course, we can distinctly point out the errors. Thus, there are urgent demands for new measurements on the viscosity of liquids in which the parameters involved should be varied within broad limits in contradistinction to what has been the case in the majority of viscosity measurements reported. Only then may we decide whether the anomalies hitherto observed are real or whether well-hidden errors in the measuring processes could perhaps be responsible for them. In this connection it appears desirable to mention that not only the material of the contact surfaces between liquid and bounding walls appears worth consideration as a parameter but also the material combinations of various parts of the complete apparatus, perhaps in relation to electric potentials, possibly playing some role in the flow processes (see for instance R. Auerbach 1930).

The transition process and the Reynolds number

The qualitative course of the transition process as interpreted from the observations of the present investigation appears to give a confirmative co-ordination of experimental results reported in the literature. In those cases where results reported by various authors apparently deviate from each other as well as from the present observations it has been possible to trace the discrepancies as due either to misinterpretation of observations or to misleading performance of the experiments. The following survey serves the purpose of giving a close description of the course of the transition process as determined in the present experiments in co-ordination with investigations due to various authors.

Laminar flow region $R < R_v$

It was reported in Part 2 that below a Reynolds number R of the order of 200, no disturbances were observed in the flow, even quite near the tube inlet, however strong disturbances were agitated in the entrance flow. These observations agree with those reported by Naumann 1931. He determined this "vorticity limit" to be $R = R_v \approx 200$. S. J. Davies & C. M. White 1928 made much the same observations on flow of water through a tube of rectangular cross-section of variable height 0.15–0.68 mm and of 25.4 mm width. They found that nothing but laminar flow occurred in any part of the tube whenever the Reynolds number was $R < 280$. (The Reynolds number is based on the hydraulic diameter as defined on p. 55.) It should, however, be noted that Davies & White did not set up any agitated disturbances in the inlet flow but merely employed a sharp edged tube inlet, so the vorticity limit is certainly $R_v < 280$.

Davies & White refer to similar observations made by S. D. Carothers 1912 on flow of oil through large smooth pipe lines; John H. Grindley & A. H. Gibson 1907/08 on flow of air through a very long coiled 'smooth' lead tube of about 3 mm diameter, and Sorkau 1911–1915 on flow of various liquids through short glass capillaries. However, it is unlikely that any of the observations reported by those authors have any bearing on the vorticity limit R_v. This statement is based on the fact that any entry disturbances in tube flow are damped and disappear within rather short distances, say maximum 50–100 tube diameters, from the tube entry as long as the Reynolds number $R < \underline{R}$, $\underline{R}$ being of the order of 2000 in the case of technically smooth tubes (see p. 34). In Grindley-Gibson's experiments the 36 m long measuring length of the tube was preceded by a 25 m long entry length of the same tube. Consequently, entry disturbance vortices cannot have been responsible for the vague increase of the flow resistance observed by those authors. Since the coil diameter of the tube was only 0.37 m it appears more credible that the effect observed was caused by secondary currents set up by centrifugal forces acting on the flow. Carothers, on the other hand, has not stated how long his pipe lines were but they were certainly of considerable lengths, so that the minor change of the flow resistance caused by any onset of entrance disturbances would hardly have been noticeable in comparison with the total flow resistance. It appears more likely that the several sharp bends of Carothers' pipe lines would set up disturbances in the flow when exceeding certain Reynolds numbers and thus be responsible for the observed vague decrease of the apparent fluidity. As regards the observations reported by Sorkau, these are due to more complicated relationships to which attention is paid later on (p. 149).

In this connection it is interesting to note that F. R. Sharpe 1905 theoretically determined a 'critical' Reynolds number of 470 below which no disturbances should be able to persist in flow through cylindrical tubes. William Orr 1907/09 corrected this limit to 360 in view of a numerical error in Sharpe's calculations. Orr himself, in an independent treatment, determined the "critical" Reynolds number 180. Of more peculiar interest is a theoretical investigation by I. Shibuya 1951 who, presuming somewhat special flow conditions and prescribed flow disturbances, attacked the eigenvalue problem as formulated by A. Sommerfeld 1908. He obtained a critical Reynolds number of about 300.

I am not qualified to judge the validity of the theoretical investigations on the instability problem mentioned above. It appears, however, that the investigations by Sharpe and Orr are the only ones hitherto presented in the literature that could reasonably be connected to any experimentally found "spontaneous transition point" for fluid flow in straight cylindrical tubes with "smooth" surfaces.

The disturbed entry flow and the initiation of turbulent flashes. The distance of accumulation

The present experiments have clearly indicated that so-called turbulent flashes (see p. 35) occur as the result of some sort of collapse of entrance flow disturbances, these being in the shape of more or less asymmetric toroidal vortices Such vortices are always damped and disappear some distance downstream of the tube inlet, unless they turn into turbulent flashes. The disturbed flow region in the entrance length of the tube is consequently to be distinguished from self-maintaining turbulent flow which possesses quite another structure of small-scale high-energetic eddies. Depending on the disturbance level at the tube inlet the disturbance vortices occur more or less readily but as already mentioned they will not appear in the tube, however high the disturbance level might be, as long as the Reynolds number R of the flow is less than the vorticity limit R_v which according to the preceding section has the value $R_v \approx 200$.

It is expressly stated in connection with the experimental observations reported that the transition process is a random phenomenon and that transition to turbulence takes place gradually by an increasing number of turbulent flashes according as the Reynolds number is increased. The experiments further indicate that each toroidal disturbance vortex has to roll some distance along the tube walls before the action of one or several wall effects might cause an instantaneous transformation of a disturbance vortex into a turbulent flash. This distance I have presently called the *distance of accumulation*.

Turbulent flashes always seem to appear with their bulk bodies in the shape of symmetrical toroidal vortices which are brought along with the flow rolling in contact with the tube walls and within which are noted very intensive small scale velocity fluctuations that are not present in corresponding primary disturbance vortices. Depending on the flow velocity distribution the turbulent flashes take the external form of arrows with the cusp in the direction of flow. (For a close description of the appearance of the turbulent flashes see pp. 33–37 and 59.)

The above scheme of the transition process as indicated by the present experiments is in agreement with and seems to co-ordinate observations reported by, for example, Reynolds 1883, Kohlrausch 1914, Davies & White 1928, Schiller 1930, Naumann 1931, Gibson 1933, Kurzweg 1933, Schiller 1934 and Binnie & Fowler 1947.

The initiation of turbulent flashes in the case of highly disturbed entry flow. The entry length, the damping limit $\underline{R}$ and the transition limit $\bar{R}$

Provided there is a high disturbance level of the flow at the tube inlet an increasing number of turbulent flashes are initiated within the disturbed entry flow region according as the Reynolds number is increased above the R_v limit. The disturbed entry flow region extends itself downstream for increasing Reynolds numbers, simultaneous with an increase of the average flash-arrow length and the average travelling distance of the flashes. However, as long as the Reynolds number is less than a certain value $\underline{R}$ all the flashes are damped and disappear after travelling rather limited distances. The longest of these travelling distances determine the *entry length.* Above the damping limit $\underline{R}$ some of the turbulent flashes begin to travel long distances with the flow through the tube without showing any sign of damping effects. On the contrary, these flashes appear to be self-maintaining by the action of some wall effects.

On further increase of the Reynolds number an increasing part of the increasing total number of turbulent flashes becomes non-fading. The distance of accumulation is fairly independent of the Reynolds number and in case of flow through technically smooth tubes the location where the turbulent spot initiation takes place might be situated at distances of 20–70 tube diameters from the inlet.

Simultaneous with the increase in the number of non-fading turbulent flashes for increasing Reynolds numbers there is also noted an increase of the entry length within which is observed the fading away of several turbulent flashes.

On a further increase of the Reynolds number the turbulent flashes follow closer and closer on each other, forming turbulent streaks and finally at the transition limit $R = \bar{R}$ the disturbed entry flow region directly transforms into continuous turbulent flow. The transition zone gradually moves nearer to the tube inlet with increasing Reynolds numbers but it never seems to be situated closer than 10–30 tube diameters to the inlet end. It is noteworthy that in the upper transition region the "continuous" turbulent flow appears to consist of turbulent flashes overlapping each other.

It has already been mentioned that the disturbed entry flow region reaches farther downstream of the tube inlet as the Reynolds number is increased. However, in the case of a high disturbance level of the entry flow, the disturbed entry flow region appears to be limited to within 70–100 hydraulic diameters from the inlet end because of direct transition to continuous turbulence already at rather low $\bar{R}$ values.

Naumann 1931, Binnie 1945 and Binnie & Fowler 1947 reported observations that in some parts directly verify the course of the transition process as indicated by the present observations described so far.

Mention should here be made that the above definition of the transition limit

$\bar{R}$ is somewhat incomplete. It might happen that the disturbed flow after travelling certain distances of accumulation transforms directly to continuous turbulent flow which, however, develops to discrete flash units further downstream within the entry length. This is a flow process which explains the dissipation effects observed on turbulent disturbances in flow of 5.8‰ and 2.5‰ bentonite sols within and above the transition region as reported in Part 2 of the paper (pp. 49–52). The transition limit $\bar{R}$, however, is meant as the Reynolds number at which the disturbed flow transforms directly to continuous flow, just at the limit at which it preserves its continuity throughout any lengths of the tube. It is noteworthy that the one or the other of those two conditions might be crucial with respect to the magnitude of the $\bar{R}$ value.

It is regrettable that it again is necessary to discuss observations reported by Rothfus & Prengle 1952, but this appears most desirable in view of a later report by Prengle & Rothfus 1955 which has misled even such competent reviewers as R. R. Hughes & A. K. Oppenheimer 1956 and consequently might lead to some general misunderstandings of the course of the transition process.

Prengle & Rothfus employed coloured liquid injectors of form similar to the common pitot tube where the mouth-piece is bent at right angle to the shaft. In Part 3 of the present paper (p. 62) it is shown that any thin probe would cause disturbances of the type mentioned by those authors. However, in spite of their statement that the "wave point" Reynolds numbers at various inserting depths increased with decreasing diameter of the mouth-piece, Prengle & Rothfus 1955 persist in their assumption that the probe is not the cause of the disturbances noted. So far as I understand, the mere indication of such a decrease of the wave-point numbers with increasing diameter implies enough evidence for the departure from the "truly viscous" flow noted by Rothfus & Prengle to be due to the probe. Those authors, however, plotted the "wave point" number versus the quotient of the diameter of the injector mouth-piece and the pipe diameter and, for various inserting depths, extrapolated wave point numbers corresponding to zero mouth-piece diameter. They concluded that the wave point numbers thus extrapolated should correspond to true wave point numbers of flow undisturbed by the probes. For control of their assumption they inclined the probe so that the tip of the dye injector just reached a chosen distance from the tube wall and determined the wave point number by observing the colour filament as before. The wave point number thus obtained agreed fairly well with the corresponding extrapolated wave point number. In this manner Prengle & Rothfus concluded that their method of observation was adequate.

Evidently the extrapolation process adopted by Prengle & Rothfus is misleading and rather gives information about the Reynolds number at which a thin probe tip without a flow-parallel mouth-piece (zero mouth-piece diameter) will cause disturbances in the flow at the inserting depth in question, which interpretation is in full agreement with the observations reported by those authors. Consequently, their determination of the "laminar film" thickness by that method also cannot be considered relevant.

The behaviour of the turbulent flashes. The critical Reynolds numbers R_k and $\bar{R}_k$.

The present experiments have shown that the self-maintaining flashes, at the Reynolds number $\underline{R}$ where they first appear, travel with unaltered dimensions along the tube with a speed which is about the same as the mean flow velocity U. When the Reynolds number is increased, the flash velocity U_F increases at a slower rate than the flow velocity U, so the relative flash velocity U_F/U decreases slowly with increasing Reynolds number. However, when approaching a certain Reynolds number, here called the critical Reynolds number R_k, any flash might begin to split into two or more units during its travel along the tube. The net effect of this splitting process is that the front of each original flash unit begins to travel faster than the corresponding tail. On further increasing the Reynolds number we pass the upper critical Reynolds number $\bar{R}_k$ above which each flash, without splitting, begins to elongate itself continuously as it travels along the tube. Above the critical Reynolds number R_k the front velocity U_F of each turbulent unit begins to increase faster than does the mean flow velocity U in such a manner that the quotient $(U_F/U)_{\mathrm{Front}}$ increases at a diminishing rate as the Reynolds number increases. The quotient $(U_F/U)_{\mathrm{Tail}}$ of the tail velocity U_F and the mean flow velocity U, on the other hand, proceeds to decrease at a rate which slowly lessens with increasing Reynolds numbers.

I have the impression that the front velocity of the turbulent regions asymptotically increases with increasing Reynolds numbers towards the maximum value of the laminar velocity profile, which would mean that laminar flow becomes turbulent at the aft end, and turbulent flow becomes laminar at the fore end of the turbulent regions even at arbitrarily high Reynolds numbers. However, this cardinal feature is particularly obvious in the region $\underline{R} < R < R_k$, where the flashes proceed with unaltered lengths, with velocities lower than the mean flow velocity. It actually implies an indication that the turbulence maintenance processes must depend on some wall effects, as has already been mentioned (Part 4, p. 98); in addition, it also accounts for the arrow-like shape of the flashes, as has been pointed out on p. 59.

It appears that the upper critical Reynolds number $\bar{R}_k$ is the limit above which continuous turbulence will establish itself sooner or later in the flow provided a high enough disturbance level is secured at the tube inlet and that the tube is long enough. In contrast to that, continuous turbulence does not seem to appear in the "splitting" region $R_k < R < \bar{R}_k$ however long the tube is.

In principle the elongation of turbulent flow disturbances at high Reynolds numbers was already mentioned by Prandtl-Tietjens (1931, vol. II, p. 40) although their rough measuring method did not allow any precise velocity determinations to be made. The present experiments are also in agreement with observations reported by Rotta 1956. Rotta's measuring method, however, only permitted determination of the rate of elongation of the turbulent regions as related to the Reynolds number.

The double meaning of the critical Reynolds number R_k

It is noteworthy that the critical Reynolds number R_k, at which value the turbulent flashes begin to split during their travel, seems to agree fairly well with the critical Reynolds number R_k' at which an abrupt increase of the flow resistance coefficient is observed, provided the entrance flow is highly disturbed and a long enough entry length is allowed for. This state of affairs, verified by measurements reported in Parts 2 and 5 of the present paper, is in agreement with and co-ordinates statements due to Schiller 1921 and Binnie & Fowler 1947. The measurements reported in Part 5 furthermore show that the great increase of the flow resistance coefficient around the R_k value is by no means a macroscopically discontinuous function of the Reynolds number although it was assumed so by Schiller 1921.

Co-ordination of apparent discrepancies between various determinations of the critical Reynolds number

The course of the transition process as presently described gives full explanation of the observations reported in Part 2 according to which transition to turbulence, as determined by pressure drop measurements, appears to take place at decreasing Reynolds numbers, the nearer to the tube inlet the measuring length of the tube is situated, provided that highly disturbed entrance flow conditions are secured. Similar observations were reported by Schiller (1921 p. 441) but he believed this tendency to be due to an accidental error. The explanation to these observations is quite simple. We remember that below the critical Reynolds number R_k there appear turbulent flashes of which quite a number fade away within shorter or longer travelling distances covered by the entry length of the tube, downstream of which, if any, only a lesser number of non-fading flashes remain. Consequently, within the flow region $R_v < R < R_k$, the number of turbulent flashes contributing to the pressure drop will increase, the closer to the tube inlet the measuring distance is located (with the exception of measuring sections situated within the distance of accumulation, very close to the tube inlet). This state of affairs also explains why the transition process, when determined by pressure drop measurements, appears to take place more gradually, the shorter the entry length allowed for is, as was already observed by Schiller 1921. Naturally, no change will be observed in the course of the transition process on varying the location of the measuring section as long as it is preceded by a tube length exceeding the true entry length (defined on p. 146).

The above statements clarify the low "critical" Reynolds numbers determined by means of pressure drop measurements on flow through cylindrical tubes as reported by E. G. Coker & S. B. Clement 1903, Wilhelm Ruckes 1908, Eberhardt Schnetzler 1910, Sorkau 1911, 1912, 1913, 1914, 1915, Giulio de Marchi 1917, and on flow through tubes of rectangular cross-section by Davies & White 1928. All those authors allowed rather a short length or none at all of each test tube to precede its measuring section. Though not on purpose, the entry flow in all cases was in quite a disturbed state of motion.

In Part 2 of the study it was reported that double pressure drop branches were determined on flow of water and bentonite sols within the turbulent region over measuring distances situated close to the tube inlet. Mention was also made that similar observations had earlier been reported by Sorkau 1911–15. No consistent interpretation was presented in this connection that could explain the peculiarities observed. However, in view of the present increased knowledge of the transition process, it appears likely that all the peculiarities reported in Part 2 should be due to irregular fluctuations of the distance of accumulation. This explanation seems to apply both to the double branches 1 in Fig. 2.10 (flow of distilled water) and to the double branches 1 and 2 in Figs. 2.11 and 2.12 (flow of bentonite sols) as well as to the singular points in Fig. 2.11 which represent unusually high pressure drop over the measuring section next to the tube inlet. Here it must be recalled that the primary measuring data are quite irregular but that they have been smoothed when plotting the diagrams, which process resulted in the double branches drawn (see p. 46). The explanation presented appears consistent also with respect to Sorkau's measurements quoted above.

The transition process at low disturbance levels of the entrance flow

By carefully arranged inlet flow conditions the appearance of disturbance vortices might be suppressed even up to quite high Reynolds numbers. The higher the Reynolds number at which the first disturbances appear, the longer the disturbances might travel before fading out and the longer is the distance of accumulation of those vortices which perhaps transform into self-maintaining turbulent flashes before disappearing. However, once the Reynolds number exceeds the value at which the first disturbance vortices appear, a further increase of it shortens the distance of accumulation necessary for the disturbance vortices to roll along the tube walls, before transformation into turbulent flashes might take place. The disturbed entry flow region, however, continues to extend itself further downstream as the Reynolds number is increased. We thus understand that even in the case of disturbed flow through a tube we might attain very high Reynolds numbers without transition to turbulence, provided only that the tube is rather short. Evidently this is the reason why Reynolds 1883, H. T. Barnes & E. G. Coker 1904/05, Ekman 1911 and Schiller 1920 obtained quite high Reynolds numbers without transition to turbulence.

On the other hand, it is often assumed that, in the case of low disturbance level of the entrance flow, transition to turbulence takes place at Reynolds numbers which decrease towards the corresponding R_k value merely by allowing for increasing distances of accumulation. This erroneous conclusion is mainly due to measurements reported by Schiller 1924, 1925 and Naumann 1931. Those authors determined the pressure drop on flow of water through cylindrical tubes at various distances from the inlet end in the case of constant rather low disturbance levels of the entrance flow. They found that the rapid increase of the flow resistance, which according to those authors means instantaneous transition to turbulence, took place at decreasing Reynolds numbers as the distance of accumulation allowed for was increased. In view of the attempts made by Prandtl (& Tietjens) 1921 to explain the initiation of turbulence as being caused by unstable velocity profiles, Schiller 1925 tried to explain his observations as being due to an instability of the laminar velocity profile as developing in the entry length of the tube. In this connection he compared his measurements on tube flow with those on Blasius flow, performed by B. G. van der Hegge-Zijnen 1924, by calculation of the "critical" Reynolds number as based on the boundary layer thickness. Schiller claimed acceptable agreement between the various results although he simultaneously had to mention inexplicable discrepancies noted.

From the present point of view it is quite clear that the observations reported by Schiller 1924, 1925 and Naumann 1931 do not mean a decrease of the "critical" Reynolds number with increasing distance from the tube inlet, neither has this decrease anything to do with an instability of the laminar velocity profile as depending on the development of the boundary layer thickness. Instead we understand that those observations are to be explained as the result of quite long distances of accumulation because of the rather low disturbance levels at the tube inlet in combination with the elongation of the turbulent regions as they travel downstream, once they have been initiated. Provided $R > \bar{R}_k$, fully developed turbulent flow will occur far enough downstream in the tube, while closer to the tube inlet there might only be disturbed flow which does not cause any substantial addition to the laminar pressure drop.

The experiments reported in Parts 4 and 5 of the present paper have shown that laminar flow persists even in very long tubes at Reynolds numbers considerably exceeding the R_k or $\bar{R}_k$ values, as long as entry flow disturbances, which are strong enough to cause breakdown to turbulence, do not occur. Evidently this scheme of the transition process is quite contradictory to current ideas on the transition process derived from the investigations performed by Schiller and co-workers as quoted above. Nevertheless it is also consistent with all the results due to those authors and furthermore it does not raise any discrepancies to be explained, which troubled Schiller when interpreting his observations 1925.

The influence of surface roughnesses on the transition process

From statements reported above we understand that the definition of the critical Reynolds number R_k as the value at which an increase of the flow resistance coefficient is observed, is a very unsuitable quantity which might vary within wide limits depending on the experimental circumstances. On the other hand the quantities R_v, $\underline{R}$, R_k, $\bar{R}_k$ (not $\bar{R}$), as defined in the preceding sections appear universal, independent of experimental particularities. This impression is, however, not true, because the present experiments have shown that surface roughnesses, even of microscopic size, considerably influence the course of the transition process. Consequently, the magnitude of the $\underline{R}$, R_k and $\bar{R}_k$ values (as also of course the $\bar{R}$ value) depend on the roughness grade of the tube walls. Whether also the vorticity limit R_v depends on the roughness grade appears uncertain at the present moment, although I have the impression that it does not.

The statements above, that the surface roughnesses of the tube walls, and especially microscopic ones, should have any bearing on the transition process is in sharp contradiction to basic ideas that by now have been common property for almost 30 years.

The ideas that the roughness of the tube surfaces should have no bearing on the transition process originate from observations reported by Schiller 1920. He determined the pressure drop on flow of water through a technically smooth brass tube of 16 mm internal diameter. The 0.52 m long measuring length of the tube was preceded by an equally long entry length. The sharp edged tube inlet was mounted flush with the inner surface of the supply reservoir. Measuring the pressure drop under these flow conditions Schiller determined a "critical" Reynolds number of about 2800, which shows that the disturbance level at the tube inlet was quite low. After providing the tube with a thread of 0.3 mm depth which extended from the tube inlet to 0.8 m downstream of the meauring length of the tube, Schiller repeated the measurements under the same flow conditions. Much to his surprise he found that the thread did not influence the magnitude of the "critical" Reynolds number which was still about 2800. Schiller then equipped the inlet of the threaded tube with a trumpet and reached Reynolds numbers of the magnitude of 20000 without transition to turbulence. From these observations it was concluded that surface roughnesses had no bearing on the "critical" Reynolds number, contrary to what had been anticipated by R. von Mises 1912. (See also Schiller 1922*b* and the discussion following on that paper.)

Experiments reported in Part 3 of the present study have shown that even very large but regularly arranged roughness elements do not agitate any disturbances in laminar flow. However, once strong enough disturbances occur in the flow they might break through the regular flow pattern close to the wall, making each roughness element a disturbance generator which casts off new disturbances into the flow. In this way a chain-reaction is started, finally balancing a higher turbulence level than that of corresponding flow when the roughness elements are of smaller size. It is also shown in Parts 3 and 4 that, within certain limits, turbulent fluctuations might be maintained at lower Reynolds numbers the larger the roughness elements are. From those facts we understand that Schiller's investigation is misleading with respect to its aim. The entrance flow conditions were the same in his tests both with the smooth and with the rough tube (without trumpet). Consequently, disturbance vortices in both cases must have appeared at the same rather high Reynolds number $R \approx 2800$. Independent of the surface roughnesses, turbulence cannot appear unless caused by entry disturbances, and consequently transition cannot take place at a Reynolds number which is lower than the value at which the disturbances appear, which Reynolds number is independent of the roughness grade of the tube. Perhaps this scheme does not present the complete interpretation of Schiller's observations, because it appears likely that a higher disturbance level should be necessary to cause transition to turbulence in a "smooth" tube than in a corresponding "rough" one, provided a long enough distance of accumulation is allowed for. In Schillers' experiments, however, the total tube length seems to have been too short (65 tube diameters only) to allow the roughnesses to cause any noticeable change of the transition point $R_k \approx 2800$. This also appears to be the reason for the rather high Reynolds number obtained without transition to turbulence in flow through the threaded tube equipped with the trumpet mouth-piece.

Had Schiller also repeated his experiments with highly disturbed entrance flow conditions, it might be suspected that the entrance disturbance vortices would have caused breakdown to turbulent flow at a noticeable lower Reynolds number in the rough tube than in the corresponding smooth one. Both of these transition limits, of course, are suspect of being considerably lower than the reported value $R_k \approx 2800$.

The observations reported in Parts 4 and 5 of the paper indicate that variations of the roughness grade, even if the roughness elements are of microscopic size as in technically smooth tubes, to some extent influence the crucial quantities $\underline{R}$, R_k $\bar{R}_k$ and $\bar{R}$. Furthermore, experiments reported in the literature indicate a considerable decrease of the R_k value for an increasing roughness grade of macroscopic order of magnitude, when there has been a high disturbance level of the entry flow. In this respect, reference can be made to experiments reported by Ruckes 1908, Schnetzler 1910 and de Marchi 1917. Ruckes obtained "critical" Reynolds numbers of the order of 800 on flow of air through rough iron and copper capillaries. Schnetzler determined "critical" Reynolds numbers on flow of water through artificially roughened capillaries and found values ranging from 100–2400 depending on the length and roughness grade of the tubes. His report is, however, somewhat incomplete, while de Marchi's experiments are rather carefully reported. De Marchi experimented with flow of water through smooth and threaded tubes in pairs, with equal hydraulic diameters of 2.9, 3.9 and 4,9 mm. The measuring distances were 170–120 tube diameters long and they were preceded by entry lengths, not quoted, but probably ranging from 80 to 50 tube diameters. The relative height of the thread compared to each tube radius was 0.10, 0.06 and 0.04 in the named order. De Marchi noted that transition took place at a Reynolds number of about 2200 in the flow through any of the smooth tubes. Corresponding transition values for flow through the threaded tubes were 1600, 1900 and 2000 according to the named order of degree of roughness. In this connection we must not forget that no intentionally agitated entrance disturbances were employed in any of the experiments quoted. Probably still greater influence of surface roughnesses on the transition data will be observed on occasions where entrance disturbances are being agitated on purpose and the tubes are long enough.

It is noteworthy that Schiller on two occasions, 1923 and 1932 (Schiller 1932, p. 191), quoted the work by de Marchi 1917 without realizing its significance. With regard to the work by Ruckes 1908, Schiller (1925 *a*, p. 584) presented quite an extensive analysis of the observations reported by that author but, in view of this own incomplete experiments of 1920, Schiller failed to realize its important bearing on the transition problem.

In this connection mention should also be made of a study by Nikuradse 1933, on flow through rough tubes. Although he has given no experimental data on the observations within the transition region, it is clearly seen from his graphically plotted values that there was a small but distinct decrease of the transition Reynolds number with increasing roughness grade. This could perhaps be considered surprising, since the entrance level must have been quite low in Nikuradse's experiments and, in addition, the relative total length of the experiment tubes was only about 70 tube diameters. However, the results appear quite natural if we observe that Nikuradse measured the pressure drop by means of pitot tubes inserted through the tube walls at the beginning and end of the measuring section. Evidently the upstream pitot tube must have caused quite strong primary disturbances which might have transformed the roughness elements into disturbance generators within the measuring distance, the more readily the rougher the tube surfaces were.

The transition process in the case of instationary conditions, following instantaneous starting of the flow

On instantaneous starting of tube flow at preadjusted stationary flow conditions there will occur a time period of gradual development of the velocity profile to its stationary shape at each cross-section. This problem has been treated analytically by P. Szymański 1930. Presuming some velocity profile to be unstable during the development period there should be observed the initiation of flow disturbances along the whole downstream length of the tube simultaneously or at discrete locations in the entry length of the tube.

Experiments of the above type, reported in Part 4 of the paper, indicated that no disturbances ever appeared in the flow unless originating from entrance flow disturbances travelling downstream with the flow. These observations, however, are referred to flow through jointless, technically smooth tubes without any macroscopic surface defects. On the other hand, pre-tests on flow through jointed tubes did show that such joints (and also borings in the tube walls) might, but need not necessarily cause turbulent disturbances, although in the case of stationary flow, those wall defects were never observed to cause any disturbances in the flow.

So far, the above statements agree perfectly with observations reported by M. R. Carstens 1956, on the transition process as appearing in instantaneously started flow of water through smooth, cylindrical brass tubes. However, Carstens determined the front velocity of the turbulent disturbances to be equal to twice the mean flow velocity of the laminar flow. This is not in agreement either with the present experiments (see pp. 90–94) or with those according to Prandtl–Tietjens (1931, p. 40). The latter authors determined the front velocity of the turbulent flow regions to be equal to the laminar mean flow velocity, which is half the value determined by

Carstens. It is to be noted that both Prandtl–Tietjens 1931 and Carstens 1956 determined various numerical values by observing the liquid jet issuing from the outlet end of the tube. This is an indirect and rather uncertain measuring method which cannot be relied upon to any degree of accuracy. In addition, Carstens also made several speculations on the estimation of the thickness of the laminar boundary layer and its critical Reynolds number which are not backed up by consistent experimental data.

Conclusion

It remains to be stated that the definition of the Reynolds number of flow of liquids and gases given on pp. 6 and 11 and pp. 55–56, and which in practice is identical with its classical definition, gives a reasonable consistency of the numerical limits of the transition process. The reproducibility of the transition data, as demonstrated by the presented review on the transition process, is surprisingly good if we consider the pronounced irregular viscous properties observed on laminar flow of liquids. This, however, does not mean that the Reynolds number in its present sense should be a universal quantity with respect to the phenomenon of transition. At most, it might be an acceptable approximation of true relationships as is already pointed out in Part 1 (p. 11) of this study as well as in a previous note (Lindgren 1956).

Evidently the experimental indications of the role of entry flow disturbances and surface roughnesses in connection with the transition process, as presented in the preceeding parts, have increased the consistency of its appearance. Thus, it is no longer necessary to explain away numerous experimental observations as being due to accidental or systematic errors. In view of the present findings they might be co-ordinated as various particularities of the same scheme which furthermore appears to be valid not only for tube flow but for any type of flow investigated, at least where it be classified as incompressible. Reference can here be made to observations reported by Couette 1890 and Mallock 1896 on flow between concentric rotating cylinders (the initiation of Taylor vortices has no bearing in these connections), Emmons 1951 on flow of a thin water layer over a smooth glass surface, Morton Mitchner 1954 and Schubauer & Klebanoff 1955 on flow of air over flat plates. All those experiments give a mental picture of the transition process as being composed of turbulent flashes or spots rolling along the surfaces in a similar manner to that observed on flow in tubes.

In this connection, however, I want to stress the point that I do not believe that all crucial variables affecting the transition process are known by mentioning such quantities as entrance disturbance vortices, surface roughnesses and viscosity anomalies. On the contrary I have the impression that there might be several other quantities unknown at the present, which might influence the mechanism of viscous flow in general and the transition process in particular, some of which are hinted at in Part 4 of the study. The present work should mainly be considered a collection of indications showing that the problem of transition could perhaps be successfully attacked from points of view other than those commonly presented in classical boundary layer research.

Turbulent flow and the laminar sub-layer hypothesis

Experimental evidence reported in the preceding parts of the paper indicates that the transition process and the maintenance of turbulent flashes are governed to a considerably extent by some surface effects of the rigid walls bounding the flow, one of these being the surface roughnesses of the walls, even when these are of microscopic size, as for instance in technically smooth tubes. This state of affairs indicates that the roughness elements ought to be of still more importance in connection with the maintenance of the vorticity in general turbulent flow, since we know that the fluctuations increase in intensity closer to the bounding walls as the Reynolds number is increased. Such a mental picture of the structure of turbulent flow is, however, inconsistent with common ideas on this concept.

On the following pages, the structure of the turbulent shear flow will be looked upon from some unconventional points of view based on the thoughts presented above.

The concept of the laminar sub-layer

According to classical ideas, the hydraulic smooth turbulent pipe flow consists of a turbulent core from which the turbulent fluctuations diffuse towards the boundary walls. In the course of this process the fluctuations gradually dissipate by the action of the viscous forces dominant in wall-close regions, so that the flow should essentially be laminar in a layer situated next to the boundary wall (the laminar sub-layer).

The introduction of the concept of the laminar sub-layer in boundary layer research is due to L. Prandtl 1910, and based on some older ideas reviewed by Benjamin Miller 1949. Taylor 1916/17 independently introduced the same concept in a criticism of a heat transfer study published by Stanton 1912/13. Taylor based his estimation of the laminar sub-layer on H. A. Lorenz's determination 1907 of the critical Reynolds number of plane Couette flow (i.e. flow caused by two ideal parallel planes moving steadily and parallel to each other). According to Lorenz no eddies should be able to exist in that type of flow below a critical Reynolds number of $R_k = Ud/\nu \approx 290$, where d is the distance between the bounding walls.

It is well known that fully developed turbulent flow has a fuller velocity profile than laminar flow of the same mean flow velocity, which means that wall-near layers in the case of turbulent flow should obtain higher velocities than in corresponding laminar flow. Should the hypothesis of the laminar sub-layer be true, which concept automatically implies an assumption of no slip at the bounding walls, this would mean that the velocity distribution should deviate from the turbulent type and approach the form of a parabola within the laminar sub-layer. In practice this would mostly imply an approximately rectilinear velocity distribution close to the wall, its gradient determining a shear force (skin friction factor) at the tube wall which ought to balance the pressure drop of the flow along the tube (see for instance Goldstein 1938, vol. II, p. 342).

The average velocity distribution of fully developed turbulent flow

Starting from the above presumtions, Stanton, Marshal & Bryant 1920 undertook to determine the velocity profile of a fully developed, turbulent flow of air through smooth cylindrical brass tubes. They employed fine pitot tubes of the ordinary type with the measuring mouth bent 90° relative to the shaft. They also made use of "straight" pitot tubes in which the surface of the experiment tube itself forms a part of the pitot tube mouth.

On measurements inside the tube on fully developed laminar flow by means of the bent pitot tube, Stanton *et al.* stated that the parabolic velocity profile was verified by the measurements as close as 0.25 mm from the wall of a tube of 7.14 mm inner diameter. However, when measuring the velocity profile of fully developed turbulent flow, Stanton stated that, if it may be assumed that the speed indicated by the pitot tube is the speed of the fluid at its geometric centre during the experiments, the observations are not inconsistent with a finite amount of slip at the boundary.

Presuming zero velocity at the wall when calibrating the "straight" pitot tube in laminar flow at distances as close as 0.05 mm to the wall in a tube of 2.7 mm diameter, it was found that the effective distance of the pitot tube centre deviated considerably from its geometric centre. (We remember here that the mouth of the straight pitot tube is limited on one side by the wall of the experiment tube itself, so consequently, the geometric centre of the pitot tube opening is situated at a distance from the tube wall equal to half the depth of the pitot tube opening.) In this manner a correction function was determined for the effective centre relative to the total depth of the pitot tube mouth.

Without use of the correction function, the measurements on fully developed turbulent flow of air through various tubes indicated considerable slip at the boundaries. On the other hand, by applying the correction quantities the measurements indicated that the velocity tended towards zero at the boundary and that there existed a laminar film beneath the turbulent core. Still, the results are quite conflicting because, in general, no agreement was found between the skin friction factors measured and those calculated on the velocity gradients determined close to the wall by use of the corrected velocity profiles.

Nikuradse 1930 reported a similar investigation on turbulent flow of water through "smooth" cylindrical brass tubes of 10 to 100 mm diameter within a wide range of Reynolds numbers, 3000 to 3000000. Nikuradse performed his measurements by means of a fine pitot tube situated 0.1–0.15 mm downstream of the sharp cut outlet end of each experiment tube. When plotting the results of these experiments in the currently adopted manner, $u^* = f(\log y^*)$, where $u^* = u/u_*$; $y^* = yu_*/\nu$ and $u_* = \sqrt{\tau_0/\varrho}$ (u = average local velocity at a distance y from the boundary; ν = kinematic viscosity and ϱ = density of the fluid while τ_0 = shear force per unit surface at the boundary), Nikuradse obtained a rectilinear relationship

$$u^* = 5.5 + 5.75 \log y^* \tag{6.1}$$

valid for all the investigated range $1 < y^* < 63000$, which result is not consistent with the laminar sub-layer hypothesis. However, in the complete report of essentially the same experiments presented two years later (Nikuradse 1932), the corresponding graph of the relationship $u^* = f(\log y^*)$ had received a somewhat different appearance. It now covered only the interval $10 < y < 63\,000$ and the rectilinear relations between u^* and $\log y^*$ appeared to be valid only in the region $y^* > 60$. It is to the credit of Miller 1949 that this point of discrepancy has been clarified. He pointed out that the primary experimental data given in Nikuradse's paper of 1932 did not agree with those prepared for and plotted in the graph of that paper.[1]

In his admirable paper, Mr. Miller gives a comprehensive and clear report about the quite arbitrary adjustments of the primary data as arranged by Nikuradse. It appears that the primary evaluated wall-close values of y^* were shifted seven units towards higher values just in order to obtain agreement with the laminar sub-layer hypothesis.

Miller's paper was seriously critisized by Stanley Corrsin in *Appl. Mech. Rev.* 1950 (see ref. Miller 1949). Corrsin called attention to the experimental investigations on velocity distributions of turbulent flow reported by Hegge–Zijnen 1924 and H. Reichardt 1940 and claimed that Miller had failed to explain away these experimental data. Corrsin furthermore stated that Miller had taken the concept of the laminar sub-layer literally and noted that no one seriously working in this research field did so. I cannot avoid mentioning that, if I have understood rightly, Miller does not take up discussion of the structure of the laminar sub-layer but merely points out that Nikuradse's measurements are adjusted to fit the laminar sub-layer hypothesis and that also some other experimental investigations appear not to agree with the same hypothesis from some other points of view, and so far the statements are based on facts that cannot be denied.

As regards the measurements of the velocity distribution of turbulent Blasius flow of air performed by Hegge-Zijnen 1924 by means of a hot-wire anemometer, it might be remarked that he excused himself for quite arbitrary corrections of the calibration data, referring to similar corrections made by Stanton, Marshal & Bryant 1920 when using pitot tubes, as already reported in the present paper (see p. 156). More serious are the objections that can be levelled against the measurements reported by Reichardt 1940 on flow of air through a rectangular duct. He stated (Reichardt 1940, p. 306) that he had obtained too high u_* values, probably because the flow was not fully developed turbulent. Reichardt then supposed that it was permissible to shift his average u_* values so that they would agree with those according to other authors. However, as reference values of u_* he used the adjusted ones of Nikuradse 1932, and Reichardt expressly excluded the values reported by Nikuradse 1930 which, as he stated, were obviously too high.

From the above statements it appears that Professor Corrsin's heavy criticism of Mr. Miller's paper is not justified from any point of view.

For a long time, the investigation of Nikuradse 1932 has been considered the very proof of the existence of the laminar sub-layer and it has hitherto appeared in the literature as the most referenced work on this subject both in standard text books and in research papers. This is quite a ridiculous state of affairs because, as we have seen, in reality Nikuradse's work contains the strongest experimental evidence *against* the laminar sub-layer hypothesis yet reported in the literature.

So far as I can see, no serious objections can be levelled against Nikuradse's original measuring data which evidently indicate slip at the boundaries of turbulent flow of water in "smooth" cylindrical tubes.

There are several other works, not quoted above, which also deal with the velocity distribution of turbulent flow. Mention is first to be made of a study by Fage 1936

---

[1] I want to remark here that the primary pressure gradient values presented in Table 2 of Nikuradse's paper should probably have the dimension pond/cm³, not dyn/cm³ as given in that table.

on turbulent flow of water through a smooth brass tube by means of an ultra-microscope and by pitot tube measurements. The test section consisted of an 0.15 m long piece of a glass tube of 27.3 mm diameter, joined to the brass tube which was of approximately the same diameter.

The measurements of the velocity distribution due to Fage do not cover regions so close to the wall that they cover the laminar sub-layer region. This is quite surprising because the ultra-microscope appears to be an instrument well fitted for such measurements. Instead, Fage used the corrected values given by Stanton, Marshal & Bryant 1920, which agree very well with Nikuradse's adjusted values.

Investigations of the velocity distribution of turbulent flow of air in pipes by means of pitot tubes are further reported by Rothfus, Monrad & Senecal 1950 and Robert G. Deissler 1950.

Rothfus, Monrad & Senecal 1950 made use of pitot tubes both of the ordinary bent type and of the straight type as previously described by Stanton *et al.* 1920. They experienced much the same calibration effects and essentially confirmed the observations reported by Stanton *et al.*. Rothfus *et al.* failed to predict skin friction from the velocity gradient at the wall, as also did Stanton, Marshal & Bryant 1920, and they stated that they could give no explanation for this discrepancy.

Deissler 1950 worked only with pitot tubes of the bent type which he calibrated in laminar flow presuming parabolic velocity distribution arbitrarily close to the wall. Deissler concluded that the geometric centre of his pitot tubes was identical with their dynamic pressure centre anon d this presumption the velocity distribution obtained by him agrees with the results according to Stanton, Marshal & Bryant 1920 and Rothfus, Monrad & Senecal 1950 in the vicinity of the wall. It is worth mentioning that the length of the bent mouth-piece of the pitot tubes was only a millimetre or so in Deissler's experiments while, usually, it is considered necessary to have quite long mouth-pieces in order to avoid interference effects with the pitot tube shaft. In view of Deissler's statement that the dynamic pressure centre was identical with the geometric centre of the pitot tubes, his results are actually not in agreement with those according to Stanton *et al.* 1920 (see p. 156).

Additional works on the velocity distribution of fully developed turbulent flow of air through rectangular and circular ducts have been presented by John Laufer 1950 and 1954 and on flow through rectangular channels by W. H. Corcoran, F. Page Jr., W. G. Schlinger & B. H. Sage 1952, Page Jr., Corcoran, Schlinger & Sage 1952, and Page Jr., Schlinger, D. K. Breaux & Sage 1952.

Laufer 1950, 1954 employed both thin ordinary bent pitot tubes and a hot-wire anemometer for determination of the various flow data. He does not give any description of the calibration processes or of the corrections of the measuring quantities necessary in the vicinity of the boundaries. According to the graphically plotted results, Laufer's determinations of the velocity distribution indicate full agreement with the laminar sub-layer hypothesis (however, see also p. 160). Furthermore, Laufer also claimed good agreement between the skin friction factor obtained by pressure drop experiments and the corresponding one determined by means of the velocity gradient measured at the flow boundary. Laufer's paper appears to be the first and as yet the only study reporting agreement between these two quantities.

Corcoran, Page *et al.* 1952, Page, Corcoran *et al.* 1952 and Page, Schlinger *et al.* 1952 performed their measurements by means of pitot tubes and the hot-wire anemometer as did Laufer 1950. Also the velocity distributions determined by those authors appear to agree with the concept of the laminar sub-layer. On the other hand, these authors point out that the generalized velocity distributions outside the laminar film (in more central parts of the flow), as determined by them and various other authors, show up considerable discrepancies relative to each other, especially at low Reynolds numbers.

Mention should also be made of a paper by F. L. Wattendorf and A. M. Kuethe 1934 and a thesis due to G. Skinner at Cal. Inst. of Techn. 1950. However, the latter paper has not been available to me at the time of writing and the former one does not appear to add anything of importance in the present connections which is not known from the papers quoted above.

All the authors cited, with the exception of Nikuradse 1930, 1932, have measured the velocity distribution at some cross-section situated along the tubes or channels. They have all calibrated their measuring devices in laminar flow by presuming parabolic velocity profile with zero velocity at the bounding walls. Some of these authors mention the observation of strong interference effects in the proximity of the walls while others did not even care to investigate that point of the problem. (Laufer does not at all mention how his wall corrections are obtained or whether there are any at all, although I have an impression that he has followed some standard procedure as, for instance, Hegge-Zijnen 1924 did.) The feature common to all these investigations is that they lack some primary calibration or experimental data and that they claim agreement with the experimental results due to Nikuradse 1930, 1932 in verifying the laminar sub-layer hypothesis. However, as pointed out in the present paper and by Miller 1949, the results claimed imply instead a most contradictory state of affairs.

Nikuradse 1930, 1932 is, on the other hand, the only investigator who has measured the velocity distribution just outside the sharp cut outlet end of experiment tubes. In contradistinction to the reports of the other authors his paper gives information about the primary experimental data and evidently these do not support the laminar sub-layer hypothesis but rather indicate a finite amount of slip of the turbulent flow at the boundaries, a possibility that was not definitely excluded in the report by Stanton, Marshal & Bryant 1920.

I can hardly judge whether one or other of the conflicting results is right or wrong, I only can state that the experimental evidences, contrary to what seems to be commonly believed, are highly in contradiction to each other. This state of affairs might perhaps be connected with peculiarities of pitot tube measurements as noted in the experimental investigations by Fry & Tyndall 1911 and Barker 1922. Mention should also be made of a theoretical investigation by Andersson 1957, which shows that a slight inclination of the pitot tube relative to the flow direction might cause noticeable errors in the pitot tube readings. Consequently it might perhaps be expected that steep velocity gradients might cause still larger errors in the pitot tube readings.

The discrepancies between various determinations of the generalized velocity distribution outside the laminar sub-layer noted by Corcoran, Page *et al.* 1952 and Page, Schlinger *et al.* 1952 (see above) are further discussed and stressed in a paper by Schlinger & Sage 1953, who recommended a further study of the velocity distribution in uniform steady turbulent flow of gases. Had these authors but known that the Nikuradse measurements referred to are adjusted, as pointed out by Miller 1949, this recommendation would certainly have been emphasized with still more urgency. It appears quite discouraging that Miller's admirable paper as yet has been so completely neglected.

The deviations of the turbulent velocity distribution pointed out by Schlinger & Sage 1953 are inexplicable from the point of view of the similarity law of turbulent flow through ducts with ideal smooth surfaces. However, the observations reported in Parts 4 and 5 of the present study, show that even microscopic roughness elements of technically smooth tube surfaces influence the turbulence maintaining effects in the transition zone and consequently also might be expected to be active in fully developed turbulent flow. On such lines we perhaps might receive a natural explanation of the deviations observed and perhaps such ideas might lead to an understanding of various characteristics of turbulent flow that cannot be explained from the point of view of classical boundary layer theory.

The structure of the turbulent-energy balance

The experiments of Fage 1936 appear to be the first ones indicating that the "laminar sub-layer" should not be laminar. Fage found that the turbulent fluctuations relative to the local speed increase towards the wall except for the relative fluctuations perpendicular to the boundary which reach a maximum somewhere in the proximity of the boundary and then decrease towards zero.

Laufer 1950, 1954 made careful measurements of the distribution of the turbulent fluctuations by means of the hot-wire anemometer and in the main confirmed Fage's observations, that the "laminar sub-layer" is by no means laminar. This state of affairs has lately induced the use of the expression "viscous layer" as a substitute for the less correct term "laminar sub-layer".

Laufer's papers are extensively concerned with the turbulent energy balance. His measurements indicate that the various turbulent energy rates show up maximum values at the edge of the viscous layer. A strong transfer of kinetic energy away from the edge of the viscous layer and an approximately equal amount of pressure energy towards it was noted. Laufer stated that the bulk of the direct viscous dissipation takes place in a very narrow region close to the tube wall and that the layer where the viscous dissipation is equal to the production of turbulence is approximately the same as the layer where the maximum amount of turbulent energy is produced, which position appears to be situated at the edge of the assumed viscous layer.

In this connection it appears desirable to point out that the hot-wire measurements of the turbulent fluctuations might give some misleading indications in the proximity of the bounding walls. It is known that the size of the turbulent "patches" decreases towards the bounding walls and becomes very small in the vicinity of the boundaries (see Fage & Townend 1932). Evidently the hot-wire anemometer cannot record fluctuations of turbulent patches of an average size some few times smaller than the length of the probing hot-wire. This statement is of course valid for sufficiently small-scale fluctuations anywhere in the turbulent flow and evidently indicates a limit of the applicability of the hot-wire anemometer. Whether this limit has any significance in connection with Laufer's measurements I do not know at present, but it appeared desirable to point out that such a limit certainly must exist. (See for instance Ralph D. Cooper & Marshal P. Tulin 1955 on this subject.)

There are some theoretical considerations on the problem of vorticity production presented by Taylor 1938, which indicate that the rate of destruction of vorticity by viscosity should be several times as great as the rate at which vorticity according to measurements actually disappears. Professor Taylor concludes that vorticity is being produced by extension of vortex filaments, which process could be the cause of the high rate of dissipation associated with turbulent flow. T. Theodorsen 1955 has presented a theoretical analysis on some kind of horse-shoe vortices which were assumed to explain the transition phenomenon. Professor Theodorsen's analysis appears, in principle, to contain about the same cardinal virtues as does that of Taylor quoted above. John R. Weske 1954 studied the Theodorsen horse-shoe vortices experimentally in the transition range of tube flow. In view of the present study it appears, however, that Weske's experiments were concerned only with the first stages of disturbed flow and did not allow any studies on transition to self-maintaining turbulent disturbances. (The tube was only 136 diameters in length and only small disturbances were present in the flow.)

The turbulence production mechanism proposed by Taylor 1938 might possibly have a bearing on the production of turbulence in the "critical layer" at the edge of the viscous layer as determined by Laufer 1950, 1954. According to the theory quoted this would imply the production of large eddies from small ones. Such a process fits very well with the present observations which indicate that turbulent fluctuations are generated at the boundaries and become larger according as they distend into the central parts of the flow where they dissipate. This postulation of the maintaining mechanism of the eddies in turbulent flow appears to be the reverse process of the currently assumed one, according to which the problem is to explain how smaller eddies diffusing towards the boundaries are maintained by larger eddies in the more central parts of the flow. (See, for instance, Taylor & A. E. Green 1937.)

Even apart from the considerations presented above, it is quite clear that the viscous layer is not laminar. I here refer to the work by Fage & Townend 1932 earlier quoted (Part 3, p. 60), which shows that the turbulent fluctuations are bodily in contact with the flow boundaries. This state of affairs is still better demonstrated in an interferometric study on a free-convection boundary layer presented by E. R. G. Eckert & E. Soehnghen 1951. The latter authors found that the interferometric lines fluctuated right up to the surface with a rather high frequency and that the scale of the turbulent fluctuations decreased towards the plate surface. They also pointed out that the scale of fluctuations was remarkably large in the outer portion of the boundary layer. We thus understand that the introduction of the concept of the laminar sub-layer in the viewpoint of Prandtl 1910 and Taylor 1917 has no bearing on current ideas regarding the viscous layer, and in view of presumptions presented in this paper the laminar sub-layer should be quite an inconceivable quantity.

The structure of turbulent-energy balance with consideration of surface roughnesses on the boundaries

Reconsidering assumptions presented in the preceding section that small-scale eddies should be generated (perhaps not only) by the action of surface roughnesses of the bounding walls and diffuse towards the central parts of the flow, we receive a natural explanation of the turbulent maintenance processes. This implies that the primary wall-generated small eddies should be enlarged in the turbulence-producing critical layer (extension of the vortex filaments) according as they diffuse towards the more central parts where dissipation takes place. The turbulence level of the flow should thus be determined by the balance between the turbulence production in the critical layer and dissipation effects in the turbulent core. Evidently the turbulence production in the critical layer depends on the number and intensity of the primary eddies available, which condition should be determined by the roughness grade of the boundaries and/or by other wall effects. Consequently the turbulence level in the flow ought to vary to some extent with the properties of the bounding walls. However, as long as the average size of the primary eddies is smaller than the distance from the wall to the turbulence-producing layer, the main character of the turbulent flow structure should be determined by the turbulence production in that layer. This scheme of the mechanism of turbulent flow could perhaps add to an understanding of the Blasius' resistance formula for smooth turbulent pipe flow. It also appears to give a satisfactory explanation of discrepancies between various determinations of the resistance of "smooth" turbulent flow which are inexplicable in terms of hydrodynamic similitude as long as the boundaries are assumed to be ideally smooth. Furthermore, it gives a natural explanation to the well-known fact that the flow resistance for smooth turbulent flow through channels of any cross-section agrees rather well with corresponding values of flow through circular pipes provided the reference dimension be the hydraulic diameter (for a definition see p. 55). In this connection reference should again be made to a study by Schiller 1923 (1925 *a*) in which he presumes a hidden crucial meaning of the concept of the hydraulic diameter.

However, in cases where the boundaries are very rough the primary disturbances become very large and are cast off directly into the flow and the "viscous layer" is destroyed. Under these conditions the roughness disturbances play the dominant role in the turbulence-maintaining processes and the Blasius' resistance formula is valid no longer but is replaced by the "square resistance law" at high enough Reynolds numbers (see Nikuradse 1933).

The scheme of the mechanism of turbulence presented implies that even microscopic roughness elements of technically smooth tubes should sooner or later cause transition from the Blasius' "law" of flow resistance to the "square" flow resistance law, provided only the Reynolds number is raised high enough. This is quite in agreement with experiments on flow of water through technically smooth steel tubes reported by B. Bauer & F. Galavics 1936 as noted by Schlichting, *Grenzschicht-Theorie* (1951, p. 380).[1]

From the above statements we understand why macroscopic roughness elements do not cause transition to the "square" law unless the Reynolds number is increased to above certain limits determined by the characteristics of the roughness elements. The classical explanation that the structure of turbulent flow should be uninfluenced by roughness elements as long as they do not protrude outside the laminar sub-layer (see Nikuradse 1933) is already not very satisfying with respect to Laufer's investigations, which show that the viscous layer is not laminar, and from the present point of view such an assumption appears to be an anachronism.

In this connection I want to draw attention to a paper by Albert van Hecke 1952 which presents some unusual aspects of the problem of viscous flow. van Hecke actually assumes that even microscopic surface roughnesses play an important role with respect to the structure of turbulent flow, and, further, he does not exclude the possibility of slip at the flow boundaries. Although van Hecke's ideas in many respects appear quite peculiar, neglecting many experimental indications reported in the literature, I believe that they should not be considered altogether valueless.

---

[1] Bauer & Galavics' paper was not available at the time of writing.

Conclusion

It is shown in preceding parts of the paper that wall effects (viz. surface roughnesses) probably play an important role with respect to the transition process, and that the introduction of such quantities seems to improve the consistency of the observations of various authors as being in agreement with indications of the present investigation. In view of these conclusions I found it desirable to examine the consequences that would follow therefrom also with respect to the fully developed self-maintaining turbulent flow.

In the course of the review undertaken it appeared that the experimental determinations on the structure of the turbulent flow (boundary layer flow) seemed in many respects rather vague and were also in a highly contradictory state both internally and relative to each other. Here, for instance, mention could be made of (1) the concept of the laminar sub-layer, which was introduced by Prandtl and Taylor on presumptions that are not consistent with experimental facts; (2) the highly contradictory state of affairs which characterizes the determinations of the velocity distribution according to various authors and which does not definitely exclude a possible slip of the turbulent flow at the walls; (3) the discrepancies between various determinations of the "smooth" turbulent flow resistance and other features of the turbulent flow which are inconsistent with von Kármán's theory of similitude (v. Kármán 1927, 1930) of the hydraulic smooth turbulent flow (on this subject see further Werner Heisenberg 1924 and H. Krey 1927).

Since, in my opinion, the introduction of wall effects as being of primary importance, with respect also to the structure of the self-maintaining turbulent flow, appears to co-ordinate, in a natural way, apparent discrepancies between various experimental findings on similar trends as was followed in connection with the transition phenomenon, I have been bold enough to present the above somewhat advanced ideas on the mechanism of turbulent flow. In this connection I want to recall the hydraulic mean diameter, a concept which is inconceivable according to classical ideas, but receives a natural and important bearing with respect to the characteristics of the turbulent flow in view of the present ideas.

I am quite aware of the fact that the advanced ideas presented above are not backed up by sufficient experimental data and they probably will have to be modified in the course of the future research. Thanks to the sponsorship of the *U.S. Air Forces Development Command* and the *Swedish State Council for Technical Research* I have now, however, been able to arrange for the continuation of the present investigation at *KTH* in order to obtain more extensive experimental data on this part of the problem.

REFERENCES

ANDERSSON, BENGT, On the stress-tensor of viscous isotropic fluids. Arkiv för Fysik *4*, 501 (1952).

—— On measurement of velocity by pitot tubes. Arkiv för Matematik *3*, 391 (1957).

AUERBACH, R., Hydrodynamische Korrosionsursachen. Jahrbuch des Forschungsinst. AEG, Berlin, *2*, 249 (1930).

BALLANTYNE, E. R., The measurement of the rheological properties of bentonite suspensions by the "moving plate" method. Commonwealth Sci. & Ind. Res. Organiz., Australia, Div. of Tribophysics, Serial no. 38, Gen. Chem. Rep. no. 5 (1949) (unpublished).

BARKER, MURIEL, On the use of very small pitot-tubes for measuring wind velocity. Proc. Roy. Soc. Lond. (A) (Proc. Roy. Soc.) *101*, 435 (1922).

BARNES, H. T., and COKER, E. G., The flow of water through pipes. Proc. Roy. Soc. *74*, 341 (1904/05).

BARR, GUY, A Monograph of Viscometry. Oxford University Press, London: Humphrey Milford, 1931.

BEATTY, K. O., FERRELL, J. K., and RICHARDSON, F. M., Radioisotopes in the study of fluid dynamics. Proc. Int. Conf. Peaceful Uses of Atomic Energy August 1955, Genève. Vol. 15, p. 194 (United Nations, New York 1956).

BINGHAM, EUG. C., and JACKSON, RICH. F., Standard substances for the calibration of viscometers. Bull. Nat. Bur. of Standards (Bull. NBS) *14*, 59 (1918).

BINGHAM, EUG. C., and THOMPSON, THEOD. R., The Fluidity of Mercury. J. Am. Chem. Soc. *50:* 2, 2878 (1928).

BINNIE, A. M., A double-refraction method of detecting turbulence in liquids. Proc. Phys. Soc. Lond. (Proc. Phys. Soc.) *57*, 390 (1945).

BINNIE, A. M., and FOWLER, J. S., A study by a double-refraction method of the development of turbulence in a long cylindrical tube. Proc. Roy. Soc. *192*, 32 (1947). Rev. in Appl. Mech. Rev. (AMR) *1* no. 489 p. 81 (1948).

BOUSSINESQ, J., Théorie du régime permanent graduellement varié qui se produit près de l'entrée évasée d'un tube fin, où les filets d'un liquide qui s'y écoule n'ont pas encore acquis leurs inégalités normales de vitesse. Comptes Rendus des Séances de l'Académie des Sciences Paris (Compt. Rend.) *110:* 1, 1160 (1890).

—— Théorie du mouvement permanent qui se produit près de l'entrée évasée d'un tube fin: application à la deuxième série d'expériences de Poiseuille. Ibid. *110:* 1, 1238 (1890).

—— Théorie du régime permanent graduellement varié qui se produit près de l'entrée évasée d'un tuyau de conduite, où les filets fluides n'ont pas encore acquis leurs inégalités normales de vitesse. Ibid. *110:* 1, 1292 (1890).

—— Sur la manière dont les vitesses, dans un tube cylindrique de section circulaire, évasé à son entrée, se distribuent depuis cette entrée jusqu'aux endroits où se trouve établi un régime uniforme. Ibid. *113:* 2, 9 (1891).

—— Calcul de la moindre longeur qui doit avoir un tube circulaire, évasé à son entrée, pour qu'un régime sensiblement uniforme s'y établisse, et de la dépense de charge qu'y entraîne l'établissement de ce régime. Ibid. *113:* 2, 49 (1891).

BRILLOUIN, MARCEL, Leçons sur la viscosité. Gauthier-Villars Paris 1907.

BROCKMAN, MARION R., Resistance of flow in teflon and brass tubes. U.S. Dept. of Commerce, NBS Report 4673 (1956).

BRODMANN, C., Untersuchungen über den Reibungscoefficienten von Flüssigkeiten. Inaug. Diss. Göttingen 1891, or Ann. d. Ph. und Ch. (Wied. Ann.) *45*, 159 (1892).

CAROTHERS, S. D., Portland experiments on the flow of oil in tubes. Proc. Roy. Soc. *87*, 154 (1912).

CARSTENS, M. R., Transition from laminar to turbulent flow during unsteady flow in a smooth pipe. 9th Int. Congr. of Appl. Mech. (ICAM), Paper I: 96 (Bruxelles 1956).

COKER, E. G., and CLEMENT, S. B., An experimental determination of the variation with temperature of the critical velocity of flow of water in pipes. Trans. Roy. Soc. Lond. (A) (Trans. Roy. Soc.) *201*, 45 (1903).

COOPER, RALPH D., and TULIN, MARSHAL P., Turbulence measurements with the hot-wire anemometer. AGARDograph (Adv. Group for Aeron. Res. and Developm., NATO) 12, August 1955.

CORCORAN, W. H., PAGE JR, F., SCHLINGER, W. G., and SAGE, B. H., Methods and apparatus for flow between parallel plates. Industr. and Engin. Chem. (IEC) *44*, 410 (1952).

COUCH, WILLIAM H., and HERRSTROM, CHARLES E., A study of fluid motion by means of color bands. Chem. Eng. Thesis, Mass. Inst. of Techn. (MIT), June 1924 (unpublished).
COUETTE, M. M., Etudes sur le frottement des liquides. Ann. de Chim. et de Phys., Paris (Ann. Ch. et Ph.) (6) *21*, 433 (1890).
DAVIES, S. J., and WHITE, C. M., An experimental study of the flow of water in pipes of rectangular section. Proc. Roy. Soc. *119*, 92 (1928).
DEISSLER, ROBERT G., Analytical and experimental investigation of adiabatic turbulent flow in smooth tubes. NACA TN 2138, 1950.
ECKERT, E. R. G., and SOEHNGHEN, E., Interferometric studies on the stability and transition to turbulence of a free-convection boundary layer. General Discussion, Heat Transfer Conference, London, Sept. 11–13, 1951, Section IV. Instn. Mech. Engnrs. New York, Am. Soc. Mech. Engnrs., 1951 (3 pp.). Rev. in AMR *5*, no. 197, p. 32 (1952).
EKMAN, V. W., On the change from steady to turbulent motion of liquids. Arkiv för Mat. Astr. och Fys. *6*, no. 12 (1911).
ELIE, M. B., Variation du coefficient de viscosité avec la vitesse. J. de Physique, Paris (J. de Phys.) (2) *1*, 224 (1882).
EMMONS, H. W., The laminar-turbulent transition in a boundary layer—Part I. Journal of the Aeronautical Sciences (JAS) *18*, 490 (1951). Rev. in AMR *5*, no. 486, p. 75 (1952).
ERK, S., Unsere Kenntnis der Zähigkeit von Quecksilber. Z. für Ph. *47*, 886 (1928).
FAGE, A., Turbulent flow in a circular pipe. Phil. Mag. (7) *21*, 80 (1936).
FAGE, A., and TOWNEND, H. C. H., An examination of turbulent flow with an ultramicroscope. Proc. Roy. Soc. *135*, 656 (1932).
FAWSITT, CHARLES E., On the determination of viscosity at high temperatures. Proc. Roy. Soc. *80*, 290 (1907/08).
FAXÉN, O. H., and OSEEN, C. W., Flüssigkeitsbewegung mit Reibung. *In* FRANK–v. MISES, Die Differential- und Integralgleichungen der Mechanik und Physik, zweiter (physikalischer) Teil. Friedr. Vieweg & Sohn A. G., Braunschweig 1927, p. 810.
FEATES, F. S., and IVES, J. G., The ionisation functions of cyanoacetic acid in relation to the structure of water and the hydration of ions and molecules. J. Chem. Soc. London (J. Ch. Soc.), p. 2798 (1956).
FORSLIND, E., Crystal structure and water adsorption of clay minerals. Int. Ceramic Congr. Nederland 1948, p. 98.
—— The clay water system II. Proc. Swed. Cem. and Concr. Res. Inst., Stockholm, no. 17 (1952) *a*.
—— A theory of water. Ibid. Nr 16 (1952) *b*.
—— Water association and hydrogels. Proc. 2nd Int. Congr. on Rheology, p. 50 (Oxford 1953).
FRY, J. D., and TYNDALL, A. M., On the value of the pitot constant. Phil. Mag. (6) *21*, 348 (1911).
GIBSON, A. H., The breakdown of streamline motion at the higher critical velocity in pipes of circular cross section. Phil. Mag. (7) *15*: 1, 637 (1933).
GLASER, H., Über die innere Reibung zäher und plastisch-fester Körper und die Gültigkeit des Poiseuilleschen Gesetzes. Inaug. Diss. Erlangen, 1907. Summary report in Ann. d. Ph. (4) *22*, p. 694 (1922).
GOLDSTEIN, S., Modern Developments in Fluid Dynamics I and II. Oxford: Clarendon Press, 1938.
GRIFFITHS, ALBERT, and GRIFFITHS CONSTANCE, H., Viscosity of water at low rates of shear. Proc. Phys. Soc. *33*, 231 (1920/21).
GRIFFITHS, ALBERT, and VINCENT, P. C., The viscosity of water at low rates of flow. Ibid. *38*, 291 (1925/26).
GRINDLEY, JOHN H., and GIBSON, A. H., On the frictional resistances to the flow of air through a pipe. Proc. Roy. Soc. *80*, 114 (1907/08).
HAGEN, G., Ueber die Bewegung des Wassers in engen cylindrischen Röhren. Ann. d. Ph. und Ch. (Pogg. Ann.) (2) *46*, 423 (1839).
—— Über den Einfluss der Temperatur auf die Bewegung des Wassers in Röhren. Abhandl. der Königl. Akad. der Wissensch. zu Berlin, Math. Abh. (Abh. Ak. Wiss. Berlin.) 1854, p. 17.
—— Über die Bewegung des Wassers in cylindrischen, nahe horizontalen Leitungen. Ibid. 1869: II, pp. 1 and 27.
HATSCHEK, EMIL, The Viscosity of Liquids. G. Bell, London 1928 (German ed. 1929, French ed. 1932).
HAUSER, E. A., and LE BEAU, D. S., Studies in colloidal clays. J. ph. Ch. *42*, 1031 (1938).
HECKE, ALBERT VAN., Théorie du mouvement des fluides I et II. Union d. Ing. sortis d'Ecoles spéciales de l'Université catholique de Louvain. Bull:s Techn. 3 et 4, Sér. techn. 16 (1952).

HEGGE-ZIJNEN, B. G. VAN DER, Measurements of the velocity distribution in the boundary layer along a plane surface. Proefschrift, Technische Hoogeschool te Delft 1924.
HEISENBERG, WERNER, Ueber Stabilität und Turbulenz von Flüssigkeitsströmen. Ann. d. Ph. (4) *74*, 577 (1924). English transl. in NACA TM 1291 (1951).
HELMHOLTZ, H., and PIOTROWSKI, G. VON, Ueber Reibung tropfbarer Flüssigkeiten. Sitzungsber. K. Akademie d. Wissensch. Wien (Sitz. Ak. Wiss. Wien) (E) *40*, 607 (1860).
HENNIKER, J. C., The depth of the surface zone of a liquid. Rev. Mod. Ph. *21*, 322 (1949).
HERMANS, J. J., Flow Properties of Disperse Systems. North-Holland Publishing Company, Amsterdam, 1953.
HIRSCHFELDER, JOSEPH O., CURTISS, CHARLES F., and BIRD, R. BYRON. Molecular Theory of Gases and Liquids. John Wiley & Sons Inc., New York, 1954.
HÖPPLER, F., Über neuere Messungen der Zähigkeit des Wassers. Z. ang. Ph. *4*, 297 (1952).
HUGHES, R. R., and OPPENHEIM, A. K., Fluid dynamics. IEC *48*, 633 (1956).
KAMPMEYER, PRESTON M., The temperature dependence of viscosity for water and mercury. J. appl. Ph. *23*, 99 (1952).
KÁRMÁN, TH. v., Gastheoretische Deutung der Reynoldschen Kennzahl. Z. für angew. Math. und Mech. (ZAMM) *3*, 395 (1923).
—— Ueber die Stabilität der Laminarströmung und die Theorie der Turbulenz. Proc. 1st ICAM, p. 97 (Delft, 1924).
—— Mechanische Ähnlichkeit und Turbulenz. Proc. 3rd ICAM Vol. I, p. 83 (Stockholm 1930).
KNIBBS, G. H., The history, theory and determination of the viscosity of water by the efflux method. J. and Proc. of the Roy. Soc., New South Wales, Sydney, *29*, 77 (1895).
—— Note on recent determinations of the viscosity of water by the efflux method. Ibid. *30*, 186 (1896).
KOHLRAUSCH, K. W. FRITZ, Über das Verhalten strömender Luft in nichtkapillaren Röhren. Ann. d. Ph. (4) *44*, 297 (1914).
KOLIN, ALEXANDER, Demonstration of parabolic velocity distribution in laminar flow. American J. of Physics (Am. J. Ph.) *21*, 619 (1953).
KREY, H., Die Quer-Geschwindigkeitskurve bei turbulenter Strömung. ZAMM *7*, 107 (1927).
KURZWEG, HERMANN, Neue Untersuchungen über die Entstehung der turbulenten Rohrströmung. Ann. d. Ph. (5) *18*, 193 (1933).
LADENBURG, R., Über die innere Reibung zäher Flüssigkeiten und ihre Abhängigkeit vom Druck. Inaug. Diss., München Univ., 1906. Summary report in Ann. d. Ph. (4) *22*, 287 (1907).
LAMB, HORACE, Hydrodynamics. Cambridge University Press, 6th ed., reprinted 1953.
LANDOLT–BÖRNSTEIN, Physikalisch-Chemische Tabellen. 5th ed., hrsg. W. A. ROTH und K. SCHEEL, Hw. I, 1923; Eg. I, 1927; Eg. II*a*, 1931; Eg. III*a*, 1935. Julius Springer, Berlin.
LAUFER, JOHN, Investigation of turbulent flow in a twodimensional channel. NACA Report 1053 (1951), supersedes NACA TN 2123 (1950). See also JAS *17*, 277 (1950). Rev. in AMR *4*, no. 345, p. 48 (1951).
—— The structure of turbulence in fully developed pipe flow. NACA Report 1174 (1954), supersedes NACA TN 2954 (1953).
LAVERGNE, MICHEL, and DROST-HANSEN, WALTER, Discontinuities in slope of the temperature dependence of the thermal expansion of water. Naturwissenschaften *43*, 511 (1956).
LINDGREN, E. RUNE, Some aspects of the change between laminar and turbulent flow of liquids in cylindrical tubes. Arkiv för Fysik *7*, 293 (1954) *a*.
—— Note on the flow of liquids in tubes. Appl. sci. Res. (A) *4*, 313 (1954) *b*.
—— Properties of certain bentonite suspensions and water. A note on the inadequate definition of the Reynolds number in hydrodynamics. Arkiv för Fysik *11*, 117 (1956).
LORENZ, H. A., Über die Entstehung turbulenter Flüssigkeitsbewegungen und über den Einfluss dieser Bewegungen bei der Strömung durch Röhren. *In* H. A. LORENZ, Abhandlungen über theoretische Physik, B. G. Teubner, Leipzig und Berlin, 1907, Vol. I, p. 43.
MALLOCK, A., Determination of the viscosity of water. Proc. Roy. Soc. *45*, 126 (1888/89).
—— Experiments on fluid viscosity. Trans. Roy. Soc. *187*, 41 (1896).
MARCHI, GIULIO DE, Nuove esperienze intorno al cambiamento di regime nel movimento dell'acqua entro condotti circolari. Memorie dell'Istituto idrotecnico di Stra, Venezia, *1*, 19 (1917).
MCADAMS, WILLIAM H., Heat Transmission. 3rd ed., McGraw-Hill Publ. Comp. Ltd., London, 1954.
MCPHERSON, M. B., and NECE, R. E., An inexpensive demonstration fluid polariscope. Spring Meeting, Middle Atl. Sect. Am. Soc. Eng. Education, Lehigh Univ., Bethlehem, Pa., May 13, 1950

METROT, R., Détermination statique de la "yield value" des systèmes plastiques par la méthode d'arrachement. Application aux boues de forage. Rev. Inst. France du Petrole *1*, 78 (1946) or Annales des Combustibles liquides *2*, 79 (1946).

MILLER, BENJAMIN, The laminar-film hypothesis. Trans ASME *71*, 357 (1949). Adapted from a lecture entitled "Exploding a heat transfer myth" delivered to the Nepa Heat Transfer Symposium at Oak Ridge, Tenn., Dec. 1947. Rev. by STANLEY CORRSIN in AMR *3*, no. 1542, p. 244 (1950).

MISES, R. v., Kleine Schwingungen und Turbulenz. Jahresbericht der deutschen Mathematiker-Vereinigung *21*, 241 (1912).

MITCHNER, MORTON, Propagation of turbulence from an instantaneous point disturbance. JAS *21*, 350 (1954).

MORRIS, W. J., and SCHNURMANN, R., Temporary reduction of viscosity of liquids at high rates of shear. Nature *167*, 317 (1951). Rev. in AMR *4*, no. 2985, p. 422 (1951).

NAUMANN, A., Experimentelle Untersuchungen über die Entstehung der turbulenten Rohrströmung. Forschung auf dem Gebiete des Ingenieurwesens, Berlin (Forsch. Geb. Ing.w.) *2*, 85 (1931).

NEWTON, ISAAC, Philosophiae naturalis principia mathematica. 1687.

NIKURADSE, J., Widerstandsgesetz und Geschwindigkeitsverteilung von turbulenten Wasserströmungen in glatten und rauhen Rohren. Proc. 3rd ICAM Vol. I, p. 239 (Stockholm 1930).

—— Gesetzmässigkeiten der turbulenten Strömung in glatten Rohren. Verein. Deutsch. Ingenieure, Forschungsheft (VDI Forsch.heft), 356 (1932).

—— Strömungsgesetze in rauhen Rohren. Ibid. 361 (1933). English transl. in NACA TM 1292 (1950).

ORR, WILLIAM, The stability or instability of the steady motions of a perfect liquid and of a viscous liquid. I: A perfect liquid. II: A viscous liquid. Proc. Roy. Irish Academy (A), *27*, 9, 69 (1907/09).

OSEEN, C. W., Das Turbulenzproblem. Proc. 3rd ICAM Vol. I, p. 3 (Stockholm 1930).

PAGE JR, F., CORCORAN, W. H., SCHLINGER, W. G., and SAGE, B. H., Temperature and velocity distributions in uniform flow between parallel plates. IEC *44*, 419 (1952).

PAGE JR, F., SCHLINGER, W. H., BREAUX, D. K., and SAGE, B. H., Point values of eddy conductivity and viscosity in uniform flow between parallel plates. Ibid. *44*, 424 (1952).

PHILIPPOFF, W., Viskosität der Kolloide. Theodor Steinkopff, Dresden und Leipzig, 1942.

POISEUILLE, J. L. M., Recherches expérimentales sur le mouvement des liquides dans les tubes de très petits diamètres. Compt. Rend. *11:* 2, 961 (1840) and *12:* 1, 112 (1841). More comprehensive report in Mém. présentés par div. sav. l'Acad. Roy. d. Sciences l'Inst. de France, Sci. Math. et Phys. (Mém. Sav. Etrangers) *9*, 433 (1846).

PRANDTL, L., Eine Beziehung zwischen Wärmeaustausch und Strömungswiderstand der Flüssigkeiten. Ph. Z. *11*, 1072 (1910).

—— Bemerkungen über die Entstehung der Turbulenz. ZAMM *1*, 431 (1921).

PRANDTL, L.–TIETJENS, O., Hydro- und Aeromechanik I and II. Julius Springer, Berlin, 1931.

PRENGLE, R. S., and ROTHFUS, R. R., Transition phenomena in pipes and annular cross sections. IEC *47*, 379 (1955).

REICHARDT, H., Die Wärmeübertragung in turbulenten Reibungsschichten. ZAMM *20*, 297 (1940).

REYNOLDS, OSBORNE, An experimental investigation of the circumstances which determine whether the motion of water shall be direct or sinuous, and of the law of resistance in parallel channels. *In* Papers on Mechanical and Physical Subjects. Cambridge University Press, 1901, Vol. II, p. 51, which reproduces the complete report of Trans. Roy. Soc. *174*, 935 (1883). The first experimental arrangements were already reported in Proc. Manch. Lit. and Phil. Soc. of the year 1874, p. 9. A summary article of the complete work is presented in Proc. Roy. Soc. *35*, 84 (1883).

RICHARDSON, FRANCES; FERREL, J. K., LAMONDS, J. A., and BEATTY, K. O., How radiotracers are used in measuring fluid-velocity profiles. Nucleonics *13*, no. 7, p. 21 (July 1955).

ROTHFUS, R. R., MONRAD, C. C., and SENECAL, V. E., Velocity distribution and fluid friction in smooth concentric annuli. IEC *42*, 2511 (1950).

ROTHFUS, R. R., and PRENGLE, R. S., Laminar-turbulent transition in smooth tubes. Ibid. *44*, 1683 (1952).

ROTTA, J., Experimenteller Beitrag zur Entstehung turbulenter Strömung im Rohr. Ing. Arch. *24*, 258 (1956).

RUCKES, WILHELM, Untersuchungen über den Ausfluss komprimierter Luft aus Haarröhrchen und dabei auftretenden Wirbelerscheinungen. Ann. d. Ph. (4) *25*, 983 (1908), or VDI Forsch.-heft *75*, 23 (1909). More comprehensive in Inaug. Diss. Univ. Würzburg, 1908.

SCHILLER, L., Rauhigkeit und kritische Zahl. Ein experimenteller Beitrag zum Turbulenzproblem. Z. für Ph. *3*, 412 (1920).

—— Experimentelle Untersuchungen zum Turbulenzproblem. ZAMM *1*, 436 (1921).

—— Die Entwicklung der laminaren Geschwindigkeitsverteilung und ihre Bedeutung für Zähigkeitsmessungen. ZAMM *2*, 96 (1922).

—— Untersuchungen über laminare und turbulente Strömung. VDI Forsch.heft 248 (1922) *a*. Contains both the reports ZAMM *1*, 436 and ZAMM *2*, 96 (Leipziger Habilitationsschrift 1921).

—— Experimentelle Feststellungen zum Turbulenzproblem. Ph. Z. *23*, 14 (1922) *b*. This article summarizes the works reported in ZAMM *1*, 436, Z. für Ph. *3*, 412 and Ph. Z. *22*, 523, and is accompanied by a discussion by HOPF, v. KÁRMÁN, and v. MISES.

—— Über den Strömungswiderstand von Rohren verschiedenen Querschnitts und Rauhigkeitsgrade. ZAMM *3*, 2 (1923).

—— Neue Versuche zum Turbulenzproblem. Ph. Z. *25*, 541 (1924).

—— Grenzschichtdicke und kritische Zahl. Ibid. *26*, 64 (1925).

—— Das Turbulenzproblem und verwandte Fragen. Ibid. *26*, 566 (1925) *a*.

—— Strömungsbilder zur Entstehung der turbulenten Rohrströmung. Proc. 3rd ICAM Vol. I, p. 226 (Stockholm 1930).

—— Handbuch der Experimentalphysik IV: 4, Hydro- und Aerodynamik. Akad. Verlagsges. m. b. H., Leipzig, 1932.

—— Neue quantitative Versuche zur Turbulenzentstehung. ZAMM *14*, 36 (1934).

SCHILLER, L., and KIRSTEN, H., Über den Widerstand strömender Flüssigkeit in kurzen Rohrstücken. Ph. Z. *22*, 523 (1921).

SCHLICHTING, H., Neuere Untersuchungen über die Turbulenzentstehung. Die Naturwissenschaften *22*, 376 (1934).

—— Grenzschicht-Theorie. G. Braun, Karlsruhe, 1951.

SCHLINGER, W. G., and SAGE, B. H., Velocity distribution between parallel plates. IEC *45*, 2636 (1953).

SCHNETZLER, EBERHARDT, Strömungserscheinungen von Wasser in rauhwandigen Kapillaren innerhalb eines grossen Bereiches von Strömungsgeschwindigkeiten. Ph. Z. *11*, 1002 (1910).

SCHUBAUER, G. B., and KLEBANOFF, P. S., Contributions on the mechanics of boundary layer transition. Symposium on Boundary Layer Effects in Aerodynamics, 31st March–2nd April 1955, National Physical Laboratory, England.

SCHUBAUER, G. B., and SKRAMSTAD, H. K., Laminar boundary layer oscillations and transition on a flat plate. NACA WR W-8 from 1943, or J. of Res. NBS *38*, 251 (1947), or NACA Rep. 909 (1948), or Laminar boundary oscillations and stability of laminar flow, JAS *14*, 69 (1947).

SHARPE, FRANCIS ROBERT, On the stability of the motion of a viscous liquid. Trans. Amer. Math. Soc. *6*, 496 (1905).

SHIBUYA, I., Theoretical study of the turbulent transition of a flow through a circular pipe. Rep. Inst. high Speed Mech. Tôhoku Univ. (B) *1*, 37 (1951). Rev. in AMR *6*, no. 2309, p. 342 (1953).

SOMMERFELD, A., Ein Beitrag zur hydrodynamischen Erklaerung der turbulenten Fluessigkeitsbewegungen. Proc. 4th Int. Congr. for Mathematics Vol. III, p. 116 (Rome 1908).

SORKAU, W., Experimentelle Untersuchungen über die innere Reibung einiger organischer Flüssigkeiten im turbulenten Strömungszustande. Ph. Z. *12*, 582 (1911), or Anales de la Sociedad Cientifica, Argentina, *73*, 237 (1911).

—— Über den Einfluss von Temperatur, spezifischem Gewicht und chemischer Natur von Flüssigkeiten auf die Turbulenzreibung. Inaug. Diss. Greifswald, 1912. Summary report in Ph. Z. *13*, 805 (1912).

—— Über den Zusammenhang zwischen Molekulargewicht und Turbulenzreibungskonstante. Ibid. *14*, 147 (1913).

—— Zur Turbulenzreibung des Wassers. I und II. Ibid. *14*, 759, 828 (1913).

—— Zur Kenntnis der Turbulenzreibung. Ibid. *15*, 582 (1914).

—— Zur Kenntnis des Überganges von der geordneten zur Turbulentströmung in Kapillarröhren. I. Ibid. *15*, 768 (1914).

—— Same. II and III. Ibid. *16*, 97, 101 (1915).

SPITSE, L. A., and RICHARDS, D. O., Surface studies of glass. Part I. Contact angles. J. Appl. Ph. *18*, 904 (1947).

STANTON, T. E., Note on relation between skin friction and surface cooling. Adv. Comm. of Aeronautics, Techn. Report (ACA Techn. Rep.) 1912/13 (Rep. & Mem. no. 94), p. 45.

STANTON, T. E., MARSHALL, DOROTHY, and BRYANT, C. N., On the conditions at the boundary of a fluid in turbulent motion. Proc. Roy. Soc. *97*, 413 (1920).

SWINDELLS, J. F., COE, J. R., and GODFREY, T. B., Absolute viscosity of water at 20°C. J. of Res. NBS *48:* 1, 1 (1952).

SZYMAŃSKI, P., Sur l'écoulement non permanent du fluide visqueux dans le tuyau. Proc. 3rd ICAM Vol. I, p. 249 (Stockholm, 1930).

TAMMAN, G., and HINNÜBER, J., Die innere Reibung von Quecksilber. Z. für anorg. und allg. Ch. *167*, 230 (1927).

TATSUMI, TOMOMASA, Stability of the laminar inlet-flow prior to the formation of Poiseuille regime, I and II. J. Ph. Soc. Jap. *7*, 489, 495 (1952). Rev. in AMR *6*, no. 1653, p. 245 (1953).

TAUSZ, J., and KŐRÖSY, F. v., Über Reibungskonstante und Wandschicht. Z. für Phys. Chem. (A) *140*, 263 (1929).

TAYLOR, G. I., Conditions at the surface of a hot body exposed to the wind. ACA Techn. Rep. 1916/17 Vol. II (Rep. & Mem. no. 272), p. 423.

—— Stability of a viscous liquid contained between two rotating cylinders. Trans. Roy. Soc. *223*, 289 (1922/23). Summary report in Proc. Roy. Soc. *102*, 541 (1923).

—— Production and dissipation of vorticity in a turbulent fluid. Proc. Roy. Soc. *164*, 15 (1938).

TAYLOR, G. I., and GREEN, A. E., Mechanism of the production of small eddies from large ones. Ibid. *158*, 499 (1937).

THEODORSEN, THEODORE, The structure of turbulence. *In* 50 Jahre Grenzschichtforschung. Hrsg. H. GÖRTLER und W. TOLLMIEN. Friedr. Vieweg & Sohn, Braunschweig 1955, p. 55.

TOLLMIEN, W., Über die Entstehung der Turbulenz. 1. Mitteilung. Nachr. v. d. Gesellschaft d. Wiss. zu Göttingen, Mat.-Ph. Kl. 1929, Heft 1, p. 21. Summary report *in* Vorträge aus d. Geb. d. Aerodyn. und verw. Geb., Aachen 1929, p. 18 (hrsg. GILLES, HOPF, KÁRMÁN), Julius Springer, Berlin, 1930. English translation in NACA TM 609 (1931).

—— Fortschritte der Turbulenzforschung. ZAMM *33*, 200 (1953). Rev. in AMR *7*, no. 865, p. 121 (1954).

WATTENDORF, F. L., and KUETHE, A. M., Investigations on turbulent flow by means of the hot-wire anemometer. Physics *5*, 153 (1934).

WEBER, WOLF, Die Temperaturabhängigkeit der Viskosität des Wassers zwischen 0° und 40°C. Z. ang. Phys. *7*, 96 (1955).

WESKE, JOHN R., Discrete vortices in the transition range of flow in a pipe. AGARD Traveling Seminar 16 June–16 July 1954, p. 7.

WEYLAND, HAROLD, La biréfringence d'écoulement comme technique pour l'étude du champ hydrodynamique. J. de Ph. et le Radium *16*, 27 (1955).

—— Streaming birefringence as a hydrodynamic research tool. Applied to a rotating cylinder apparatus above the transition velocity. J. of Appl. Ph. *26*, 1197 (1955).

Tryckt den 25 april 1957

Uppsala 1957. Almqvist & Wiksells Boktryckeri AB

Arkiv för Fysik

Arkiv för Fysik, the journal of physics issued by the Royal Swedish Academy of Sciences, was first published in 1949, having earlier formed part of the former *Arkiv för Matematik, Astronomi och Fysik.* The journal aims at making the research work of Swedish physicists known to the international public. The Swedish title of the journal – and of other such periodicals published by the Academy – by no means implies that Swedish is the main language used. In fact, in the volumes published so far, all papers but one are in English, German or French: Swedish authors are of course interested in making their papers understandable to all those who are working in the same field.

Arkiv för Fysik appears at irregular intervals but on an average with nine issues pro year. Six issues form one volume with a total of approx. 600 pages. Subscription rate per volume, Sw. kr. 50.–.

Requests for subscription should be addressed to

ALMQVIST & WIKSELL, Import & Export Department, Gamla Brogatan 26, Stockholm, Sweden.